INCLUSION OF ALKYLPARABENS IN CYCLODEXTRINS

BY: ELISE JANINE CHRISTL DE VRIES

B.Sc.(Hons.) University of Cape Town

THESIS PRESENTED TO THE UNIVERSITY OF CAPE TOWN FOR THE DEGREE OF DOCTOR OF PHILOSOPHY

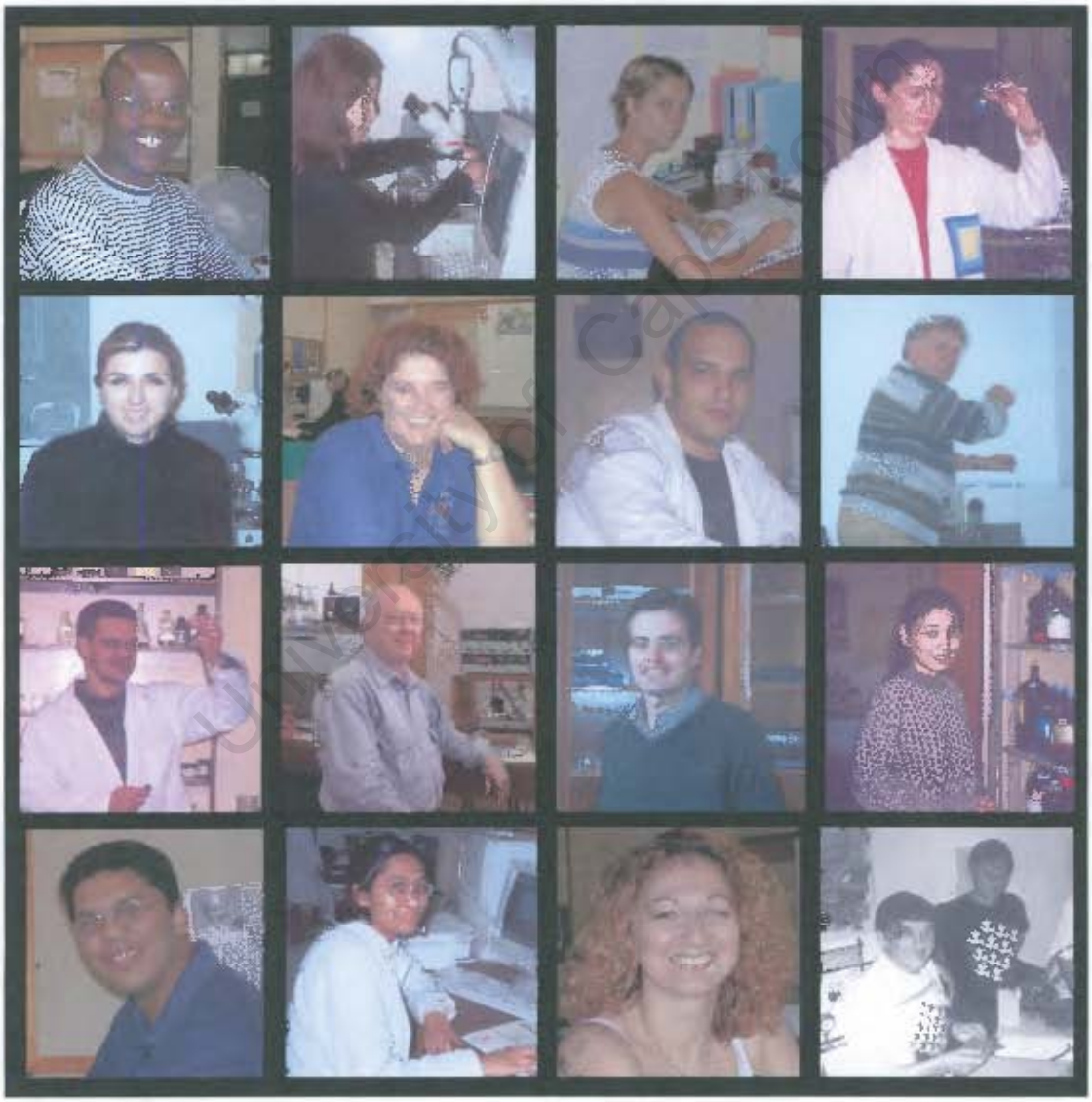

April 2003

ACKNOWLEDGEMENTS

I would like to thank:

my supervisors, Professor M. R. Caira and Professor L. R. Nassimbeni, for their guidance and supervision, as well as Professor S. A. Bourne for her help and advice

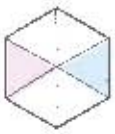

Dr. J. Bacsa and Dr. H. Su for data collection on the Kappa CCD diffractometer and solving other problems

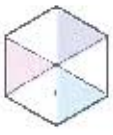

Mr. N. W. Hendricks for collecting NMR data and Professor G. E. Jackson for his help in interpreting the data

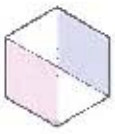

D. Bogdan, M. Bogdan and S. I. Farcas at the National Institute for Research and Development of Isotopic and Molecular Technologies, Cluj-Napoca, Romania for their assistance and valuable instruction on NMR analysis

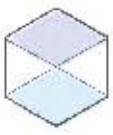

the members of the Crystallography Research Group for their assistance, especially V. Smith for his input and help, as well as the rest of the group for their movie reviews and lunch time entertainment

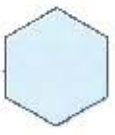

the National Research Foundation and the University of Cape Town for financial support

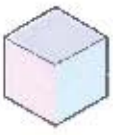

my friends and family for their support and efforts to understand what I was talking about

PUBLICATIONS AND CONFERENCES

➢ Parts of this thesis that have been published:

M. R. Caira, E. J. C. de Vries, L. R. Nassimbeni, *Cyclodextrin Inclusion of p-Hydroxybenzoic Acid Esters* in *J. Thermal Analysis and Calorimetry*, 2003 in press.

➢ Parts of this thesis have been presented at the following conferences:

A poster entitled "Inclusion of Paraben Molecules in β-cyclodextrin" was presented at the *Academy of Pharmaceutical Science*, 21st Annual Congress, Pharmacy in the New Millennium, 10 - 13 September 2000, Rhodes University, Grahamstown, South Africa.

A poster entitled "Inclusion of Paraben Molecules in Heptakis(2,3,6-tri-*O*-methyl)-β-cyclodextrin" was presented at the *International Immunopharmacology Congress*, 16 - 20 September 2001, Sun City, Pilanesberg, South Africa.

A presentation entitled "Inclusion of Paraben Molecules in Heptakis(2,3,6-tri-*O*-methyl)-β-cyclodextrin" was presented at the annual meeting of the *South African Crystallographic Society*, 4 - 5 April 2002, Department of Chemistry, University of Stellenbosch, South Africa.

A poster entitled "Inclusion of Paraben Molecules in Heptakis(2,3,6-tri-*O*-methyl)-β-cyclodextrin" was presented at the *XIX Congress and General Assembly of the International Union of Crystallography*, 6 - 15 August 2002, Geneva, Switzerland.

Abstract

The aim of this thesis was to prepare crystalline inclusion complexes with cyclodextrins (CDs), as hosts, and drugs, as guests, characterise them using various methods and attempt to elucidate their structures by X-ray diffraction methods to establish the detailed mode of drug inclusion in the solid state.

Cyclodextrins and their derivatives have a low polarity central void formed by linked glucose residues of varying numbers. This annular cavity is able to encapsulate low molecular weight molecules and is therefore responsible for the great interest in CDs in host-guest chemistry. In addition, inclusion of drug molecules in cyclodextrins can significantly improve aspects of their performance, such as increased aqueous solubility and dissolution rates which lead to their increasing application in the pharmaceutical industry.

p-Hydroxybenzoic acid esters (alkylparabens) are widely used as antimicrobial preservatives for aqueous based pharmaceutical formulations, cosmetics and food products. In general, the elongation of the alkyl chain increases their antispectic action and clinical safety. However, practical use of parabens with longer alkyl chains has been limited because of their low solubility in water. Previous studies have demonstrated that complexation with cyclodextrins can be used to increase the solubilities of these molecules.

In this thesis the inclusion of alkylparabens with cyclodextrins was studied in solution and in the solid state. Co-precipitation and kneading methods were used to effect drug inclusion. The physicochemical methods employed to assess these compounds can be divided into three categories. Ultraviolet spectrophotometry, microanalysis and thermogravimetric analyses were the principal techniques employed to determine the chemical composition. This was followed by the analysis of the thermal behaviour of the compounds by hot stage microscopy, differential scanning calorimetry and thermogravimetric analysis. Finally, the study involved the determination of structural features of the respective inclusion complexes by X-ray diffraction analysis of powder samples and single crystals.

Among the cyclodextrins used were the native species β- and γ-CD and two methylated derivatives of β-CD, namely heptakis(2,6–di–*O*–methyl)–β–CD and heptakis(2,3,6–tri–*O*–methyl)–β–CD, commonly abbreviated as DIMEB and TRIMEB respectively. Complexes with alkylparabens were prepared and thermal analysis, Fourier transform infrared spectroscopic and X-ray diffraction techniques indicated that complexation had occurred with each host, as modifications in the properties of the pure host and guest were observed. In addition X-ray powder diffraction patterns were recorded in order to characterise the structures according to their packing schemes. This technique was useful in determining isostructural series and was the approach used in cases where it was difficult to grow suitable single crystals, as in the γ-CD complexes.

The β-CD complexes were studied both in solution and in the solid state. In solution, NMR was used to determine the stoichiometry of the complexes as well as the association constants to evaluate the stability of the host-guest system. In the solid state it was found that the β-CD-methyl paraben inclusion complex crystallised in two different space groups under different temperature conditions. This novel indication of polymorphism of a β-CD inclusion complex is reported in detail.

The crystal structures of three β-CD complexes, four DIMEB and four TRIMEB inclusion compounds were elucidated. Successful analyses clearly indicated i) the details of inclusion of the drug in the CD cavities and ii) the generally extensive hydrogen bonding networks mediated by water molecules. Guest molecules maintained similar conformations on the whole as those observed in other crystal structures and the conformations of the hosts were akin to those found in known crystal structures.

Guest disorder, a common feature observed in the β-CD inclusion complexes, was successfully resolved and modelled in the polymorphs containing methyl paraben. The DIMEB inclusion complexes of methyl- and ethyl paraben are isostructural, while those of propyl- and butyl paraben crystallise in a different isostructural series. The guest orientations are "reversed" in the two series. With TRIMEB as host, the included ethyl paraben molecule behaves anomalously in having an orientation which is reversed with respect to its homologues.

ABBREVIATIONS AND SYMBOLS

COMPOUNDS

MP	Methyl paraben
EP	Ethyl paraben
PP	Propyl paraben
BP	Butyl paraben
CD	Cyclodextrin
γ-CD	Gamma cyclodextrin
β-CD	Beta cyclodextrin
2-HP-β-CD	2-hydroxypropyl-β-cyclodextrin
DIMEB	Heptakis(2,6-di-*O*-methyl)-β-cyclodextrin
TRIMEB	Heptakis(2,3,6-tri-*O*-methyl)-β-cyclodextrin
MPGCD	γ-cyclodextrin-methyl paraben inclusion complex
EPGCD	γ-cyclodextrin-ethyl paraben inclusion complex
PPGCD	γ-cyclodextrin-propyl paraben inclusion complex
BPGCD	γ-cyclodextrin-butyl paraben inclusion complex
MPBCD	β-cyclodextrin-methyl paraben inclusion complex
EPBCD	β-cyclodextrin-ethyl paraben inclusion complex
PPBCD	β-cyclodextrin-propyl paraben inclusion complex
BPBCD	β-cyclodextrin-butyl paraben inclusion complex
MPDMB	DIMEB-methyl paraben inclusion complex
EPDMB	DIMEB-ethyl paraben inclusion complex
PPDMB	DIMEB-propyl paraben inclusion complex
BPDMB	DIMEB-butyl paraben inclusion complex
MPTMB	TRIMEB-methyl paraben inclusion complex
EPTMB	TRIMEB-ethyl paraben inclusion complex
PPTMB	TRIMEB-propyl paraben inclusion complex
BPTMB	TRIMEB-butyl paraben inclusion complex

TECHNIQUES

DSC	Differential Scanning Calorimetry
HSM	Hot Stage Microscopy
FTIR	Fourier Transform Infrared Spectroscopy
NMR	Nuclear Magnetic Resonance Spectroscopy
SEM	Scanning Electron Microscopy
TGA	Thermogravimetric Analysis
XRD	X-ray Powder Diffraction
UV	Ultraviolet Spectrophotometry

SYMBOLS

α	The angle between *b* and *c* unit cell axes
β	The angle between *a* and *c* unit cell axes
γ	The angle between *a* and *b* unit cell axes
CSD	Cambridge Structural Database
$\Delta\delta$	Change in chemical shift
E	Normalised structure factor
Endo	Endotherm
e.s.d	Estimated standard deviation
F	Structure factor
F(000)	Number of electrons in the unit cell
G	Guest compound
H	Host compound
H:G	Host to guest ratio
I	Intensity
K	Association constant
M_r	Molecular mass
S	Goodness of fit (F^2)
s.o.f.	Site-occupancy factor
τ	Torsion angle
T	Temperature
T_{on}	Onset temperature
μ	Linear absorption coefficient
W	Water
Z	Number of asymmetric units in the unit cell

TABLE OF CONTENTS

CHAPTER 2: EXPERIMENTAL

CHAPTER 3: γ-CD INCLUSION COMPLEXES

CHAPTER 4: β-CD INCLUSION COMPLEXES

CHAPTER 5: DIMEB INCLUSION COMPLEXES

CHAPTER 6: TRIMEB INCLUSION COMPLEXES

Chapter 1

INTRODUCTION

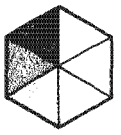

INCLUSION COMPOUNDS

In the last two decades there have been great advances in the field of supramolecular chemistry. As described by J.–M. Lehn[1] in his Nobel lecture, "supramolecular chemistry may be defined as chemistry beyond the molecule". Hence supramolecular chemistry can be described as a discipline of chemistry that involves all intermolecular interactions where covalent bonds are not established between the interacting species, namely molecules, ions or radicals. The majority of these are host-guest type interactions, leading to the formation of inclusion compounds.[2] Inclusion compounds may be defined as those compounds in which one type of molecule [the host] is able to incorporate one or several smaller molecules [the guest] in its crystal structure without changing the covalent bonding network of either molecule.

In consideration of this, Vögtle[3] proposed that there are two distinct classifications of inclusion compounds. Firstly, he refers to *lattice clathrates*, in which the host molecules assemble to form a host framework containing intermolecular voids in which the guest molecules can be accommodated. Secondly, there are *molecular complexes*, in which the host component comprises a single molecule and the guest component [or components] are located within the host. Examples of such hosts are cavitands, coronands, crown ethers, and cryptands. Cyclodextrins can be thought of as a combination of the two classifications, as cyclodextrin inclusion complexes usually consist of a tertiary system [of host, guest and solvent, which is often water] and in most cases the solvent molecules are found in the intermolecular spaces. The versatility of cyclodextrins as supramolecular hosts prompted the work in this thesis and further reference to other types of hosts will be omitted.

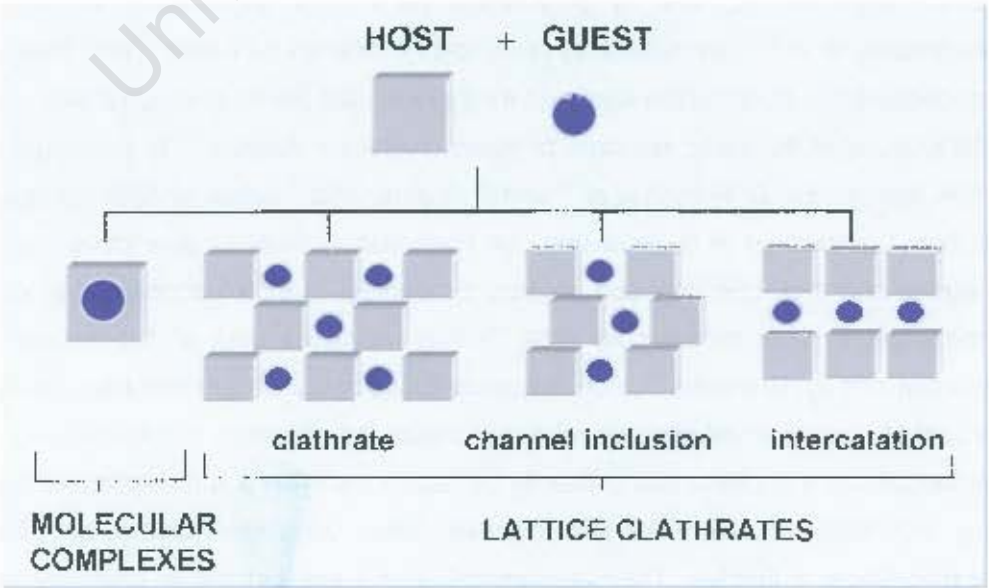

Figure 1.1 Schematic representation of inclusion compounds

NATURAL ORIGIN OF CYCLODEXTRINS

The term cyclodextrins [hereinafter CDs], also known as Schardinger dextrins, cycloamyloses and cycloglucoamyloses, encompasses those starch derivatives characterised by a ring built with glucose units. These compounds are obtained from enzymatic degradation of amylose, the linear unbranched fraction of starch, in a two-step process involving the cleavage of polysaccharidic chains into oligosaccharides followed by the resealing of the two open ends to form a cyclic structure. The starch helix is hydrolysed and its ends are joined together through α(1,4)-linkages. The enzyme used is a bacterial amylase called cyclodextrin glycosyltransferase [CGTase] which was first isolated from *Bacillus macerans*.[4] This enzyme is generally unspecific with respect to the site of hydrolysis, thus producing a family of cycloamyloses containing different numbers of glucopyranose units.[4-5] The most abundant of the cyclodextrins produced consist of 6 (α-CD), 7 (β-CD) and 8 (γ-CD) glucopyranose units, referred to as native cyclodextrins [Figure 1.2]. Whereas larger cyclodextrins with more than 100 glucopyranose units and beyond have been prepared by the action of disproportionating enzyme on amylose,[6] smaller molecules would be sterically strained and are therefore not produced by the glucosyltransferase enzymes.

BRIEF HISTORICAL OVERVIEW

The first reference to a substance that later proved to be a cyclodextrin was published by Villiers in 1891,[7] when he isolated the CD as crystals from a culture medium of *Bacillus amylobacter* grown on a starch-containing medium. This degradation product of starch was later characterised, in 1904, by Schardinger as a cyclic oligosaccharide.[8] In the 1930s Freudenberg *et al* [9-10] concluded, by using data published by Karrer[11] and Miekeley,[12] that cyclodextrins are constructed from α(1,4)-glycosidically linked glucopyranose units and in 1936 postulated the cyclic structure of these crystalline dextrins.[13] At the beginning of the 1950s, two groups, D. French *et al* [14] and F. Cramer *et al* [5] began to work intensively on the enzymatic production of cyclodextrins, on fractionating them to pure components and on characterising their chemical and physical properties. French[14] observed the existence of some larger cyclodextrins and in 1954 Cramer published work on the inclusion complex formation with cyclodextrins.[5] Once adequate toxicological studies had been performed and the cost of purchase had become relatively cheap, the utilisation of cyclodextrins increased dramatically, to the extent that presently cyclodextrins have a wide variety of applications. They are utilised in cosmetics and toiletries, foods, pesticides, biomedical products and pharmaceutical industries. They also exhibit useful applications in chemical technology, analytical chemistry and diagnostics.[15]

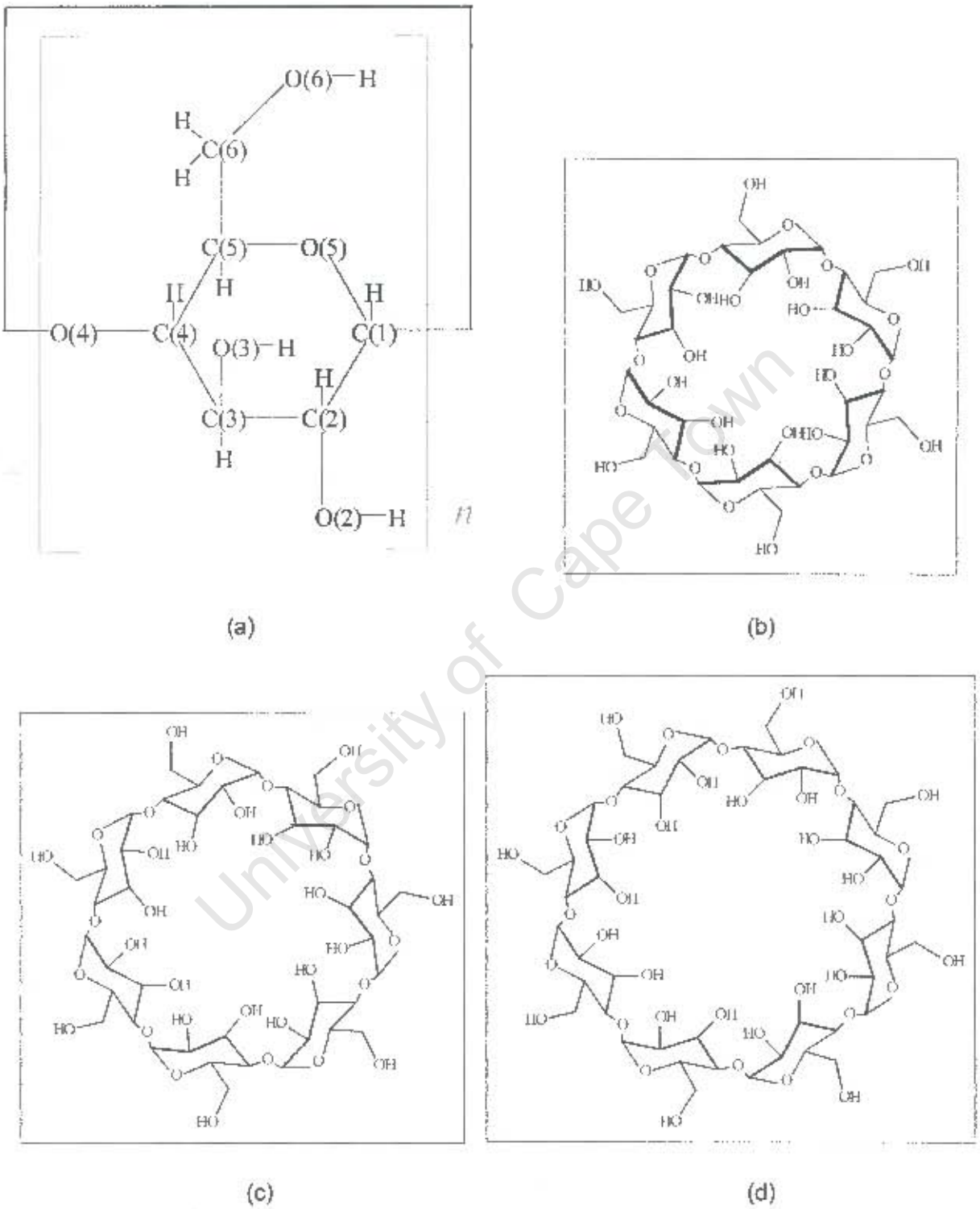

Figure 1.2 (a) The glucopyranose unit with the numbering scheme, (b) α-CD, (c) β-CD, (d) γ-CD

STRUCTURAL FEATURES

The glucopyranose units adopt a $^4C_1$-chair conformation and can be considered a fairly rigid building block.[16-18] This chair conformation and the intramolecular ring of hydrogen bonds formed between the secondary hydroxyl groups of adjacent glucopyranose units account for the structural rigidity and stability of CDs. The only real conformational flexibility is the rotational freedom of the O(6)–H hydroxyl groups around the axis of the C(5)–C(6) bond and the limited rotational movement about the C(1)–O(4')–C(4') glycosidic link [the primed atom belongs to the adjacent glucose unit].

Intramolecular hydrogen bonding

Since the glucopyranose units are orientated *cis* in the cyclodextrin, all the secondary O(2) and O(3) hydroxyl groups are situated on one side of the macrocycle. This enables the formation of intramolecular hydrogen bonds of the type O(2)•••O(3') between adjacent glucopyranose units. Neutron diffraction studies have shown that this intramolecular hydrogen bonding is of a "flip-flop" nature in β- and γ-CD crystal structures, constantly oscillating between O(2)–H•••O(3') and O(2)•••H–O(3') in the solid state.[19-20] The average O(2)•••O(3') distance decreases from α- [3.05 Å], to β- [2.92 Å], to γ-CD [2.84 Å],[18] indicating that the hydrogen bonds become increasingly stronger as the number of glucose units increases. Methylation of all the hydroxyl groups results in the loss of this intramolecular hydrogen bonding and consequently, an increase in conformational flexibility is observed in the heptakis(2,3,6–tri–O–methyl)–β–cyclodextrin (TRIMEB) molecule.[21]

The primary hydroxyl groups

The primary O(6) hydroxyl groups are located on the narrow primary rim of the macrocycle. They may rotate around the C(5)–C(6) bond with the preferred orientation of the O(5)–C(5)–C(6)–O(6) torsion angle (ω) being (–)*gauche* [ω = –60°]. In this conformation the O(6) hydroxyl groups will be pointing away from the centre of the cavity. However, if the O(6) hydroxyl groups are involved in hydrogen bonding with an enclosed guest molecule the less preferred (+)*gauche* conformation [ω = +60°], with the O(6) hydroxyl groups directed towards the cavity, is observed. The *trans* orientation [ω = 180°] has not been observed thus far, probably due to the adverse steric interactions which might occur between the O(6)–H and atoms of the adjacent glucose residues.

Parameters describing the conformation of cyclodextrins

The macrocyclic conformation of cyclodextrins and an indication of its deviation from the *n*-fold symmetry can be described by certain parameters.[17-18] Amongst these are the distances between the linking glycosidic oxygen atoms O(4)•••O(4') (*l*), the radius of the O(4) polygon (*r*), the O(4)•••O(4')•••O(4'') angle (*a*) and the torsion angle O(4)•••O(4')•••O(4'')•••O(4''') (*t*), as indicated in Figure 1.3. The average radius of the O(4) polygon is defined as the mean distance measured from the centre of gravity (C) of the polygon to each O(4) atom. For a planar regular macrocycle the deviation (*d*) of each O(4) atom from the mean plane of the macrocycle would be zero and the torsion angles would all be zero degrees. In practice, polygons composed of glycosidic O(4) atoms offer a good idealisation of the macrocyclic ring and generally these oxygen atoms are virtually coplanar, with *ca.* 0.3 Å deviation from the common mean plane.[18] The mean values of the principal geometrical parameters of the O(4) polygon for α-, β- and γ-CD are shown in Table 1.1.

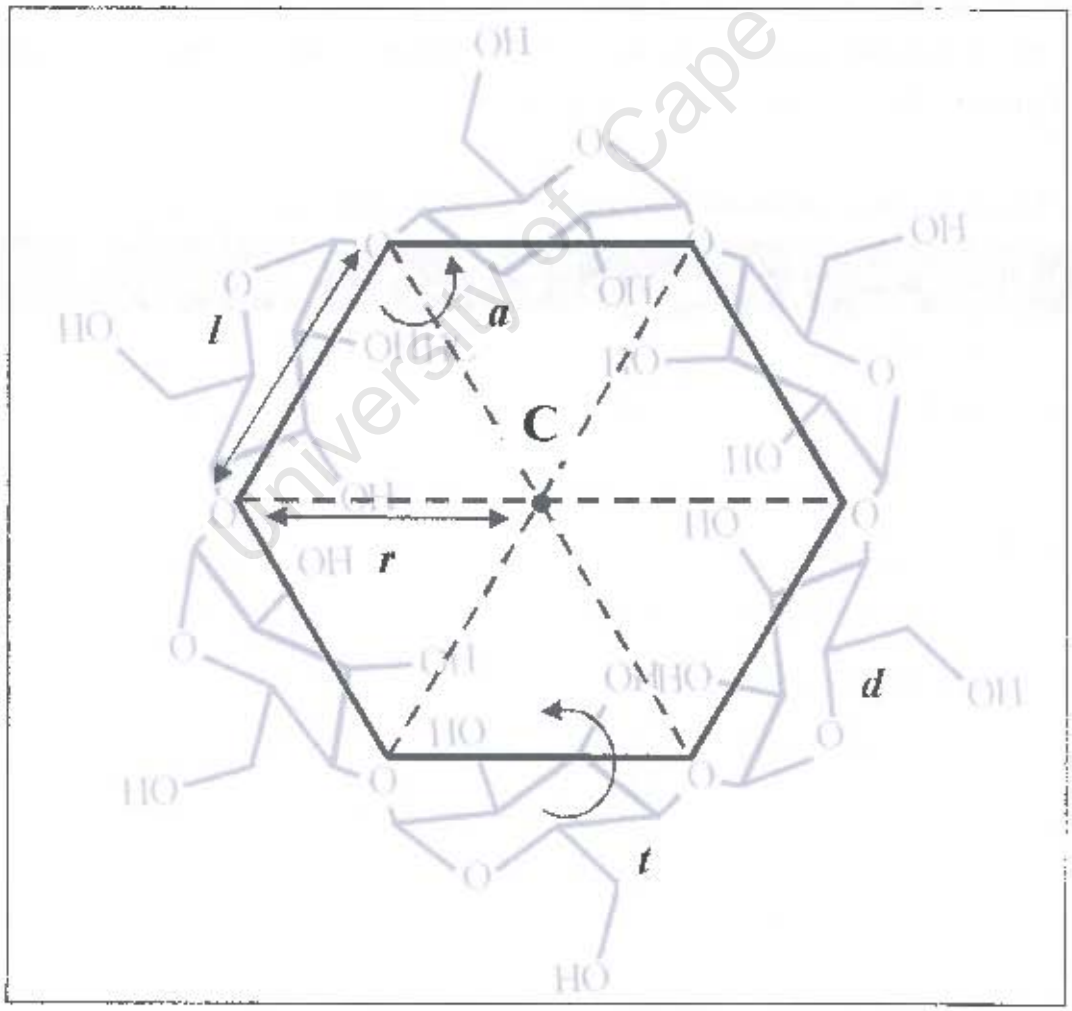

Figure 1.3 Principal geometrical parameters of the O(4) polygon

Other useful parameters are the O(2)•••O(3') distance, the intersaccharidic bond angle (φ) and the tilt angle (τ). The intersaccharidic bond angle is defined as φ = C(1')•••O(4)•••C(4), while the tilt angle can be defined in two ways. The mean values for these parameters are shown in Table 1.1 and were obtained from average structure values in the literature.

The tilt angle evaluates the relative inclinations of each glucose unit from the ideal *n*-fold symmetry. The tilt angle, τ_1, is defined as the angle made between the mean O(4) plane and the mean plane through the six pyranose ring atoms [namely C(1), C(2), C(3), C(4), C(5) and O(5)] of each glucose unit. The tilt angle, τ_2, is defined as the angle made by the mean O(4) plane and the mean plane through the atoms O(4'), C(1), C(4) and O(4) of each glucose unit.[22] Each glucose unit is not orthogonal to the mean O(4) plane but is inclined with the O(6) side towards the inside or outside of the macrocycle. If the glucose unit is inclined with its O(6) side towards the centre of the cavity, the tilt angle is positive, while a negative tilt angle denotes that the glucose unit is inclined with the O(6) side towards the outside of the macrocyclic cavity.

Table 1.1 Geometrical parameters describing the macrocyclic conformation

		α-CD	β-CD	γ-CD
O(4)•••O(4') distance[18]	(l / Å)	4.2	4.3	4.5
Radius of the O(4) polygon[18]	(r / Å)	4.2	5.0	5.9
O(4)•••O(4')•••O(4'') angle[23]	(a / °)	120	128	132
Torsion angle[23]	(t / °)	5	5	2
Planarity of the O(4) polygon[23]	(d / Å)	0.07	0.08	0.02
O(2)•••O(3') distance[24]	(l / Å)	3.05	2.92	2.84
Intersaccharidic bond angle[24]	(ϕ / °)	118.4	117.7	115.0
Tilt angle (τ_1)[24]	(τ_1 / °)	+ 11.4	+ 9.5	+ 14.5
Tilt angle (τ_2)	(τ_2 / °)	+ 13 [25]	+ 14 [26]	+ 19 [27]

Hydrophobic cavity

The shape of the cyclodextrin is that of a hollow, truncated cone [which is frequently compared to a bottomless bucket] with a wider secondary rim formed by the O(2) and O(3) atoms. The secondary hydroxyl groups are in equatorial positions with the O(2) groups pointing towards the cavity and the O(3) groups pointing away from the cavity. The primary rim is narrower, as the free rotation of the primary O(6) hydroxyl groups reduces the effective diameter of the cavity [Figure 1.4].

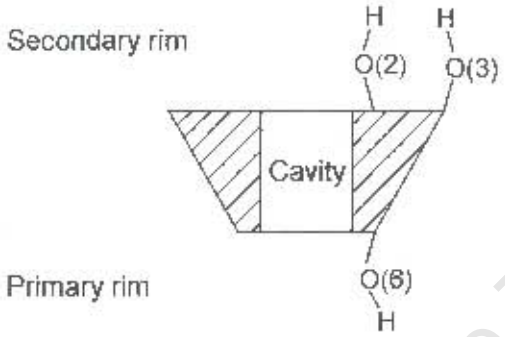

Figure 1.4 Schematic diagram of CD showing the cavity, primary and secondary faces

The inner wall of the cavity is lined with atoms of the glycosidic oxygen bridges and hydrogen atoms from the methine [C(3)–H and C(5)–H] and methylene groups [C(6)–H_2]. The non-bonding electron pairs of the glycosidic oxygen bridges are directed towards the inside of the cavity producing a high electron density there. The hydroxyl groups are lined on a circle at both ends of the cavity, such that there are twice as many secondary hydroxyl groups as there are primary hydroxyl groups. This produces an uneven charge distribution caused by the dipole moment parallel to the pseudo-symmetry axis of the molecule. As a result of this special arrangement of the functional groups, the cavity is relatively apolar and hydrophobic compared to water while the external faces are relatively polar and hydrophilic. The physical dimensions and cavity volumes of α-, β- and γ-CD are presented in Figure 1.5.

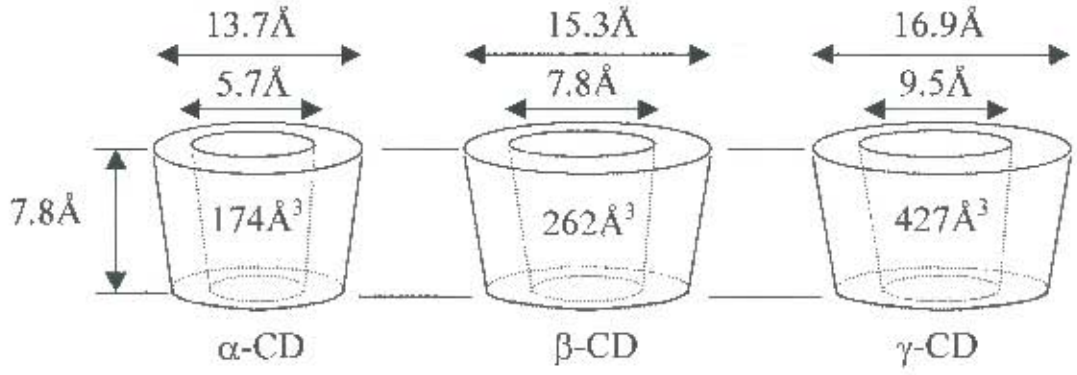

Figure 1.5 The physical dimensions of α-CD, β-CD and γ-CD[2]

INCLUSION COMPLEXES

The affinity of a guest towards cyclodextrins depends on the conformity between the guest molecule and the cyclodextrin cavity [i.e. the shape and size matching], the hydrogen bonding ability of the guest, the position of a substituent in the guest, and the flexibility of the guest molecule.

The structure of an inclusion complex is determined by an energetic balance between the maximal inclusion of the guest within the cavity, and the optimal orientation of the host and guest to enhance the interaction of the polar portions of the guest with the cyclodextrin or the solvent [Figure 1.6]. Thus, the guest can be completely or partially included in the cyclodextrin cavity.[28] In general, the stability of the cyclodextrin inclusion compounds increases with the extent to which the cavity is filled by the hydrophobic part of the guest.

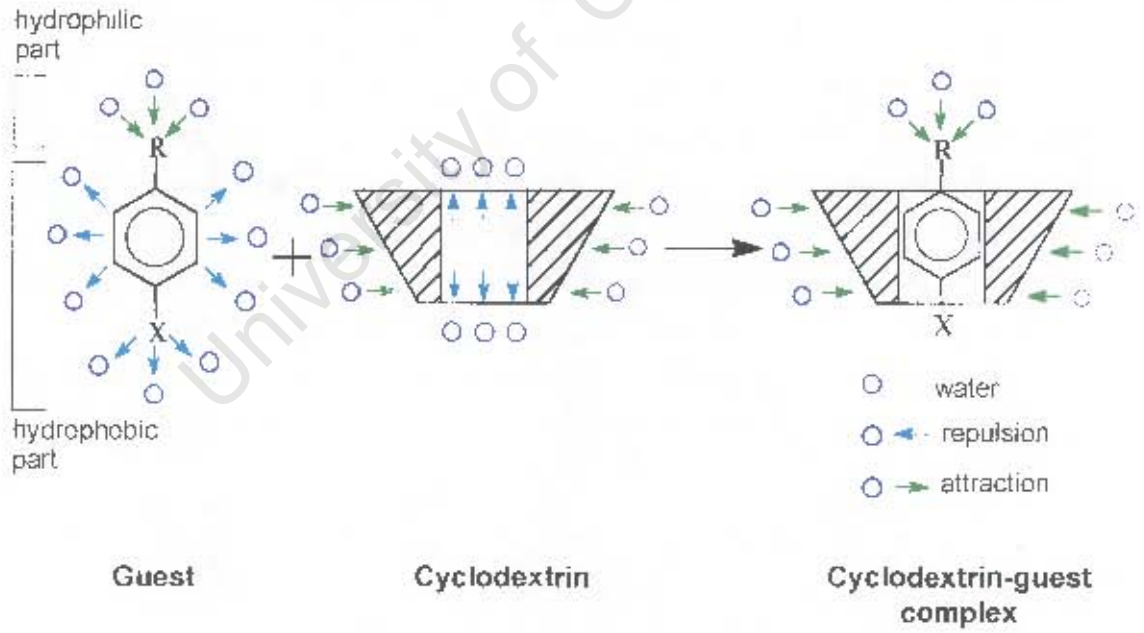

Figure 1.6 Schematic representation of guest inclusion by cyclodextrin on the expulsion of water

The most probable mode of binding involves the insertion of the less polar part of the guest molecule into the cavity, the direction of insertion presumably being from the wider, secondary hydroxyl rim of the cavity. The more polar group is located near the secondary hydroxyl groups or may even be exposed to the bulk solvent just outside the cavity.

In an aqueous solution, the slightly apolar cyclodextrin cavity is occupied by water molecules which are energetically unfavoured. On complexation these water molecules are readily substituted by appropriate guest molecules, which are less polar than water. The liberated water molecules are taken up by the bulk water and contribute to the stability of the complex owing to the resulting increase in entropy. This release of high enthalpy water from the cyclodextrin cavity into the bulk water is thus viewed as one of the driving forces of complexation.

Driving force of complexation

Many studies are aimed at elucidating this aspect of CDs. To date several factors have been postulated: van der Waals interactions, hydrogen bonding, hydrophobic interactions, release of high-energy cavity water, release of macrocyclic ring strain and the effect of solvent surface tension. However there is still no clear agreement on the mechanism of formation of cyclodextrin inclusion complexes.[4, 28-30] Although it is suggested that host-guest interactions are mainly due to van der Waals forces, hydrophobic interactions and hydrogen bonding, the extent to which these forces contribute is dependent on the nature of the guest.[16]

Hydrogen bonding in the complex

The involvement of the cyclodextrin hydroxyl groups in hydrogen bonding to the guest molecules is restricted mainly to the primary O(6)–H groups because they are more flexible. In addition to direct hydrogen bonding between the guest and the cyclodextrin molecules, there can be water-mediated hydrogen bonds as water may also be enclosed within the cavity if the guest molecule is too small to fit properly.

CRYSTAL PACKING

The packing arrangements found in the crystal structures of cyclodextrins and their complexes can be broadly classified into channel and cage type packing, according to the overall appearance of the formed cavities.[17, 31] The solid state structural arrangement adopted is determined predominantly by the dimensions [i.e. size and shape] of the guest molecule as well as the intra- and intermolecular interactions achievable within the cavity.

Channel type structures are formed by cavity-to-cavity alignment of the cyclodextrin macrocycles, either in a head-to-head or head-to-tail fashion [or a combination of these], thus forming infinite columns. Guest molecules are embedded in these columns and those which are longer than the depth of the cavity can be included in two or more cyclodextrin molecules. Frequently, the channels are not straight and individual cyclodextrin molecules are tilted with respect to the channel axis. Cage type structures are formed when the cavity of each cyclodextrin is blocked on both sides by adjacent cyclodextrin molecules in the crystal structure. Cage type structures can either be herringbone or brickwork type packing, the latter having a layered appearance. These layered structures are observed when the guest molecule is too large to be fully accommodated within the host cavity. These broad classifications can be further subdivided and this is best illustrated by considering β-CD.

Packing arrangements within β-CD

Monomeric Structures [Figure 1.7]

There are five different types of monomeric packing arrangements, namely: herringbone ($P2_1$), zigzag ($P2_12_12_1$), brickwork ($P2_1$), layer ($P2_1$) and helical channel ($P6_1$).[32] A search of the Cambridge Structural Database[33] indicates that the majority of monomeric β-CD complexes have cage type herringbone packing.

The monomeric herringbone packing arrangement allows for very efficient packing of the β-CD molecules and is preferred with small guest molecules that do not protrude from the cavity. The cyclodextrin molecules are stacked along the two-fold screw axis to form the characteristic herringbone pattern. The cavity of the cyclodextrin molecule is blocked on one end by a screw-related cyclodextrin molecule. The other end is blocked by a cyclodextrin molecule, which is related by translation along the *b*-axis.

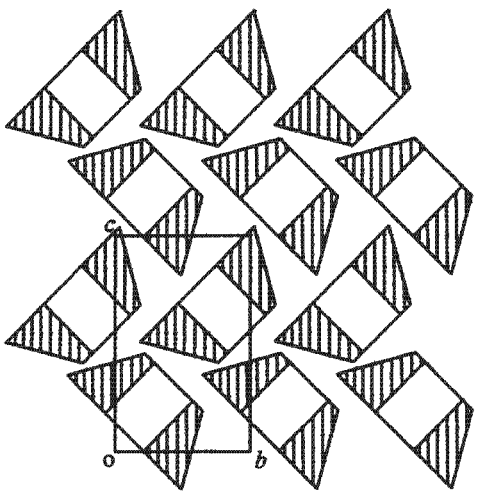

HERRINGBONE

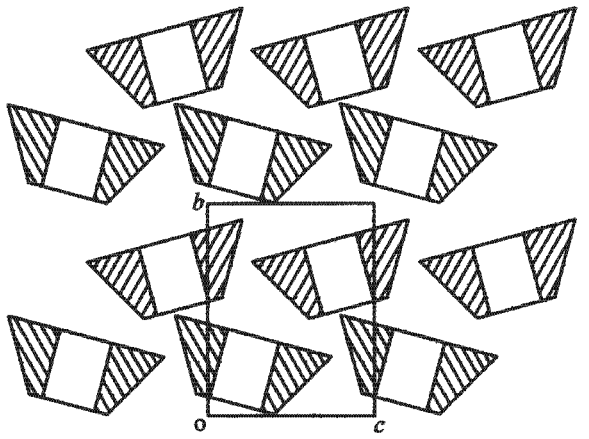

LAYER

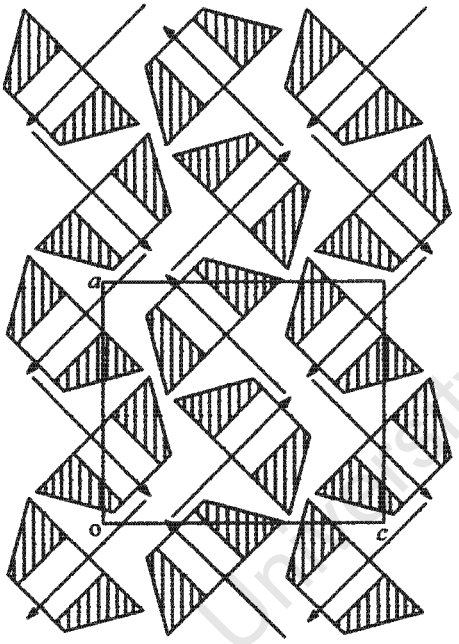

ZIGZAG

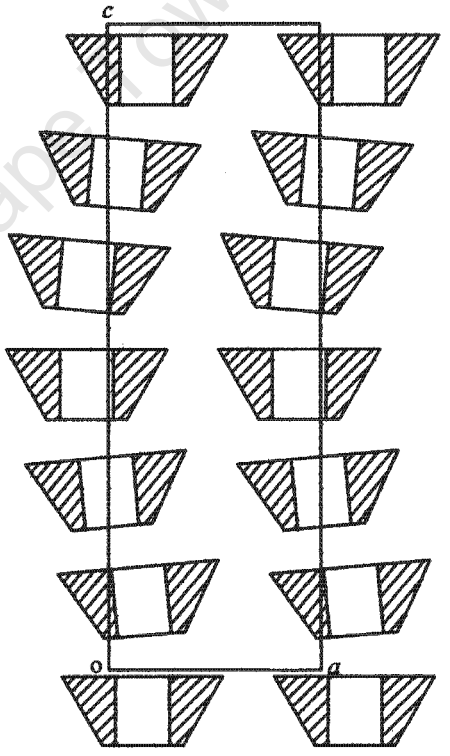

HELICAL CHANNEL

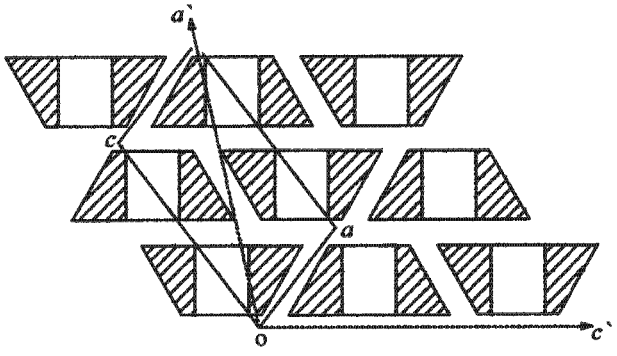

BRICKWORK

Figure 1.7 The packing arrangements of β-CD monomers[32]

Dimeric Structures [Figure 1.8]

The cyclodextrin conformation in the monomeric packing arrangements is slightly more distorted in comparison with that found in the dimeric complexes, where the macrocyclic conformation is round and symmetrical. The majority of β-CD complexes are dimeric whereby two cyclodextrin molecules form a head-to-head dimer stabilised by multiple hydrogen bonds across the secondary rim and are stacked in the crystal with their seven-fold axes appfoximately parallel.[34] A larger cavity is formed in this manner and can thus accommodate more bulky guests or more than one guest molecule. The dimers always pack in layers and four different types of dimer packing have been described, namely: channel (P1 or C2), screw channel ($P2_1$), intermediate (P1) and chessboard ($C222_1$).[24, 34] Further subdivisions of these general categories have recently been identified based on X-ray powder diffraction patterns of isostructural series.[32] According to Mentzafos *et al*[27] the packing of the dimer structures can generally be considered to consist of C-centred or pseudo-C-centred dimeric layers.

In the channel class, the dimers are aligned one above the other by lattice translation forming columns. In the screw channel class, the layers form a deformed channel located on a two-fold screw axis. In the intermediate class the layers are interrelated by a lattice translation, as in the channel type, but the intramolecular cavities of dimers belonging to adjacent layers are far from being aligned. In the chessboard class, the dimers of adjacent layers are related by a two-fold screw axis. The dimer is thus located above a space filled by solvent.

The dimers are linked together by a two-dimensional hydrogen bond network involving the water molecules and the cyclodextrin hydroxyl groups, characteristic of all four classes, and are divided into two sub-networks.[35] One is associated with the primary hydroxyl groups of the host and links the layers of the dimers via water molecules. The other is associated with the secondary hydroxyl groups of the host and therefore extends the intramolecular and intra-dimer hydrogen bond network.

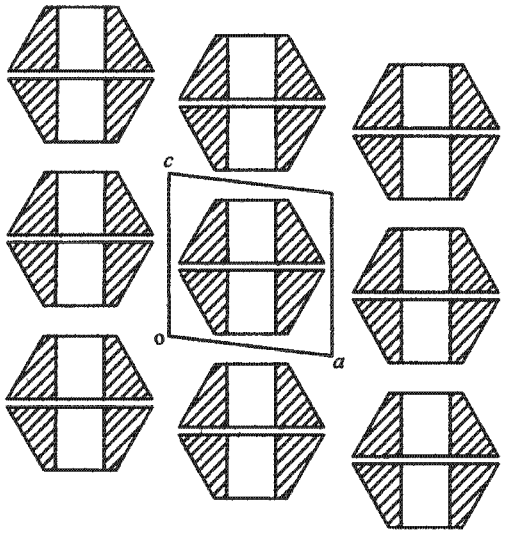

CHANNEL

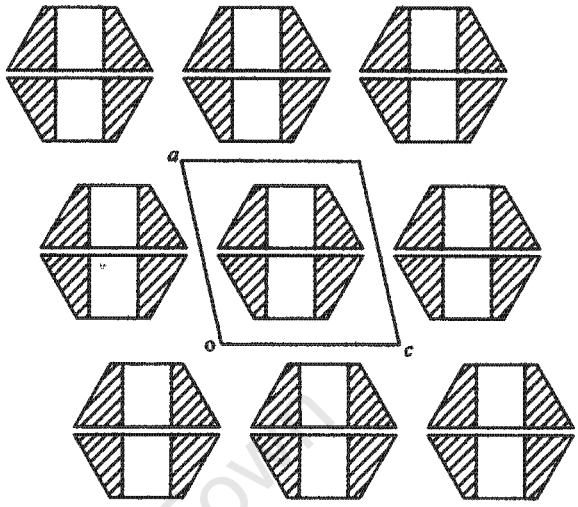

INTERMEDIATE

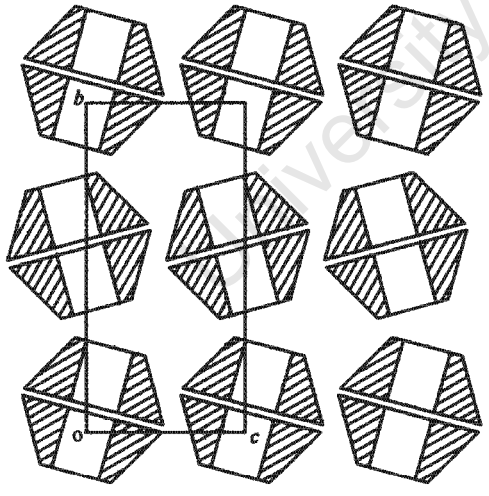

SCREW CHANNEL

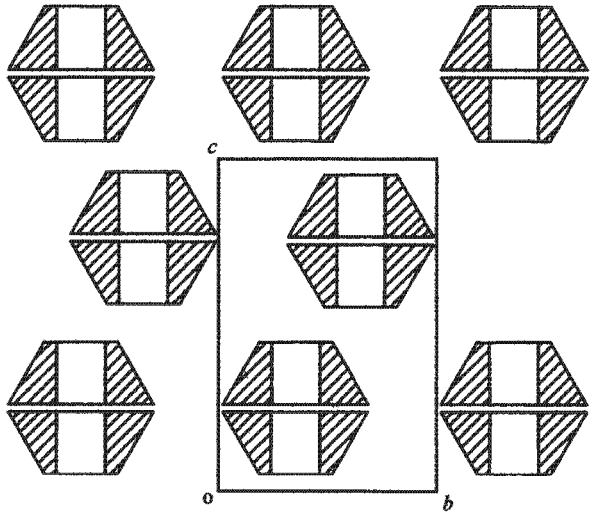

CHESSBOARD

Figure 1.8 The packing arrangements of β-CD dimers[32]

METHYLATED CYCLODEXTRINS

One of the main limitations of native cyclodextrins is their relatively low solubility, particularly in the case of β-CD.[4, 15] At 25°C the solubilites of α-, β-, and γ-CD in water are 0.1211, 0.0163, and 0.168 mol dm^{-3}, respectively.[36] Consequently, in an effort to improve the aqueous solubility while retaining and in some cases enhancing the complexing ability, chemical modification of cyclodextrins has been extensively investigated.[37-43]

The hydroxyl groups of the cyclodextrins are characterised by different reactivities and can be selectively substituted.[41] Methylation of the hydroxyl group is one of the simplest modifications and causes significant changes in some physical and chemical properties of the cyclodextrins. Geometrically, the replacement of the hydroxyl groups with methoxyl groups extends the depth of the cavity by *ca.* 2 Å, which will affect host-guest interactions. Physically, methylation causes both ends of the cavity to change from hydrophilic to hydrophobic. Chemically, methylated cyclodextrins are more soluble in water and organic solvents at room temperature than native CDs. Two methylated derivatives of β-CD, heptakis(2,6–di–O–methyl)–β–cyclodextrin and heptakis(2,3,6–tri–O–methyl)–β–cyclodextrin, commonly abbreviated as DIMEB and TRIMEB, have been proposed as drug carriers in the pharmaceutical industry, and have formed part of this study. The structures of these compounds are given in Figure 1.9. A comparison between the mean values for the geometrical parameters of β-CD, DIMEB and TRIMEB is given in Table 1.2 and these parameters were obtained from average structure values in the literature.

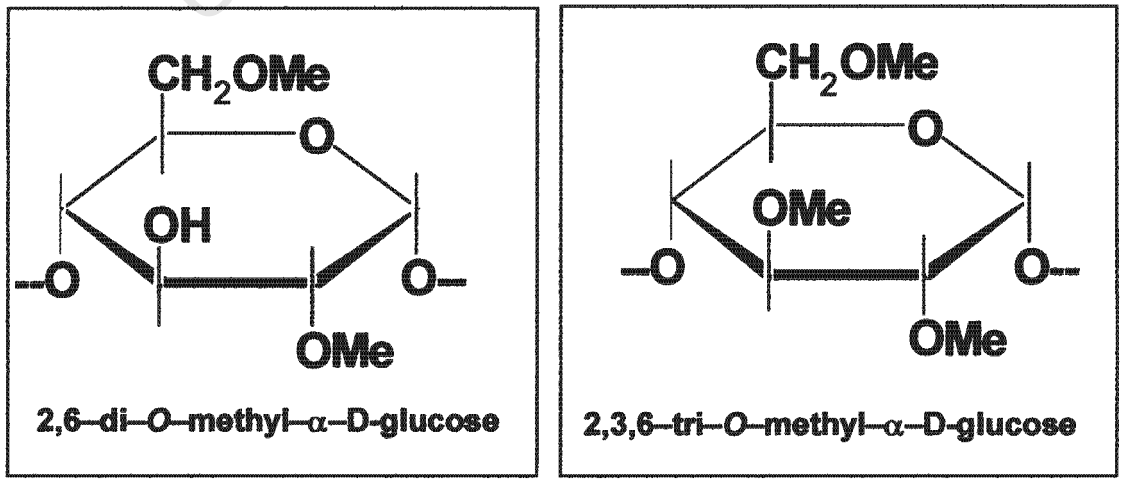

Figure 1.9 Structure of DIMEB and TRIMEB subunits

DIMEB is produced on methylation of the O(2) and O(6) hydroxyl atoms. The round structure of the macrocyclic ring is still maintained by the intramolecular O(2)•••H–O(3') hydrogen bonds.[44,45] There is less difference in the hydrophilic character of the intra- and intermolecular spaces of DIMEB than β-CD, due to the presence of the methyl groups and this enhances the inclusion ability of DIMEB. The guest can be found inside and outside the cavity,[47-49] though interaction between guests is unusual.

The macrocyclic ring of TRIMEB is produced on full methylation, which leads to marked distortion of the ring as the O(2)•••H–O(3') hydrogen bonds are absent.[2] Hence the macrocyclic ring becomes more flexible and less symmetrical. Hydrogen bonding of the weaker C(6)–H•••O(5') interaction persists [Figure 1.10]. Full methylation also leads to steric hindrance and thus the O(2), O(3) ends of the cavity are enlarged. The crystal structure of the permethylated β-CD shows that the cavity is no longer open, but is closed by "inward" rotation of O(6)–CH_3 groups so that the cavity becomes bowl shaped.[50] Although the average radius and side length of the O(4) heptagon are nearly the same as those of β-CD, the seven O(4) atoms are no longer on a plane, as indicated by the root-mean-square deviation of 0.44 Å.[51] Permethylation not only affects the macrocyclic conformation but also the pyranose conformation of the glucose residues as one of the glucose residues adopts the $^{1}C_{4}$ conformation. This is most unusual as the inverted chair conformation is less stable and has not been previously observed in CDs or their complexes in the solid state.[52]

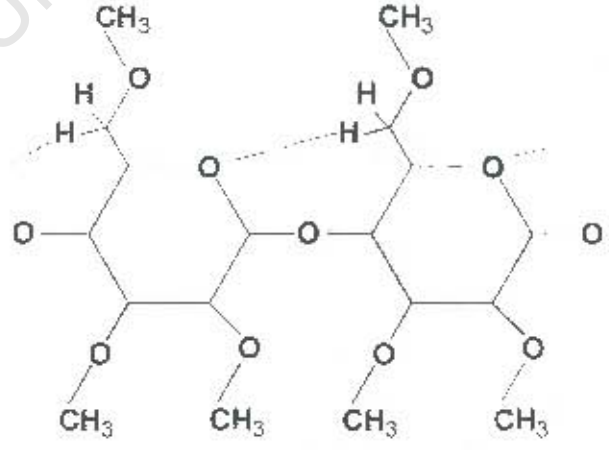

Figure 1.10 Illustrates hydrogen bonding of the type C(6)–H•••O(5') in TRIMEB

Table 1.2 Geometrical parameters describing the macrocyclic conformation

		β-CD[18, 23-24]	DIMEB[48]	TRIMEB[51]
O(4)•••O(4') distance	(l / Å)	4.3	4.3	4.5
Radius of the O(4) polygon	(r / Å)	5.0	5.0	5.0
Planarity of the O(4) polygon	(d / Å)	0.08	0.09	0.44
O(2)•••O(3') distance	(l / Å)	2.92	2.91	3.46
Glucosidic angle	(φ / °)	118	117	117

Packing arrangement within DIMEB

DIMEB and its complexes crystallise in both the monoclinic space group $P2_1$ and the orthorhombic space group $P2_12_12_1$.[33] Various packing modes are observed in DIMEB complexes. These include channel type packing with head-to-tail stacking of the host molecules, but with adjacent columns anti-parallel, modified brickwork type packing and modified herringbone type packing. A search of the Cambridge Structural Database[33] indicates that guest molecules can be either included in the cyclodextrin cavity, as with 2-naphthoic acid,[53] or can be located in the interstitial sites while the cavity is occupied by water molecules, as with *p*-iodophenol and *p*-nitrophenol.[49] There is no explanation for the guest occupying the intermolecular space instead of the cyclodextrin cavity in some of the DIMEB complexes, except that perhaps the intermolecular space has a more hydrophobic character than the intramolecular spaces of the parent cyclodextrin because of the presence of the methyl groups.[49]

Packing arrangement within TRIMEB

TRIMEB and its complexes crystallise in the space group $P2_12_12_1$.[33] Most TRIMEB crystal structures have a screw channel type packing arrangement in a head-to-tail fashion with the axis of the cyclodextrin almost parallel to the *b*-axis and adjacent columns of complex units anti-parallel. The guest molecules are never fully immersed in the TRIMEB cavity and a portion of the guest molecules protrudes from the O(2), O(3) side of the macrocycle.[54-57] However, in the case of the *m*-iodophenol TRIMEB complex,[51, 56] the axis of the TRIMEB molecule makes an angle of 26.2° with the *b*-axis, resulting in a cage type packing arrangement and one of the methylglucose residues adopts the $^4S_2$ twist conformation.

APPLICATIONS OF CYCLODEXTRINS IN THE PHARMACEUTICAL INDUSTRY

Over the past twenty years, cyclodextrins and their derivatives have received a considerable amount of interest in the pharmaceutical industry, due to their potential to form complexes with a wide variety of drug molecules. [4, 15, 58]

Complexation increases the chemical stability of pharmaceuticals that are sensitive to the environment. Encapsulation provides protection from photodegradation, hydrolysis, decomposition, oxidation and reduction, racemisation, isomerisation and it eliminates drug polymorphism. Improved stability often results in significant decreases in the degradation rate of the drug.

Pharmaceuticals which are poorly soluble in water and frequently only slightly soluble in body fluids, can be made more readily available by the formation of inclusion compounds. The increase in aqueous solubility facilitates simpler formulation and an improved uptake of the drug, resulting in better oral bioavailability. Recently there has been a great interest in the solubilisation of insulin[59] and steroid hormones[60] as well as antiviral drugs[61] by cyclodextrins for nasal application.

In addition, complexation can be used to slow down the rate of release of a drug, thus increasing the duration of effectiveness. Complexation may also be used to stabilise volatile drugs and mask unpleasant odors or tastes associated with certain drugs.

Administration of most pharmaceutically active therapeutic agents is as a solid dosage form,[62] and thus cyclodextrins can also function as an auxiliary additive, such as carriers, solubilisers, diluents or tablet ingredients.

Because of their incorporation in pharmaceutical preparations, cyclodextrins have undergone detailed investigations of their toxicity, mutagenicity, teratogenicity and carcenogenicity.[63] Native cyclodextrins are quite safe for oral administration as most of the cyclodextrins are degraded by intestinal flora in the colon, although high concentrations can cause damage to human erythrocytes.[64] The relative amounts of unmetabolised cyclodextrins that are absorbed are less than 2% for α-CD, 0.1% for γ-CD and from 1-6% for β-CD.[65] The breakdown products, glucose and short-chain oligosaccharides, are non-toxic and readily assimilated. The potential toxicity of methylglucose and other derivatives may limit the use of substituted cyclodextrins.

MOTIVATION AND OBJECTIVES OF THE STUDY

In pharmaceutical products, cyclodextrins act as drug carriers,[38] improve dissolution[66-67] and enhance absorption of drugs.[68] It is believed that the same complexation effect occurs with preservatives, which are present in pharmaceutical products.[69]

Parabens [esters of 4-hydroxybenzoic acid, Figure 1.11] are widely used as typical preservatives for cosmetics, food products and pharmaceutical formulations. Parabens are often used in combination to take advantage of synergistic effects, are active over a wide pH range, have a broad spectrum of antimicrobial activity and are most effective against yeasts and moulds.[70]

The antimicrobial activity, antiseptic action and clinical safety of parabens increase with the elongation of the alkyl moiety.[71] However, practical use of parabens with longer alkyl chains has been limited because of their low solubility in water, and so the sodium or potassium salts of the paraben are frequently used in formulation. An alternative approach to increasing their solubility is cyclodextrin complexation.[72]

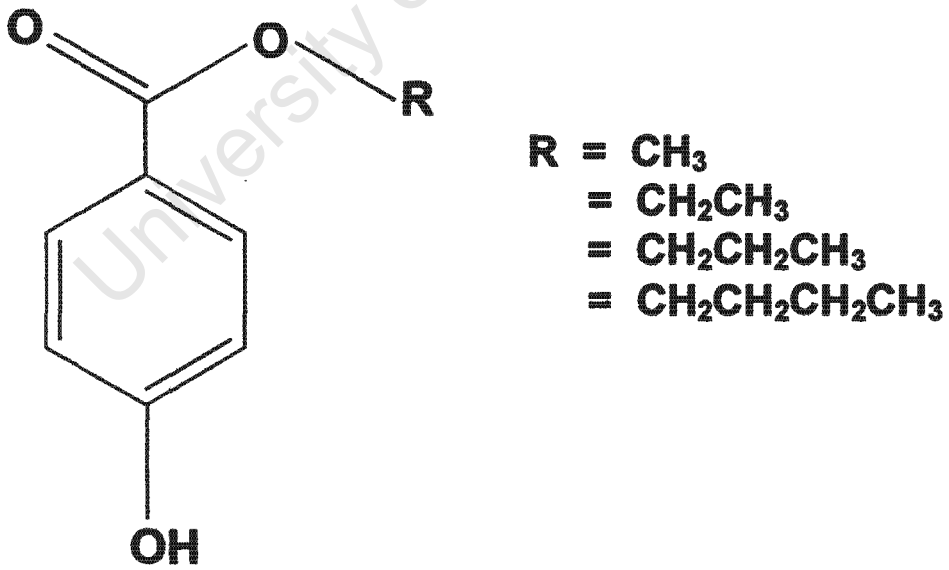

Figure 1.11 Paraben guest compounds

The solubilities of parabens in both pure water and in the presence of 2-hydroxypropyl-β-cyclodextrin [2-HP-β-CD] have been the subject of recent studies.[73-74] Matsuda *et al* [75] showed that the aqueous solubility of parabens, particularly those having long alkyl chains, was significantly improved by inclusion with 2HP-β-CD, and suggested that the higher solubilisation of 2-HP-β-CD with parabens with a longer alkyl group may be ascribed to the preferred inclusion of the hydrophobic alkyl chain.

Complexation of parabens with 2-HP-β-CD has furthermore been studied in detail by nuclear magnetic resonance. Matsuda *et al* [75] proposed that the hydrophobic alkyl chain of the paraben molecules entered the hydrophobic cavity of 2-HP-β-CD, with the phenol moiety of the preservative located at the wider secondary rim of the cavity. Chan *et al* [76] studied the interaction of *p*-hydroxybenzoic esters with β-CD using ^{1}H-NMR. The results of the ^{1}H-NMR spectral studies showed that the hydrophobic part of the paraben molecule entered the hydrophobic cavity of β-CD. The phenol moiety of the preservative was located at the wider secondary rim of the CD and in the case of propyl- and butyl paraben, the alkyl chain was allowed to orientate itself to assume a low energy conformation. Chan suggests that the extent of host-guest interaction is dependent on i) the concentration of β-CD, ii) the length of the alkyl chain which affects, iii) the spatial relationship between the host and paraben guest molecule.

AIM

The difference between the methyl-, ethyl-, propyl- and butyl parabens, used in this study, lies in the alkyl group. Hence the aim of this study was to investigate the effect of the size, shape and degree of hydrophobicity of the alkyl group on the extent of interaction with cyclodextrins and their derivatives and to assess current proposals for the mode of inclusion of alkylparabens in CDs. Another interest was to establish the role of cyclodextrins as a solubiliser and carrier for these poorly soluble drug molecules. The host cyclodextrins used in the study were β-CD, γ-CD, DIMEB and TRIMEB. The investigation mainly focussed on i) preparation, ii) determination of chemical composition, iii) analysis of thermal behaviour and iv) investigating the structure of CD guest complexes on the molecular level in solution and in the solid state. By characterising the complexes and solving the crystal structures, information about the i) thermal stability, ii) mode of drug inclusion in the CD cavity iii) nature of host-guest interaction [related to the association constant and hydrogen bonding / hydrophobic contacts] and iv) spatial distribution and structural role of water in the crystal structure could be elucidated.

REFERENCES

1) J.–M. Lehn, *Angew. Chem. Int. Ed. Engl.*, **1990**, 29, 1304.
2) J. Szejtli, *Chem. Rev.*, **1998**, 98, 1743.
3) F. Vögtle, in *Supramolecular Chemistry - an Introduction,* John Willey & Sons, New York, **1991**.
4) J. Szejtli, in *Topics in Inclusion Science - Cyclodextrin Technology,* J. E. D. Davies (ed.), Kluwer Academic Publishers, Dordrecht, The Netherlands, **1988**.
5) F. Cramer, Einschlussverbindungen (Inclusion Compounds), Spinger-Verlag, Berlin, **1954**.
6) T. Takaha, M. Yanase, S. Takata, S. Okada, S. M. Smith, *J. Biol. Chem.,* **1996**, 271, 2902.
7) A. Villiers, *Compt. Rend.,* **1891**, 112, 536.
8) F. Z. Schardinger, *Unters. Nahr. U. Genussum.,* **1903**, 6, 865.
9) K. Freudenberg, W. Rapp, *Ber. Dtsch. Chem. Ges.,* **1936**, 69, 2041.
10) K. Freudenberg, H. Boppel, M. Meyer-Delius, *Naturwissenschaften,* **1938**, 26, 123.
11) P. Karrer, *Helv. Chim. Acta,* **1921**, 4, 169.
12) A. Miekeley, *Ber. Dtsch. Chem. Ges.,* **1932**, 65, 69.
13) K. Freudenberg, G. Blomquist, L. Ewald, K. Soff, *Ber. Dtsch. Chem. Ges.,* **1936**, 69, 1258.
14) D. French, *Adv. Carbohydr. Chem.,* **1957**, 12, 189.
15) K-H. Frömming, J. Szejtli, *Topics in Inclusion Science - Cyclodextrins in Pharmacy,* (Vol. 5), Kluwer Academic Publishers, Dordrecht, The Netherlands, **1993**.
16) W. Saenger, *Angew. Chem., Int. Ed. Engl.*, **1980**, 19, 344.
17) W. Saenger, *Inclusion Compounds,* (Vol. 2), J. L. Atwood, J. E. D. Davies, D. D. MacNicol (eds.), Oxford University Press, London, **1984**, Ch 8.
18) K. Harata, *Inclusion Compounds,* (Vol. 5), J. L. Atwood, J. E. D. Davies, D. D. MacNicol (eds.), Oxford University Press, London, **1984**, Ch 9.
19) W. Saenger, C. Betzel, B. E. Hingerty, G. M. Brown, *Nature,* **1982**, 296, 581.
20) W. Saenger, C. Betzel, B. E. Hingerty, G. M. Brown, *Angew. Chem., Int. Ed. Engl.,* **1983**, 22, 883.
21) K. Harata, K. Uekama, M. Otagiri, F. Hirayama, *J. Incl. Phenom.,* **1984**, 1, 279.
22) K. Harata, *Bull. Chem. Soc. Jpn.,* **1979**, 52, 2451.
23) K. B. Lipkowitz, K. Green, J. Yang, *Chirality*, **1992**, 4, 205.
24) F. W. Lichtenthaler, S. Immel, *Liebigs Ann.,* **1996**, 27.
25) P. C. Manor, W. Saenger, *J. Am. Chem. Soc.,* **1976**, 96, 3630.
26) K. Lindner, W. Saenger, *Carbohydr. Res.,* **1982**, 99, 103.

27) D. Mentzafos, I. M. Mavridis, G. le Bas, G. Tsoucaris, *Acta Crystallogr.*, **1991**, B47, 746.
28) M. I. Bender, M. Komiyama, *Cyclodextrin Chemistry,* Springer-Verlag, Berlin, **1978**.
29) K. A. Connors, *Chem. Rev.*, **1997**, 97, 1325.
30) M. V. Rekharsky, Y. Inoue, *Chem. Rev.*, **1998**, 98, 1875.
31) W. Saenger, *Isr. J. Chem.*, **1985**, 25, 43.
32) D. R. Dodds, *PhD Thesis, Physicochemical Study of Inclusion of Drug Molecules in Cyclodextrins,* University of Cape Town, South Africa, **1999**.
33) *Cambridge Structural Database and Cambridge Structural Database System,* Version 5.23, April **2002**, Cambridge Crystallographic Data Centre, University Chemical Laboratory, Cambridge, England.
34) G. le Bas, G. Tsoucaris, *Mol. Cryst. Liq. Cryst.*, **1986**, 137, 287.
35) G. le Bas, G. Tsoucaris, *Supramol. Chem.*, **1994**, 4, 13.
36) M. J. Jozwiakowski, K. A. Connors, *Carbohydr. Res.*, **1985**, 143, 51.
37) B. Casu, M. Reggiani, G. R. Sanderson, *Carbohydr. Res.*, **1979**, 76, 59.
38) J. Szejtli, *J. Incl. Phenom.*, **1983**, 1, 135.
39) B. W. Müller, U. Brauns, *Int. J. Pharm.*, **1985**, 26, 77.
40) J. Pitha, J. Pitha, *J. Pharm. Sci.*, **1985**, 74, 987.
41) J. Szejtli, *J. Incl. Phenom.*, **1992**, 14, 25.
42) G. Wenz, *Angew. Chem., Int. Ed. Engl.*, **1994**, 33, 803.
43) D. Duchêne, *New Trends in Cyclodextrins and Derivatives,* de Santé (ed.), Paris, France, **1991**.
44) K. Harata, *Chem. Lett.*, **1986**, 2057.
45) M. Czugler, E. Eckle, J. J. Stezowski, *J. Chem. Soc., Chem. Commun.*, **1981**, 1291.
46) K. Harata, *Chem. Lett.*, **1984**, 1644.
47) K. Harata, F. Hirayama, K. Uekama, G. Tsoucaris, *Chem. Lett.*, **1988**, 1585.
48) K. Harata, *J. Chem. Soc., Chem. Commun.*, **1993**, 546.
49) K. Harata, *Bull. Chem. Soc. Jpn.*, **1988**, 61, 1939.
50) T. Steiner, W. Saenger, *Carbohydr. Res.*, **1996**, 282, 53.
51) K. Harata, *J. Chem. Soc., Chem. Commun.*, **1988**, 928.
52) M. R. Caira, V. J. Griffith, L. R. Nassimbeni, B. van Oudtshoorn, *J. Chem. Soc., Perkin Trans. 2*, **1994**, 2071.
53) K. Harata, *Chem. Commun.*, **1999**, 191.
54) K. Harata, K. Uekama, M. Otagiri, F. Hirayama, *Bull. Chem. Soc. Jpn.*, **1983**, 56, 1732.
55) K. Harata, K. Uekama, T. Imai, F. Hirayama, M. Otagiri, *J. Incl. Phenom.*, **1988**, 6, 443.

56) K. Harata, F. Hirayama, H. Arima, K. Uekama, T. Miyaji, *J. Chem. Soc., Perkin Trans. 2,* **1992**, 1159.

57) D. Mentzafos, I. M. Mavridis, H. Schenk, *Carbohydr. Res.,* **1994**, 253, 39.

58) D. Duchêne, *Cyclodextrins and Their Industrial Uses,* Editions de Santé, Paris, France, **1987**.

59) H. Arima, K. Wakamatsu, H. Aritomi, T. Irie, K. Uekama, in *Minutes of the 5th International symposium on Cyclodextrins,* O. Huber, J. Szejtli (eds.), Kluwer Academic Publishers, Dordrecht, The Netherlands, **1988**.

60) B. Pfannemüller, W. Burchard, *Macromol. Chem.,* **1969**, 121, 1.

61) W. Al-Nakib, P. G. Higgins, G. I. Barrow, D. A. J. Tyrell, K. Andries, G. V. den Bussche, N. Taylor, P. A. J. Janssen, *Antimicrob. Agents Chemother.,* **1989**, 33, 522.

62) T. Irie, M. Sunada, M. Otagiri, K. Uekama, Y. Ohtani, Y. Yamada, Y. Sugiyama, *J. Pharmacobi-Dyn.,* **1982**, 5, 741.

63) M. E. Brewster, in *New Trends in Cyclodextrins and Derivatives,* D. Duchêne (ed.), Editions de Santé, Paris, France, **1991**.

64) Y. Ohtani, T Irie, K. Uekama, K. Fukunaga, J. Pitha, *Eur. J. Biochem.*, **1989**, 186, 117.

65) G. Antlsperger, H. Reuscher, G. Schmid, Wacker-Chemie GmbH, unpublished studies, **1987-1995**.

66) P. Montassier, D. Duchêne, M. C. Poelman, *Int. J. Pharm.,* **1997**, 153, 199.

67) M. D. Veiga, P. J. Diaz, F. Ahsan, *J. Pharm. Sci.,* **1998**, 87, 891.

68) R. Iwaoku, K. Arimori, M. Nakano, K. Uekama, *Chem. Pharm. Bull.,* **1982**, 30, 4, 1416.

69) T. Loftsson, O. Stefansdottir, H. Frioriksdottir, O. Guomundsson, *Drug Dev. Ind. Pharm.,* **1992**, 18, 13, 1477.

70) A. Wade, P. J. Weller (eds.) *Handbook of Pharmaceutical Excipients,* 2nd ed., American Pharmaceutical Association, Washington DC, **1994**.

71) K. Schubel, *Münchener Med. Wochenschrift,* **1930**, 77, 13.

72) M. E. Brewster, J. W. Simpkins, M. S. Hora, W. C. Stern, *J. Parenteral Sci. Technol.,* **1989**, 43, 231.

73) C. McDonald, L. Palmer, M. Boddy, *Drug Dev. Ind. Pharm.,* **1996**, 22, 1025.

74) F. Giordano, R. Bettini, C. Donini, A. Gazzaniga, M. R. Caira, G. G. Z. Zhang, D. J. W. Grant, *J. Pharm. Sci.,* **1999**, 88, 1210.

75) H. Matsuda, K. Ito, Y. Sato, D. Yoshizawa, M. Tanaka, A. Taki, H. Sumiyoshi, T. Utsuki, F. Hirayama, K. Uekama, *Chem. Pharm. Bull.,* **1993**, 41, 8, 1448.

76) L. W. Chan, T. R. R. Kurup, A. Muthaiah, J. C. Thenmozhiyal, *Int. J. Pharm.,* **2000**, 195, 71.

Chapter 2

EXPERIMENTAL

MATERIALS

The host compounds β-cyclodextrin, γ-cyclodextrin, DIMEB and TRIMEB were obtained from Cyclolab [H-1097 Budapest, Illatos út 7, Hungary] and were used as received. The guest compounds methyl-, ethyl-, propyl- and butyl paraben were purchased from Sigma Chemical Company [St. Louis, Missouri, USA] and were used without any further purification. The D_2O [deuterium content 99.7%] was obtained from the Institute of Cryogenics and Isotope Separation [Rm. Vălcea, Romania]. The D_2O [deuterium content 99.9%] was additionally obtained from Aldrich Chemical Company, Inc, USA.

INCLUSION COMPLEX PREPARATION AND CRYSTAL GROWTH

Inclusion complexes of the host with a paraben guest molecule were obtained by the method of co-precipitation and/or kneading. Co-precipitated material was prepared with β- and γ-CD by the addition of equimolar amounts of drug to a hot, saturated aqueous solution of the cyclodextrin. Kneaded material was prepared with each of the host compounds by initially preparing a homogeneous paste of the cyclodextrin by mixing the CD in a mortar with water. To this CD paste the paraben was added and the mixture was kneaded for an hour. During this process, an appropriate quantity of water was added to the mixture in order to maintain a suitable consistency. Attempts to grow single crystals of complexes of β- and γ-cyclodextrin with the paraben drugs were conducted by adding an equimolar quantity of each paraben to a hot aqueous solution of cyclodextrin, with prolonged stirring. Crystals of these compounds were obtained by filtering the hot solution through micofilters of pore size 0.45 μm and allowing the aqueous solutions to slowly evaporate. Inclusion complexes with DIMEB and TRIMEB were prepared by dissolving the CD and guest in fixed molar ratios and concentrations at room temperature. Single crystals were prepared by filtering the solution with a 0.45 μm micofilter and placing the aqueous solutions at an elevated temperature of 50°C in an incubation oven. Further details of the preparation of individual complexes are given in the appropriate chapters.

UV SPECTROPHOTOMETRY (UV)

Since cyclodextrins are UV inactive and parabens are UV-active, UV can be used to determine the amount of drug present in a specific mass of the sample or in the CD solution. In this study UV was used to determine the CD:drug molar ratio. UV spectra were recorded on a Philips *PU8700* series UV / visible spectrophotometer over a wavelength range of 190 nm to 300 nm at a scanning rate of 200 nm / min.

MICROANALYSIS

A Fisons EA1108 CHNS-O Elemental Analyser was used to determine the amount of carbon and hydrogen that was present in the inclusion compound. Microanalysis was used to validate the H:G ratio found for each inclusion compound from the UV experiments. The samples were not dried under vacuum prior to the analysis and the water content of each sample was taken into account for each calculation. These values were then compared with the results obtained from microanalysis to see if they correlated.

THERMAL ANALYSIS

Thermal analysis is a technique which measures the changes in physical properties of a sample as a function of temperature, whilst the sample is subjected to a controlled temperature program. The three thermal analytical methods used were Hot Stage Microscopy [HSM], Thermogravimetric Analysis [TGA] and Differential Scanning Calorimetry [DSC].

HSM can be used to observe physical changes in a sample, which are often related to thermal events that can then be measured on the TGA and DSC apparatus. Mass loss, resulting from such processes as dehydration, can be measured by TGA. These reactions are usually accompanied by absorption of heat that can be detected using DSC. DSC measures the onset temperature [T_{on}] of dehydration, which is a reliable indication of the stability of a given inclusion compound. Thermal analysis can therefore be used to characterise compound purity, solvation, and degradation[1] and can also be used to detect complexation and/or polymorphism.

Both TGA and DSC experiments were performed on a Perkin-Elmer PC7-Series instrument, namely the PE TGA7 Thermogravimetric Analyser and the PE DSC7 Differential Scanning Calorimeter. The results obtained were plotted by a Hewlett Packard Colour Plotter which was connected to the thermal station. All TGA and DSC runs were performed at a heating rate of 10°C / min under dry nitrogen with a flow rate of 30 ml / min.

Hot Stage Microscopy (HSM)

Visual characterisation of the crystals was performed on a Nikon SMZ-10 stereoscopic microscope fitted with a Linkam THMS600 hot stage and Linkam TP92 temperature control unit. Images were captured using a real-time Sony Digital Hyper HAD colour video camera and analysed using the Soft Imaging System program, analySIS.[2] A heating rate of 10°C / min was used and the crystals, in most cases, were submerged in an inert medium of silicone oil to observe the evolution of gas bubbles upon dehydration. Other events such as opacity of the crystal, fusion and the onset of degradation were recorded for comparison with data for crystals of native cyclodextrins. This proved useful for preliminary identification of inclusion complexes.

Thermogravimetric Analysis (TGA)

TGA experiments measure the change in sample mass, determined by a thermobalance, as a function of temperature. Both crystalline and powder samples of weight 0.8-5 mg were analysed on the TGA, whilst being heated in an open platinum pan. Weight loss was used to determine the number of water molecules of crystallisation per host molecule for each complex.[3] Calibration of the TGA instrument was performed against the Curie points of alumel [163°C] and nickel [354°C] and the balance calibrated using a standard mass.

Differential Scanning Calorimetry (DSC)

DSC experiments measure the difference in energy inputs [i.e. the enthalpy] between the sample and the reference, in a controlled atmosphere, as a function of temperature. The crystalline sample, of weight 0.8-5 mg, was sealed in a crimped, vented aluminum pan while a sealed and empty pan was used as the reference. Endothermic and exothermic peaks appearing in the DSC traces were analysed in terms of their onset temperatures, temperature range of the peak [determined from the first derivative of the trace] and the enthalpy of the peak [measured in J/g]. DSC can therefore be used to accurately establish the melting point and the onset of other thermal events.[3] Calibration of the DSC instrument was performed by measuring the onset temperatures of the melting of indium [156.6°C] and zinc [419.5°C] while the heat flow was calibrated from the enthalpy of fusion of indium [28.62 J/g].

FOURIER TRANSFORM INFRARED SPECTROSCOPY (FTIR)

The formation of an inclusion compound is known to have an effect on the spectroscopic properties of the guest molecule.[4-5] In this study FTIR was used to determine the effect of cyclodextrin complexation on the C=O stretching frequency of the guest molecules. FTIR spectra were recorded on a Perkin-Elmer 983 FTIR spectrophotometer for pure and complexed materials. Samples were prepared by grinding the material in nujol mull® and run over the range 1000–4000 cm^{-1}. Percentage transmittance was recorded against frequency. For the cyclodextrin complexes, shifts in certain characteristic bands of the appropriate drug molecule were indicative of interaction between the cyclodextrin and drug.

SCANNING ELECTRON MICROSCOPY (SEM)

Scanning electron microscopy was carried out on a Leica Stereoscan 440I scanning electron microscope. An accelerating potential of 10 kW and a probe current of 20 pA were used. The working distance was 15 mm and scans were recorded at magnifications of 5000x and 10 000x.

X-RAY POWDER DIFFRACTION (XRD)

This is a technique whereby diffraction patterns are obtained by irradiating a powdered crystalline material with X-rays. The apparatus used was a Philips PW1050/25 vertical goniometer. Ni-filtered CuKα-radiation [λ = 1.5418 Å], generated by a Philips PW1130/90 X-ray generator was used. The generator was operated at 40 kV and 25 mA. The system was calibrated with a silicon standard which yielded a peak position 28.45 ± 0.01° 2θ before each scan. The powder samples were manually ground and packed successively in the same sample holder for reproducibility of conditions, taking care to minimise preferred orientation. A 2θ scanning range of 6.0° to 40.0° was used. X-ray powder scans were carried out in a step mode at a scan speed of 0.1° 2θ min^{-1}, step size 0.1° 2θ.

Comparisons were made between the XRD traces of complexed material and a physical mixture of host and guest in the relevant molar ratio. The appearance of new peaks and the disappearance of peaks relative to the pattern for the physical mixture is evidence in favour of the formation of an inclusion complex. This follows from the fact that the crystal packing arrangement of the inclusion complex is generally quite different from those of the components. The XRD patterns of the β-CD, γ-CD, DIMEB and TRIMEB complexes were overlaid with reference patterns to see if these complexes were isostructural with known structures.[5]

For each crystal structure determined in this study, refined unit cell parameters, space group symmetry, atomic co-ordinates and thermal parameters were used as input to the program *LAZY PULVERIX*[6] in order to generate an idealised X-ray powder pattern. Calculated powder patterns can also be used to conveniently assess the purity of a sample and were compared with the corresponding experimental patterns to prove that the crystallographic model is correct.

NUCLEAR MAGNETIC RESONANCE SPECTROSCOPY (NMR)

NMR parameters such as chemical shift, spin coupling and relaxation time are sensitive to short-range intermolecular interactions[7-10] and ever since Demarco and Thakkar[11] presented direct evidence of complexation of β-CD with aromatic guest molecules in aqueous solution, NMR spectroscopy has become more widely used for studies of CD inclusion phenomena.

^{1}H chemical shift changes of the CD protons within the cavity, namely the H3, H5 and to a lesser extent the H6, are generally accepted to be evidence of the formation of an inclusion complex in solution. In addition shifts of the guest protons can also be observed upon complexation and subsequently an advantage of NMR spectroscopy is that both the host and guest components can be observed simultaneously. Difficulties may be encountered, however, when there is overlap of the host and guest signals. These changes in chemical shift allow for the determination of the stoichiometry and association constant of the complex.

The continuous variation [Job's] method[12] has been used extensively to establish the H:G stoichiometry in solution. This method involves preparing a series of solutions containing both the host and the guest in varying proportions so that a complete range of the mole ratios, r, is sampled and where the total concentration $[H]_t + [G]_t$ is constant for each solution. The experimentally observed parameter is a host or guest chemical shift that is sensitive to complex formation. The data are plotted in the form $\Delta\delta_{obs}$ [X] versus r, where $\Delta\delta_{obs}$ is the measured change in chemical shift referenced to that of the uncomplexed species and r, the mole fraction of the host / guest in equilibrium mixture. The position of the maximum indicates the stoichiometry of the complex in solution. It is worth mentioning that the stoichiometry in solution may, however, not be the same as that in the solid state.[13-18]

Once the stoichiometry of the complex has been ascertained the change in chemical shift of the host and/or guest proton/s can be used to estimate the association constant. The determination of the association constant, K, of a complex usually contains some approximations. The most commonly used methods for the determination of K were the methods due to Scatchard[19], Benesi and Hildebrand[20] and Scott.[21] They each require a graphical representation of the experimental parameters and the global consideration of $[H]_t >> [G]_t$. The latter requirement is not always either possible or mathematically correct. Experimentally, $\Delta\delta_i$ is determined for each of the studied protons and, consequently, the use of the corresponding expression for K yields a different K value for each one of the studied protons.[22] Additionally, if $[G]_t$ is very small the difficulty in determining the chemical shift for a signal increases with its complexity [coupling]. And finally, the standard range of work only permits H:G ratios no larger than 9/1, a ratio which cannot mathematically be considered as satisfying the condition $[H]_t >> [G]_t$. This limitation led to the production of new methods and new programs, such as CALCK,[22] MULTIFIT,[23-24] EMUL[24-25] to determine K. The determination of the association constant for a 1:1 complex, is based on the consideration of the general equations:

$$G + H \overset{K}{\rightleftharpoons} H{:}G \qquad (1)$$

$$K = \frac{[H{:}G]}{[H][G]} \qquad (2)$$

We define f_o and f_1 as the fractions of the host or guest in the free and bound states respectively and hence $f_o + f_1 = 1$. The equations below are related to the guest where $[G]_t = [G] + [H:G]$ (i.e. the total concentration of the guest) and could alternatively be expressed in terms of the host.

$$f_o = \frac{[G]}{[G]_t} = \frac{[G]}{[G]+[H:G]} = \frac{[G]}{[G]+K[H][G]} = \frac{1}{1+K[H]} \quad (3)$$

$$f_1 = \frac{[H:G]}{[G]_t} = \frac{K\cdot[H]\cdot[G]}{[G]+[H:G]} = \frac{K[H]\cdot[G]}{[G]+K[H][G]} = \frac{K[H]}{1+K[H]} \quad (4)$$

The chemical shift parameter is usually a weighted average of all the species present; in consequence when the complex is in fast equilibrium with the isolated molecules, the experimental δ_{obs} corresponds to the intermediate situation and can be expressed by the weighted average between the unbound / isolated (f_o) and the bound / complexed (f_1) chemical shifts. The observed chemical shift can therefore be expressed as the following, if the observed proton is located on the guest:

$$\delta = f_o\delta_G + f_1\delta_{H:G} \quad (5)$$

$$\delta - \delta_G = f_1(\delta_{H:G} - \delta_G) \quad (6)$$

$$\Delta\delta_{obs} = f_1\Delta\delta_c \quad (7)$$

$$\Delta\delta_{obs} = \frac{K[H]}{1+K[H]}\cdot\Delta\delta_c \quad (8)$$

$$\frac{1}{\Delta\delta_{obs}} = \frac{1}{K\cdot\Delta\delta_c[H]_t} + \frac{1}{\Delta\delta_c} \quad (9)$$

Equation (9) is the Benesi-Hildebrand equation, where $[H] \cong [H]_t$ and $[H]_t = [H] + [H:G]$ i.e. the total concentration of the host. Equation (13) can be obtained by substituting Equations (12) into Equation (8) and can be further developed into a second order equation whose solution is Equation (18), where [X] is the concentration of the host or guest of a sample and $M = [G]_t + [H]_t$.

$$f_1 = \frac{[H:G]}{[G]_t} \quad (4)$$

$$[H:G] = \frac{\Delta\delta_{obs} \cdot [G]_t}{\Delta\delta_c} \quad (10)$$

$$[H]_t = [H] + [H:G] \quad (11)$$

$$[H] = [H]_t - \frac{\Delta\delta_{obs} \cdot [G]_t}{\Delta\delta_c} \quad (12)$$

$$\Delta\delta_{obs} = \frac{K\,(\Delta\delta_c\,[H]_t - \Delta\delta_{obs}[G]_t)}{\Delta\delta_c + K\,(\Delta\delta_c[H]_t - \Delta\delta_{obs}[G]_t)}\,\Delta\delta_c \quad (13)$$

$$\Delta\delta_{obs}\Delta\delta_c + K\Delta\delta_{obs}(\Delta\delta_c\,[H]_t - \Delta\delta_{obs}\,[G]_t) = K\Delta\delta_c(\Delta\delta_c\,[H]_t - \Delta\delta_{obs}\,[G]_t) \quad (14)$$

$$K\Delta\delta_{obs}^2\,[G]_t - \Delta\delta_{obs}(K\Delta\delta_c\,[G]_t + K\Delta\delta_c\,[H]_t + \Delta\delta_c) + K\Delta\delta_c^2\,[H]_t = 0 \quad (15)$$

$$K\Delta\delta_{obs}^2\,[G]_t - K\Delta\delta_{obs}\Delta\delta_c\,([G]_t + [H]_t + {}^1/_K) + K\Delta\delta_c^2\,[H]_t = 0 \quad (16)$$

$$\Delta\delta_{obs} = \left[K\Delta\delta_c\,([G]_t + [H]_t + {}^1/_K) \pm \left\{([G]_t + [H]_t + {}^1/_K)^2K^2\Delta\delta_c{}^2 - 4[G]_t[H]_tK^2\,\Delta\delta_c{}^2\right\}^{1/2}\right] \div 2K[G]_t \quad (17)$$

$$\Delta\delta_{obs}^{[X]} = \frac{\Delta\delta_c^{[X]}}{2[X]}\left[M + {}^1/_K - \left\{(M + {}^1/_K)^2 - 4[G]_t[H]_t\right\}^{1/2}\right] \quad (18)$$

Only the negative square root solution is to be considered because the ratio $\Delta\delta_{obs}$ / $\Delta\delta_C$ is always smaller than 1. Equation (18) must be satisfied for each sample studied, i.e., we have a set of n equations [as many as there are samples] with two independent variables ($\Delta\delta_C$ and K) which can be solved using the experimental $\Delta\delta_{obs}$ values as reference values.

Apparatus

Proton NMR experiments were performed at 300 MHz with a Varian-Gemini 300 spectrometer. The ^1H NMR spectra were recorded in D_2O solution at 298 ± 0.5 K. Typical conditions were as follows: 32 K data points, sweep width 4500 Hz giving a digital resolution of 0.28 Hz / point. The pulse width was 13 μs (90°) and the spectra were collected by co-addition of 32 or 64 scans. Homonuclear Overhauser effect [NOE] difference experiments were performed at 300 MHz with a Varian-Mercury 300 spectrometer with a three-second mixing time.

Continuous variation method

In order to determine the stoichiometry of the β-CD complexes, the paraben under investigation and β-CD were prepared in D_2O as two individual equimolar stock solutions. The concentration of the stock solution was determined by the solubility of each paraben in water [Table 2.1]. The equimolar stock solutions of the host and guest were mixed to a constant volume (1.5 ml) at varying proportions, so that a complete range ($0 < r < 1$) of ratios $r = [X] / ([H]_t + [G]_t)$ was sampled. This maintained the total concentration of each sample solution constant. In the preceding equation [X] is equivalent to the concentration of the host or of guest for the sample and $[H]_t$ and $[G]_t$ are the total concentrations of the host (β-CD) and guest (paraben), respectively. From the NMR data the quantity $\Delta\delta_{obs}$ [X] was obtained by subtracting the observed shift value for a given sample from the chemical shift of the free X. $\Delta\delta_{obs}$ [X] was then plotted against r and the maximum of the curve corresponded to the stoichiometry.

Table 2.1 Solubility and concentration of the stock solutions

	Solubility (Mmol)[26]	Concentration of the stock solutions (mM)
Methyl paraben	16.1	10.0
Ethyl paraben	5.6	5.0
Propyl paraben	2.2	1.5
Butyl paraben	1.1	0.7

Determination of the association constant

The same set of samples that was used for the determination of the stoichiometry, was used in the determination of the association constant. Once the stoichiometry had been determined as 1:1, the association constant was calculated using a C[11] program.[27] This program evaluates the data by a non-linear least squares regression analysis of the observed chemical shift changes of the guest and β-CD NMR lines, as a function of β-CD concentration, according to Equation (18). This equation involves no approximations and correlates the total concentration of the host and guest molecules with the observed difference in chemical shift, $\Delta\delta_{obs}$.

The program is based on an iteration procedure following specific algorithms in order to fit the experimental values of $\Delta\delta_{obs}$ to the appropriate equation. Each iteration sets up a quadratic program to determine the direction of the search and the loss function E, defined as the sum of the squared deviation about the predicted values, until the search converges [Equation (19), where "i" counts the sample number and "j" the studied proton which can belong to the guest or host molecule]. The fitting procedure reaches an end when the difference between two consecutive E values is smaller than 10^{-6}.

$$E = \sum_i \sum_j \left(\Delta\delta^{ij}_{obs} - \Delta\delta^{ij}_{c} \right)^2 \qquad (19)$$

The treatment of the whole set of protons studied yields one single K value for the whole process and a set of calculated $\Delta\delta_C$ values. $\Delta\delta_C$ represents the chemical shift difference [for a given proton] between the free molecule and the pure complex.[28] The program is quite flexible as both the host and the guest can be observed for spectroscopic perturbations as a function of variable host and guest concentrations.[29] However it can only be used for 1:1 host-guest stoichiometries.

CRYSTAL STRUCTURE DETERMINATION

Single crystals were obtained from β-CD and methyl paraben [MPBCD, MPBCDP1], β-CD and propyl paraben [PPBCD], from DIMEB with each paraben [MPDMB, EPDMB, PPDMB, BPDMB] and from TRIMEB with each paraben [MPTMB, EPTMB, PPTMB, BPTMB]. In each case single crystals of suitable quality [typically between 0.2 and 0.5 mm in all dimensions] were selected for their ability to uniformly extinguish plane-polarised light. Crystals were mounted on a glass fiber and coated with Paratone N oil,[30] which was necessary to prevent decomposition owing to dehydration and to provide a rigid mount in the instance of low-temperature data collection. The glass fiber was then mounted on a goniometer head.

Photography

The preliminary cell dimensions and crystal systems were obtained by using X-ray photography. Oscillation and Weissenberg photographs were both taken on a Stoë goniometer with a film radius of 28.65 mm. Photography was performed using Nickel-filtered CuKα radiation [λ = 1.5418 Å]. The X-ray generator was operated at 20 mA and 40 kV.

Oscillation

When the crystal was mounted on the goniometer head it was done so that one of the crystallographic axes would be orientated parallel to the axis of rotation [which was orthogonal to the X-ray beam]. The reflections were recorded on film placed in a cylindrical cassette which surrounded the crystal. From the oscillation photography it was possible to align the crystal. This enabled the determination of the unit cell dimension that was parallel to the oscillation axis, as well as being a necessary requirement before a Weissenberg photograph could be taken.

Weissenberg

Weissenberg photography allows a one-dimensional layer line in the oscillation photograph to be expanded into two dimensions.[31] This was achieved by simultaneously rotating the crystal and moving the X-ray film. A screen was used to ensure that only those diffraction spots corresponding to the selected layer line reach the film.

The film was moved parallel to the oscillation axis so that the diffraction pattern from the chosen layer line was spread over the entire film. The resulting photograph appeared as a distorted image of the selected reciprocal lattice plane. This photograph was placed on a transparent Weissenberg co-ordinate chart, from which the co-ordinates of each point were located and plotted onto graph paper to give a representation of the reciprocal lattice. From this plot a reasonable estimate of the remaining two cell dimensions, as well as one of the angles could be determined. Additionally the Laue symmetry could be inspected leading to the establishment of the crystal system and space group.

Diffractometry

This technique uses the diffraction of X-rays from a single crystal to determine the accurate unit cell parameters and intensities of the X-ray reflections. The reflection intensity data were measured on a Nonius Kappa CCD Single Crystal X-ray Diffractometer, using graphite-monochromated MoK_α radiation [λ = 0.71069 Å] generated by an Nonius FR590 generator operated at 50 kV and 30 mA. Data were measured at 173 K for all the crystal structures, except where indicated otherwise. The reduced temperature of 173 K was maintained by a constant stream of N_2 gas with a flow rate of 20 cm^3 / min produced by a Cryostream cooler [Oxford Cryosystems]. Data were corrected for Lorentz-polarisation effects and cell refinement and data reduction were performed using the programs *DENZO* and *SCALEPACK*.[32] The space group was determined by examining the systematic absences and matching the observed conditions to a known space group.[33] Assignment of the correct space group was confirmed using the Xprep program.[34]

CRYSTAL STRUCTURE SOLUTION AND REFINEMENT

The structures were solved either by the optimisation of the orientation and position of a molecular fragment with the program *PATSEE*[35-36] or by isomorphous replacement, using the published co-ordinates for the non-hydrogen atoms of cyclodextrins from an isomorphous structure. The refinement was performed using *SHELXL*-97[37] which employs full-matrix least-squares refinement on F^2 and was operated through the X-Seed interface.[38]

In all cases, several low angle reflections were omitted from the final refinement because of their abnormally low measured intensities caused by beam-stop truncation. Further details of specific structure solutions and refinements are discussed under individual structures in the relevant chapters.

PATSEE

PATSEE attempts to position a fragment of known geometry in a unit cell by integrating the merits of Patterson, packing and direct methods. The reflection data are processed with *SHELXS*[39] using the *PSEE* command to calculate the sharpened Patterson map and a set of the largest E-values. A fragment search is then performed with *PATSEE*, the procedure being a rotational search followed by a translation search.

The orientation of the search model is determined by a conventional but highly automated real-space Patterson rotation search. A comparison between the weights of a number of vectors (n) produced by the orientations of the search model (w_i) and the closest matching Patterson map vectors (P_i) is used to calculate rotational figures of merit (RFOMs), Equation (20).

The translation positions of a set of the fragments with the highest RFOM values is located by maximising the weighted sum of cosines of a small number of strong translation-sensitive triple-phase invariants, Equation (21).

For the solutions obtained, the correlation between the Patterson function and the intermolecular vector set is used to determine a translation figure of merit (TFOM), Equation (22), in an analogous manner to that for CFOM. An R-index (R_E), Equation (23), based on E magnitudes is computed for sets of solutions with the best TFOM values.

The best solutions are sorted according to a combined figure of merit (CFOM), Equation (24), based upon agreement with the Patterson function (TFOM), triple-phase consistency (TPRSUM) and the R-index involving E_{obs} and E_{calc} (R_E). *PATSEE* produces a list of the best solutions found for the fragment. The fractional co-ordinate sets of these positions can then be chosen for partial structure expansion in *SHELXS*. If the partial structure expansion is successful, atomic co-ordinates can be input for refinement.

$$RFOM = [\Sigma P_i / w_i] / n \quad (20)$$

$$TPRSUM = [\Sigma E_h E_k E_{-h-k} \cos (\varphi_h + \varphi_k + \varphi_{-h-k})] / [\Sigma E_h E_k E_{-h-k}] \quad (21)$$

$$TFOM = [\Sigma P_i / w_i] / n \quad (22)$$

$$R_E = [\Sigma \{ |E_{obs}| - |E_{calc}| / p \}] / \Sigma |E_{obs}| \quad (23)$$

$$CFOM = [0.2 \times \{ (RFOM + TFOM) / 2 \} + \times TPRSUM^{\frac{1}{2}}] / R_E \quad (24)$$

SHELXL-97

Refinement in *SHELXL-97* involves minimisation of the function $\Sigma w (F_o^2 - F_c^2)^2$ using the full-matrix least squares technique. The agreement between the observed (F_o) and calculated (F_c) structure factor is expressed by the residual index (R_1), Equation (25), which should be low for a satisfactory model. Refinement against F^2 tends to magnify the deviations of the Goodness of Fit, S, from unity compared with refinement against F and therefore these values are not directly comparable to structures refined against F.

The weighting scheme (*w*) in Equation (26) and the parameters a and b were refined for each structure using Equations (27) and (28) below. The terms a and b are chosen in the above weighting scheme to yield constant distributions of $[w (F_o^2 - F_c^2)^2]$ with $\sin\theta$ and $(F_o / F_{max})^{\frac{1}{2}}$. S is defined by Equation (29), where n is the number of reflections and p is the total number of parameters refined. For a well-behaved structure S should be close to unity, and the over-determination should be of the order n / p = 10.

$$R_1 = [\Sigma | \, |F_o| - |F_c| \, |] / \Sigma |F_o| \quad (25)$$

$$wR_2 = \{ [\Sigma w (F_o^2 - F_c^2)^2] / [\Sigma w (F_o^2)^2] \}^{1/2} \quad (26)$$

$$w = 1 / [\sigma^2 (F_o^2) + (aP)^2 + bP] \quad (27)$$

$$P = [\max (0, F_o^2) + 2 F_c^2] / 3 \quad (28)$$

$$S = [\Sigma [w (F_o^2 - F_c^2)^2] / (n - p)]^{\frac{1}{2}} \quad (29)$$

ADDITIONAL RESOURCES

The Cambridge Structural Database [CSD][40] was used to investigate published crystal data for comparison with structures reported in this study. Molecular parameters and geometrical data with their associated e.s.d.s and non-bonding distances were calculated using the program *PARST95*.[41] Molecular diagrams were created through POV-Ray for Windows,[42] while molecular packing diagrams were produced with the program *PLUTO*.[43] CPK diagrams were constructed using the program WebLab ViewerPro Version 3.5.[44] Slices through the unit cell were viewed using the Section program in X-Seed.[38]

Final atomic co-ordinates, temperature factors, bond angles, bond lengths, torsion angles and structure factor tables for the each of the solved structures have been recorded under the abbreviation of the complex in the file named Appendix C on a compact disk, attached to the inside back cover of the thesis. The files have been saved as text files and can be opened in a text editor such as WORDPAD in Windows95 and Windows98. The file extension and file contents are listed in the table below.

Table 2.2 File types found in the Appendix

EXTENSION	CONTENTS
.HKL	Reflection data
.RES .CIF	SHELX type co-ordinate file Crystallographic information file
.SFT .FCF	Structure factor tables
.TEX	atomic co-ordinates bond lengths bond angles torsion angles displacement parameters
.LST	atomic co-ordinates bond lengths bond angles torsion angles displacement parameters geometry between non-bonded atoms intermolecular and inter-atomic contacts

REFERENCES

1) D. Giron, *Thermochim. Acta*, **1965**, 248, 1.
2) Soft Imaging System GmbH, *Digital Solutions for Imagining and Microscopy*, Version 3.1 for Windows (Copyright **1987 - 2000**).
3) M. E. Brown, *Introduction to Thermal Analysis: Techniques and Applications*, Chapman and Hall, London, New York **1988**, p. 1-39.
4) K-H. Frömming, J. Szejtli, *Topics in Inclusion Science - Cyclodextrins in Pharmacy*, (Vol. 5), Kluwer Academic Publishers, Dordrecht, The Netherlands, **1993**.
5) M. R. Caira, *Roum. Chim. Rev.*, **2001**, 46. 4, 371.
6) K. Yvon, W. Jeitschko, E. Parthe, *J. Appl. Crystallogr.*, **1977**, 10, 73.
7) Y. Inoue, *JEOL NEWS*, **1987**, 23A, 36.
8) Y. Yamamoto, Y. Inoue, *J. Carbohyr. Chem.*, **1989**, 8, 29.
9) D. J. Wood, F. E. Hruska, W. Saenger, *J. Am. Chem. Soc.*, **1977**, 99, 1735.
10) Y. Ymmoto, Y. Kanda, Y. Inoue, R. Chûjô, S. Kobayashi, *Chem. Lett.*, **1988**, 495.
11) P. V. Demarco, A. L. Thakkar, *J. Chem. Soc., Chem. Commun.*, **1970**, 2.
12) P. Job, *Ann. Chim. Phys.*, **1928**, 9, 113.
13) K. Harata, *Bull. Chem. Soc. Jpn.*, **1976**, 49, 1493.
14) Y. Yamamoto, M. Onda, M. Kitagawa, Y. Inoue, R. Chujo, *Carbohyr. Res.*, **1987**, 167, C11.
15) R. L. Gelb, L. M. Schwartz, B. Cardelino, H. S. Fuhrman, R. F. Johnson, D. A. Laufer, *J. Am. Chem. Soc.*, **1981**, 103, 1750.
16) M. Sakurai, M. Kitagawa, H. Hoshi, Y. Inoue, R. Chujo, *Bull. Chem. Soc. Jpn.*, **1989**, 62, 2067.
17) K. Harata, H. Uedaira, J. Tanaka, *Bull. Chem. Soc. Jpn.*, **1978**, 51, 1627.
18) Y. Inoue, T. Okuda, R. Chujo, *Carbohyr. Res.*, **1985**, 141, 179.
19) G. Scatchard, *Ann. N. Y. Acad. Sci.*, **1949**, 51, 660.
20) H. A. Benesi, J. H. Hildebrand, *J. Am. Chem. Soc.*, **1949**, 71, 2703.

21) R. L. Scott, *Recl. Trav. Chim. Pays-Bas.*, **1956**, 75, 787.

22) D. Salvatierra, C. Diez, C. Jaime, *J. Incl. Phenom.*, **1997**, 27, 215.

23) M. A. Petti, T. J. Shepodd, R. E. Jr. Barrans, D. A. Dougherty, *J. Am. Chem. Soc.*, **1988**, 110, 6825.

24) R. E. Jr. Barrans, D. A. Dougherty, *Supramol. Chem.*, **1994**, 4, 121.

25) P. C. Kearney, L. S. Mizoue, R. A. Kumpf, J. E. Forman, A. McCurdy, D. A. Dougherty, *J. Am. Chem. Soc.*, **1993**, 115, 9907.

26) F. Giordano, R. Bettini, C. Donini, A. Gazzaniga, M. R. Caira, G. G. Z. Zhang, D. J. W. Grant, *J. Pharm. Sci.*, **1999**, 88, 11, 1210.

27) D. Mosich, N. Shammas, B. Flamig, *Advanced TurboC Programmer's Guide*, **1988**, John Wiley & Sons.

28) L. Fielding, *Tetrahedron*, **2000**, 56, 6151.

29) M. Bogdan, M. R. Caira, S. I. Farcas, *Supramol. Chem.*, **2002**, 14, 5, 427.

30) Paratone N oil (Exxon Chemical Co., TX, USA).

31) G. H. Stout, L. H. Jensen, *X-ray Structure Determination: a Practical Guide*, Macmillan Company, New York, **1968**, p. 83-109.

32) Z. Otwinowski, W. Minor, *Processing of X-ray Diffraction Data in Oscillation Mode in Methods in Enzymology*, (Vol. 276), C. W. Carter, R. M. Sweet (eds.), Academic Press, New York, **1996**, p. 307.

33) *International Tables for Crystallography*, Vol. C: Mathematical, Physical and Chemical Tables, A. J. C. Wilson (ed.), Kluwer Academic Publishers, Dordrecht, **1992**, p. 691-778.

34) *Data Preparation and Reciprocal Space Exploration*, Version 5.1, (Copyright Bruker Analytical X-ray Systems, **1997**).

35) E. Egert, *Acta Crystallogr.*, **1983**, A39, 936.

36) E. Egert, G. M. Sheldrick, *Acta Crystallogr.*, **1985**, A41, 262.

37) G. M. Sheldrick, *SHELXL-97, Program for the Refinement of Crystal Structures*, University of Göttingen, Germany, **1997**.

38) L. J. Barbour, *X-Seed, A Software Tool for Supramolecular Crystallography*, *Supramol. Chem.*, **2001**, 1, 189.

39) G. M. Sheldrick, *Crystallographic Computing*, (Vol. 3) G. M. Sheldrick, C. Krüger, R. Goddard (eds.), Oxford University Press, London, **1985**, p. 175.

40) *Cambridge Structural Database and Cambridge Structural Database System*, Version 5.23, April **2002**, Cambridge Crystallographic Data Centre, University Chemical Laboratory, Cambridge, England.

41) M. Nardelli, *J. Appl. Cryst.*, **1995**, 28, 659.

42) Pov-Ray for Windows, v. 3.1e.watcom.win32, The Persistence of Vision Development Team, © **1991-1999**, (www.povray.org).

43) W. D. S. Motherwell, *PLUTO89, Program for Plotting Molecular and Crystal Structures*, University of Cambridge, England, **1989**.

44) *WebLab ViewerPro Version 3.5* (Copyright **1999** by Molecular Simulations Inc., San Diego, CA).

Chapter 3

γ-CD INCLUSION COMPLEXES

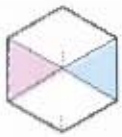

COMPLEX PREPARATION

Crystalline complexes of γ-CD with each paraben were prepared by mixing equimolar amounts of CD and drug in a hot aqueous solution [45°C]. The solution was then filtered and allowed to undergo slow cooling and slow evaporation. Crystalline powdered material was obtained on standing for a period of one to two weeks. The complexes of γ-CD with methyl-, ethyl-, propyl- and butyl paraben will be referred to as MPGCD, EPGCD, PPGCD and BPGCD respectively.

UV SPECTROPHOTOMETRY (UV)

Since cyclodextrins are UV inactive, UV spectrophotometry was used to determine the host to guest ratio for the γ-CD complexes. Each of the MPGCD, EPGCD, PPGCD and BPGCD complexes contains 1:2 stoichiometric amounts of host to guest. The total water content of the sample to be analysed was calculated from the initial mass losses obtained from thermogravimetric analysis and the results are reported in Table 3.1.

Table 3.1 UV spectrophotometry results for the γ-CD complexes

COMPLEX	H:G RATIO
MPGCD • 16.2 H_2O	1 : 2
EPGCD • 16.8 H_2O	1 : 2
PPGCD • 15.7 H_2O	1 : 2
BPGCD • 12.6 H_2O	1 : 2

THERMAL ANALYSIS

DSC results of the γ-CD complexes and physical mixtures of their components

The DSC traces of the MPGCD, EPGCD, PPGCD and BPGCD complexes are shown in Figure 3.1 together with the traces of the appropriate uncomplexed drug and the 1:1 γ-CD to drug physical mixture. The characteristic melting endotherms for methyl-, ethyl-, propyl-, and butyl paraben are 126, 116, 96 and 69°C respectively. These fusion endotherms are clearly visible in the DSC traces of the uncomplexed drug and physical mixtures of these drugs with γ-CD.

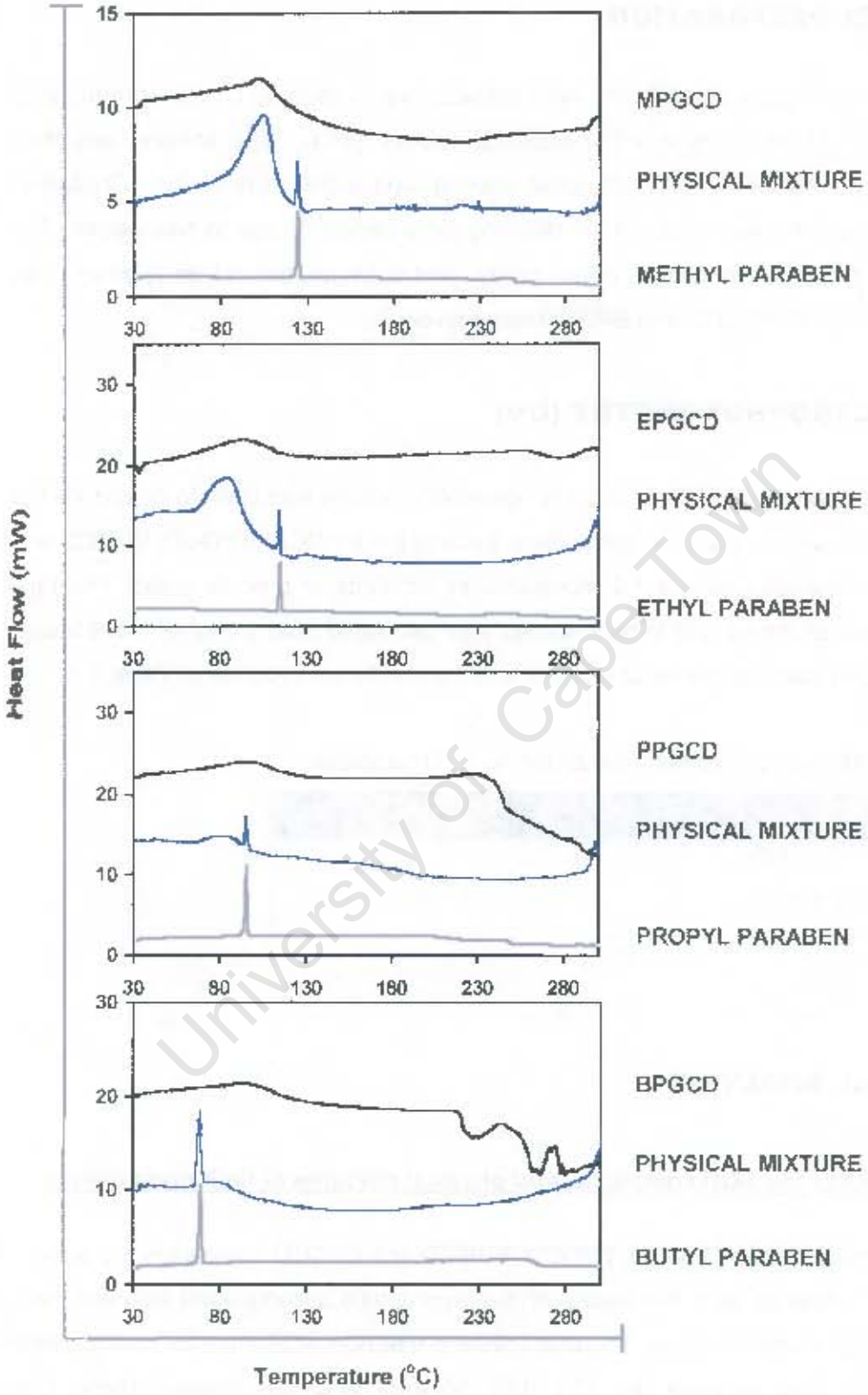

Figure 3.1 DSC traces of the γ-CD paraben complexes, 1:1 physical mixtures and uncomplexed paraben drugs

In all cases the disappearance of the pure drug fusion endotherm was observed in the DSC traces of the complexes, indicating that an inclusion complex has been formed in the solid state. Individual drug molecules are separated from one another and contained within the cavities of the cyclodextrin molecules and therefore will no longer exhibit the characteristics of their original crystalline phase.

TGA results for the γ-CD complexes

The TGA results for the MPGCD, EPGCD, PPGCD and BPGCD complexes are shown in Figure 3.2 (a), (b), (c) and (d) respectively. A summary of the observed percentage weight losses is presented in Table 3.2. Weight losses from 30 to 160°C represent water loss from the complexes. From 160 to 200°C a small weight loss is observed, indicating initial decomposition. From 200°C onwards weight losses due to chemical decomposition are observed.

Table 3.2 The percentage weight losses for the γ-CD complexes

Temp (°C)	MPGCD		EPGCD		PPGCD		BPGCD	
	Sample weight (%)	Δ Weight loss (%) *	Sample weight (%)	Δ Weight loss (%) *	Sample weight (%)	Δ Weight loss (%) *	Sample weight (%)	Δ Weight loss (%) *
30	100	-	100	-	100	-	100	-
160	83.2	16.8	82.9	17.1	83.9	16.1	86.8	13.2
170	83.1	0.1	82.7	0.2	83.8	0.1	86.6	0.2
180	83.1	0.0	82.4	0.3	83.6	0.2	86.5	0.1
190	83.0	0.1	82.3	0.1	83.2	0.4	86.1	0.4
200	83.0	0.0	82.0	0.4	82.7	0.9	85.6	0.9
220	82.8	0.2	81.4	0.6	81.6	1.1	83.8	2.0
260	82.3	0.5	79.2	2.2	78.7	2.9	79.4	4.4
300	80.9	1.4	75.4	3.8	74.5	4.2	74.3	5.1
350	18.5	62.4	13.7	61.7	13.2	61.3	25.2	49.1
Average number of water molecules per H:G unit								
	16.2		**16.8**		**15.7**		**12.6**	

* Δ Weight loss (%) = [Sample weight (%) at temperature (n-1)] - [Sample weight (%) at temperature (n)]

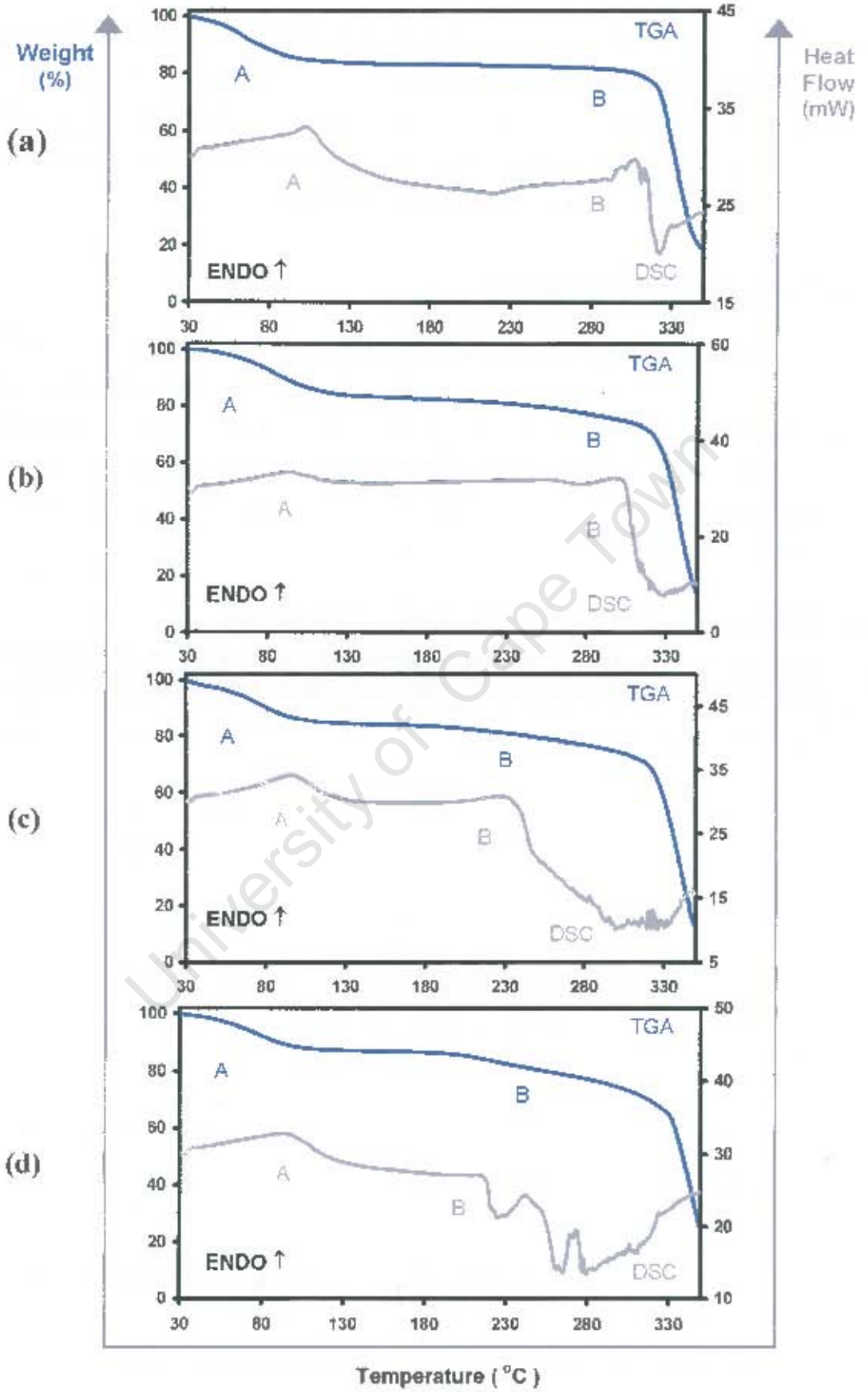

Figure 3.2 TGA and DSC traces for the (a) MPGCD (b) EPGCD (c) PPGCD and (d) BPGCD co-precipitated complexes

DSC results for the γ-CD complexes

The DSC results for the MPGCD, EPGCD, PPGCD and BPGCD complexes are shown in Figure 3.2 (a), (b), (c) and (d) respectively and the results are summarised in Table 3.3. The four γ-CD complexes show a broad endothermic event corresponding to water loss in the range 30-160°C, which is consistent with the observed mass loss in the TGA traces [labelled A in Figure 3.2 (a), (b), (c) and (d)].

The asymmetric shapes of the dehydration endotherms suggest that water loss from these complexes is a multi-stage process. The onset of decomposition is indicated by further mass loss on the TGA traces from 200°C [labelled B]. The DSC onset of decomposition occurs at 265, 247, 232 and 209°C for the MPGCD, EPGCD, PPGCD and BPGCD complexes respectively. This decomposition begins, in all cases, earlier than the decomposition of the γ-CD molecule, which occurs above 290°C, and is therefore associated with decomposition of the complex. Interpretation of the thermal events occurring during the final stages of decomposition is complicated by the significant loss of mass relative to the original sample, which affects the baseline of the trace.

The thermal stability of the inclusion complexes was based on the analysis of the onset of decomposition for the complexes. The stability follows the order MPGCD > EPGCD > PPGCD > BPGCD, which follows the same thermal stability as that of the pure parabens.

Table 3.3 Summarised DSC results for the γ-CD complexes

			MPGCD	EPGCD	PPGCD	BPGCD
Temperature range	A	(°C)	30-166	30-149	30-155	30-166
Endotherm A	T_{on}	(°C)	76	51	64	75
	Peak	(°C)	103	94	96	96
Endotherm B	T_{on}	(°C)	265	247	232	209
			METHYL	**ETHYL**	**PROPYL**	**BUTYL**
Endotherm for fusion of pure paraben[1]		(°C)	126	116	96	69

SCANNING ELECTRON MICROSCOPY (SEM)

SEM was undertaken to demonstrate the morphology of the γ-CD powder complexes. γ-CD complexes typically have a square, bipyramidal or tetragonal rod-like morphology and this was observed in the MPGCD, EPGCD, PPGCD and BPGCD complexes [as shown in Figure 3.3].

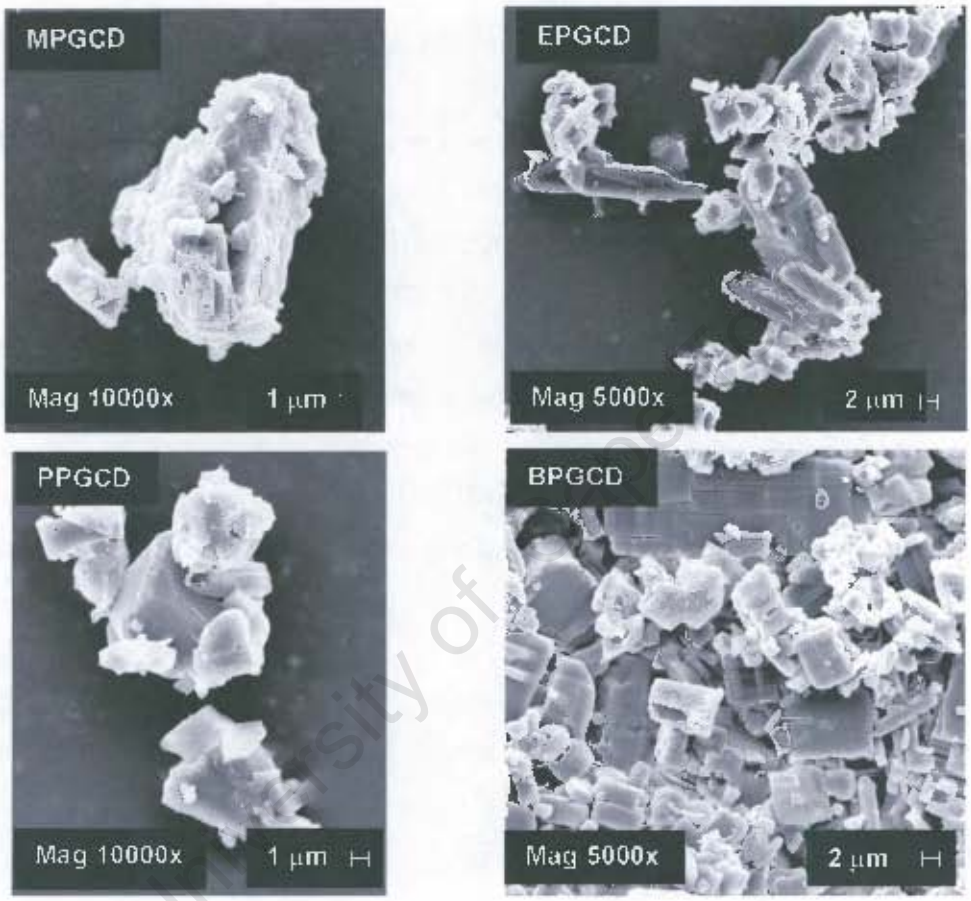

Figure 3.3 SEM photographs of the γ-CD complexes

FOURIER TRANSFORM INFRARED SPECTROSCOPY (FTIR)

FTIR spectroscopy was used to determine how the carbonyl stretching frequency was affected by complexation. The C=O stretching frequencies of the MPGCD, EPGCD, PPGCD and BPGCD complexes are displaced to 1700, 1691, 1689, 1688 cm^{-1} respectively from the measured values of 1679, 1672, 1675, 1678 cm^{-1} for the pure methyl-, ethyl-, propyl- and butyl paraben [Figure 3.4]. This significant frequency shift also indicates that the guest is included in the host. Furthermore, this is consistent with the known presence of strong hydrogen bonding (C=O···H–O) in the crystals of the guests[7] and the probable absence of hydrogen bonding of this type in the CD complexes.

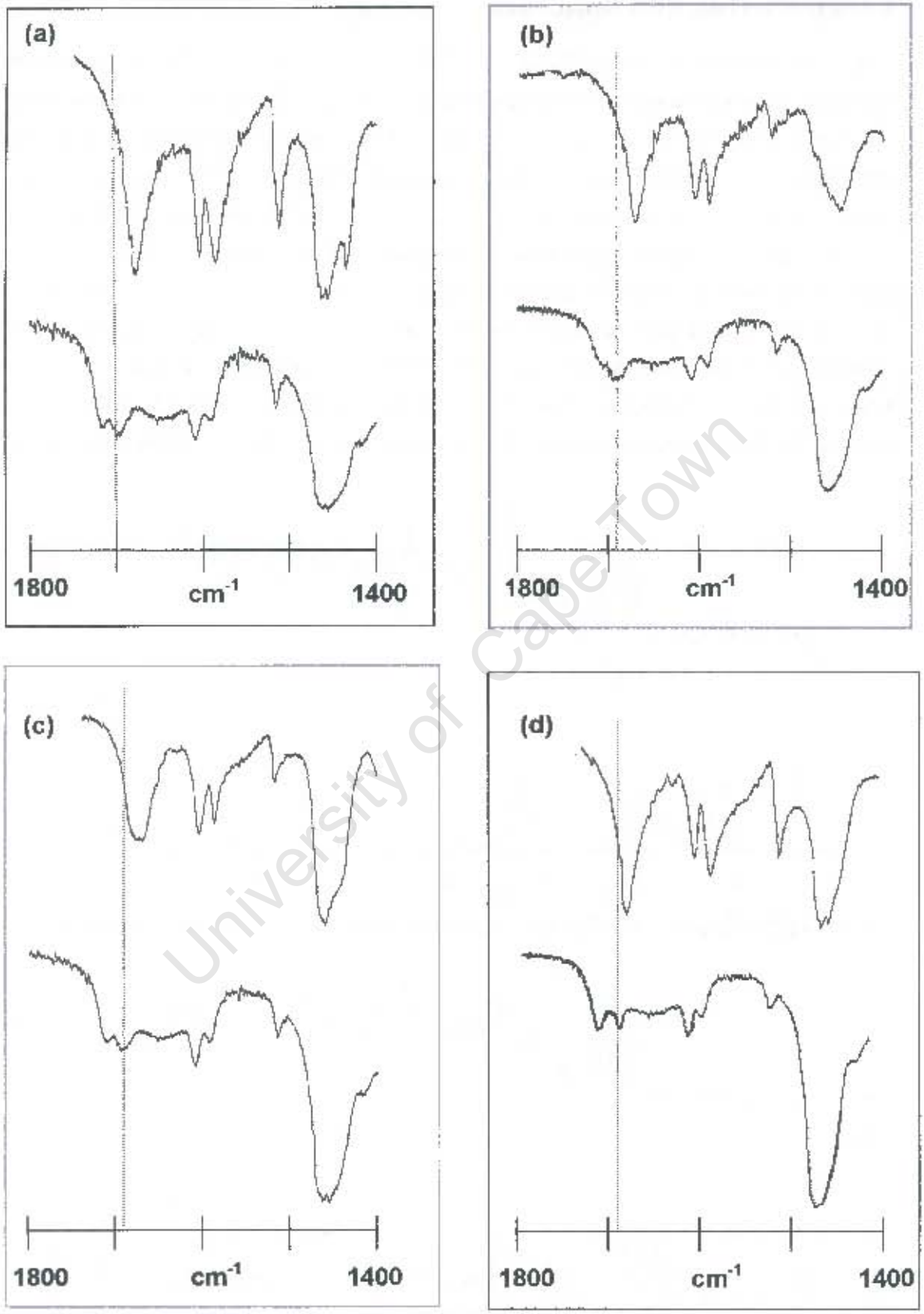

Figure 3.4 FTIR spectra (a) MP and MPGCD, (b) EP and EPGCD, (c) PP and PPGCD, (d) BP and BPGCD. The top spectrum is that of the pure paraben.

EXPERIMENTAL XRD ANALYSIS

The XRD patterns for the MPGCD, EPGCD, PPGCD and BPGCD co-precipitated materials, kneaded materials and the physical mixtures of γ-CD with the appropriate drugs are shown in Figures 3.5, 3.6, 3.7 and 3.8 respectively. The diffraction patterns of the co-precipitated and kneaded material were compared with those of the physical mixture [consisting of a 1:1 molar ratio of drug and γ-CD]. When the XRD trace for the latter differs from the others i.e. by the appearance of new peaks and the disappearance of old peaks, inclusion complex formation is considered "very probable".[2] This can be explained by the fact that the crystal packing arrangement of the inclusion complex is generally quite different from those of the components, and thus the complex will have a distinct crystalline phase with its own "fingerprint". The XRD traces represented in Figures 3.5 - 3.8 therefore indicate that complexation occurred by the co-precipitation method, but not by the kneading method.

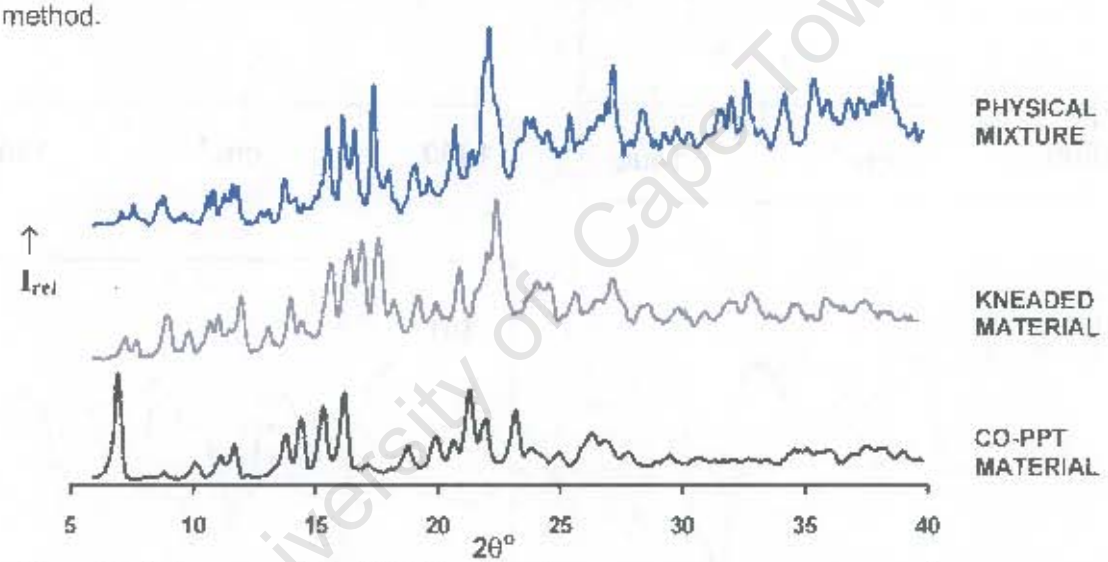

Figure 3.5 XRD patterns of the MPGCD co-precipitated and kneaded materials and a 1:1 physical mixture

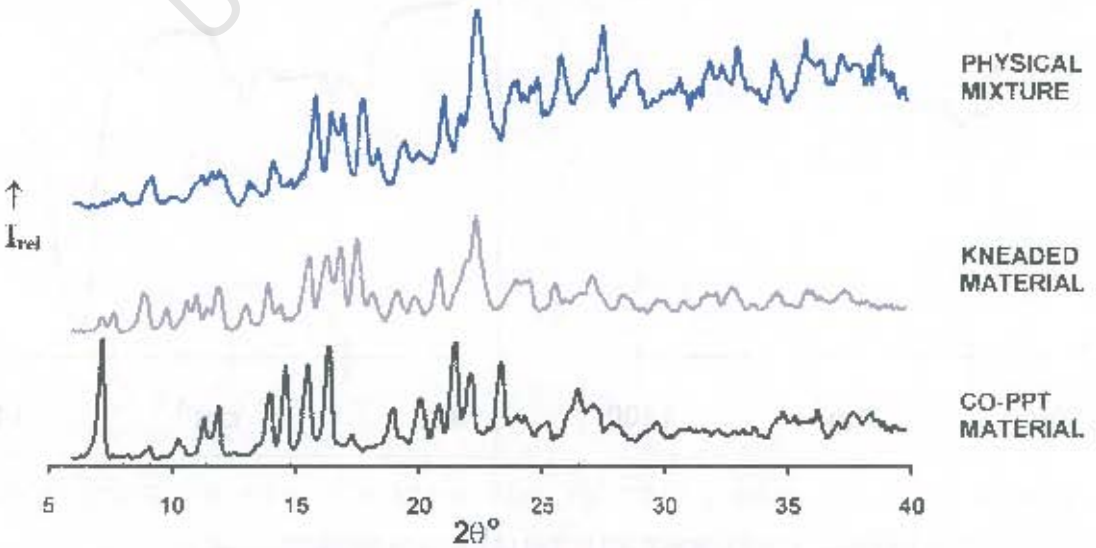

Figure 3.6 XRD patterns of the EPGCD co-precipitated and kneaded materials and a 1:1 physical mixture

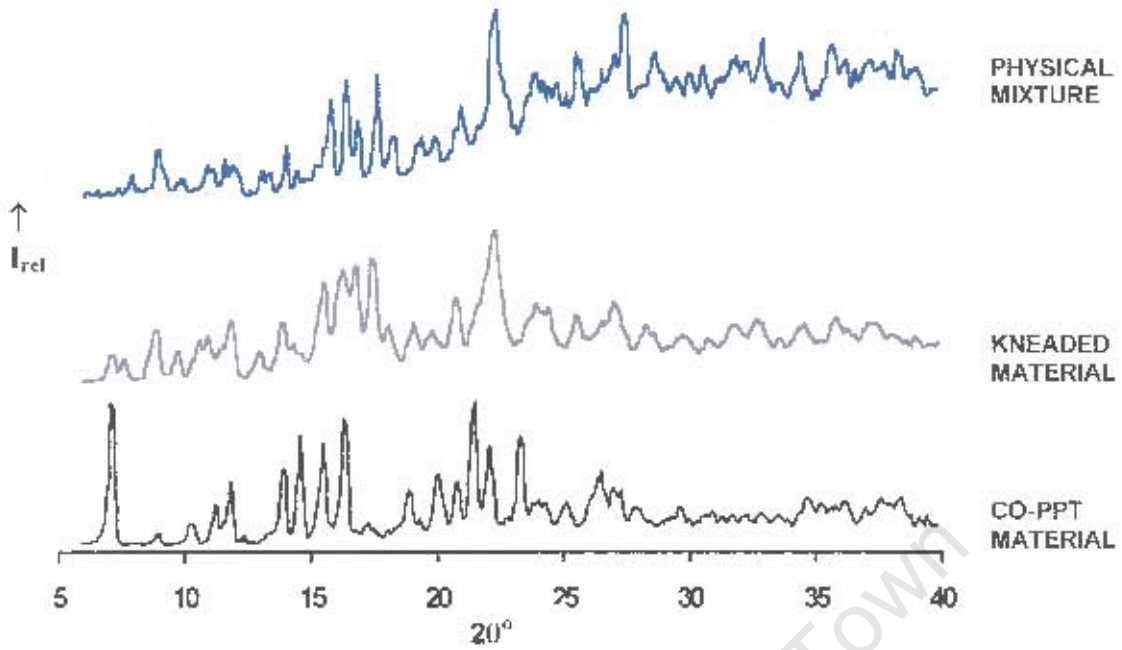

Figure 3.7 XRD patterns of the PPGCD co precipitated and kneaded materials and a 1:1 physical mixture

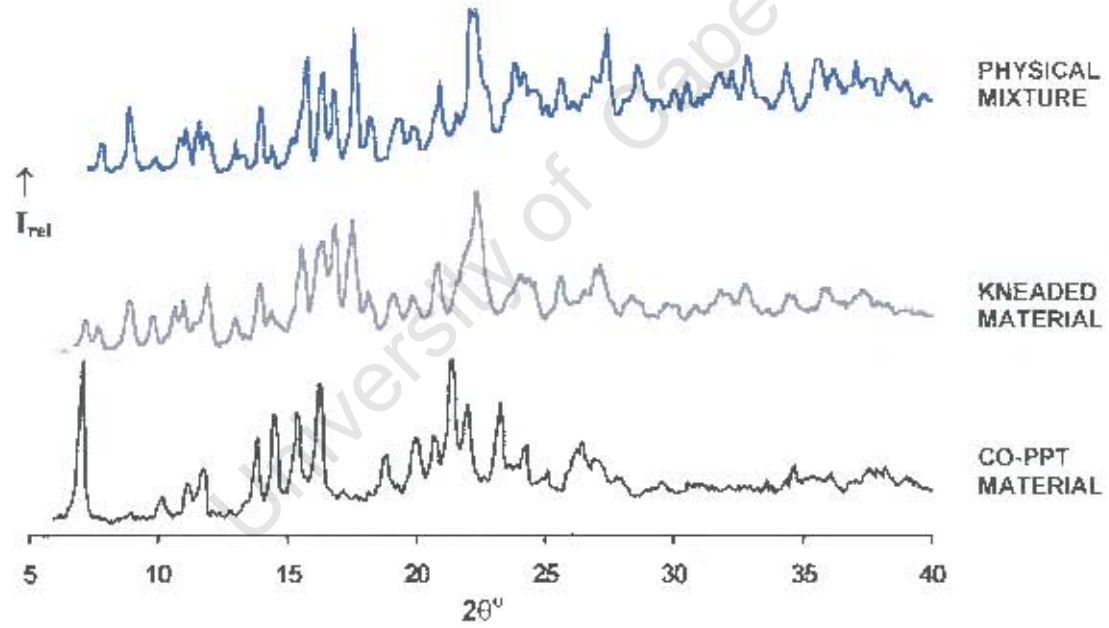

Figure 3.8 XRD patterns of the BPGCD co-precipitated and kneaded materials and a 1:1 physical mixture

The XRD patterns of all four of the γ-CD complexes [Figure 3.9] are closely matching and they can therefore be considered as isostructural to each other and with all other γ-CD complexes, based on work published by Caira.[3] The term "isostructural" is used here in the sense defined by Kálmán and Párkányi[4] to denote the fact that the complexes have the same space group with similar unit cell dimensions and a similar internal arrangement of molecules. This implies that for closely related structures, common atoms of the two structures have approximately the same co-ordinates.[5]

Only a few crystal structures have been published as yet for γ-CD and these fall into two structural categories: γ-CD•16H_2O crystallises in the space group $P2_1$, forming a cage type structure in which the water-filled molecular cavities are closed on both ends by neighbouring γ-CD molecules. In this crystal packing the γ-CD molecules are somewhat distorted with no internal symmetry.[5-7] All other γ-CD complexes crystallise in the tetragonal space group $P42_12$ with channel type packing.

The analysis of the XRD traces in Figure 3.9 for the γ-CD complexes reveals that the pattern is relatively "simple", in that the XRD trace has relatively few peaks. This is characteristic of compounds belonging to highly symmetrical space groups. Specifically, these traces confirm that the complexes crystallise in the tetragonal system, space group $P42_12$, with unit cell dimensions a ~ b ~ 23.8 and c ~ 23.2 Å.[3]

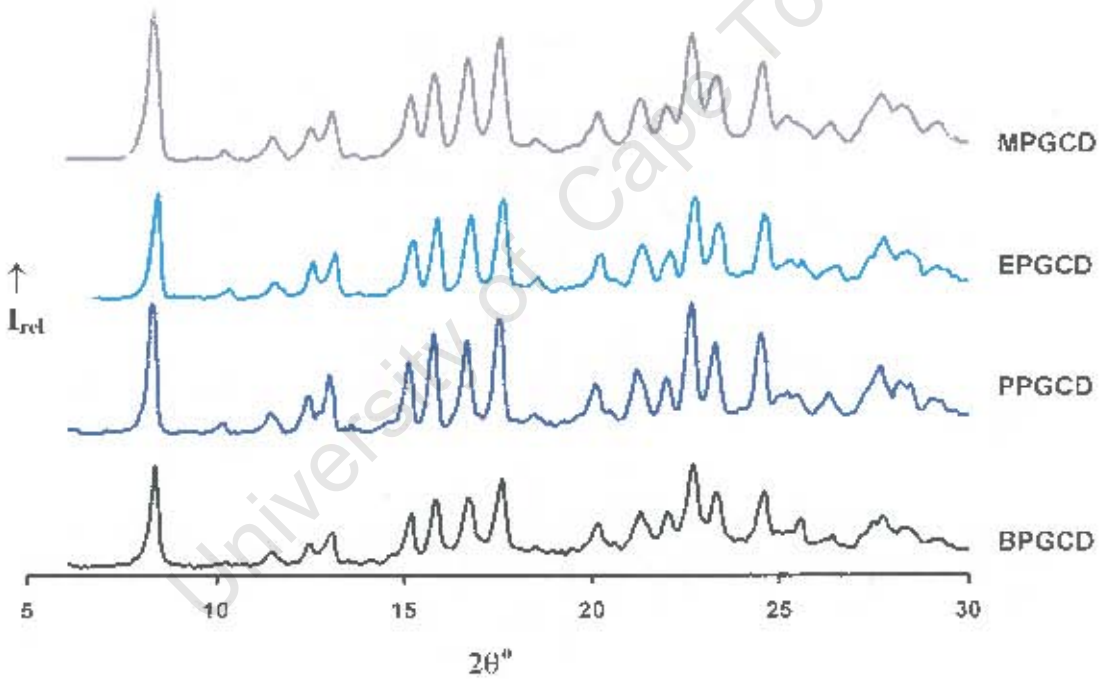

Figure 3.9 XRD traces of the MPGCD, EPGCD, PPGCD and BPGCD complexes

The packing mode of a γ-CD complex is shown in Figure 3.10 and Figure 3.11.[8] In Figure 3.10 the crystallographic symmetry elements of the space group $P42_12$ are indicated. In the crystalline phase, γ-CD molecules with their inherent eight-fold symmetry, are stacked parallel to the tetragonal c-axis to produce linear infinite channels [Figure 3.11]. These channels are unique in that they have three cyclodextrin molecules in one asymmetric unit. Consequently, the number of symmetry-independent glucose residues is six, amounting to $^3/_4$ of a γ-CD molecule.

The three crystallographically independent γ-CD molecules A, B, C, form a trimer arranged in head-to-head [A-B], tail-to-tail [B-C] and head-to-tail [C-A`] relationships. This stacking sequence is unusual, as CD columns typically stack with the molecules parallel [head-to-tail arrangement] or neighbouring molecules antiparallel.[8-10] The four-fold rotation axis runs through the centre of the γ-CD cavity and any guest molecule included in the cavity will of necessity be disordered around the four-fold axis, unless it possesses four-fold symmetry itself.[6]

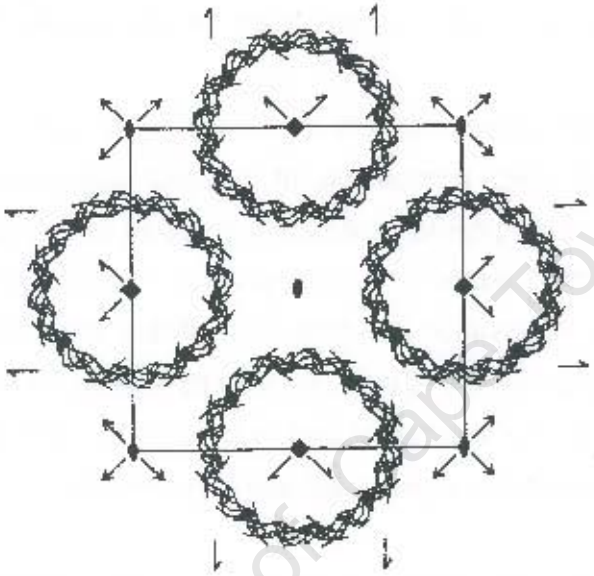

Figure 3.10 Crystal packing shown in projection on the *x,y* plane

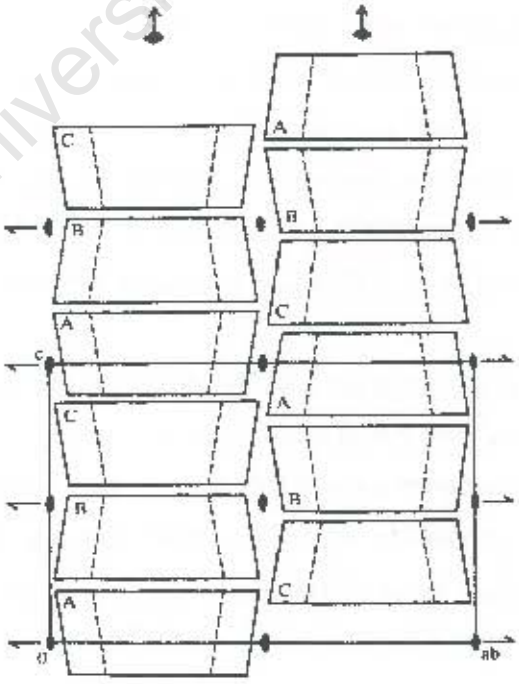

Figure 3.11 A projection of the stacking sequence within the molecular channel

DISCUSSION

γ-CD has been shown to have more favourable toxicological properties than α- and β-CD because it can be degraded in the upper intestinal tract while α- and β-CD cannot. α- and β-CD can only be degraded in the caecum and colon by bacterial flora and may therefore affect the kidneys by resorption [depending on the dosage].[11] γ-CD has therefore some more favourable properties than other CDs and this is what promoted the investigation of γ-CD complexation with the paraben drugs.

The γ-CD to guest stoichiometries were of a 1:2 host to guest ratio for each of the complexes. DSC and XRD comparison of inclusion complexes and the physical mixtures of their constituents demonstrated that inclusion complexes have been formed in the solid state by the method of co-precipitation. Furthermore FTIR spectroscopy confirmed this by the observation of a frequency shift of the C=O bond. The thermal stabilities of the complexes were found to be directly affected by the thermal stability of the included guest, as the thermal stability of the γ-CD complexes increased with increasing fusion temperatures of the guest that they included.

The XRD traces of the γ-CD complexes were in close agreement with each other. This indicated an analogous packing arrangement of the four complexes. They were determined to be isostructural with each other and with all other γ-CD inclusion complexes with the space group $P42_12$.[3] Although the space group $P42_12$ [no. 90] and the unit cell content Z = 6 are extremely rare this is the favourite crystal packing arrangement of γ-CD inclusion complexes. The Cambridge Structural Database[12] which archived 257 162 entries in April 2002, yielded 23 hits [i.e., 0.009%] for structures with this space group, and 79 hits [i.e., 0.03%] for structures with a unit cell content of 6.

These γ-CD complexes are positioned with the centre of the γ-CD molecules situated on a four-fold rotation axis. The guest molecules included in the cavities will inevitably be crystallographically disordered around this rotation axis by at least four-fold. This is the main reason why complexes of γ-CD molecules are structurally much less frequently characterised than those of the lower homologues α- and β-CD.

REFERENCES

1) F. Giordano, R. Bettini, C. Donini, A. Gazzaniga, M. R. Caira, G. G. Z. Zhang, D. J. W. Grant, *J. Pharm. Sci.*, **1999**, 88, 11, 1210.

2) L. Szente, *In Comprehensive Supramolecular Chemistry*, (Vol. 3), J. L. Atwood, J. E. D. Davies, D. D. MacNicol, F. Vögtle (eds.), Pergamon, UK, **1996**, Ch 8, p. 253-278.

3) M. R. Caira, *Roum. Chim. Rev.*, **2001**, 46, 4, 371.

4) A. Kálmán, L. Párkányi, *Advances in Molecular Structure Research*, (Vol. 3), M. Hargittai, I. Hargittai (eds.), JAI Press, Greenwich, CT., **1997**, p. 206.

5) L. Fábián, A. Kálmán, *Acta Crystallogr.*, **1999**, B55, 1039.

6) K. Harata, *Bull. Chem. Soc. Jpn.*, **1987**, 60, 2763.

7) J. Ding, T. Steiner, V. Zabel, B. E. Hingerty, S. A. Mason, W. Saenger, *J. Am. Chem. Soc.*, **1991**, 113, 8081.

8) T. Steiner, W. Saenger, *Acta Crystallogr.*, **1998**, B54, 450.

9) W. Saenger, *Isr. J. Chem.*, **1985**, 25, 43.

10) W. Saenger, *Inclusion Compounds*, (Vol. 2), J. L. Atwood, J. E. D. Davies, D. D. MacNicol (eds.), Oxford University Press, London, **1984**.

11) G. Antlsperger, H. Reuscher, G. Schmid, *Wacker-Chemie GmbH*, **1996**, Hanns-Seidel-Platz 4, D-81737 München, Germany.

12) *Cambridge Structural Database and Cambridge Structural Database System*, Version 5.23, April **2002**, Cambridge Crystallographic Data Centre, University Chemical Laboratory, Cambridge, England.

Chapter 4

β-CD INCLUSION COMPLEXES

The present section consists of two parts and describes a parallel study of the inclusion of the paraben drugs in β-CD, both in the solid state and in solution. The combination of the two studies provides more insight into the nature of the inclusion process than either of the studies by itself.

In the solid state study, thermal analysis and X-ray techniques were used to elucidate the thermal properties and crystal structures of the inclusion complexes and these results are described in Part 1.

In solution, ^{1}H NMR spectroscopy was used to determine the stoichiometry and formation constants of the paraben-CD complexes. These results are presented in Part 2.

Part 1

SOLID STATE STUDY

COMPLEX PREPARATION

Crystalline complexes of methyl-, ethyl-, propyl- and butyl paraben with β-CD were obtained from slow cooling and slow evaporation of hot aqueous solutions [~ 45°C] of cyclodextrin and drug in 1:1 molar ratios at 7°C and ambient temperature. Crystalline material was obtained on standing for a period of one to two weeks at RT and one month at 7°C. The density of the crystals was not measured due to the high solubility of the host in both aqueous solution and organic solvents. The complexes of β-CD with each paraben, grown under ambient conditions, will be referred to as MPBCD, EPBCD, PPBCD and BPBCD and will be described herein.

MICROANALYSIS

The host to guest ratios of the β-CD complexes were determined by carbon and hydrogen microanalysis of the fully hydrated complexes. Each of the MPBCD, EPBCD, PPBCD and BPBCD complexes contains 1:1 stoichiometric amounts of host to guest. This stoichiometry was confirmed by UV spectrophotometric experiments. The total water content of the sample to be analysed was calculated from the initial mass losses obtained from thermogravimetric analysis and the results are reported in Table 4.1.

Table 4.1 Carbon and hydrogen microanalysis results for the β-CD complexes

COMPLEX	CALCULATED (%)		EXPERIMENTAL (%)	
	C	H	C	H
MPBCD • 7.2 H_2O	42.38	6.57	42.54	6.37
EPBCD • 7.0 H_2O	42.90	6.64	42.79	6.35
PPBCD • 7.0 H_2O	43.33	6.71	43.54	6.48
BPBCD • 7.3 H_2O	43.57	6.80	43.61	6.56

THERMAL ANALYSIS

DSC analysis of the β-CD complexes and physical mixtures of their components

Figure 4.1 shows the DSC traces of the MPBCD, EPBCD, PPBCD and BPBCD complexes respectively together with the traces of the appropriate uncomplexed drug and the 1:1 β-CD-drug physical mixture. The characteristic fusion endotherms for methyl-, ethyl-, propyl-, and butyl paraben are 126, 116, 96 and 69°C respectively, and are clearly visible in the DSC traces of the uncomplexed drug and physical mixtures of these drugs with β-CD. In each case the disappearance of the fusion endotherm was observed in the DSC traces of the complexes, which indicated that an inclusion complex had been formed.

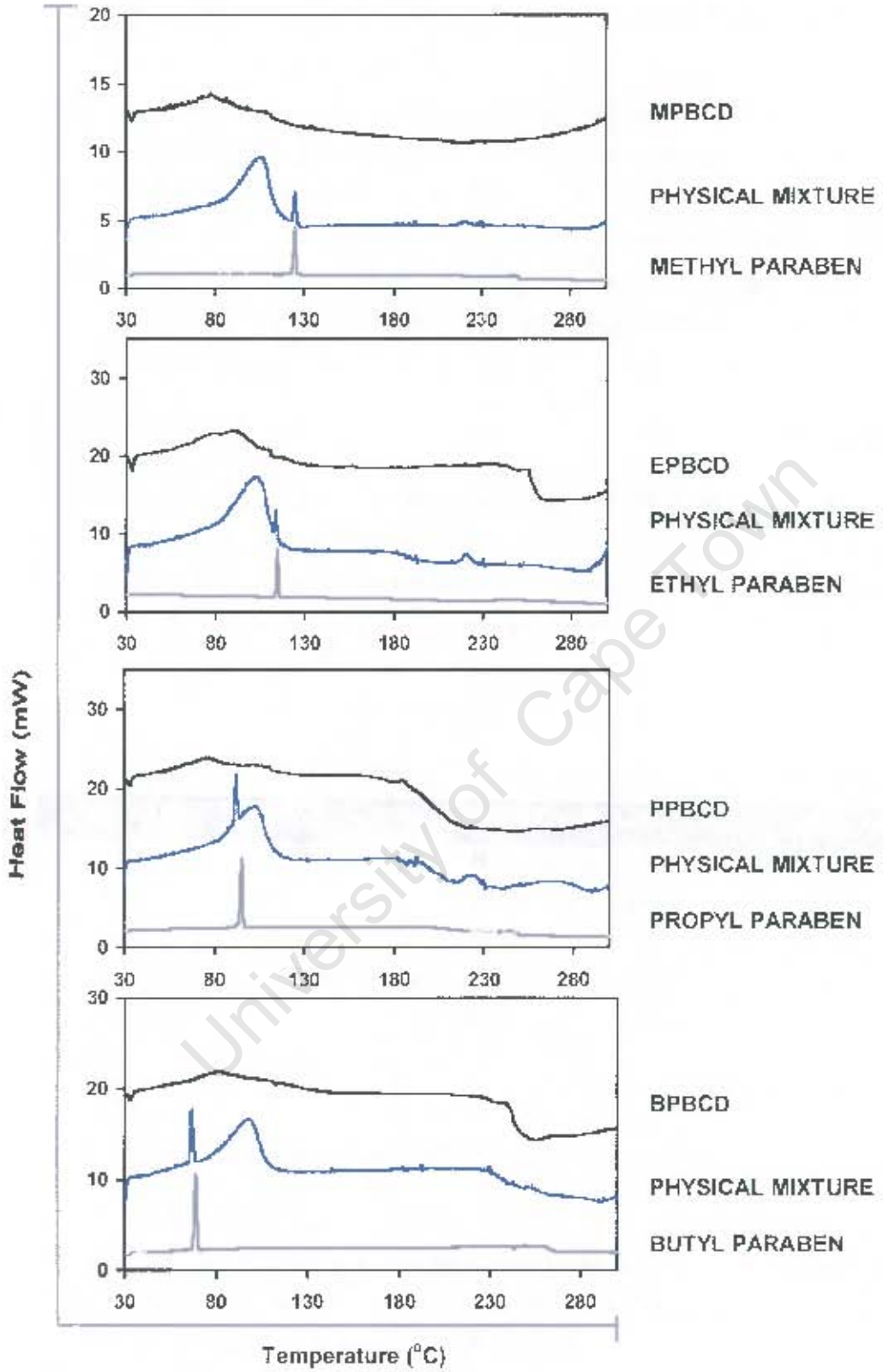

Figure 4.1 DSC traces of the β-CD paraben complexes, 1:1 physical mixtures and uncomplexed paraben drugs

TGA results for the β-CD complexes

The TGA results for the MPBCD, EPBCD, PPBCD and BPBCD complexes are shown in Figure 4.2 (a), (b), (c) and (d) respectively. A summary of the observed percentage weight losses over the temperature intervals between 30, 110, 200, 250, 300 and 350°C are presented in Table 4.2.

Table 4.2 The percentage weight losses for the β-CD complexes

Temp (°C)	MPBCD		EPBCD		PPBCD		BPBCD	
	Sample weight (%)	Δ Weight loss (%) *	Sample weight (%)	Δ Weight loss (%) *	Sample weight (%)	Δ Weight loss (%) *	Sample weight (%)	Δ Weight loss (%) *
30	100	-	100	-	100	-	100	-
110	90.8	9.2	90.1	9.9	91.2	8.8	89.8	10.2
200	89.6	1.2	89.2	0.9	86.0	5.2	88.2	1.6
250	86.7	2.9	86.7	2.5	83.4	2.6	86.1	2.1
300	77.8	8.9	81.2	5.5	79.6	3.8	83.6	2.5
350	20.8	57.0	18.2	63.0	22.6	57.0	23.4	60.2
Average number of water molecules per H:G unit								
	7.2		7.0		7.0		7.3	

* Δ Weight loss (%) = [Sample weight (%) at temperature (n-1)] - [Sample weight (%) at temperature (n)]

DSC results for the β-CD complexes

The DSC results for the MPBCD, EPBCD, PPBCD and BPBCD complexes are shown in Figure 4.2 (a), (b), (c) and (d) respectively and the results are summarised in Table 4.3. The DSC traces of MPBCD, EPBCD, PPBCD and BPBCD appear to have similar profiles. The complexes show a broad asymmetric endotherm [labelled A] with a leading edge, which is associated with water loss. This corresponds to an observed mass loss in the TGA trace. For the MPBCD complex the endotherm peaks at 80°C with a shoulder at 110°C. For the EPBCD complex the major peak occurs at 85°C and has a number of shoulders occurring at 110 and 120°C indicating that water loss from this complex is clearly a multi-step process. The water loss peak of the PPBCD complex occurs at 77°C and has a shoulder that occurs at 106°C. The BPBCD complex has one broad endotherm associated with water loss peaking at 83°C. The asymmetric shape of the dehydration endotherm is an indication that the water loss from these complexes is a multi-step process.

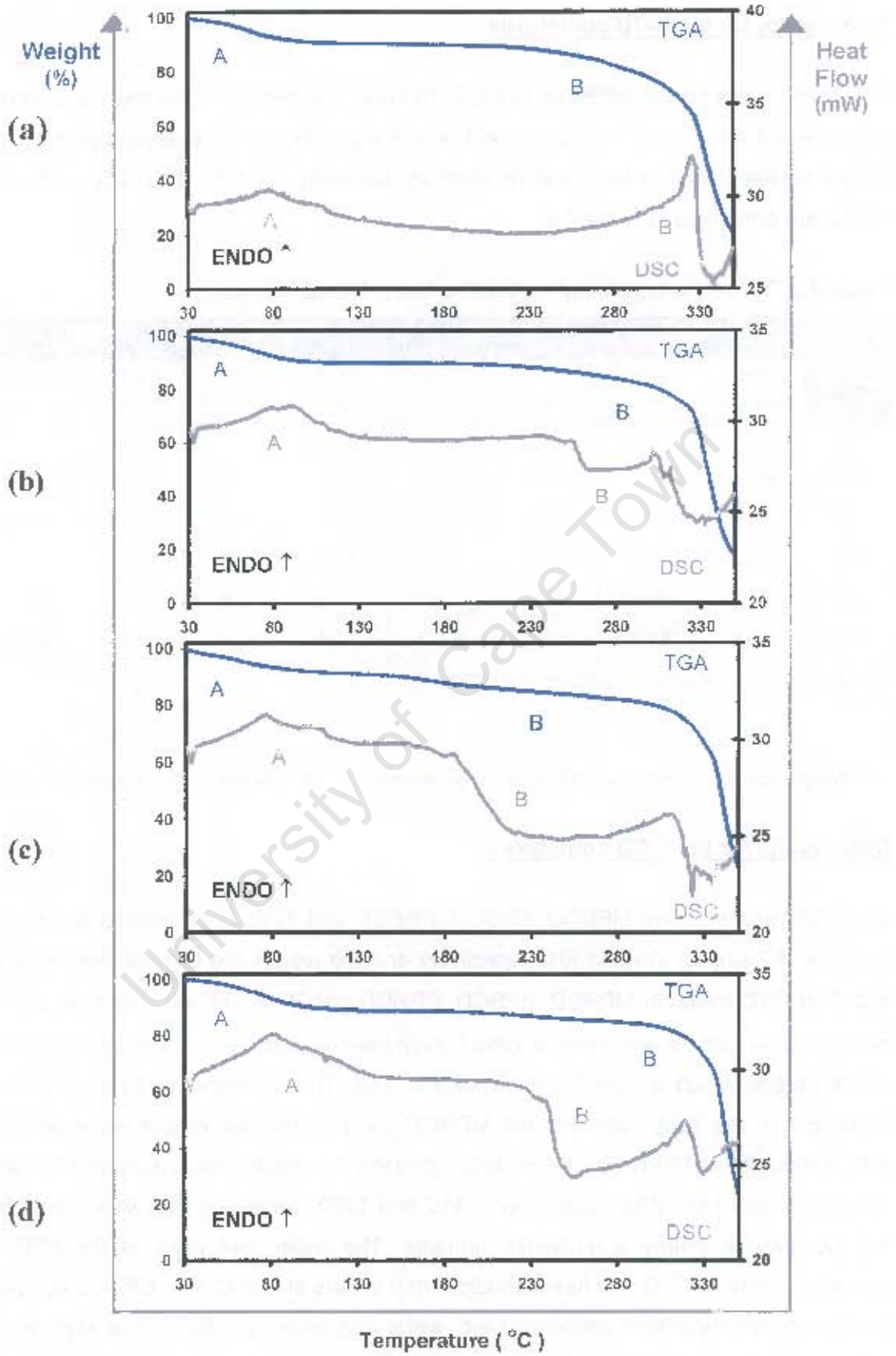

Figure 4.2 TGA and DSC traces for the (a) MPBCD (b) EPBCD (c) PPBCD and (d) BPBCD complexes

As is usually the case for cyclodextrin complexes where the host is unsubstituted, there is no well-defined melting point. The onset of decomposition is indicated by further mass loss on the TGA traces from 200°C [labelled B]. The decomposition peak is asymmetric with a leading edge and thus the onset of decomposition occurs at approximately 268, 256, 196 and 209°C for the MPBCD, EPBCD, PPBCD and BPBCD complexes respectively. In all four complexes, this decomposition begins well below the decomposition of the β-CD molecule, which occurs above 290°C, and is therefore associated with loss or decomposition of guest molecules included in the complex. Very large weight losses are observed in the TGA traces from 300°C onwards for all the complexes, confirming the decomposition of the β-CD molecules. The thermal stability of the inclusion complexes was based on the analysis of the onset of decomposition for the complexes. The stability follows the order MPBCD > EPBCD > BPBCD ~ PPBCD, which follows a similar thermal stability to that of the pure parabens.

Table 4.3 Summarised DSC results for the β-CD complexes

			MPBCD	EPBCD	PPBCD	BPBCD
Temperature range	A	(°C)	30-127	30-135	30-138	30-139
Endotherm A	T_{on}	(°C)	30	30	30	30
	Peak	(°C)	80	85	77	83
Endotherm B	T_{on}	(°C)	268	256	196	209
			METHYL	**ETHYL**	**PROPYL**	**BUTYL**
Endotherm for fusion of pure paraben[1]		(°C)	126	116	96	69

FOURIER TRANSFORM INFRARED SPECTROSCOPY (FTIR)

The carbonyl stretching frequencies of the pure methyl-, ethyl-, propyl- and butyl paraben were measured and found to occur at 1679, 1672, 1675, 1678 cm^{-1} respectively. The carbonyl stretching frequencies for the complexes were displaced to 1715, 1708, 1712, 1708 cm^{-1} for the MPBCD, EPBCD, PPBCD and BPBCD complexes respectively [Figure 4.3]. It is evident that the υ(C=O) of the complexed drug is significantly higher than in the pure drug in each case. This suggests that the C=O bond is stronger in the complexed drug due to the absence of the strong hydrogen bonding (C=O···H–O) found in the crystals of the uncomplexed guest molecules.[1]

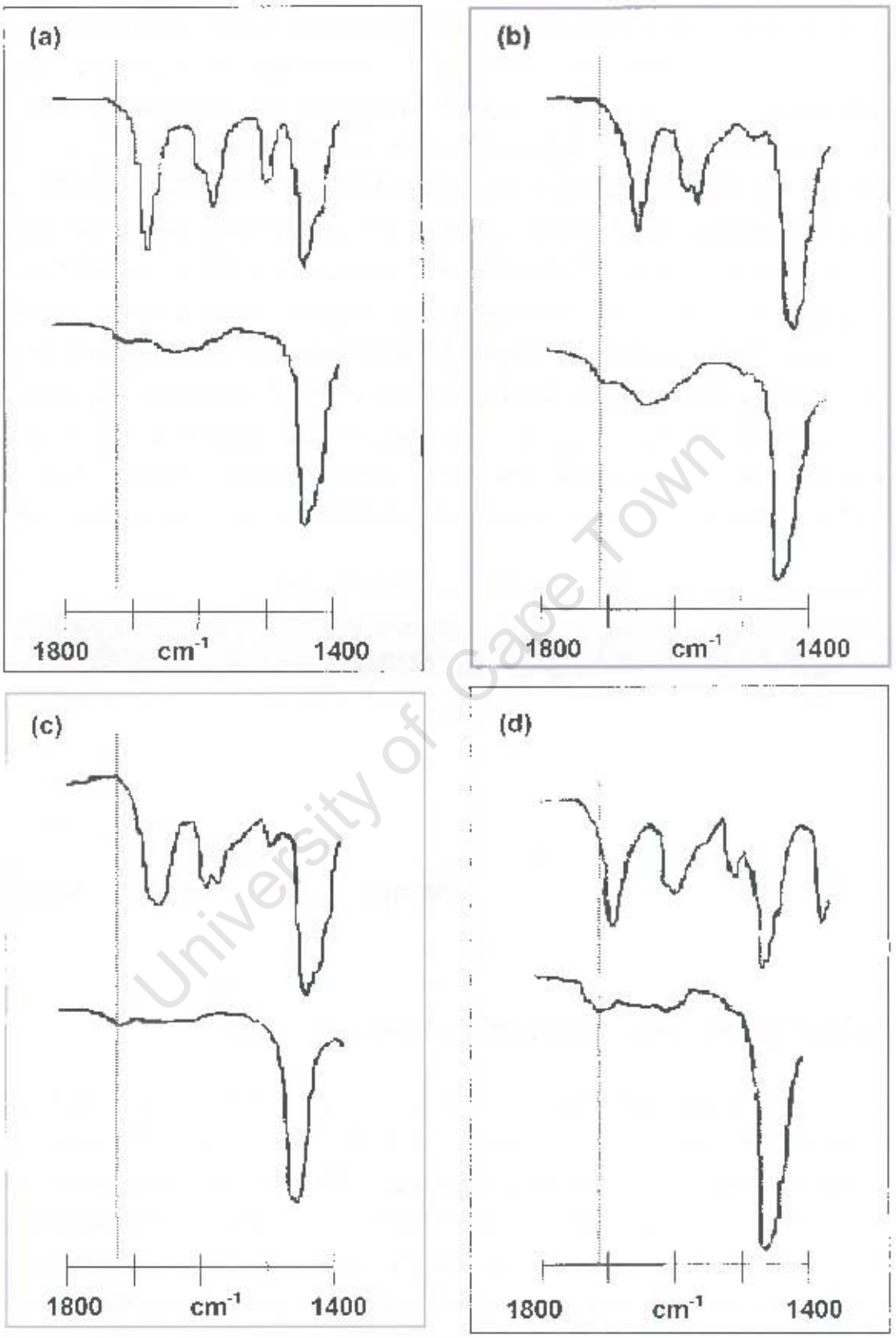

Figure 4.3 FTIR spectra (a) MP and MPBCD, (b) EP and EPBCD, (c) PP and PPBCD, (d) BP and BPBCD. The top spectrum is that of the pure paraben.

EXPERIMENTAL XRD ANALYSIS

The XRD patterns for the MPBCD, EPBCD, PPBCD and BPBCD complexes, obtained from kneading and the co-precipitation method, are shown in Figures 4.4, 4.5, 4.6 and 4.7 respectively together with the XRD patterns of the physical mixture of β-CD with the appropriate drug. The diffraction patterns of the kneaded and co-precipitated materials were compared with those of the physical mixture [consisting of a 1:1 molar ratio of drug and β-CD]. In each case, the diffraction patterns of the co-precipitated and kneaded materials were different from that of the physical mixture, demonstrating that complexation had occurred.[7] The diffraction patterns of the kneaded and co-precipitated materials were similar, indicating that they are the same crystalline phase. The relative intensities of the peaks do not coincide and this could be attributed to some degree of preferred orientation of the sample in the XRD sample holder.

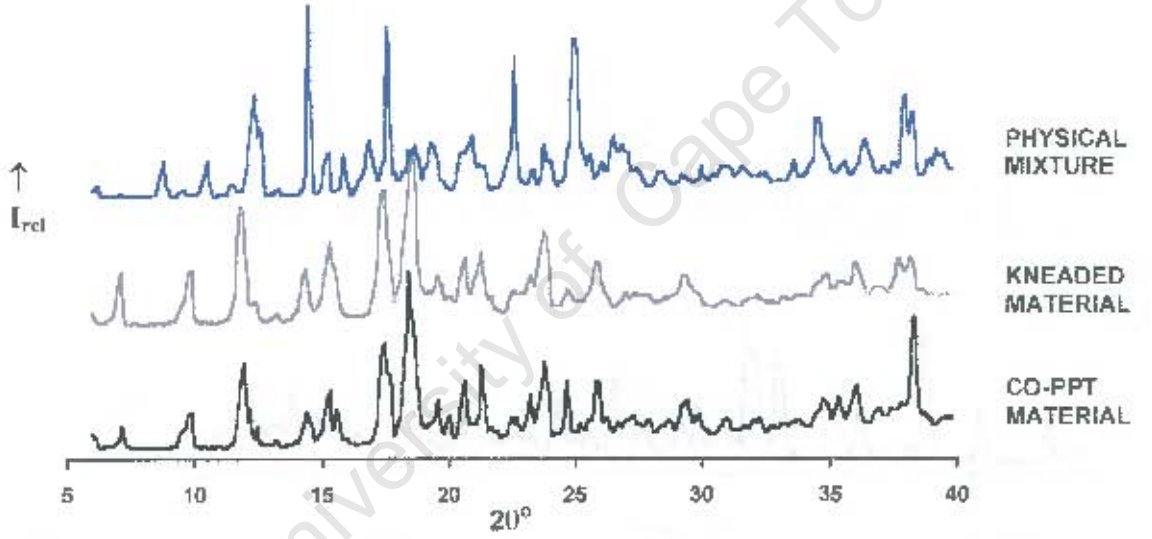

Figure 4.4 XRD patterns of the MPBCD co-precipitated and kneaded materials and a 1:1 physical mixture

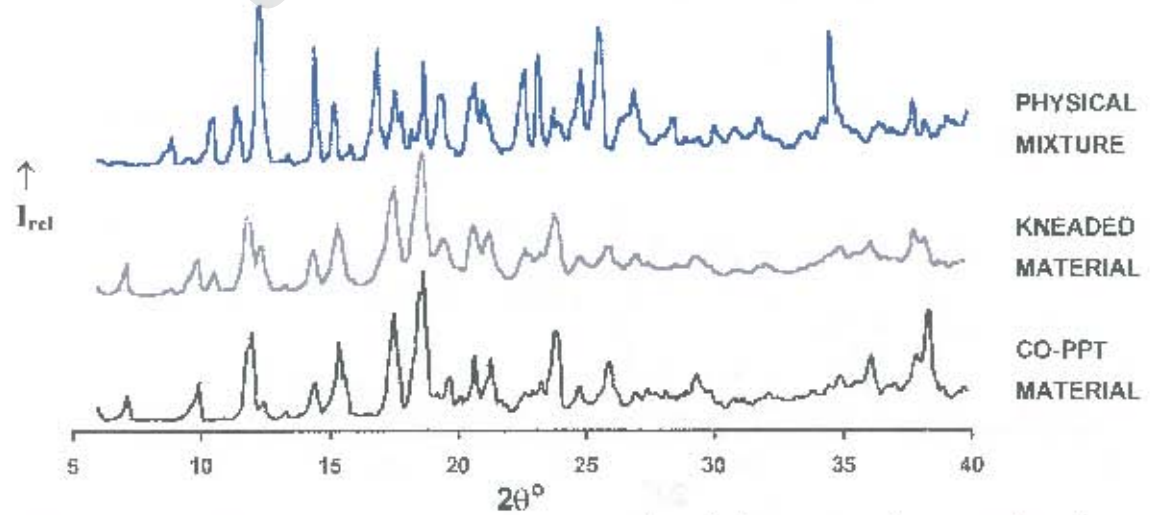

Figure 4.5 XRD patterns of the EPBCD co-precipitated and kneaded materials and a 1:1 physical mixture

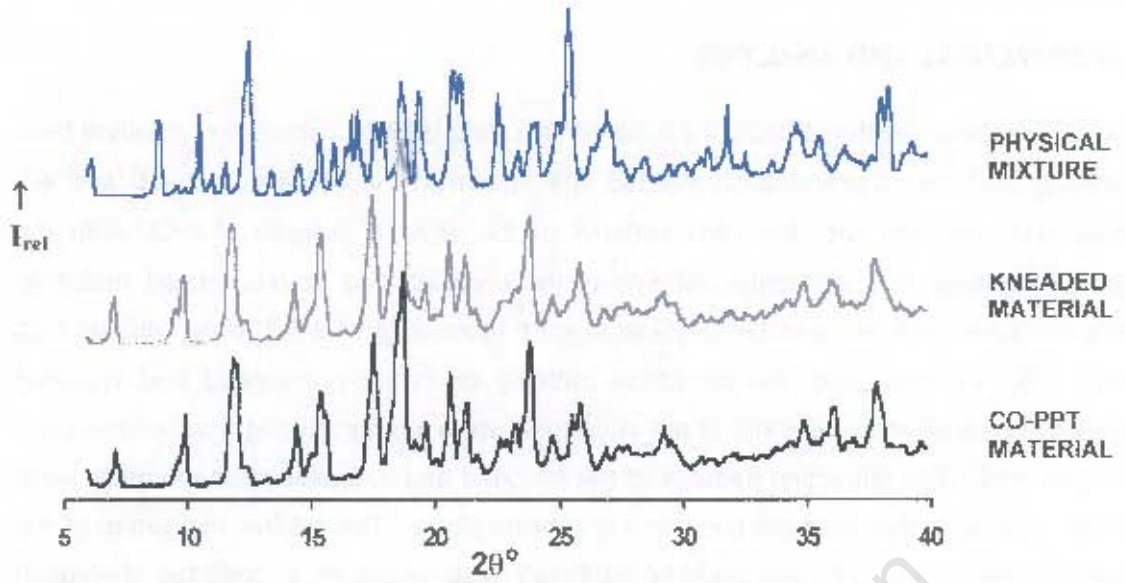

Figure 4.6 XRD patterns of the PPBCD co-precipitated and kneaded materials and a 1:1 physical mixture

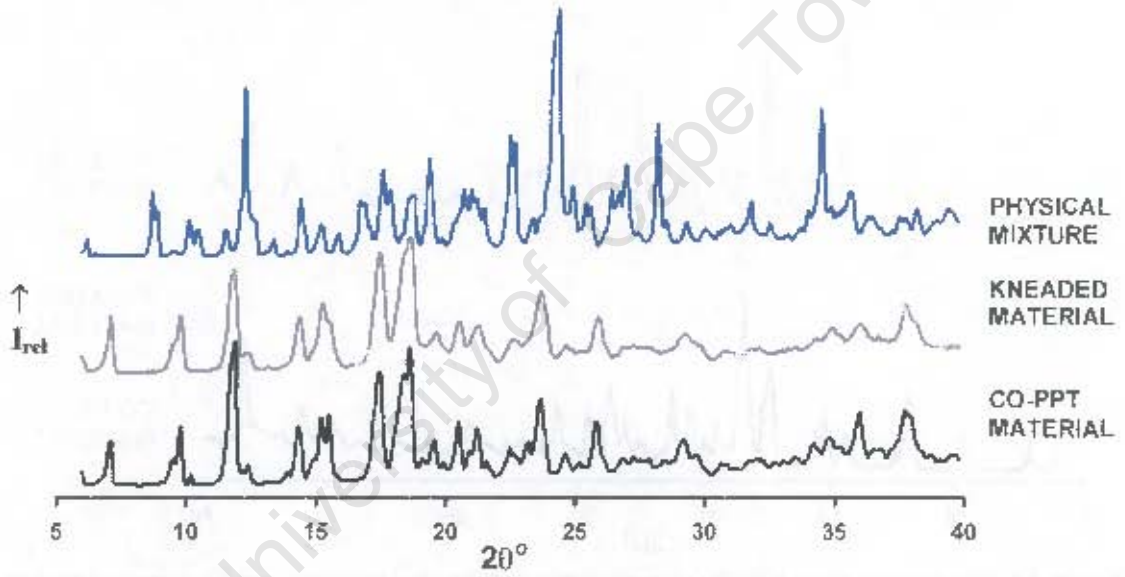

Figure 4.7 XRD patterns of the BPBCD co-precipitated and kneaded materials and a 1:1 physical mixture

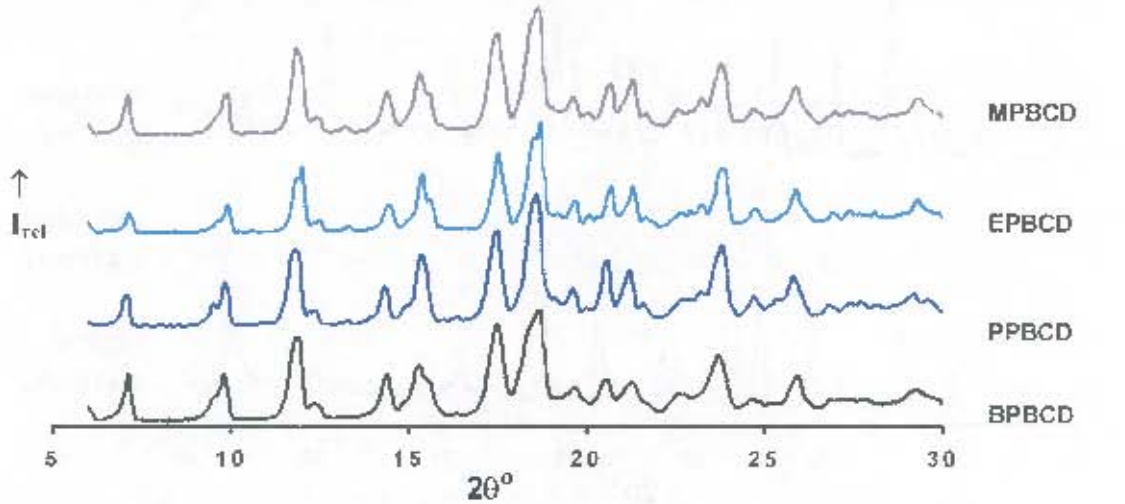

Figure 4.8 XRD traces of the MPBCD, EPBCD, PPBCD and BPBCD complexes

The XRD traces of the four complexes resemble one another closely [Figure 4.8] and these phases can therefore be considered as isostructural.[3] On comparison of these XRD traces with those published by Caira,[3] it can be deduced that the space group will either be C2 or P1, both with channel type packing, the unit cell dimensions being approximately 19.3, 24.5, 15.9 Å and β = 109° for the C2 complexes and 15.6, 15.6, 15.9 Å, α = 101, β = 101 and γ = 103° for the P1 complexes. β-CD complexes crystallising in these space groups have practically indistinguishable XRD traces as the respective unit cells are related by a simple lattice transformation[4] and the differences between them are subtle. The β-CD dimer complex of space group P1 possesses a pseudo-twofold symmetry, while the β-CD dimer complex of space group C2 has a crystallographic diad passing through the dimer interface. Consequently, in more then one instance, the wrong space group has been used for complex crystal structure refinement.[5-6] Corrections from P1 to C2 or *vice versa* are minor and the molecular dimensions and co-ordinates are effectively unchanged, explaining why the powder patterns are so similar.[7] Preliminary inspection of the cell parameters may hint at the fact that the wrong space group has been selected, i.e. the equality of two axes and two angles suggesting that the space group P1 is incorrect. Once the cell dimensions have been determined, the assignment of the correct space group can be determined by using the tools of the reduced cell and Niggli matrix. X-ray photography does distinguish these cases, yielding Laue symmetries $\bar{1}$ and 2/m for space groups P1 and C2 respectively.

UNIT CELL DETERMINATION OF THE β-CD COMPLEXES

X-ray photographic analysis was used to determine the unit cell parameters, crystal system and space group for crystal complexes. Suitable single crystals for X-ray photographic analyses were obtained from the MPBCD and PPBCD complexes. A single crystal of each complex was mounted on a glass fiber and covered in Paratone N oil[8] to prevent cracking due to dehydration. The unit cell parameters determined from photography for the MPBCD and PPBCD complexes were very similar with a = 19.0, b = 24.3, c = 15.4 Å and β = 110°. Photography revealed Laue *2/m* symmetry and reflection conditions listed below.

hkl: h + k = 2n
h0l: (h = 2n)
0k0: (k = 2n)

This indicated the monoclinic space group C2, C*m* or C2/*m*. These absences together with the absence of possible mirror planes or centers of inversion, due to the chiral nature of the cyclodextrin, indicated that the correct space group is C2.

Smaller crystals were obtained for the EPBCD and BPBCD complexes. These crystals diffracted poorly and the long exposure time needed to obtain interpretable photographs led to crystal decay. Cell determination was therefore performed directly on the Nonius Kappa CCD diffractometer using graphite-monochromated MoKα radiation. For both complexes the crystals were highly unstable in air and were mounted on a glass fibre and covered in Paratone N oil.[8] The unit cell parameters for the EPBCD complex were a = 18.88, b = 24.44, c = 15.73 Å and β = 109.8° and for the BPBCD complex a = 19.05, b = 24.48, c = 15.73 Å and β = 110.9°. These parameters are very similar to those of the MPBCD and PPBCD complexes.

To confirm that the space group of the complexes is C2 [as observed from photography], the crystal data of the MPBCD and PPBCD complexes were initially collected as P1. From the computer program Xprep[9] it was found, by way of the Niggli matrix, that the data fit the higher [monoclinic] symmetry. The metric tensor [Niggli matrix] is given by [**a.a b.b c.c / b.c c.a a.b**] (conveniently abbreviated as [*ABC / DEF*]), with standard ordering of the axes as $a \leq b \leq c$. The general background is given by Giacovazzo,[10] while specifics on the use of reduced cells to determine correct symmetries have been summarised by de Wolff.[11]

The unit cell and atomic co-ordinates were therefore transformed to acquire the new cell and co-ordinates were averaged according to the demands of the higher symmetry. The relationship between the monoclinic and triclinic co-ordinates is $x_M = (x_T + y_T) / 2 - 0.57$, $y_M = (-x_T + y_T) / 2$ and $z_M = z_T - 0.48$, the translation being needed to place the origin on a C_2 axis in the space group C2. However, it should be remembered that the true symmetry is revealed by intensity rather than by metric relationships and the photographic observation of Laue 2/m symmetry is conclusive.

The MPBCD and PPBCD complexes are included in the next section, in which the complete three-dimensional structure analyses are reported. Structures for the EPBCD and BPBCD complexes are not included, as suitable single crystals of these complexes could not be obtained, despite repeated efforts to grow them.

X-RAY CRYSTALLOGRAPHIC ANALYSIS OF THE MPBCD STRUCTURE

Data-collection

X-ray intensity data-collection was performed at 293(2) K on the Nonius Kappa CCD diffractometer using graphite-monochromated MoKα radiation. A single crystal was mounted on a glass fibre and covered in Paratone N oil[8] to provide a rigid mounting for the low-temperature data collection and to prevent cracking due to loss of water of crystallisation. Crystal data and data-collection parameters are listed in Table 4.4.

Structure determination and refinement

The MPBCD complex crystallises in the monoclinic space group C2 with a single β-CD molecule, a guest molecule and 7.2 water molecules comprising the asymmetric unit of the structure. The complex is dimeric, the asymmetric unit being rotated through a diad parallel to the *b*-axis to produce the other half of the dimer. The structure was solved using published co-ordinates for the non-hydrogen cyclodextrin atoms [excluding the primary hydroxyl oxygen atoms] of the isomorphous β-CD-ibuprofen complex.[12]

After refinement in SHELX-97,[13] the difference Fourier map revealed the positions of most of the primary hydroxyl oxygen atoms. After further refinement it was found that five of these atoms had full site-occupancy, while the other two [O(63) and O(66)] were disordered over two positions. For a given pair, a fixed U_{iso} of 0.08 Å^2 [the mean of U_{eq} for the chemically equivalent ordered atoms] was assigned and site-occupancy factors [s.o.f.'s] of x and 1-x were assigned, with x variable. The major positions refined to s.o.f.'s of 0.81 and 0.60 for O(63A) and O(66A) respectively. All the host atoms except the disordered primary hydroxyl oxygen atoms and O(6G2) were refined anisotropically.

Once all the non-hydrogen atoms of the host and the water molecules had been located from subsequent difference electron density maps, all the cyclodextrin hydrogen atoms were placed. These hydrogen atoms were geometrically fixed at idealised positions in a riding-model. All the primary hydroxyl hydrogen atoms were assigned a common variable isotropic temperature factor and were placed using the AFIX 83 or AFIX 147 instruction. The remaining hydrogen atoms of each glucose moiety were assigned common variable isotropic temperature factors.

Table 4.4 Details of the data collection and refinement parameters for the MPBCD structure

Empirical formula	$C_{42}H_{70}O_{35}•C_8H_8O_3•7.2H_2O$
Formula weight	1416.8
Crystal system	Monoclinic
Space group	C2
a / Å	18.8632 (4)
b / Å	24.4542 (5)
c / Å	15.5942 (5)
α / °	90
β / °	110.668 (1)
γ / °	90
Volume / $Å^3$	6730.4 (3)
Z	4
$Density_{calc}$ / g cm^{-3}	1.398
μ (MoKα) / mm^{-1}	0.125
F(000)	3016
Temperature of data collection / K	293 (2)
Crystal size / mm^3	0.32 x 0.18 x 0.10
Range scanned θ / °	$2 \leq \theta \leq 28$
Index ranges	h: -22, 24 k: -31, 31 l: -19, 20
ϕ scan angle / °	1.0
ϕ scan range, frames	183.0°, 183
ω scan angle / °	1.0
ω scan ranges, frames	44.0°, 44 and 23.0°, 23 and 68.0°, 68
Dx / mm	33
Total no. of reflections collected	21970
No. of independent reflections	14557
No. of reflections with $I > 2\sigma(I)$	10463
No. of parameters	771
R_{int}	0.0200
S	1.067
R_1 (for 8090 reflections)	0.1004
Reflections omitted	(0 0 2); (0 -2 1); (-1 1 2); (1 3 0); (1 -3 0); (-1 3 1); (1 5 0); (1 -5 0); (2 0 0); (2 2 0); (-2 2 1); (-2 -2 2); (-2 2 2); (3 1 0); (3 -3 0)
wR_2	0.2548
Weighting scheme	a = 0.1996 b = 1.8270
$(\Delta / \sigma)_{mean}$	< 0.103
Δρ excursions / e.$Å^{-3}$	0.83 and -0.83

Fourteen positions were located for the water molecules and each was assigned a fixed U_{iso} of 0.11 $Å^2$ while the site-occupancy factors were allowed to refine. The site occupancies of the water molecules varied in the range 0.23-0.86 and are listed in Table 4.5. The total number of accounted water molecules per asymmetric unit was 6.8, as compared to the 7.2 water molecules expected from the TGA results. The hydrogen atoms of the water molecules were not located.

Table 4.5 Site occupancy values of the water molecules per asymmetric unit

Water molecule	s.o.f.	Water molecule	s.o.f.
O(1WA)	0.45	O(1WB)	0.44
O(2WA)	0.47	O(2WB)	0.25
O(3W)	0.29	O(4WA)	0.46
O(4WB)	0.54	O(4WC)	0.23
O(5W)	0.70	O(6W)	0.86
O(7WA)	0.70	O(7WB)	0.40
O(8WA)	0.53	O(8WB)	0.44

Modelling of the methyl paraben guest

The UV spectrophotometry experiments indicated that a single methyl paraben molecule was included per β-CD molecule. It became apparent during the course of the refinement that this guest molecule was disordered within the CD cavity, as additional residual density was found around the guest atomic positions. After careful inspection of the difference map, the two positions of the hydroxyl oxygen atoms of the guest were found to be located at the primary rim of the CD cavity. The two peaks, of approximately equal electron density, were assigned s.o.f.'s of 0.5 each. Initial placement of the two phenyl rings was challenging. After analysing the electron density map very carefully, peaks were chosen that corresponded to two geometrically reasonable positions for the phenyl rings consistent with the position of the hydroxyl oxygen atoms. The atoms of each phenyl ring were assigned s.o.f.'s of 0.5 and the rings were constrained as rigid hexagons using the AFIX 66 instruction. Refinement of these two positions was successful, yielding an electron density map that led to the placement of the two ester substituents. The ester substituents were refined with s.o.f.'s of 0.5 each. The two positions of the guest will be referred to with the suffixes **A** and **B**.

The geometries of the models were then optimised with distance and angular constraints on certain bonds, namely: O(1)–C(2) 1.354 Å; C(5)–C(8) 1.469 Å; C(8)–O(9) 1.217 Å; C(8)–O(10) 1.334 Å; O(10)–C(11) 1.436 Å [all with σ = 0.005 Å]. The values chosen were taken from Lin.[14] A single isotropic temperature factor was used for the non-hydrogen atoms of each position and these refined to final values of 0.19 and 0.15 $Å^2$ for **A** and **B** respectively. The hydrogen atoms attached to the carbon atoms of the guest were also inserted at idealised positions and assigned a common isotropic temperature factor. The hydrogen atom of the hydroxyl group was placed using the rotating group refinement strategy [AFIX 147]. The two positions and the numbering scheme [labelled **A** in blue and **B** in green] for the methyl paraben molecules can be seen in Figure 4.9.

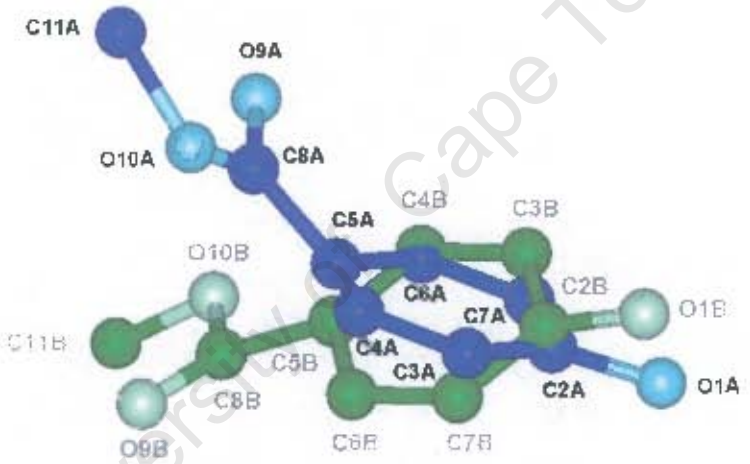

Figure 4.9 A plot of the two disordered positions [**A** and **B**] of the methyl paraben guest

At the end of the refinement there were still three significant electron density peaks unaccounted for with heights between 0.83 and 0.81 $e.Å^{-3}$. One of these peaks was found at a distance of 0.7 Å from O(6G2). Hydrogen atoms were placed on O(6G2) before and after isotropic temperature refinement, but the remaining electron density was still not accounted for. The possibility that this electron density peak represented a disordered oxygen atom was rejected on the basis of the unfavourable geometric position relative to those atoms already placed. Attempts to refine the other two peaks as water molecules were unsuccessful as clusters of electron density would collect around these atoms after further refinement and would invariably lead to unsuitable close contacts with the CD atoms.

Geometrical analysis of the MPBCD structure

The asymmetric unit of the MPBCD structure contains a single β-CD molecule, its associated guest and 7.2 water molecules. The structure and numbering scheme of the β-CD molecule and water molecules are shown in Figure 4.10. The glucose units will be referred to as G1, G2, G3, G4, G5, G6 and G7. The guest is disordered over two positions which will be referenced with the suffixes **A** [in blue] and **B** [in green]. The geometrical data for the β-CD molecule are listed in Tables 4.6 and 4.7 [e.s.d.s are in the range 0.005-0.007 Å for distances and 0.12-0.47° for angles].

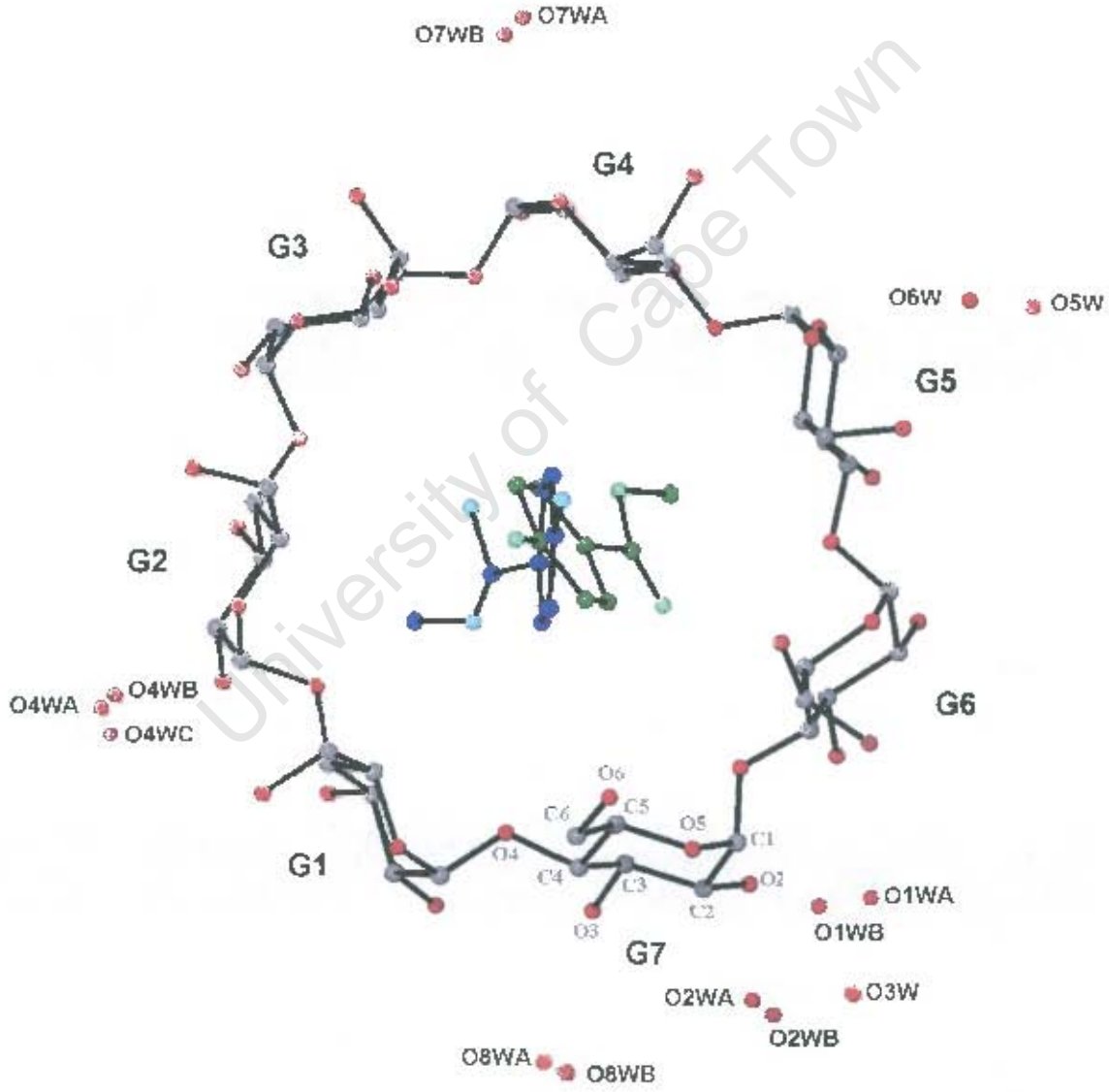

Figure 4.10 Macrocyclic structure and numbering scheme of glucose residues and water oxygen atoms, with the hydrogen atoms excluded. The host is viewed from the primary face.

The glucose residues are all in the $^{c}C_1$ chair conformation. The C(6)–O(6) bonds of the G1, G2, G4 and G5 residues are directed away from the cavity and are in the (-) *gauche* conformation to the C(4)–C(5) and O(5)–C(5) bonds. The C(6)–O(6) bonds of the G7 residue points towards the cavity in the (+) *gauche* conformation. The O(6) atoms of the G3 and G6 residues are disordered over two sites. The major position of the O(6) atom of the G3 residue adopts the (+) *gauche* conformation while the minor position adopts the (-) *gauche* conformation. The reverse of this is seen for the G6 residue, with the major position adopting the (-) *gauche* conformation and the minor position adopting the (+) *gauche* conformation. The geometric parameters of the O(4) heptagon of the MPBCD structure are listed in Table 4.6. These include the radii, the O(4)•••O(4') distances, the O(4)•••O(4')•••O(4'') angles, the O(4)•••O(4')•••O(4'')•••O(4''') torsion angles and the deviations of each of the O(4) atoms from the mean O(4) plane. Table 4.7 lists the other important features of the macrocyclic structure such as the intersaccharidic bond angle (φ), the O(2)•••O(3') distance and the tilt angles [τ_1 and τ_2]. These parameters are defined in Chapter 1.

Table 4.6 Geometrical parameters of the O(4) heptagon for the MPBCD structure

Glucose unit	Radii (Å)	O(4)•••O(4') (Å)	O(4) angle (°)	Torsion angle (°)	Deviation (Å)
G1	4.88 (1)	4.50	132	2.3 (3)	0.02
G2	5.02 (1)	4.29	129	-4.5 (2)	0.10
G3	5.23 (2)	4.39	124	-0.1 (2)	-0.06
G4	4.98 (1)	4.42	131	4.7 (2)	-0.06
G5	4.93 (1)	4.41	130	-2.2 (2)	0.09
G6	5.12 (2)	4.31	127	-3.1 (2)	0.02
G7	5.15 (1)	4.33	126	3.2 (2)	-0.10
Average	**5.04**	**4.38**	**128**	**2.8**	**0.06**

Table 4.7 φ, O(2)•••O(3') distance, τ for the MPBCD structure

Glucose unit	φ (°)	O(2)•••O(3') (Å)	τ_1 (°)	τ_2 (°)
G1	119	2.78	1.0 (2)	3.9 (2)
G2	117	2.76	7.4 (2)	10.4 (2)
G3	117	2.82	8.9 (2)	13.8 (2)
G4	118	2.90	3.9 (2)	7.5 (2)
G5	120	2.83	8.0 (1)	10.1 (2)
G6	118	2.78	7.0 (2)	10.7 (2)
G7	119	2.84	5.5 (2)	8.0 (3)
Average	**118**	**2.82**	**6.0**	**9.2**

On the whole, the O(4) heptagon has a high degree of planarity and shows a seven-fold symmetry based on the O(4)•••O(4') distances and O(4)•••O(4')•••O(4") angles. The shape of the macrocycle is defined by the tilt angles. The dihedral angles between the plane of the macrocycle and the optimum planes that define the relative orientation of each glucose residue show that all have a positive tilt angle and lean towards the centre of the cavity. This gives the cyclodextrin the characteristic truncated cone shape with the secondary rim being wider than the primary rim. The complex unit forms a dimer whose geometry is described below.

Guest geometry and interactions for the MPBCD structure

Two torsion angles can be used to define the three-dimensional conformation of the methyl paraben molecule. These torsion angles define the rotational orientations that can be adopted by the ester residue. The torsion angles δ_1 [C(6)–C(5)–C(8)–O(9)] and δ_2 [C(5)–C(8)–O(10)–C(11)], will be used to describe rotation around the C(5)–C(8) and C(8)–O(10) bonds respectively. They were compared with the conformation of the free methyl paraben molecule [Figure 4.11].[14] The torsion angles of the complexed methyl paraben have a larger out-of-plane twist than those of the uncomplexed paraben, indicating that inclusion allows for more rotational freedom around the C(5)–C(8), and C(8)–O(10) bonds. The torsional changes could reflect changes in conformation which would assist in the more efficient inclusion of the methyl paraben molecules in the β-CD dimer. The close contact distances for the relevant interactions between the host and guest molecule are listed in Table 4.8.

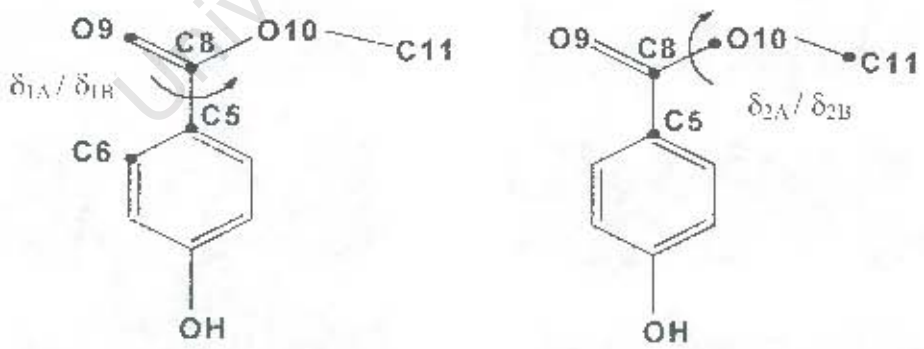

MP in complex A	δ_{1A} = 14 (2)	δ_{2A} = 173 (2)
MP in complex B	δ_{1B} = 25 (2)	δ_{2B} = 173 (1)
MP uncomplexed:[14]	δ_1 = -0.6	δ_2 = -177

Figure 4.11 Torsion angles δ_1 and δ_2 of the methyl paraben

Table 4.8 Close contact distances for the MPBCD structure

Interaction	Distance (Å)
C(11A) ••• H(321)	2.69 (2)
H(11A) ••• C(3G2)	2.88 (5)
H(11A) ••• H(321)	2.20
H(11B) ••• H(321)	2.29
H(3B) ••• H(531)	2.39
C(11B) ••• H(351)	2.85 (2)
H(11D) ••• H(351)	2.26

Figure 4.12 shows the CPK diagrams for a dimer of the MPBCD structure. The upper half of the dimer includes the position of **A** [with the carbon atoms in blue, oxygen atoms in light blue and hydrogen atoms in purple]. The lower half includes the position of **B** [with the carbon atoms in green, oxygen atoms in light green and hydrogen atoms in yellow]. The hydroxyl group of the guest is situated near the primary rim of the dimer with the ester moiety contained within the secondary hydroxyl interface of the dimer. This figure illustrates how the two methyl paraben molecules are completely contained within the β-CD dimer. This is achieved by tilting the guest molecule with respect to the mean O(4) plane of the CD. The phenyl rings of **A** and **B** form angles of 82.9 (6)° and 72.6 (4)° respectively with the mean O(4) plane. The tilting permits the guest to occupy most of the available space in the cavity and is necessary to avoid abnormally close contacts of the ester residues.

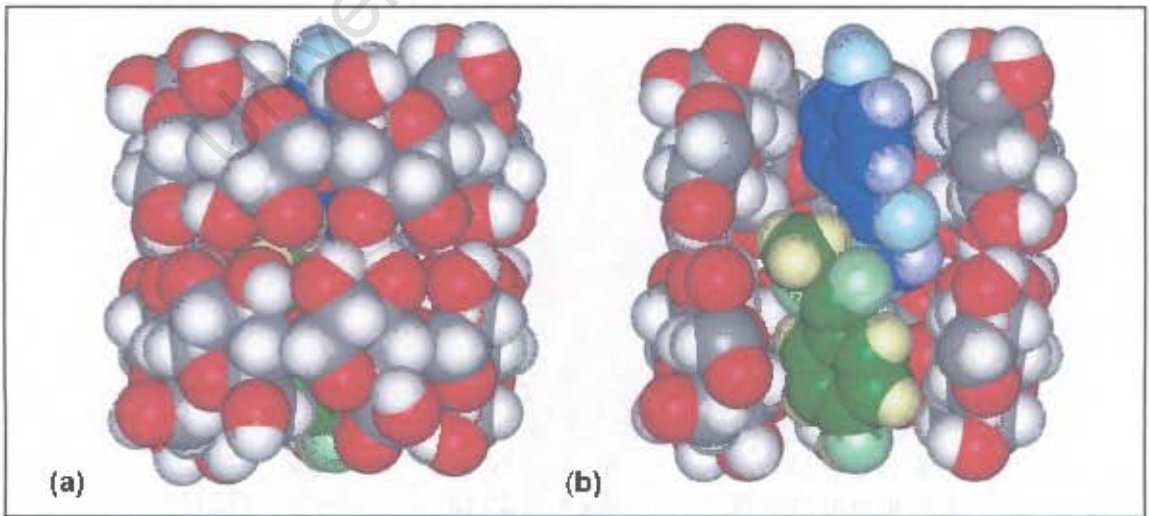

Figure 4.12 Space-filling diagram of the MPBCD structure (a) side view (b) sectioned view of the same orientation, showing guest **A** and **B**§ [the C_2-related counterpart of molecule **B** of the asymmetric unit]

An important feature of the disorder of the guest molecule is that the ester portions of both **A** and **B** are involved in unacceptably close contacts with their two-fold related counterparts [C(11A)•••C(11A)§ distance is 1.1 Å and the C(11B)•••C(11B)§ distance is 1.5 Å]. This implies that **A** [or **B**] and its two-fold related position cannot be present in a single β-CD dimer of the MPBCD structure. Therefore, the two-fold symmetry required by the space group C2 cannot always be maintained within a single dimer. However, it is possible that if the two positions were present in equal proportions in the crystal of the complex then the average structure would still maintain C2 symmetry [Figure 4.13]. A likely scenario for the disorder is one where, in any given dimer, **A** and **B** are present in opposite halves of the dimer as shown in Figure 4.12(b) [C(11A)•••C(11B)§ distance is 5.3 Å].

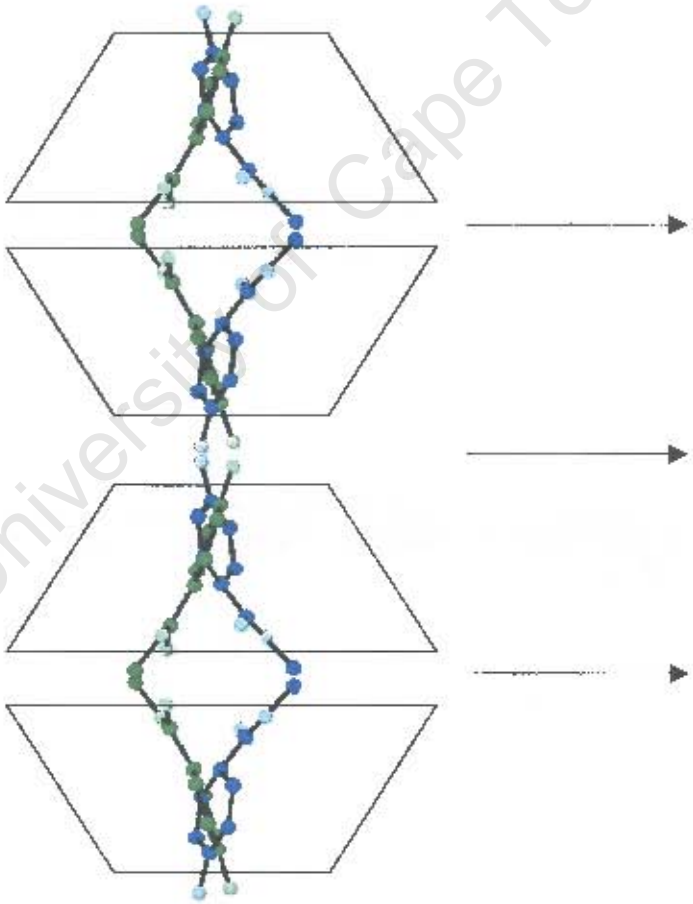

Figure 4.13 A schematic diagram of the guest **A** [blue] and **B** [green] in the dimer unit, viewed down the a-axis [excluding the hydrogen atoms]

Hydrogen bonding interactions of the MPBCD structure

Host interactions

The host molecules are stabilised by seven intramolecular O(2)•••O(3') hydrogen bonds on their secondary faces, as reported with other β-CD structures.[5-25] These hydrogen bonds contribute to the rigidity and highly symmetrical conformation of the cyclodextrin. Two host molecules form a head-to-head dimer with C_2 symmetry. The dimers are stabilised by seven intermolecular O–H•••O hydrogen bonds which involve the O(3) hydroxyl groups. The O(3)•••O(3) bonds were chosen over and above the O(2)•••O(2) and O(2)•••O(3) type hydrogen bond candidates as they were found to have shorter and more favourable O–H•••O geometries. Additionally, inter-dimer hydrogen bonds occur between cyclodextrin layers. Table 4.9 lists these lengths.

The conformation of each β-CD molecule is further stabilised by one intra- and four intermolecular C–H•••O hydrogen bonds [Table 4.10] These encompass a C(6)–H•••O(5') hydrogen bond, a C(1)–H•••O(2) hydrogen bond, a C(2)–H•••O(3) hydrogen bond and two C(6)–H•••O(6) hydrogen bonds. The latter two bonds involve the disordered O(6G6) atoms, and are an indication that disorder in the CD adds to the overall stability of the structure. All the C•••O distances are in the range 3.1-3.4 Å.

Table 4.9 Summary of the appropriate contacts for the cyclodextrin and inter-layer interactions

Type		Number / dimer	Range (Å)	Mean (Å)
Cyclodextrin interactions				
	O(2)•••O(3')	7	2.76 - 2.90	2.82
Dimer formation:	O(3)•••O(3[§])	7	2.76 - 2.89	2.85
Intra-layer interactions				
O(2G1)•••O(2G6)[']		2	2.76	2.76
O(6G1)•••O(6G4)['']		2	2.86	2.86
O(6G2)•••O(6G4)[''']		2	2.90	2.90

[§] Two-fold related counterpart
['] Related by symmetry operation: $1^1/_2$-x, $^1/_2$+y, 1-z
[^] Related by symmetry operation: $^1/_2$+x, $^1/_2$+y, z
[#] Related by symmetry operation $^1/_2$-x, $^1/_2$+y, -z

Table 4.10 C–H•••O hydrogen bonds in the MPBCD structure*

				Distance (Å)		Angle (°)
C	H	O	C–H	H•••O	C•••O	C–H•••O
Intramolecular hydrogen bonds						
C(6G4)	H(642)	O(5G5)	0.97	2.57	3.361 (8)	138.4 (5)
Intermolecular hydrogen bonds						
C(1G1)	H(111)^{i}	O(2G5)^{i}	0.98	2.50	3.294 (7)	138.4 (4)
C(2G6)	H(261)^{ii}	O(3G2)^{ii}	0.98	2.44	3.304 (8)	147.3 (4)
C(6G4)	H(641)^{iii}	O(66A)^{iii}	0.97	2.54	3.16 (2)	122.0 (5)
C(6G5)	H(651)^{iii}	O(66B)^{iii}	0.97	2.52	3.28 (2)	135.6 (5)

^{i} Related by symmetry operation: $^{1}/_{2}$+x, $^{1}/_{2}$+y, z
^{ii} Related by symmetry operation: $^{1}/_{2}$+x, -$^{1}/_{2}$+y, z
^{iii} Related by symmetry operation: -x, y, -z
* Hydrogen bonding parameters based on idealised hydrogen atom positions.

In addition to these hydrogen bonds a direct hydrogen bond is found between adjacent O(6) layers along the channel. The minor position of O(63B) is bonded to a symmetry related atom O(63B) [symmetry operation -x, y, -z]. The length of this bond is 2.61(4) Å, with a C(6G3)-O(63B)•••O(63B) angle of 121°.

Guest interactions

The hydrogen bonding distances for the relevant interactions between the host and guest molecule are listed in Table 4.11. The atom O(1A) is within hydrogen bonding contact of the primary hydroxyl atoms O(66B) and O(6G7). The O(66B) host oxygen atom is one of the disordered positions of the O(6) atom of glucose residue G6. The atom O(1B) is within hydrogen bonding contact of the primary hydroxyl atom O(6G7). The O(1B)•••O(6G7) bond may be classified as a strong hydrogen bond from the O•••O distance of 2.55(3) Å.[26] The O(66B) and O(6G7) atoms adopt a (+) *gauche* orientation on account of this hydrogen bonding to the guest molecule, thus adding to the overall stability of the inclusion complex.

Table 4.11 Hydrogen bonding distances between the host and the guest molecule*

				Distance (Å)		Angle (°)
Donor(D)	H	Acceptor(A)	D–H	H•••A	D•••A	D–H•••A
O(66B)	H(66B)	O(1A)^{i}	0.82	2.14	2.70 (4)	125 (2)
O(1A)		O(6G7)^{i}			2.76 (4)	
O(1B)		O(6G7)^{i}			2.55 (3)	
C(3B)	H(3B)	O(6G7)^{i}	0.93	2.67	3.33 (2)	128 (1)

^{i} Related by symmetry operation: 1-x, y, -z
* Hydrogen bonding parameters based on idealised hydrogen atom positions.

Water interactions

Thermogravimetric analysis gave a weight loss that corresponds to 7.2 water molecules per 1:1 complex unit, of which 6.8 water molecules were accounted for in the crystallographic analysis. Many of the water molecules were found to be disordered over two positions. All of these waters are situated at the periphery of the cyclodextrin molecule, filling the intermolecular space between complex units. All the primary hydroxyls [except O(6G2) and O(6G7)] are attached to at least one water molecule.

Two water molecules O(5W) and O(8WB) do not bond directly to a cyclodextrin molecule but are connected to other water molecules. The water molecules that interact with the O(6) rim of the cyclodextrin, O(1WA), O(2WA), O(6W), and O(7WA) form bridges between adjacent dimers in the same layer, while those that interact with the secondary rim, O(2WB), O(3W), O(4WA-C) and O(8WA) indirectly form part of an infinite sub-layer of water molecules that run between the cyclodextrin channels. Two networks of water molecules form hydrogen bonds to primary and secondary hydroxyl groups. Hence the water molecules were found to be involved in many hydrogen bonds, which stabilise the crystal packing. There are no water molecules positioned inside the cyclodextrin cavity. Hydrogen bonding distances between the host and these water molecules are listed in Tables 4.12 and 4.13 and are illustrated in Figure 4.14.

Table 4.12 C–H•••O hydrogen bonds between the host and the water molecules*

			Distance (Å)			Angle (°)
Donor(D)	H	Acceptor(A)	D–H	H•••A	D•••A	D–H•••A
O(66A)	H(66A)	O(1WA)	0.82	2.00	2.77 (2)	156 (1)
O(2G7)	H(272)	O(3W)	0.82	2.01	2.67 (3)	137 (1)
O(2G2)	H(222) ^{i}	O(4WC) ^{i}	0.82	2.12	2.92 (4)	164 (1)
O(6G5)	H(653)	O(6W)	0.82	2.03	2.74 (1)	144.5 (6)
C(6G2)	H(622) ^{ii}	O(6W) ^{ii}	0.97	2.93	3.42 (1)	112.2 (6)
C(1G4)	H(141)	O(7WA)	0.98	2.83	3.42 (2)	119.4 (6)
C(1G4)	H(141)	O(7WB)	0.98	2.49	3.14 (4)	123.6 (9)
O(2G3)	H(232) ^{i}	O(8WA) ^{i}	0.82	2.13	2.80 (3)	139.0 (7)

^{i} Related by symmetry operation: $1^{1}/_{2}$-x, $-^{1}/_{2}$+y, 1-z
^{ii} Related by symmetry operation: $^{1}/_{2}$-x, $^{1}/_{2}$+y, -z
* Hydrogen bonding parameters based on idealised hydrogen atom positions.

Table 4.13 Hydrogen bonding distances involving the water molecules

Interaction	Distance (Å)	Symmetry operator for the second oxygen atom listed
O(2WA) ••• O(63A)	2.81 (2)	1-x, y, -z
O(2WA) ••• O(63B)	2.84 (4)	1-x, y, -z
O(2WB) ••• O(3G3)	2.92 (4)	1+x, y, z
O(4WA) ••• O(2G2)	2.63 (3)	x, y, z
O(4WA) ••• O(3G6)	2.83 (3)	$-^1/_2$+x, $^1/_2$+y, z
O(4WB) ••• O(2G2)	2.81 (3)	x, y, z
O(4WB) ••• O(3G1)	2.79 (2)	1-x, y, 1-z
O(4WB) ••• O(3G6)	2.67 (2)	$-^1/_2$+x, $^1/_2$+y, z
O(4WC) ••• O(2G4)	2.81 (5)	$^1/_2$-x, $^1/_2$+y, 1-z
O(7WA) ••• O(6G1)	2.70 (3)	$-^1/_2$+x, $-^1/_2$+y, z
O(7WA) ••• O(6G4)	2.89 (2)	-x, y, -z
O(8WA) ••• O(3G5)	2.74 (2)	1-x, y, 1-z
O(1WA) ••• O(2WA)	2.86 (3)	x, y, z
O(1WA) ••• O(7WA)	2.56 (4)	1+x, y, z
O(1WA) ••• O(7WB)	2.69 (5)	1+x, y, z
O(1WB) ••• O(2WB)	2.72 (3)	x, y, z
O(1WB) ••• O(7WA)	2.80 (4)	1+x, y, z
O(1WB) ••• O(7WB)	2.72 (5)	1+x, y, z
O(2WA) ••• O(5W)	2.75 (3)	$^1/_2$+x, $^1/_2$+y, z
O(2WB) ••• O(3W)	2.56 (4)	2-x, y, 1-z
O(3W) ••• O(4WA)	2.71 (4)	$^1/_2$+x, $-^1/_2$+y, z
O(3W) ••• O(4WC)	2.64 (5)	$^1/_2$+x, $-^1/_2$+y, z
O(5W) ••• O(6W)	2.74 (2)	x, y, z
O(5W) ••• O(8WA)	2.85 (2)	$1^1/_2$-x, $-^1/_2$+y, 1-z
O(8WB) ••• O(8WB)[§]	2.61 (4)	2-x, y, 1-z

[§] Two-fold related counterpart

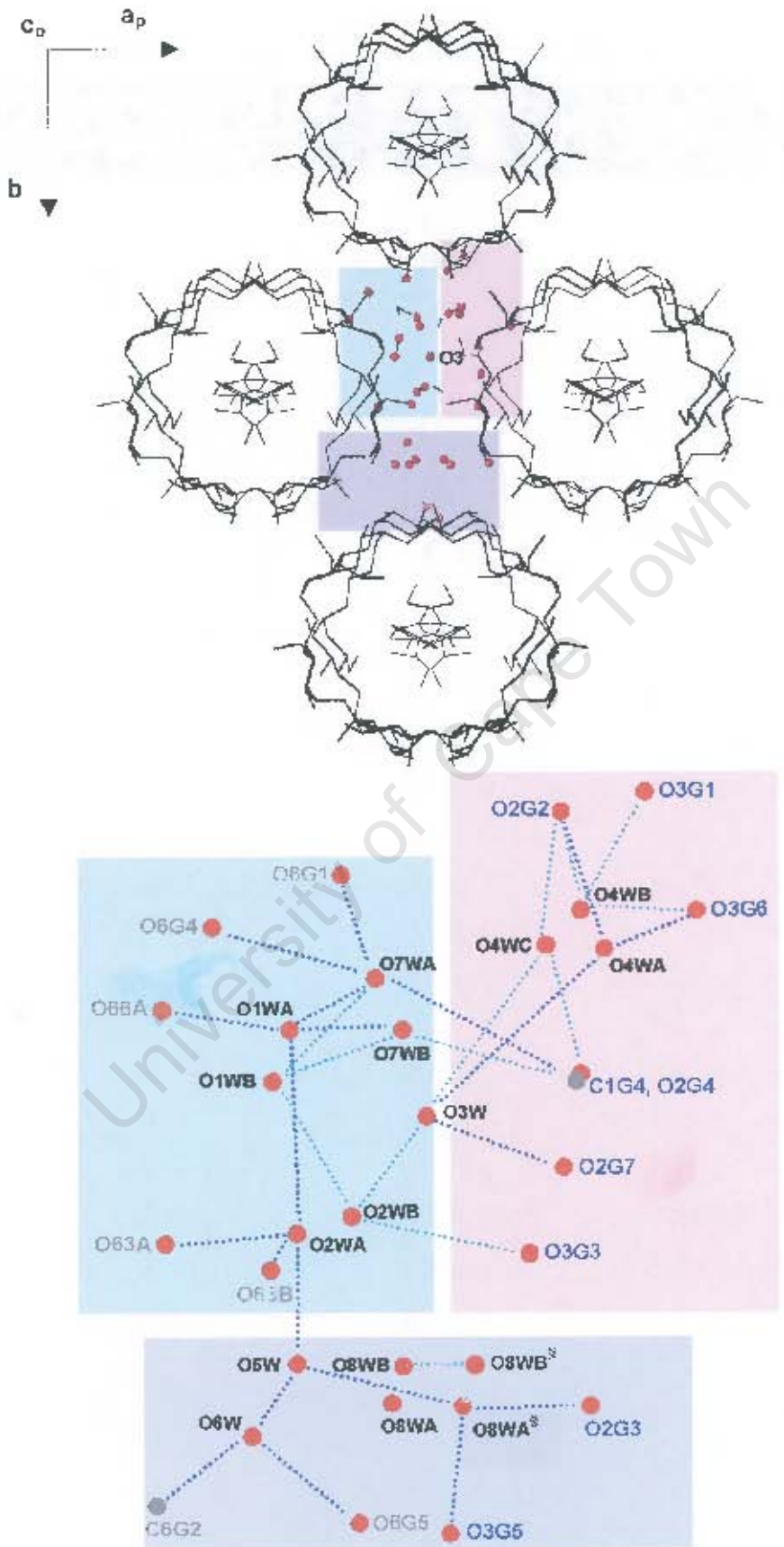

Figure 4.14 A schematic representation of the water molecules that connect adjacent host units

Crystal packing of the MPBCD structure

Figure 4.15 is an extended stereo packing diagram of the MPBCD structure projected down the *c*-axis and illustrates the "endless" channels formed by the dimer columns along the *c*-axis. Successive dimers within a channel are directly linked by hydrogen bonding between the primary hydroxyl groups. The two-fold axes [indicated as arrows in Figure 4.15] run parallel to the *b*-axis and are present at positions 0, $^1/_2$ and 1 along both the *a*- and *c*-axes. The two-fold axes relate the two β-CD molecules of a dimer to one another as well as relating adjacent dimers. The MPBCD structure is characteristic of the channel type packing motif for β-CD dimers.[15,25] The dimers are arranged in C-centred layers and are stacked upon each other parallel to the *c*-axis to form almost linear channels. The relative average shift of consecutive dimers, when the dimers are viewed perpendicular to their mean O(4) planes is reported as 2.7 (2) Å for the channel type structures crystallising in the space group C2.[4] These dimeric layers are a feature of all dimeric β-CD structures. The dimeric layers stack on top of one another with a single dimer layer forming the repeating array of the structure. Disorder of the included guest is often observed in structures of the channel type packing mode crystallising in the space group C2,[15-20, 22, 24-25] as was observed in the MPBCD structure. In only a few cases [e.g. ethyl-*p*-amino-benzoate,[16] paracetamol,[27] sesquikis coumarin,[28] dimethyl coumarin[29] and cinnamic acid[30]] has it been possible to resolve the disorder of the guest in this structural arrangement.

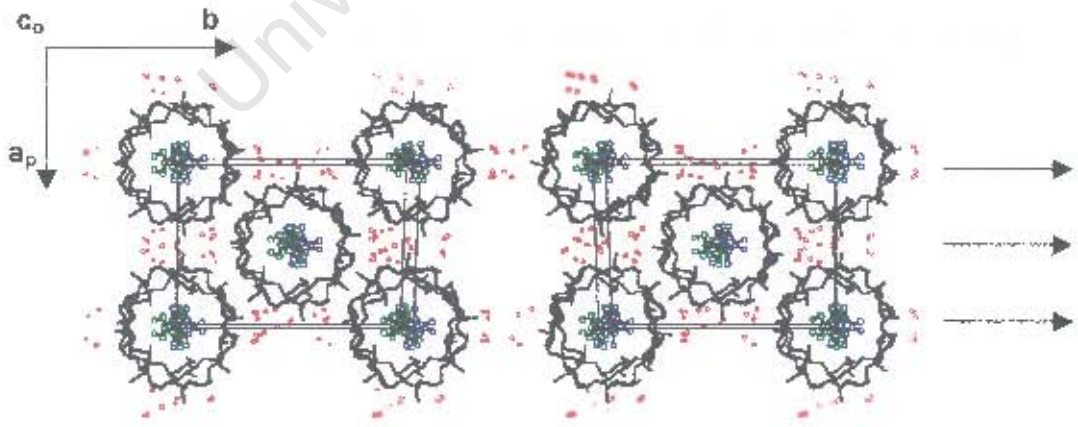

Figure 4.15 Stereo packing diagram of the MPBCD structure [*c*-axis projection]

Comparative XRD

The experimental X-ray powder diffraction pattern of MPBCD was successfully matched with that calculated from the single crystal structure data [Figure 4.16]. This indicates that the sample has the same crystalline structure as that of the MPBCD complex whose single crystal X-ray structure is reported here.

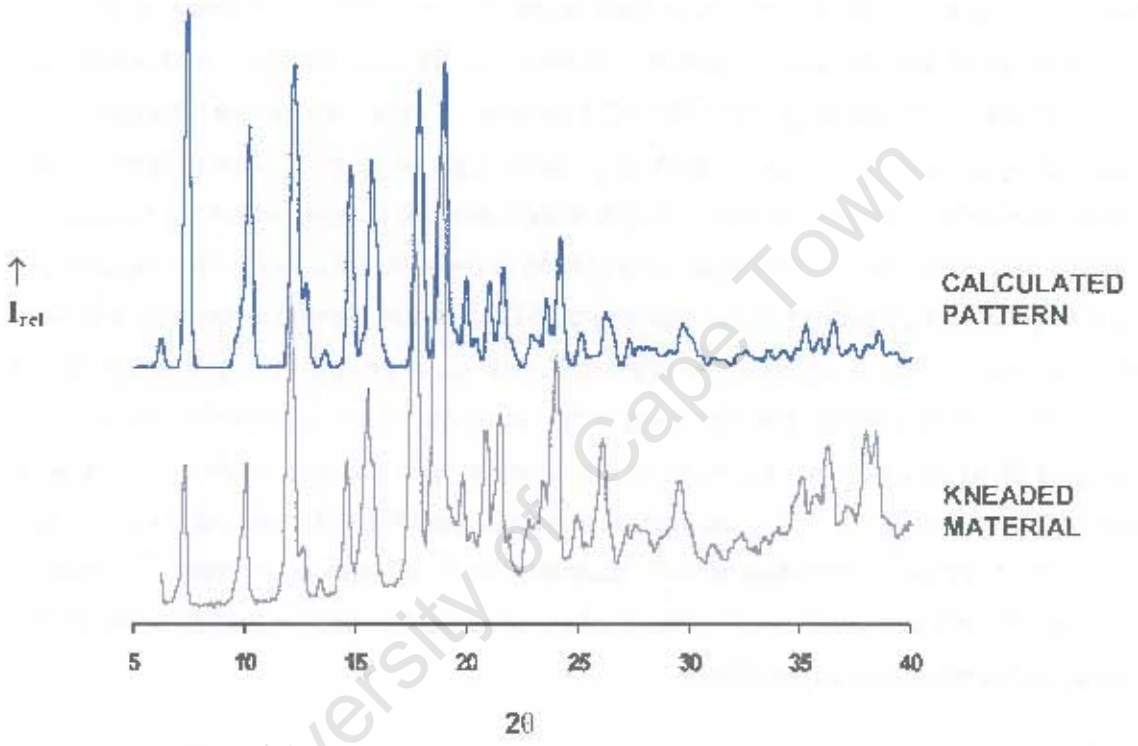

Figure 4.16 Experimental and calculated XRD traces for the MPBCD structure

ISOLATION OF A SECOND CRYSTALLINE MODIFICATION OF THE β-CD METHYL PARABEN COMPLEX

In addition to the MPBCD inclusion complex, crystals of a second complex between β-CD and methyl paraben were grown at 7°C [hereinafter MPBCDP1]. The crystals were prepared by heating and stirring a solution of cyclodextrin and drug in a 1:1 molar ratio, in a sealed flask at 45°C for 2 hours. This was followed by a hot filtration to remove any undissolved material. The solution was then allowed to cool to room temperature before being placed in the refrigerator at 7°C. Block-shaped transparent crystals of the complex were obtained after 1 month.

Preliminary physicochemical studies indicated that an inclusion complex had formed and that these crystals were different from those grown under ambient conditions. These two complexes can therefore be considered to be polymorphs of each other, as they are chemically identical but have different physical properties owing to the different internal organisation within the solid. According to McCrone "A polymorph is a solid crystalline phase of a given compound resulting from the possibility of at least two different arrangements of the molecules of that compound in the solid state".[31] The situation is however complicated by the ternary nature of the complex [containing host, guest and water molecules] and the term "polymorphic pseudo-polymorphs" may be a better description of the relationship between the monoclinic and triclinic species.

THERMAL ANALYSIS OF THE INCLUSION COMPLEXES

HSM results for the MPBCD and MPBCDP1 complexes

HSM proved to be a useful technique to observe the thermal differences between the two complexes. HSM results for the MPBCD and MPBCDP1 complexes are presented in Figure 4.17. Both complexes have similar crystal habits in that they both have a flat plate-like appearance. Additionally both complexes display similar thermal events, i.e. initial cracking and bubbling indicating dehydration, followed by decomposition. However, the corresponding events occur at different temperatures.

The MPBCD crystals displayed signs of cracking after removal from the mother liquor, as they began to lose their water of crystallisation. Thereafter significant cracking was observed and by 125°C the crystals had become totally opaque. These dehydrated crystals remained unchanged till shortly before 200°C. Decomposition of the complex was evident by the discoloration of the crystals from 194°C onwards and by 350°C extensive decomposition of the complex had taken place.

The MPBCDP1 crystals started to crack at 39°C and became more and more opaque as the temperature increased to 63°C. Bubbles were observed at 103°C and became more vigorous by 115°C. This dehydration process caused the crystals to crack and break apart. Decomposition was observed as the crystals started to discolour only at a temperature of 251°C. Hence this complex had a much higher decomposition temperature than MPBCD.

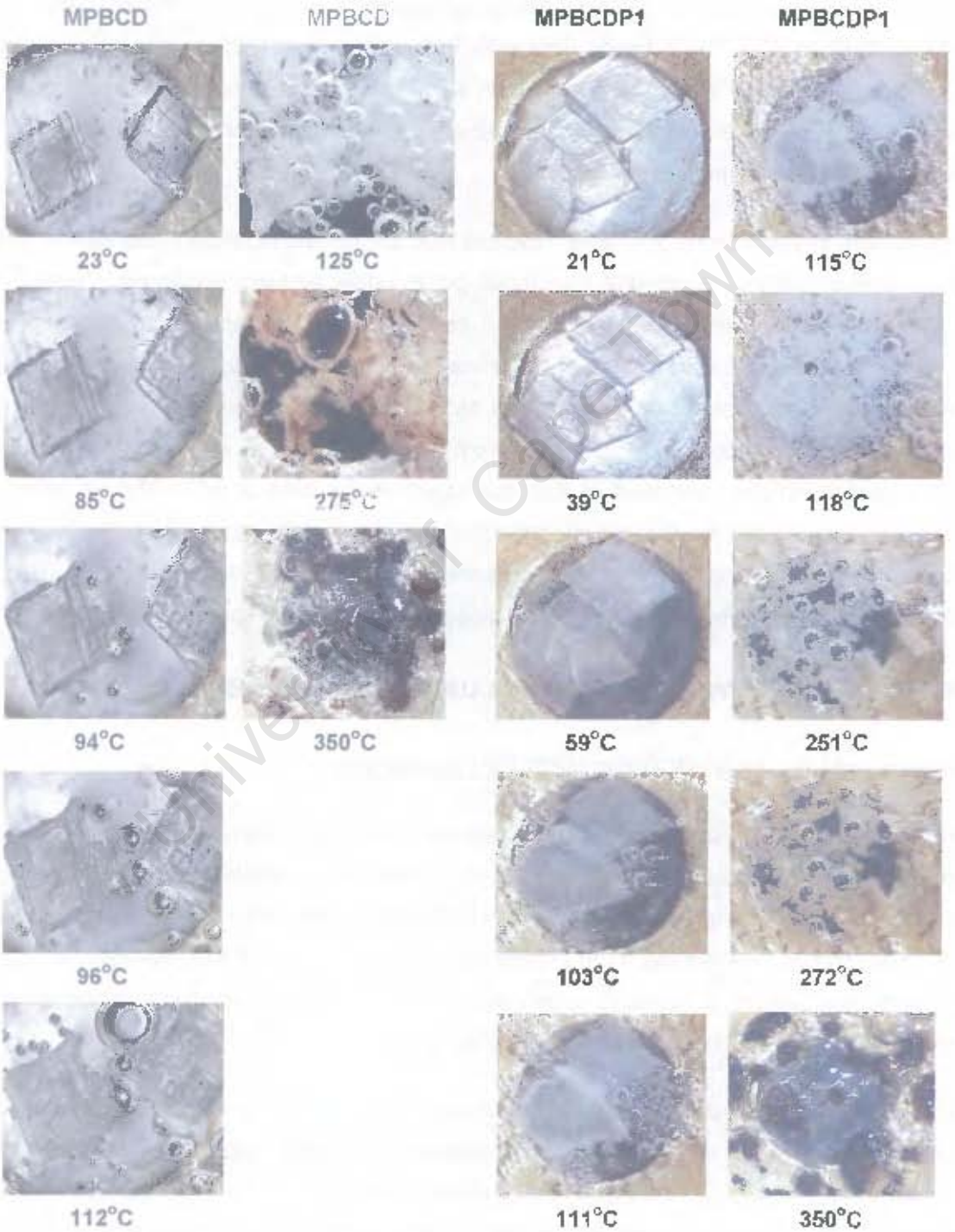

Figure 4.17 HSM photographs taken at various temperatures for crystals of the MPBCD and the MPBCDP1 complexes

TGA and DSC results for the MPBCDP1 complex

The TGA and DSC results for the MPBCDP1 complex are shown in Figure 4.18 and the results are summarised in Table 4.14. TGA results show that water loss is complete by 110°C and this event corresponds to a broad asymmetric endotherm [labelled A] in the DSC trace. The calculated number of water molecules per CD from the TGA weight loss was 14. The asymmetric shape of the dehydration endotherm is an indication that the water loss from this complex is a multi-step process as seen from the HSM results. The onset of decomposition is indicated by further mass loss on the TGA traces from 250°C [labelled B] and can be seen as a broad endotherm in the DSC trace.

Table 4.14 Summaries of TGA and DSC results for the MPBCDP1 complex

TGA results						
Temp (°C)	30	110	200	250	300	350
Sample weight (%)	100	83.6	81.0	77.7	70.4	9.85
Δ Weight loss (%) *	-	16.4	2.6	3.3	7.3	60.55
DSC results						
Temperature range	A	(°C)		30-114		
Endotherm A	T_{on}	(°C)		30		
	Peak	(°C)		71		
Temperature range	B	(°C)		307-350		
Endotherm B	T_{on}	(°C)		313		
	Peak	(°C)		331		

* Δ Weight loss (%) = [Sample weight (%) at temperature (n-1)] - [Sample weight (%) at temperature (n)]

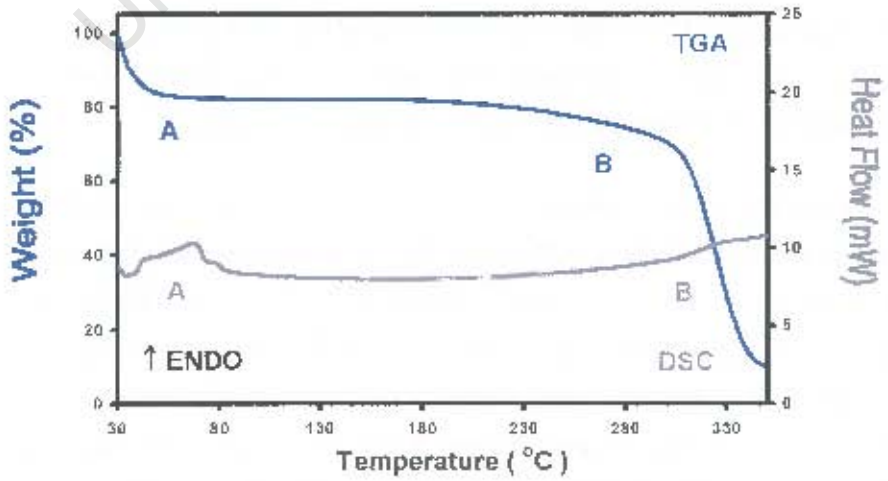

Figure 4.18 TGA and DSC traces for the MPBCDP1 complex

X-RAY CRYSTALLOGRAPHIC ANALYSIS OF THE MPBCDP1 STRUCTURE

Data-collection

The preliminary unit cell parameters and space group for the MPBCDP1 structure were determined by X-ray photographic techniques. Laue symmetry $\bar{1}$ indicated the triclinic crystal system. The chiral nature of the CD molecule determined the space group as P1.

Intensity data were collected at 173 K on the Nonius Kappa CCD diffractometer using graphite-monochromated MoKα radiation [λ = 0.71073 Å]. A single crystal was mounted on a glass fibre and covered in Paratone N oil[8] to provide a rigid mounting for the low-temperature data collection and to prevent cracking due to loss of water of crystallisation. Crystal data and data-collection parameters are listed in Table 4.15.

Structure determination and refinement

The MPBCDP1 complex crystallises in the triclinic space group P1 with two crystallographically independent β-CD molecules, two guest molecules and 28 water molecules comprising the asymmetric unit. The structure was solved using published co-ordinates for the non-hydrogen β-CD atoms of the isomorphous β-CD-4-*t*-butylbenzoic acid complex[32] [deprived of the primary hydroxyl O atoms]. This fragment was refined with SHELX-97,[13] generating a difference Fourier map that revealed the positions of the primary hydroxyl oxygen atoms. From subsequent difference Fourier maps the minor occupancy sites of three disordered primary hydroxyl groups were located [labelled **C** and **D**]. For a given pair, site-occupancy factors of x and 1-x were assigned, with x variable. The population parameters of the major sites refined to 0.69, 0.80 and 0.73 for O(6A3), O(6A5) and O(6B5) respectively. Refinement was carried out with all the host oxygen atoms anisotropic, except the disordered primary hydroxyl oxygen atoms.

Once all the non-hydrogen atoms of the host had been located the cyclodextrin hydrogen atoms were placed. The hydrogen atoms of the host molecule were calculated at idealised positions. They were included as riding, with U_{iso} set equal to 1.2 times the U_{iso} of the parent atom. All the primary hydroxyl hydrogen atoms were assigned a common variable isotropic temperature factor and were placed using the AFIX 83 instruction. After a cycle of refinement some of these H atoms were fixed, as further refinement would lead to abnormally close contacts with H atoms on the adjacent β-CD molecule.

Table 4.15 Details of the data collection and refinement parameters for the MPBCDP1 structure

Empirical formula	$(C_{42}H_{70}O_{35})_2 \cdot (C_8H_8O_3)_2 \cdot 28H_2O$
Formula weight	3078.80
Crystal system	Triclinic
Space group	P1
a / Å	18.0187 (3)
b / Å	15.3431 (4)
c / Å	15.4140 (3)
α / °	103.464 (1)
β / °	113.122 (1)
γ / °	99.254 (1)
Volume / Å^3	3656.65 (1)
Z	1
Density$_{calc}$ / g cm^{-3}	1.398
μ (MoKα) / mm^{-1}	0.128
F(000)	3288
Temperature of data collection / K	173 (2)
Crystal size / mm^3	0.45 x 0.39 x 0.25
Range scanned θ / °	2 < θ < 23
Index ranges	h: -20, 19 k: -16, 17 l: -17, 16
φ scan angle / °	1.0
ψ scan range, frames	183.0°, 183
ω scan angle / °	1.0
ω scan ranges, frames	51.0°, 51 and 27.0°, 27
Dx / mm	35
Total no. of reflections collected	18382
No. of independent reflections	18382
No. of reflections with I > 2σ(I)	16651
No. of parameters	1213
R_{int}	0.0000
S	1.071
R_1 (for 10403 reflections)	0.0937
Reflections omitted	(0 -1 1); (-1 -1 0); (1 -1 1); (1 -2 0); (-1 2 0)
wR_2	0.2574
Weighting scheme	a = 0.1573 b = 10.5453
$(\Delta / \sigma)_{max}$	< 0.028
Δρ excursions / e Å^{-3}	0.67 and -0.67

The R_{int} of < 0.0001 is not an artefact as the data were checked and Friedel opposites were present.

Oxygen atoms of water molecules were located over thirty sites. O(1W) to O(9W) with full site-occupancy were placed and refined anisotropically with a final temperature factor U_{eq} in the range 0.05–0.10 Å^2. The remaining water molecules were refined isotropically with a constant U_{iso} of 0.08 Å^2 [the mean of the preceding U values]. O(10W) to O(17W) were refined with varying site-occupancies, while the remaining water molecules were, in most cases, disordered over two positions. The site-occupancies of the water molecules are listed in Table 4.16. A total of 25.8 water molecules per complex unit were accounted for, which compared favourably with the 28 water molecules found from thermogravimetric analysis. In view of the extensive disorder of many water molecules, no attempt was made to locate water hydrogen atoms.

Table 4.16 Site-occupancy values of the water molecules per asymmetric unit

Water molecule	s.o.f.	Water molecule	s.o.f.	Water molecule	s.o.f.
O(1W)	1.00	O(18A)	0.80	O(18B)	0.20
O(2W)	1.00	O(19A)	0.67	O(19B)	0.33
O(3W)	1.00	O(20A)	0.59	O(20B)	0.41
O(4W)	1.00	O(21A)	0.56	O(21B)	0.44
O(5W)	1.00	O(22A)	0.67	O(22B)	0.33
O(6W)	1.00	O(23A)	0.52	O(23B)	0.48
O(7W)	1.00	O(24A)	0.71	O(24B)	0.29
O(8W)	1.00	O(25A)	0.64	O(25B)	0.36
O(9W)	1.00	O(26A)	0.73	O(26B)	0.27
O(10W)	0.40	O(27A)	0.53	O(27B)	0.47
O(11W)	0.46	O(28A)	0.56	O(28B)	0.44
O(12W)	0.38	O(29A)	0.67	O(29B)	0.33
O(13W)	0.63	O(30A)	0.33	O(30B)	0.33
O(14W)	0.61	O(30C)	0.33		
O(15W)	0.51				
O(16W)	0.56				
O(17W)	0.29				

The highest residual electron density peak of 0.67 e.Å^{-3} was found within the cavity. When refined as an oxygen atom and assigned a constant U_{iso} of 0.08 Å^2 the site-occupancy factor refined to only 0.2. It was found at favourable O•••O distances [2.61 (4) and 2.68 (6) Å] from the guest O(10A) and O(10B) oxygen atoms respectively. However it additionally made unfavourable contacts with the atom C(11) of these guests and was therefore not assigned in the final refinement.

Modelling of the methyl paraben guest

The subsequent difference Fourier map revealed the position of the guest atoms. These were assigned and refined. However, the atoms of the guest displayed large isotropic displacement parameters, indicating the possibility of some disorder of the guest molecule within the β-CD cavity. The UV spectrophotometric experiments indicated that a single methyl paraben molecule was included per β-CD molecule. A difference map calculated near the end of the refinement revealed an alternative position with much lower occupancy for each of the two independent paraben guest molecules. Initial placement of the phenyl rings was challenging. After careful inspection of the map, peaks were chosen that corresponded to two geometrically reasonable positions for the phenyl ring, each of which could be reconciled with a co-planar hydroxyl oxygen atom. The atoms of each phenyl ring were constrained as rigid hexagons using the AFIX 66 instruction. This was followed by the placement of the ester substituents. Each guest and its disordered counterpart were assigned a s.o.f. of x and 1-x, with variable x. The population parameters of the major sites refined to 0.77 and 0.71 for guest **A** and **B** respectively. A single isotropic temperature factor was used for all the non-hydrogen atoms of each guest and this refined to a final value of 0.10 $Å^2$. The guest hydrogen atoms were included in geometrically calculated positions and were assigned a common isotropic temperature factor. The minor component molecules, **C** and **D**, were included in the final cycles with a conformation restrained to be similar to that of the major component molecules, **A** and **B**. The bond lengths and angles were set equal to those found in the uncomplexed methyl paraben crystals.[14] The four positions, numbering scheme and the relative position of the guest in the CD dimer can be seen in Figure 4.19. Guests with the suffixes **A**, **B**, **C** and **D** are represented in purple, green, dark red and blue respectively.

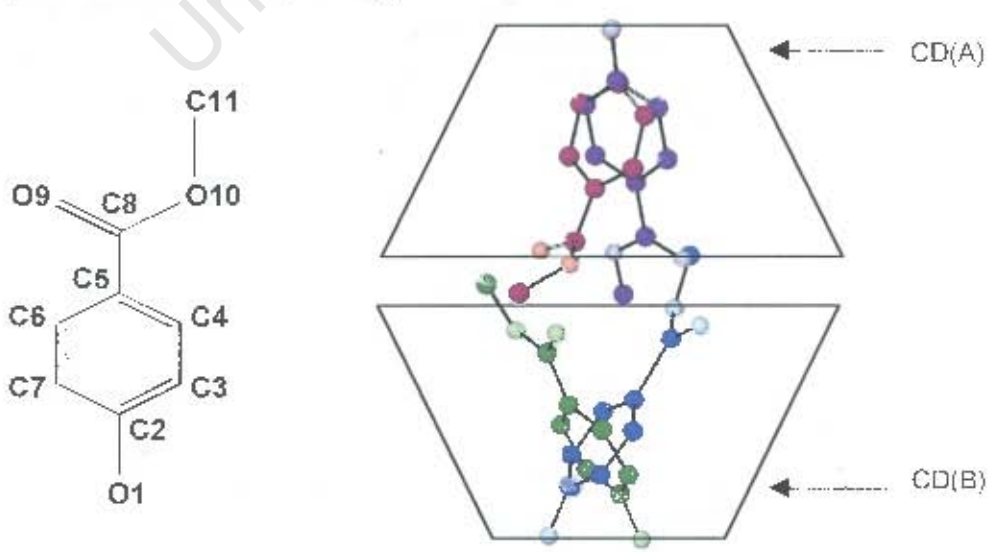

Figure 4.19 A plot of the disordered positions of the methyl paraben guest in the CD cavity

Geometrical analysis of the MPBCDP1 structure

The asymmetric unit comprises two crystallographically independent host molecules, two disordered guest molecules and 28 water molecules. The two CDs will be referred to as CD(A) and CD(B). Disordered positions on CD(A) and CD(B) were denoted C and D respectively. The glucose residues of each of the CDs are numbered one to seven, so that the glucose residues of CD(A) are A1, A2, A3, A4, A5, A6 and A7. The host numbering scheme is illustrated in Figure 4.20. The guest molecules associated with CD(A) will be referred to with the suffixes **A** and **C**, while the guest molecules associated with CD(B) will be referred to with suffix **B** and **D**. The geometrical data for the β-CD molecule are listed in Tables 4.17 and 4.18 [e.s.d.s are in the range 0.008-0.013 Å for distances and 0.19-0.77° for angles].

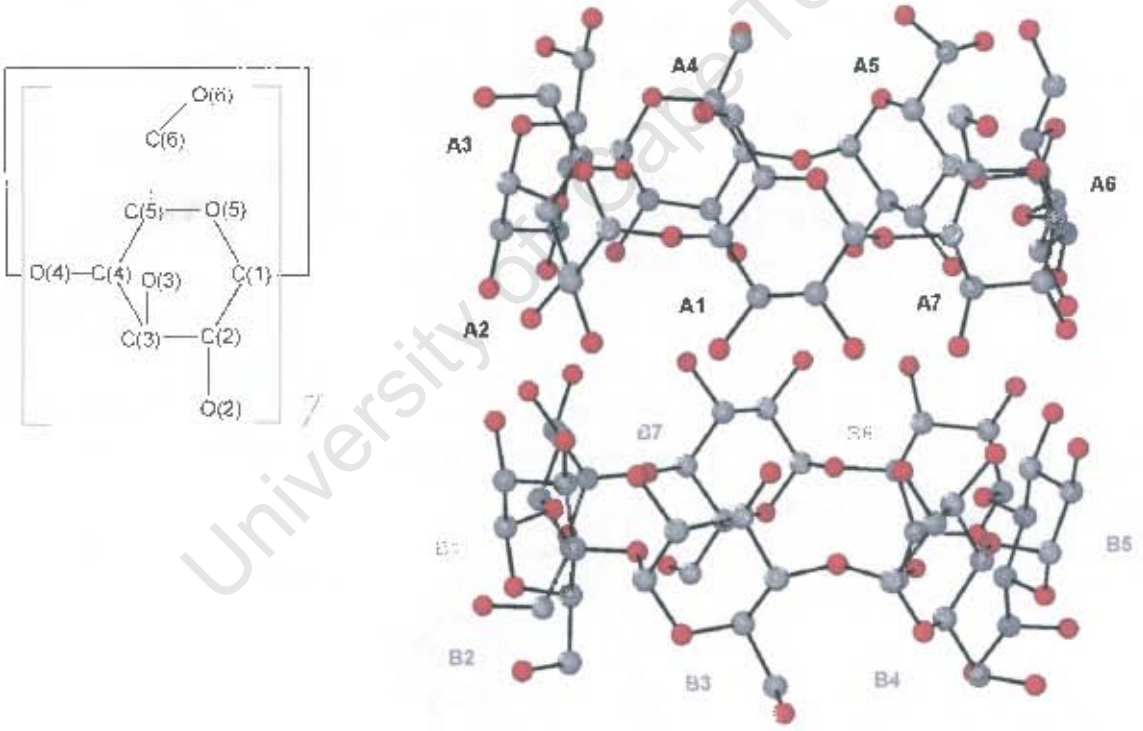

Figure 4.20 Macrocyclic structure and numbering scheme of glucose residues

The shape of the macrocycle resembles that of a hollow cylinder. All fourteen glucose residues adopt the usual $^4C_1$ chair conformation. In the host molecules A and B, two and one of the primary hydroxyl groups are disordered over two sites respectively [host A: O(6A3), O(6C3), O(6A5) and O(6C5): host B: O(6B5) and O(6D5)].

The orientations of the majority of the primary hydroxyl groups are associated with the (-) *gauche* conformation, pointing outwards. Exceptions occur for the atom O(6A6), as well as the atoms O(6C5), O(6D5) [minor positions] and O(6A3) [major position] which all point inwards [(+) *gauche* conformation].

Table 4.17 lists the geometric parameters of the O(4) heptagon of the MPBCDP1 structure for the two independent β-CD molecules A, B comprising the dimer. These include the radii, the O(4)•••O(4') distances, the O(4)•••O(4')•••O(4'') angles, the O(4)•••O(4')•••O(4'')•••O(4''') torsion angles and the deviations of each of the O(4) atoms from the mean O(4) plane. Table 4.18 lists the other important features of the macrocyclic structure such as the intersaccharidic bond angle (φ), the O(2)•••O(3') distance and the tilt angles [τ_1 and τ_2]. These parameters are defined in Chapter 1.

Table 4.17 Geometrical parameters of the O(4) heptagon for the MPBCDP1 structure

Glucose unit	Radii (Å)	O(4)•••O(4') (Å)	O(4) angle (°)	Torsion angle (°)	Deviation (Å)
CD(A)					
A1	4.93 (1)	4.28	130	2.3 (4)	-0.03
A2	5.16 (1)	4.39	126	-0.9 (4)	0.01
A3	5.09 (1)	4.31	127	0.3 (4)	0.00
A4	4.88 (1)	4.47	131	-0.2 (4)	0.00
A5	5.00 (1)	4.33	130	-0.7 (4)	-0.01
A6	5.26 (1)	4.29	123	2.4 (4)	-0.01
A7	4.89 (1)	4.50	133	-3.4 (4)	0.04
CD(B)					
B1	5.12 (1)	4.30	126	1.3 (4)	-0.01
B2	4.95 (1)	4.46	131	-3.1 (4)	-0.02
B3	5.00 (1)	4.23	129	3.3 (4)	0.04
B4	5.07 (1)	4.40	128	-1.7 (4)	-0.04
B5	5.01 (1)	4.33	129	0.0 (4)	0.00
B6	5.00 (1)	4.39	128	0.3 (4)	0.01
B7	5.00 (1)	4.37	130	-0.2 (4)	0.00
Average	**5.03**	**4.36**	**128.6**	**|1.4|**	**|0.02|**

Table 4.18 φ, O(2)•••O(3') distance.τ for the MPBCDP1 structure

Glucose unit	φ (°)	O(2)•••O(3') (Å)	τ_1 (°)	τ_2 (°)
CD(A)				
A1	120	2.83	11.9 (3)	14.8 (3)
A2	118	2.83	4.4 (3)	9.8 (4)
A3	118	2.84	8.4 (2)	12.0 (3)
A4	119	2.81	3.3 (2)	6.2 (3)
A5	117	2.73	3.4 (3)	6.6 (5)
A6	117	2.76	4.1 (2)	7.1 (4)
A7	118	2.79	2.2 (2)	6.7 (4)
CD(B)				
B1	120	2.79	4.8 (2)	9.1 (4)
B2	119	2.79	3.3 (2)	8.3 (4)
B3	117	2.82	8.8 (2)	12.8 (3)
B4	117	2.77	2.2 (2)	4.9 (4)
B5	116	2.82	9.2 (2)	12.2 (3)
B6	118	2.76	2.5 (2)	5.9 (5)
B7	119	2.76	3.4 (2)	6.6 (4)
Average	**118**	**2.79**	**5.1**	**8.8**

There is no significant difference in the conformations of the two independent β-CD molecules, A and B, and the geometric data for MPBCDP1 closely resemble those of the MPBCD structure. On the whole, the O(4) heptagon has a high degree of planarity and shows a seven-fold symmetry based on the O(4)•••O(4') distances and O(4)•••O(4')•••O(4") angles. The O(4) angles [Table 4.17] do not differ significantly from 128.6°, the angle of the regular heptagon, denoting that the cavity has not become distorted due to the inclusion of the guests. In addition the high degree of planarity is illustrated in the small deviation of the O(4) atoms from the mean O(4) plane. The planes formed by the glycosidic O atoms are almost parallel for CD(A) and CD(B). The tilt angles of the glucose units are all small and positive. This gives the cyclodextrin the characteristic truncated cone shape with the secondary rim being wider than the primary rim.

Guest geometry and interactions for the MPBCDP1 structure

Two torsion angles can be used to define the three-dimensional conformation of the methyl paraben molecule. These torsion angles define the rotational orientations that can be adopted by the ester residue. The torsion angles δ_1 [C(6)–C(5)–C(8)–O(9)] and δ_2 [C(5)–C(8)–O(10)–C(11)], will be used to describe rotation around the C(5)–C(8) and C(8)–O(10) bonds respectively. They were compared with the conformation of the uncomplexed methyl paraben molecule [Figure 4.21].[14]

In each of the modelled guests the torsion angles of the complexed methyl paraben have a larger out-of-plane twist than those of the uncomplexed MP, indicating that inclusion allows for more rotational freedom around the C(5)–C(8), and C(8)–O(10) bonds. The guest molecule **C** has the largest out-of-plane twist, while the torsion angles of the guest molecule **B** resemble those in MP. The torsional changes could represent changes in conformation, which would allow for the best possible fit of the methyl paraben molecules in the host structure. The close contact distances for the relevant interactions between the host and guest molecule are listed in Table 4.19.

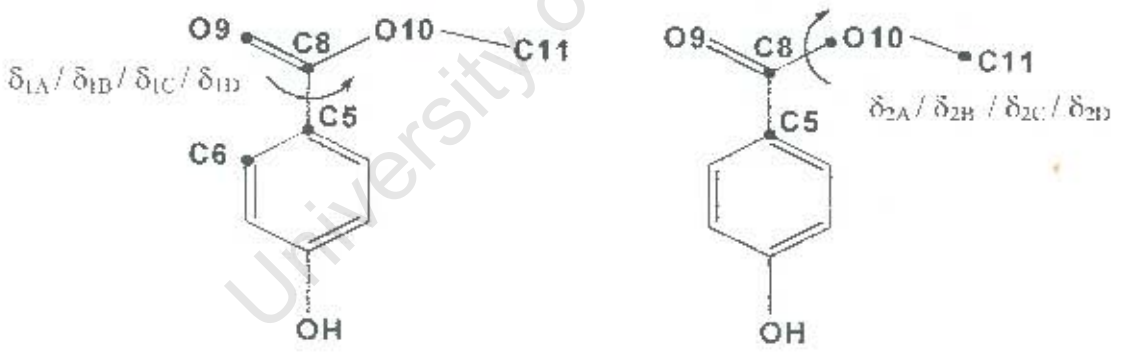

MP in conformer **A**	δ_{1A} = -8 (2)	δ_{2A} = 162 (2)
MP in conformer **B**	δ_{1B} = -5 (2)	δ_{2B} = 171 (1)
MP in conformer **C**	δ_{1C} = 11 (2)	δ_{2C} = 136 (1)
MP in conformer **D**	δ_{1D} = 1 (2)	δ_{2D} = 157 (1)
MP uncomplexed:[14]	δ_1 = -0.6	δ_2 = -177

Figure 4.21 Torsion angles δ_1, δ_2, δ_3 and δ_4 of the methyl paraben

Table 4.19 Close contact distances for the MPBCDP1 structure

Interaction	Distance (A)
H(7A) ••• H(521)	2.29
C(11A) ••• H(224)	2.74 (2)
H(11B) ••• H(342)	2.22
H(11B) ••• H(374)	2.33
H(11C) ••• H(224)	2.39
H(3B) ••• H(574)	2.11
H(7B) ••• H(544)	2.24
H(11D) ••• H(322)	2.19
H(11D) ••• H(324)	2.35
H(11E) ••• H(331)	2.24
H(3C) ••• H(571)	2.25
C(11C) ••• H(321)	2.81 (4)
C(11C) ••• H(325)	2.51 (3)
H(11H) ••• C(3A2)	2.68 (1)
H(11H) ••• H(321)	1.90
H(11H) ••• H(322)	2.27
H(11H) ••• H(325)	2.20
H(11I) ••• H(325)	2.22
H(11I) ••• H(334)	2.30
H(3D) ••• H(514)	2.16
H(7D) ••• H(544)	2.21
C(11D) ••• C(3A5)	3.29 (4)
C(11D) ••• H(351)	2.42 (3)
H(11K) ••• H(351)	1.94
H(11L) ••• H(351)	2.13

Figure 4.22 show CPK diagrams for a dimer of the MPBCDP1 structure. In Figure 4.22 (a) and (b) the upper half of the dimer includes the position of **A** [in purple, with the oxygen atoms in light purple and the hydrogen atoms in light blue]. The lower half includes the position of **B** [in green, with the oxygen atoms in light green and the hydrogen atoms in yellow]. In Figure 4.22 (c) and (d) the upper half of the dimer includes the position of **C** [in dark red, with the oxygen atoms in orange and the hydrogen atoms in yellow]. The lower half includes the position of **D** [in blue, with the oxygen atoms in light blue and the hydrogen atoms in purple].

This figure illustrates how the two methyl paraben molecules are completely enclosed within the β-CD dimer. This is achieved by tilting the guest molecule with respect to the mean O(4) plane of the CD in which they are included. The phenyl rings of **A**, **C**, **B** and **D** make angles of 72.4 (3)°, 77.4 (8)°, 56.2 (2)°, and 57.6 (6)° with the mean O(4) planes of their corresponding host molecules. These tilt angles show that the guest in the bottom half of the dimer has a greater tilt angle than the guest in the top half of the dimer. The hydroxyl groups of the guests are situated in the vicinity of the primary rim of the dimer while the ester moiety is contained within the secondary hydroxyl interface of the dimer. The orientation of the guest shows that the solvation of the polar group is an important factor in the positioning and stability of the guest in the cavity.

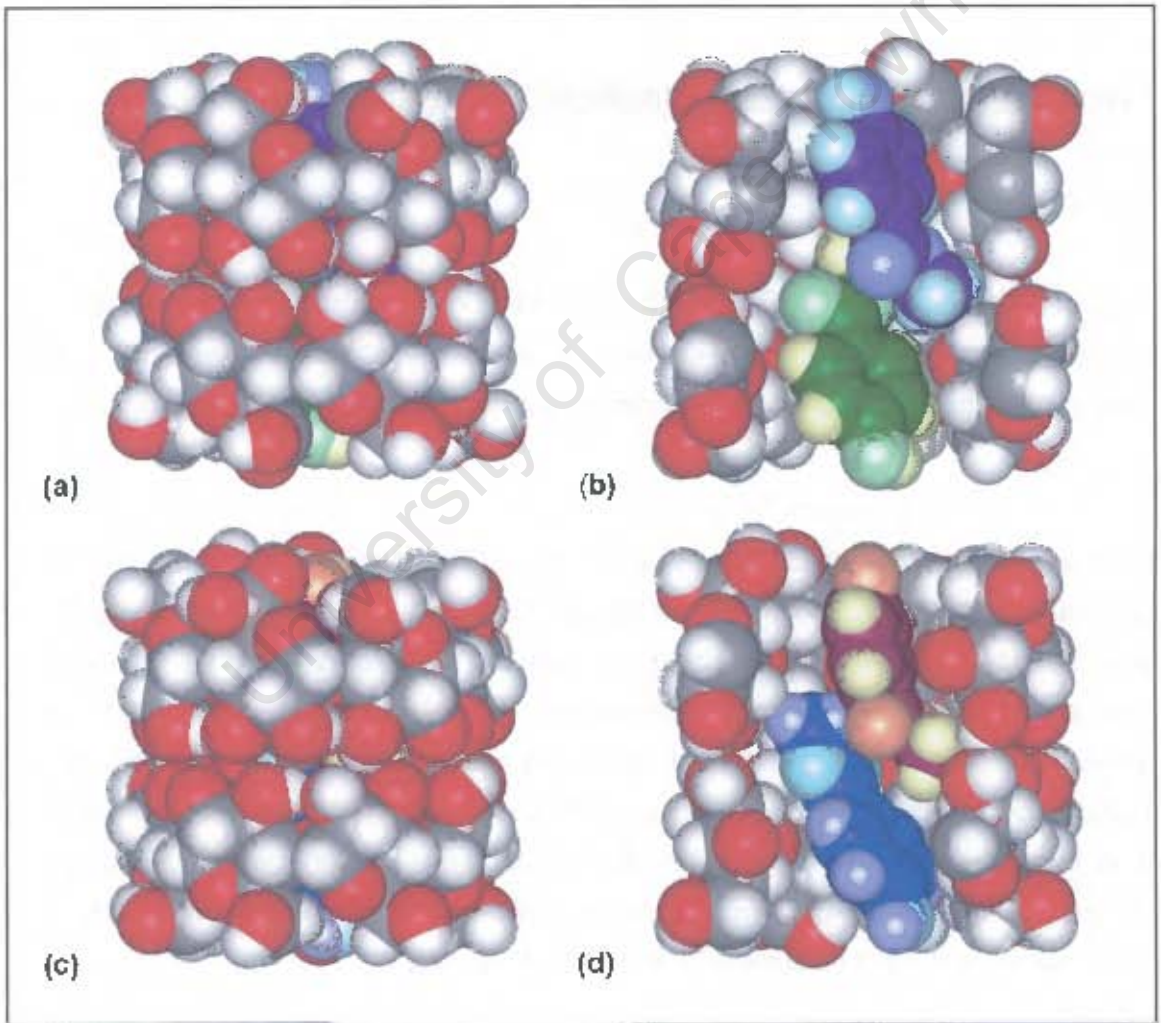

Figure 4.22 Space-filling diagram of the MPBCDP1 structure (a) side view (b) sectioned view of the same orientation, showing guest **A** and **B** (c) side view (d) sectioned view of the same orientation, showing guest **C** and **D**

An important feature of the disorder of the guest molecule is that the ester portions of **A** and **D**, as well as **B** and **C** are involved in unacceptably close contacts with each other [C(11A)•••C(11D) distance is 1.5 Å and the C(11B)•••C(11C) distance is 2.1 Å]. This implies that **A** and **D** [or **B** and **C**] cannot be present simultaneously in a single β-CD dimer. The most likely situation for the disorder is one where, in any given dimer, **A** and **B** are present in opposite halves of the dimer as shown in Figure 4.22(b) or alternatively **C** and **D** are present in opposite halves of the dimer as shown in Figure 4.22(d). The C(11A)•••C(11B) distance is 4.3 Å and the C(11C)•••C(11D) distance is 5.2 Å.

Hydrogen bonding interactions of the MPBCDP1 structure

Host interactions

A number of intramolecular O(2)•••O(3') hydrogen bonds stabilise the cyclodextrin, as has been reported with other β-cyclodextrin structures.[15-25] These hydrogen bonds contribute to the rigidity and highly symmetrical conformation of the cyclodextrin.

The β-CD dimer is formed by self-association of each monomer through hydrogen bonding between their secondary hydroxyl groups. The stability of this dimeric motif is well established in cyclodextrin structural chemistry.[4] The secondary hydroxyl groups are therefore involved in an invariant network of hydrogen bonds connecting neighbouring dimers directly or alternatively through water molecules. The self-association of the monomer through hydrogen bonding thus produces an elongated hydrophobic cavity, and the sandwiched area found between the two secondary rims is thus rather hydrophobic. The O(3)•••O(3) bonds were chosen over and above the O(2)•••O(2) and O(2)•••O(3) type hydrogen bond candidates as they were found to have shorter and more favourable O–H•••O geometries.

Additionally, intra-dimer hydrogen bonds occur between cyclodextrin layers. The primary -OH groups form a network of hydrogen bonds connecting dimers. However, these hydroxyl groups are influenced by the type of crystal packing and the presence of the guest that emerges from these faces.[33] Table 4.20 lists these lengths.

The conformation of each β-CD molecule is further stabilised by four intramolecular C(6)–H•••O(5') hydrogen bonds [Table 4.21].

Table 4.20 Summary of the appropriate contacts for the cyclodextrin and inter-layer interactions

Type			Number / dimer	Range (Å)	Mean (Å)
Cyclodextrin interactions					
	O(2)•••O(3')	**A**	7	2.73 - 2.84	2.80
	O(2)•••O(3')	**B**	7	2.76 - 2.82	2.78
Dimer formation:	O(3)•••O(3)	**A-B**	7	2.72 - 2.92	2.81
Intra-layer interactions					
O(6A2)•••O(6A5) [i]			2	2.93	2.93
O(6A4)•••O(6A7) [ii]			2	2.76	2.76
O(2A2)•••O(2B6) [i]			2	2.75	2.75
O(2A4)•••O(2B4) [ii]			2	2.84	2.84
O(6B2)•••O(6B6) [iii]			2	2.74	2.74
O(6B4)•••O(6B7) [ii]			2	2.83	2.83

[i] Related by symmetry operation: x, 1+y, z
[ii] Related by symmetry operation: x, y, 1+z
[iii] Related by symmetry operation: x, y, -1+z

Table 4.21 C–H•••O hydrogen bonds in the MPBCDP1 structure*

				Distance (Å)		Angle (°)
C	H	O	C–H	H•••O	C•••O	C–H•••O
Intramolecular hydrogen bonds						
C(6A1)	H(611)	O(5A2)	0.99	2.72	3.41 (2)	127 (1)
C(6A7)	H(672)	O(5A1)	0.99	2.65	3.44 (2)	136(1)
C(6B2)	H(625)	O(5B3)	0.99	2.66	3.45 (2)	138 (1)
C(6B3)	H(635)	O(5B4)	0.99	2.76	3.44 (2)	127 (1)

* Hydrogen bonding parameters based on idealised hydrogen atom positions.

Guest interactions

The hydrogen bonding distances for the relevant interactions between the water molecules and guest molecules are listed in Table 4.22. None of the atoms of the guest are within direct hydrogen bonding distance of the host molecules and therefore the water molecules, which are located in the vicinity of the primary rim, act as bridging atoms linking the guests to the host. All the hydroxyl oxygen atoms of the guests **A**, **B**, **C** and **D** are within hydrogen bonding contact of a water oxygen atom and are therefore linked via the water molecules to a primary hydroxyl atom of the opposite CD to that in which it was included e.g. **A** to CD(B) via O(29A). Additionally the water network connects the hydroxyl group of guest **A** / **C** with the hydroxyl group of the adjacent guest **B** / **D**. The O(1D)•••O(15W) interaction is an extremely strong hydrogen bond.[26] These interactions are illustrated in Figure 4.23.

Table 4.22 Hydrogen bonding contacts involving the guest molecule*

				Distance (Å)		Angle (°)
Donor(D)	H	Acceptor(A)	D–H	H•••A	D•••A	D–H•••A
O(1A)	H(1A)	O(6W)	0.84	1.84	2.64 (2)	173 (1)
O(1A)		O(8W)			2.85 (3)	
O(1A)		O(29A)^{i}			2.68 (5)	
C(7A)	H(7A)	O(6W)	0.95	2.63	3.28 (1)	126 (1)
O(1B)	H(1B)	O(21A)^{ii}	0.84	2.02	2.82 (2)	160 (1)
O(1B)		O(13W)			2.58 (4)	
C(7B)	H(7B)	O(13W)	0.95	2.87	3.45 (3)	121 (1)
O(1C)	H(1C)	O(6W)	0.84	1.98	2.64 (5)	129 (3)
O(1C)		O(8W)			2.89 (7)	
O(1C)		O(29A)^{i}			2.98 (6)	
C(3C)	H(3C)	O(6W)	0.95	2.73	3.33 (3)	122 (2)
O(1D)	H(1D)	O(15W)	0.84	1.79	2.59 (1)	160 (3)
C(7D)	H(1D)	O(13W)	0.95	2.85	3.43 (4)	121 (1)

^{i} Related by symmetry operation: x-1, y, z
^{ii} Related by symmetry operation: x+1, y, z+1
* Hydrogen bonding parameters based on idealised hydrogen atom positions

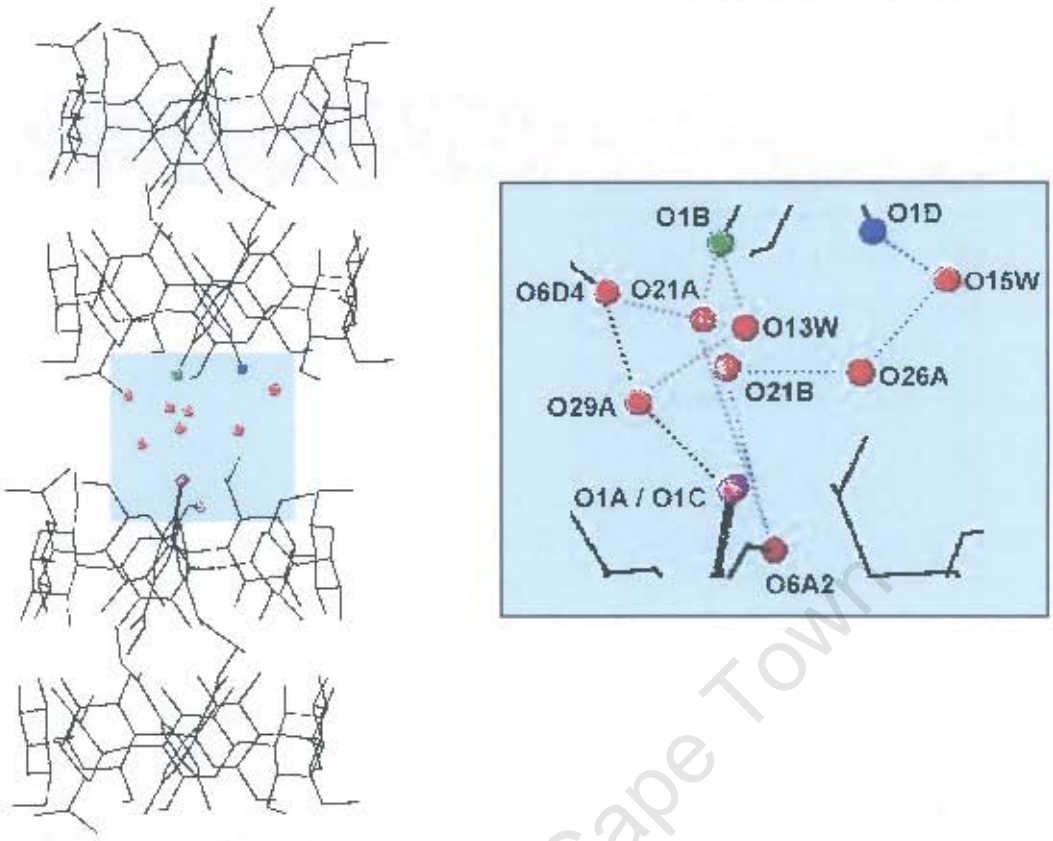

Figure 4.23 A schematic diagram showing the guest, water and host interactions for the MPBCDP1 structure

Water interactions

Thermogravimetric analysis gave a weight loss that corresponds to 28 water molecules per 2:2 complex unit of which 25.8 were accounted for. Only a few of these water molecules had full s.o.f.'s. The water molecules are distributed over 30 sites, 24 of them being within hydrogen bonding distance of primary and secondary hydroxyl groups of β-CD. These water molecules play the important role of the mediators which construct the host matrix structure or connect the host and guest molecules, as well as acting as spacers which fill the packing space among the β-CD dimer units. In the host structure there are four C(6)-O(6) bonds which point towards the cavity, namely C(6A3)-O(6A3), C(6A5)-O(6C5), C(6B5)-O(6D5) and C(6A6)-O(6A6) and these atoms are involved in hydrogen bonding interactions with water molecules that are either directly, or indirectly via a water molecule, hydrogen bonded to the guest molecules. It is assumed that distances of O•••O(W) of 2.43-3.07 Å and angles of O-H•••O(W) of 133-165° indicate hydrogen bonding. Hydrogen bonding distances between the host and these water molecules are listed in Tables 4.23.

Table 4.23 Hydrogen bonding distances involving the water molecules

				Distance (Å)		Angle (°)
Donor(D)	H	Acceptor(A)	D–H	H···A	D···A	D–H···A
O(6A1)	H(613)	O(4W)	0.84	1.95	2.74 (2)	156 (1)
O(6A3)	H(631)	O(13W) [i]	0.84	2.09	2.83 (2)	145 (1)
O(6C5)	H(652)	O(23B)	0.84	1.90	2.74 (4)	173 (3)
O(6A5)	H(651)	O(30C)	0.84	1.70	2.52 (4)	164 (2)
O(6B1)	H(616)	O(4W) [ii]	0.84	1.99	2.72 (1)	146 (1)
O(2B2)	H(225)	O(9W)	0.84	1.99	2.81 (3)	165 (1)
O(6B2)	H(626)	O(7W)	0.84	1.96	2.74 (2)	153 (1)
O(2B3)	H(235)	O(19A)	0.84	2.01	2.74 (2)	145 (1)
O(2B3)	H(235)	O(19B)	0.84	1.94	2.76 (4)	164 (2)
O(6B3)	H(636)	O(17W) [iii]	0.84	1.93	2.70 (4)	153 (2)
O(6B3)	H(636)	O(30C) [iii]	0.84	1.83	2.61 (4)	155 (2)
O(6D5)	H(655)	O(29B)	0.84	2.03	2.73 (7)	140 (3)
O(2B7)	H(275)	O(22A)	0.84	2.15	2.74 (3)	133 (2)

Interaction with H_A	Distance (Å)	Interaction with H_B	Distance (Å)
O(2W) ··· O(6A6) [ii]	2.72 (1)	O(1W) ··· O(6B7) [viii]	2.65 (2)
O(4W) ··· O(6A5) [iv]	2.61 (1)	O(1W) ··· O(6B3)	2.74 (2)
O(5W) ··· O(2A5)	2.68 (1)	O(2W) ··· O(6B6)	2.69 (1)
O(7W) ··· O(6A4) [iii]	2.72 (1)	O(3W) ··· O(6B4)	2.73 (1)
O(11W) ··· O(6C3)	2.74 (3)	O(6W) ··· O(6B7) [viii]	2.78 (2)
O(16W) ··· O(6A3)	2.71 (3)	O(14W) ··· O(2B5)	2.73 (2)
O(17W) ··· O(6A2) [v]	2.70 (4)	O(19B) ··· O(3B5) [iv]	2.73 (4)
O(18A) ··· O(6A2)	2.72 (2)	O(22A) ··· O(3B4) [vi]	2.73 (2)
O(18B) ··· O(6A2)	2.76 (8)	O(22B) ··· O(2B7)	2.64 (5)
O(19B) ··· O(3A1)	2.86 (5)	O(24B) ··· O(3B3) [vi]	2.76 (5)
O(21A) ··· O(6A7)	2.68 (2)	O(24B) ··· O(2B1)	2.71 (4)
O(21B) ··· O(6A7)	2.75 (3)	O(30B) ··· O(6B5) [i]	2.63 (5)
O(22A) ··· O(3A4)	2.70 (2)		
O(24A) ··· O(3A3)	2.86 (3)		
O(24A) ··· O(2A1) [vi]	2.72 (3)		
O(25A) ··· O(2A3) [vii]	2.71 (2)		
O(26A) ··· O(6A1)	2.86 (2)		
O(26B) ··· O(6A1)	2.75 (4)		
O(27B) ··· O(2A7)	2.84 (4)		
O(30B) ··· O(6C5)	2.73 (7)		

Table 4.23 Hydrogen bonding distances involving the water molecules [continued]

Interaction	Distance (Å)	Interaction	Distance (Å)
O(1W) ••• O(4W)^{iii}	2.82 (1)	O(14W) ••• O(25A)	2.71 (4)
O(1W) ••• O(8W)^{ix}	2.80 (2)	O(14W) ••• O(27A)	2.81 (4)
O(2W) ••• O(3W)^{vi}	2.71 (2)	O(14W) ••• O(20B)	2.58 (4)
O(2W) ••• O(6W)^{ii}	2.81 (1)	O(15W) ••• O(26A)^{iii}	2.67 (3)
O(3W) ••• O(9W)^{viii}	2.75 (1)	O(15W) ••• O(26B)^{iii}	2.79 (5)
O(3W) ••• O(23B)^{ix}	2.61 (4)	O(17W) ••• O(30B)	2.76 (6)
O(7W) ••• O(18A)^{ix}	2.82 (2)	O(18A) ••• O(27B)^{x}	2.64 (3)
O(7W) ••• O(18B)^{ix}	2.62 (7)	O(19A) ••• O(20A)^{iv}	2.72 (3)
O(7W) ••• O(30A)^{iii}	2.85 (4)	O(19B) ••• O(20B)^{iv}	2.78 (4)
O(7W) ••• O(30B)^{iii}	2.68 (4)	O(19A) ••• O(28B)	2.78 (4)
O(9W) ••• O(25A)^{x}	2.75 (4)	O(20B) ••• O(24A)^{vii}	2.69 (4)
O(9W) ••• O(25B)^{x}	3.06 (4)	O(21A) ••• O(26B)	2.46 (4)
O(10W) ••• O(30C)^{xi}	2.77 (5)	O(21B) ••• O(26B)	2.45 (4)
O(11W) ••• O(12W)^{x}	2.70 (4)	O(23A) ••• O(29B)^{i}	2.54 (4)
O(11W) ••• O(26A)^{vi}	2.69 (4)	O(23B) ••• O(29B)^{i}	2.72 (4)
O(12W) ••• O(18A)^{vii}	2.74 (4)	O(24B) ••• O(28A)^{vi}	2.60 (4)
O(13W) ••• O(29A)	2.77 (4)	O(25A) ••• O(28A)^{v}	2.80 (4)

Related by symmetry operation:

i)	x-1, y, z	iv)	x, y+1, z	vii)	x, y-1, z-1	x)	x, y+1, z+1
ii)	x+1, y, z+1	v)	x, y-1, z	viii)	x, y, z-1	xi)	x+1, y+1, z+1
iii)	x+1, y+1, z	vi)	x, y, z+1	ix)	x+1, y, z		

* Hydrogen bonding parameters based on idealised hydrogen atom positions.

The two separate water networks are formed between the dimers, one connecting the primary and the other connecting the secondary hydroxyl groups and these are summarised in Table 4.24 and illustrated in Figure 4.24. The water molecules that interact with the O(6) rim of the cyclodextrin form bridges between adjacent dimers in the same layer, while those that interact with the secondary rim form part of an infinite sub-layer of water molecules that run between the cyclodextrin channels. The O(3) atoms of the host A and B interact with similar water molecules. At the secondary hydroxyl side, the water molecules would act as H atom donors, since the hydroxyl O atoms donate their H atoms in the hydrogen bonding scheme within the dimer / between dimers in the lattice. Four water molecules are exclusively within hydrogen bonding distance to CD(A) and six to CD(B), while six water molecules do not interact with the host at all, but are connected to the CD by other water molecules.

Table 4.24 Summary of the water interactions for the MPBCDP1 structure

Type	Number of interactions	Range (Å)	Mean (Å)
O(2A_) ••• water	3	2.70 - 2.88	2.80
O(2B_) ••• water	3	2.73 - 2.75	2.74
O(3A_) ••• water	4	2.69 - 2.84	2.74
O(3B_) ••• water	7	2.65 - 2.81	2.74
O(6A_) ••• water	17	2.52 - 2.85	2.71
O(6B_) ••• water	11	2.61- 2.78	2.70
water ••• water	34	2.46 - 3.06	2.74

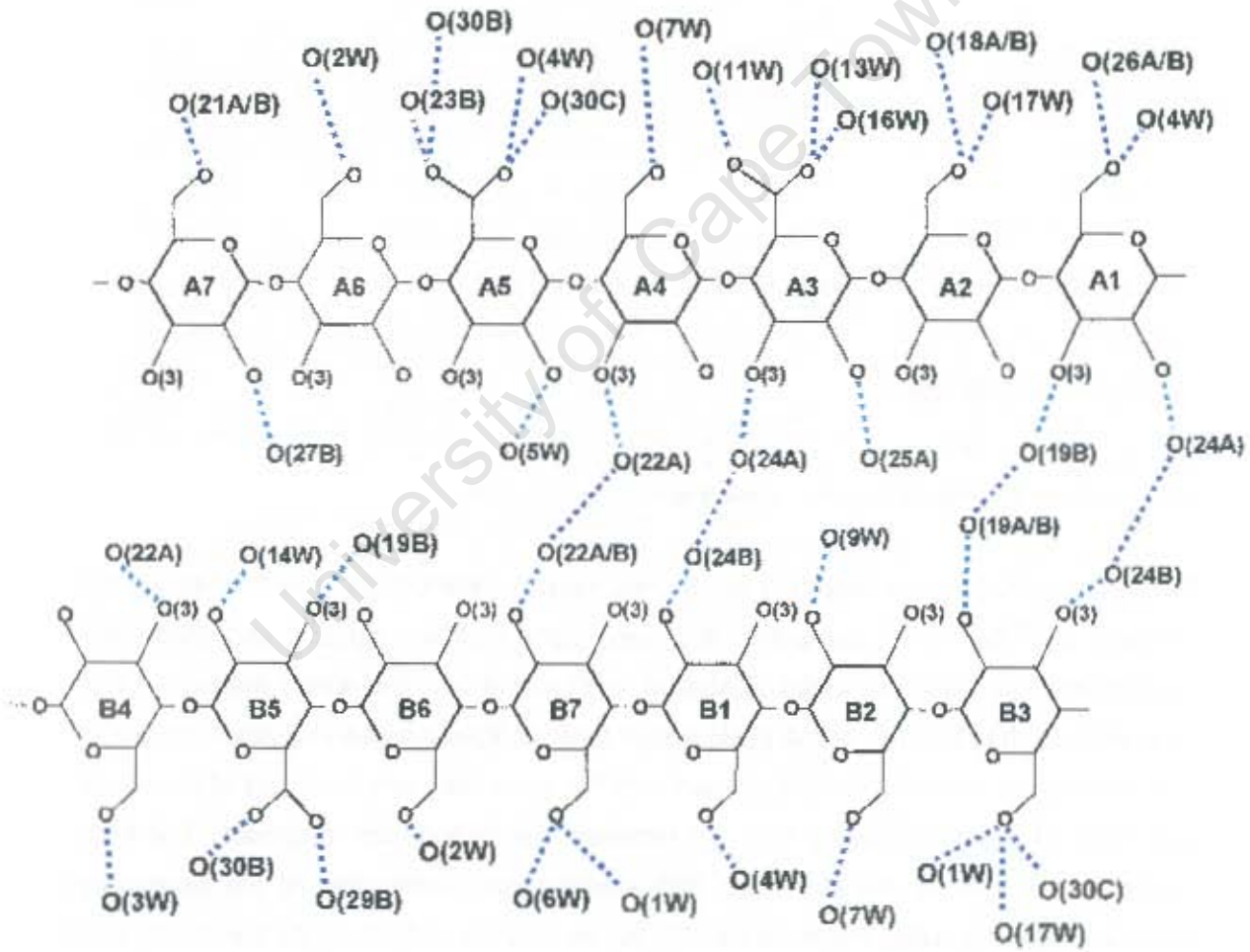

Figure 4.24 Schematic diagram showing the hydrogen bonding of the hydroxyl groups with water molecules

Crystal packing of the MPBCDP1 structure

The crystalline MPBCDP1 inclusion complex consists of head-to-head β-CD dimers and includes two disordered guest molecules. Figure 4.25 is an extended stereo packing diagram of the MPBCDP1 structure projected down the *a*-axis and illustrates the "endless" channels produced by the cavities of the dimers. Hence the dimeric layers are stacked parallel to the *yz*-plane of the structure.

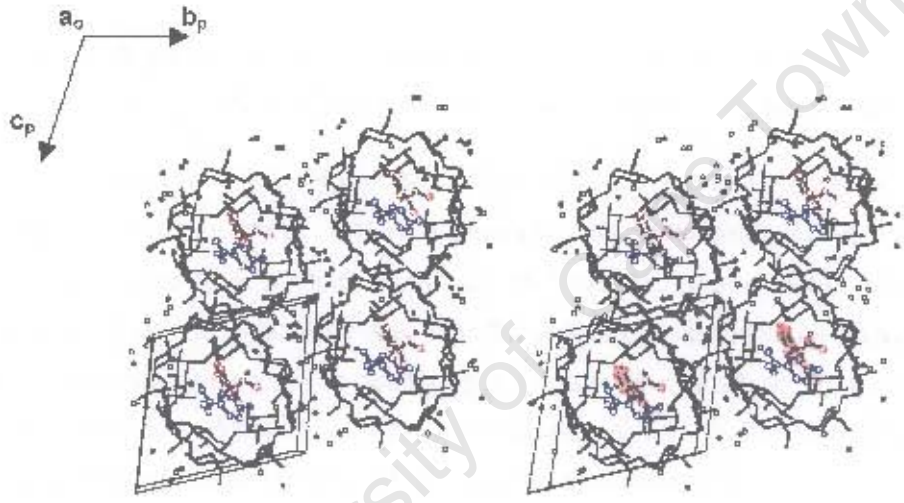

Figure 4.25 Stereo packing diagram of the MPBCDP1 structure [*a*-axis projection], with the water molecules represented as black spheres and guests **C** and **D** in red and blue respectively

Figure 4.26 (a) and (b) are extended packing diagrams of the MPBCDP1 structure showing projections as viewed down the *c*- and *b*-axes. These figures illustrate the stacking of the dimers in columns parallel to the *a*-axis.

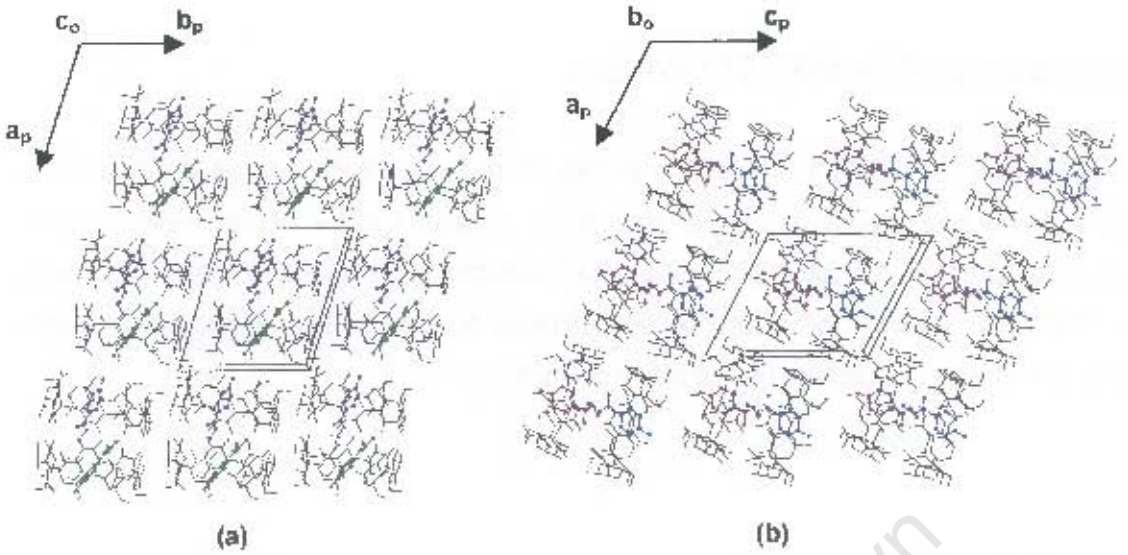

Figure 4.26 Packing diagrams of the (a) *c*-axis projection, including guests **A** and **B** and (b) *b*-axis projection, including guest **C** and **D** of the MPBCDP1 structure

This stacking mode is classified as an intermediate type packing mode, which is characteristic for β-CD complexes that crystallise in the space group P1 with cell dimensions similar to those reported here.[4] In the intermediate type structures, the β-CD dimers are arranged as close packed layers with the layers stacking on top of each other with a significant shift. The distance between the projection of two consecutive dimers onto the O(4) mean plane is 7.07 Å. The relative average shift of consecutive dimers along the *c*-axis, when the dimers were viewed perpendicular to their mean O(4) plane, is 6.0 (2) Å for intermediate type structures crystallising in the space group P1.[4] This value is almost equal to the inner diameter of the primary face of the β-CD molecule and is slightly larger than the average radius of 5.03 Å of the O(4) heptagon.[33] This shift therefore places the seven-fold axis of a dimer near the rim of a dimer below, as seen in Figure 4.26. The seven-fold axis of a dimer forms an angle of ~ 20° with the stacking axis and consequently adjacent layers are far from exactly aligned.[4] Hence the channels are more deformed at the interdimeric interface than for the channel type structures. The large shift and angle result in the discontinuation of the channel and justify the term "intermediate" i.e. between channel and chessboard mode. "Intermediate" has also been termed as "cage type" by Saenger.[34-35] The guest molecules therefore find themselves in a nearly cage-like environment and so interactions with guest molecules in neighbouring β-CD dimers were not found.

The isolation and structure elucidation of two distinct crystalline modifications of a cyclodextrin inclusion complex containing the same organic guest is noteworthy. The author is unaware of a precedent in the literature on CD inclusion complexes.

X-RAY CRYSTALLOGRAPHIC ANALYSIS OF THE PPBCD STRUCTURE

Data-collection

A single crystal of suitable size was extracted from a batch. The crystal was highly unstable in air and was mounted on a glass fibre and covered in Paratone N oil[8] to provide a rigid mounting for the low-temperature data collection and to prevent cracking of the crystal surface. X-ray intensity data-collection was performed at 173(2) K on the Nonius Kappa CCD diffractometer using graphite-monochromated MoKα radiation. Data collection parameters are outlined in Table 4.25.

Structure determination and refinement

The structure was solved using published co-ordinates for the non-hydrogen cyclodextrin atoms [excluding the primary hydroxyl oxygen atoms] of the isomorphous β-CD-ibuprofen complex.[12] After refinement in SHELX-97,[13] the difference Fourier map revealed the positions of most of the primary hydroxyl oxygen atoms. After further refinement it was found that two of these atoms were disordered over two positions [O(63) and O(66)]. For a given pair, a fixed U_{iso} of 0.08 $Å^2$ [the mean of U_{eq} for the chemically equivalent ordered atoms] was assigned and site-occupancy factors [s.o.f.'s] of x and 1-x were assigned, with x variable. The major positions refined to a s.o.f. of 0.63 and 0.74 for O(63A) and O(66A) respectively. All the oxygen atoms on the host, except the disordered primary hydroxyl oxygen atoms, O(5G2), O(6G2) and O(6G7) were refined anisotropically while the C atoms were refined isotropically.

Hydrogen atoms were included in idealised positions in a riding-model with U_{iso} set at 1.2 times those of the parent atoms. All the primary hydroxyl hydrogen atoms were assigned a common variable isotropic temperature factor and placed using the AFIX 83 or AFIX 147 instruction. The remaining hydrogen atoms of each glucose moiety were assigned common variable isotropic temperature factors.

Table 4.25 Details of the data collection and refinement parameters for the PPBCD structure

Empirical formula	$C_{42}H_{70}O_{35}{\cdot}C_{10}H_{12}O_3{\cdot}7.0H_2O$
Formula weight	1441.3
Crystal system	Monoclinic
Space group	C2
a / Å	19.137 (2)
b / Å	24.534 (1)
c / Å	15.793 (1)
α / °	90
β / °	109.52 (2)
γ / °	90
Volume / $Å^3$	6988.8 (2)
Z	4
$Density_{calc}$ / g cm^{-3}	1.370
μ (MoKα) / mm^{-1}	0.121
F(000)	3072
Temperature of data collection / K	173 (2)
Crystal size / mm^3	0.25 x 0.24 x 0.14
Range scanned θ / °	$2 \leq \theta \leq 24$
Index ranges	h: -20, 16 k: -26, 27 l: -11, 17
φ scan angle / °	1.0
φ scan range, frames	200.0°, 200
Dx / mm	40
Total no. of reflections collected	9174
No. of independent reflections	6733
No. of reflections with $I > 2\sigma(I)$	4758
No. of parameters	512
R_{int}	0.0411
S	1.096
R_1 (for 4757 reflections)	0.1465
Reflections omitted	(0 0 1); (0 0 5); (0 2 0); (1 3 0); (1 -3 0); (2 0 1); (2 2 0); (2 -2 0); (2 2 1); (-2, 2, 1); (2 -2 1); (-2, -2 1); (-3 1 2); (-3 -1 2)
wR_2	0.3575
Weighting scheme	a = 0.1731 b = 136.6262
$(\Delta / \sigma)_{mean}$	< 0.000
Δρ excursions / $e.Å^{-3}$	0.83 and -0.46

Oxygen atoms of water molecules were located over nine positions. Three of these water molecules [O(2W), O(3W) and O(4W)] were found to be disordered over two alternative positions. For a given pair, a fixed U_{iso} of 0.08 Å^2 was assigned and s.o.f.'s of x and 1-x were assigned, with x variable. The s.o.f.'s of the major position refined to 0.63, 0.65 and 0.57 for O(2WA), O(3WA) and O(4WA) respectively. The remaining waters [O(1W) and O(5W) to O(9W)] were assigned a fixed isotropic thermal factor of 0.08 Å^2 while the site-occupancies were allowed to vary. The site-occupancies of these six water molecules were 0.57, 0.95, 0.55, 0.77, 0.42, 0.34 for O(1W), O(5W), O(6W), O(7W), O(8W) and O(9W) respectively, amounting to an additional 3.6 water molecules per asymmetric unit. This amounts to a total of 6.6 water molecules per asymmetric unit which were accounted for, as compared to the 7.0 water molecules expected from the TGA results. The hydrogen atoms of the water molecules were not located.

The guest could not be located beyond a diffuse electron density cloud located within the cyclodextrin cavity and could not be modelled, due to abnormal distances and angles between electron density peaks. Since the guest molecule could not be resolved the refinement converged to a relatively high R_1 of 0.15 for observed data [$I > 2\sigma(I)$]. Fourteen low-angle reflections were omitted owing to their truncation by the beam-stop. The maximum and minimum residual electron densities were 0.83 and 0.46 e.Å^{-3} respectively.

Geometrical analysis of the PPBCD structure

The asymmetric unit comprises a single host molecule, 7.0 water molecules, and a severely disordered guest molecule. The PPBCD complex crystallises in the monoclinic space group C2 and the β-CD molecule is rotated through a diad parallel to the *b*-axis to produce the other half of the dimer.

The structure of the cyclodextrin molecule and the numbering scheme adopted for the β-CD molecule and water molecules are illustrated in Figure 4.27. The seven glucosidic residues have been assigned the Gn notation. Disordered positions were denoted A and B respectively. The glucose units will be referred to as G1, G2, G3, G4, G5, G6 and G7. The geometrical data for the β-CD molecule are listed in Tables 4.26 and 4.27 [e.s.d.s are in the range 0.014-0.019 Å for distances and 0.28-1.47° for angles].

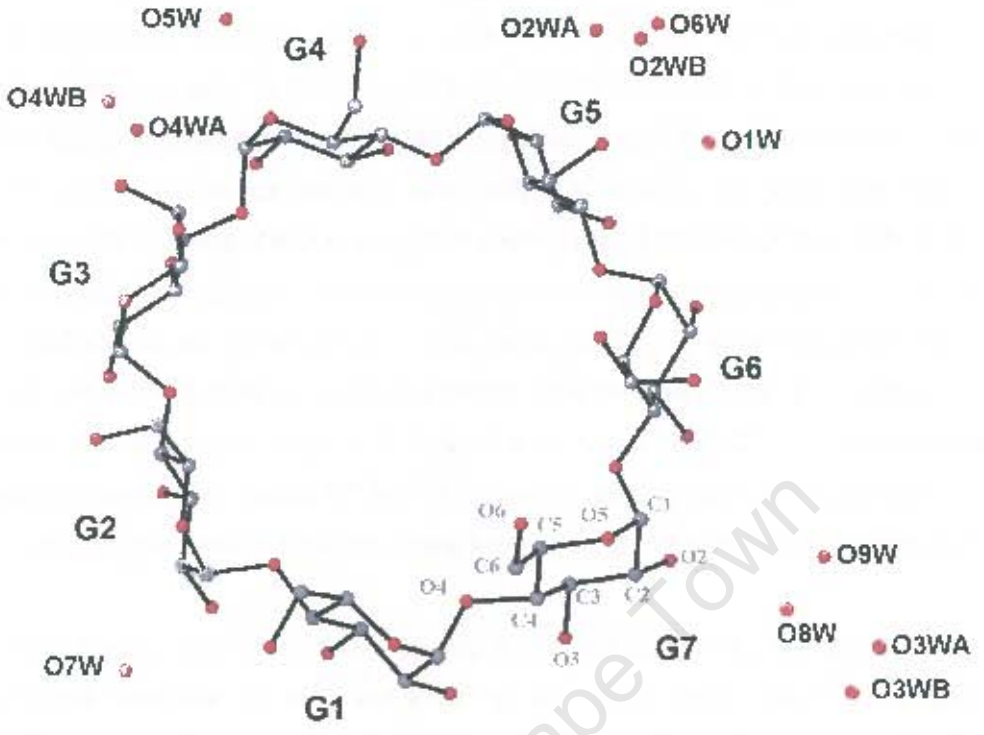

Figure 4.27 Macrocyclic structure and numbering scheme of glucose residues and water oxygen atoms, with the hydrogen atoms excluded. The host is viewed from the primary face.

The glucose residues are all in the $^4C_1$ chair conformation. The C(6)–O(6) bonds of the G1, G2, G4 and G5 residues are directed away from the cavity and are in the (-) *gauche* conformation to the C(4)–C(5) and O(5)–C(5) bonds. The C(6)–O(6) bond of the G7 residue points towards the cavity in the (+) *gauche* conformation. The O(6) atoms of the G3 and G6 residues are disordered over two sites. The major position of the O(6) atom of the G3 residue adopts the (+) *gauche* conformation while the minor position adopts the (-) *gauche* conformation. The reverse of this is seen for the G6 glucose unit.

The geometric parameters of the O(4) heptagon of the PPBCD structure are listed in Table 4.26. These include the radii, the O(4)•••O(4') distances, the O(4)•••O(4')•••O(4'') angles, the O(4)•••O(4')•••O(4'')•••O(4''') torsion angles and the deviations of each of the O(4) atoms from the mean O(4) plane.

Table 4.27 lists the other important features of the macrocyclic structure such as the intersaccharidic bond angle (φ), the O(2)•••O(3') distance and the tilt angles [τ_1 and τ_2]. These parameters are defined in Chapter 1.

Table 4.26 Geometrical parameters of the O(4) heptagon for the PPBCD structure

Glucose unit	Radii (A)	O(4)•••O(4') (A)	O(4) angle (°)	Torsion angle (°)	Deviation (A)
G1	4.92 (1)	4.56	133	3.3 (7)	0.01
G2	5.09 (2)	4.33	129	-5.4 (6)	0.10
G3	5.29 (2)	4.44	124	0.3 (6)	-0.08
G4	5.04 (2)	4.51	130	5.9 (7)	-0.06
G5	4.99 (2)	4.43	130	-4.5 (7)	0.13
G6	5.19 (2)	4.39	127	-1.1 (7)	-0.01
G7	5.21 (2)	4.35	126	2.0 (7)	-0.09
Average	**5.10**	**4.43**	**129**	**3.2**	**0.07**

Table 4.27 φ, O(2)•••O(3') distance, τ for the PPBCD structure

Glucose unit	φ (°)	O(2)•••O(3') (A)	τ_1 (°)	τ_2 (°)
G1	117	2.81	0.2 (5)	1.0 (3)
G2	119	2.76	3.9 (5)	7.6 (6)
G3	118	2.85	6.7 (4)	14.3 (5)
G4	117	2.85	3.6 (4)	9.6 (5)
G5	120	2.85	6.5 (4)	10.4 (7)
G6	119	2.80	6.5 (5)	8.5 (6)
G7	117	2.78	3.6 (6)	6.4 (8)
Average	**118**	**2.81**	**4.4**	**8.2**

The seven-fold symmetry of the β-CD appears to be well maintained. This is reflected in the O(4)•••O(4') distances and O(4)•••O(4')•••O(4") angles. Moreover, the deviations of the glycosidic O(4) atoms from their optimum plane are small. The similarity in O(4) lengths and angles, and the relatively small deviations indicate that a highly rigid conformation is adopted by the β-CD molecule.

Hydrogen bonding interactions of the PPBCD structure

Host interactions

The conformation of the β-CD macrocycle is stabilised through seven intramolecular O(2)•••O(3') hydrogen bonds corresponding to the flip-flop system described by Saenger *et al.*[36-37] The O(3)•••O(3) distances and the angles C(3)-O(3)•••O(3') [average 117°, range 114-122°] indicate that hydrogen bonds link the O(3) hydroxyl groups of two adjacent β-CD molecules to form a dimer. Inter-dimer hydrogen bonds also occur between cyclodextrin layers. Table 4.28 lists the appropriate contacts for the cyclodextrin, dimer and intra-layer interactions. The listed contacts are all in the range 2.75-2.94 Å and the e.s.d.s are in the range 0.02-0.04 Å.

The conformation of the β-CD molecule is further stabilised by four intermolecular C–H•••O hydrogen bonds [Table 4.29]. These encompass a C(1)–H•••O(2) hydrogen bond, a C(2)–H•••O(3) hydrogen bond and two C(6)–H•••O(6) hydrogen bonds. The latter two bonds involve the disordered O(6G6) atoms, indicating that disorder in the CD adds to the overall stability of the structure.

Figure 4.28 is a projection viewed down [010]. The figure shows the generation of the dimer by the two-fold rotation axis parallel to the *b*-axis, the channel packing arrangement and hydrogen bonding between adjacent dimers parallel to the *c*-axis. The dimers are arranged in C-centred layers and these layers are held together via a hydrogen bonding network through water molecules which link dimers within a layer and dimers of one layer to those of adjacent layers. The dimers are stacked upon one another parallel to the *c*-axis to form channels. Direct hydrogen bonding between adjacent O(6) layers along the channel is only found with the minor position of O(63B), which is bonded to a symmetry related atom O(63B). The length of this bond is 2.73 (5) Å, with a C(6G3)–O(63B)•••O(63B) angle of 129°. Other hydrogen bonds are formed between dimers which are parallel to each other in the *ab*-plane.

Table 4.28 Summary of the appropriate contacts for the cyclodextrin and inter-layer interactions

Type		Number / dimer	Range (Å)	Mean (Å)
Cyclodextrin interactions				
	O(2)•••O(3')	7	2.76 - 2.86	2.82
Dimer formation:	O(3)•••O(3[§])	7	2.75 - 2.94	2.86
Intra-layer interactions				
O(2G1)•••O(2G6) [i]		2	2.78	2.78
O(6G1)•••O(6G4) [ii]		2	2.88	2.88
O(6G2)•••O(6G4) [iii]		2	2.85	2.85

[§] Two-fold related counterpart
[i] Related by symmetry operation: $^{1}/_{2}$-x, $^{1}/_{2}$+y, 1-z
[ii] Related by symmetry operation: $^{1}/_{2}$+x, $^{1}/_{2}$+y, z
[iii] Related by symmetry operation: - $^{1}/_{2}$-x, $^{1}/_{2}$+y, -z

Table 4.29 C–H•••O hydrogen bonds in the PPBCD structure*

				Distance (Å)		Angle (°)
C	H	O	C–H	H•••O	C•••O	C–H•••O
Intermolecular hydrogen bonds						
C(1G1)	H(111) [i]	O(2G5) [i]	1.00	2.55	3.34 (2)	136 (1)
C(2G6)	H(261) [ii]	O(3G2) [ii]	1.00	2.45	3.33 (2)	146 (1)
C(6G4)	H(641) [iii]	O(66A) [iv]	0.99	2.56	3.16 (3)	119 (1)
C(6G5)	H(651) [iii]	O(66B) [iv]	0.99	2.41	3.24 (5)	141 (2)

[i] Related by symmetry operation: $^{1}/_{2}$+x, $^{1}/_{2}$+y, z
[ii] Related by symmetry operation: $^{1}/_{2}$+x, - $^{1}/_{2}$+y, z
[iii] Related by symmetry operation: -x, y, -z
* Hydrogen bonding parameters based on idealised hydrogen atom positions.

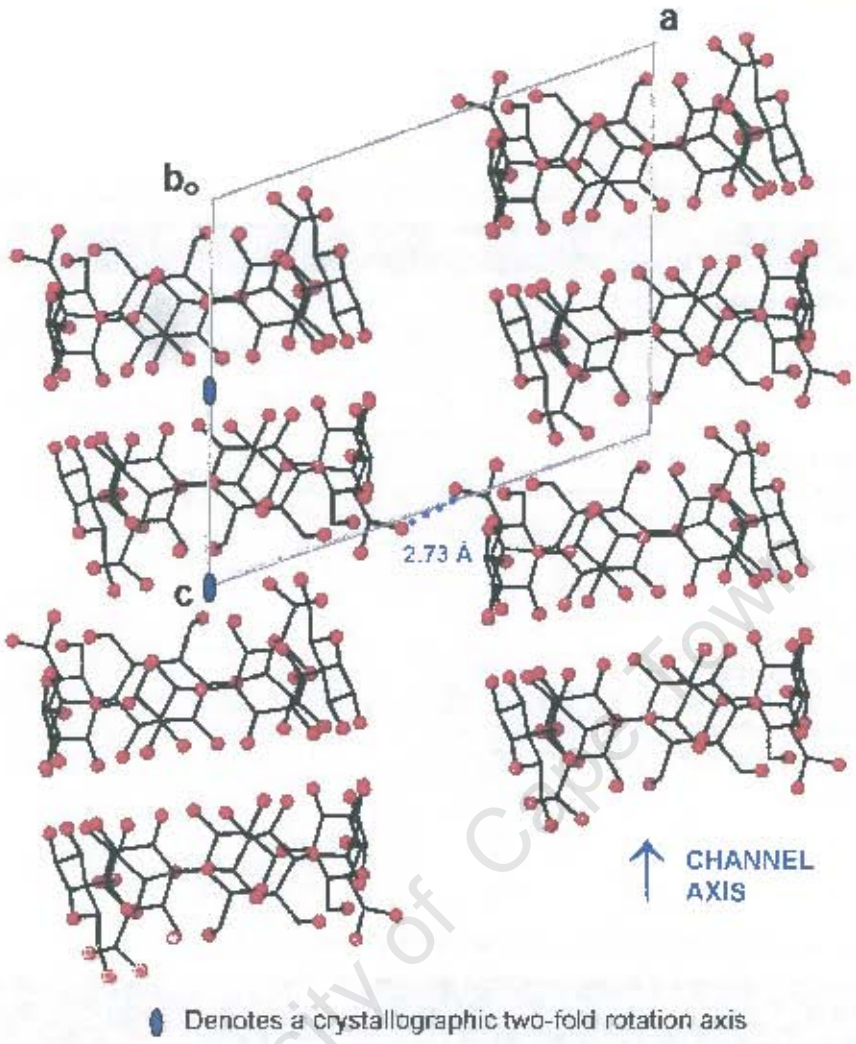

Figure 4.28 *b*-axis projection illustrating the arrangement of the β-CD dimer, the channel packing of the complex and hydrogen bonding between adjacent dimers [C-centred positions, water molecules and hydrogen atoms omitted]

Guest interaction

The guest molecule is located within the cavity, but is severely disordered and cannot be visualised beyond a diffuse electron density cloud. This and the abnormal bond angles and lengths made it difficult to model the guest. The disposition of the electron density cloud in relation to the β-CD dimer is shown in Figure 4.29 and Figure 4.30 by the positions of peaks that were identified [having values of 0.35-0.83 e.Å^{-3}]. A group of six peaks, arranged in a rough hexagon could be discerned, although attempts to model these as a phenyl ring were unsuccessful. Subsequent difference electron density maps did reveal possible positions for the guest substituent groups although the bond distances and angles were unsatisfactory.

This type of guest disorder is inherent in cyclodextrin complexes of this channel type packing and few structures have been reported where the guest is revealed and successfully modelled. [12, 17, 19-20, 22, 25, 38] It is difficult to assess whether the disorder is statistical or whether the guest molecule is undergoing a high degree of thermal motion or is actually migrating through the channels. The channels formed by the cyclodextrin molecules are almost perfectly linear and the disordered guest is observed in positions near the centre of the cavity as a long chain of overlapping peaks, generated by symmetry, suggesting several possible positions for the guest.

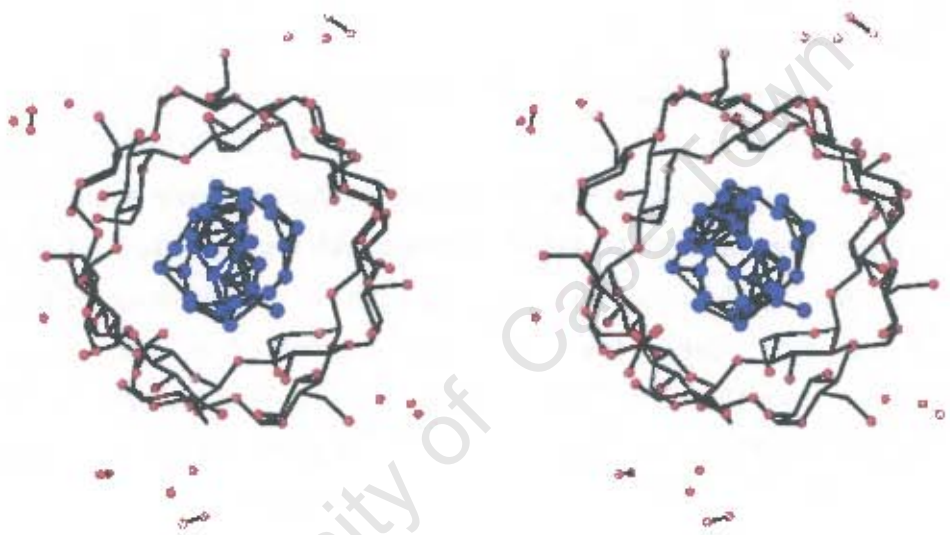

Figure 4.29 Stereo-view down the *c*-axis illustrating low electron-density candidate guest peaks

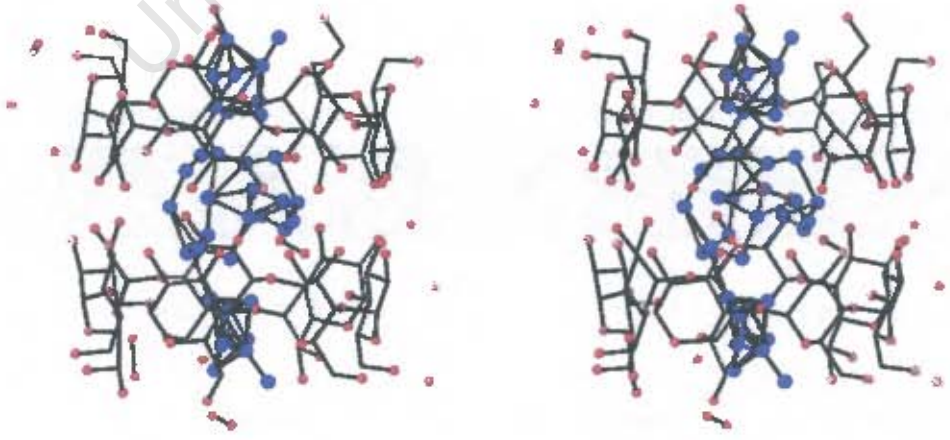

Figure 4.30 Stereo-view down the *b*-axis illustrating low electron-density candidate guest peaks

Water interactions

Thermogravimetric analysis gave a weight loss that corresponds to 7.0 water molecules per 1:1 complex unit, of which 6.6 water molecules were accounted for in the crystallographic analysis. All of these water molecules are situated at the periphery of the cyclodextrin molecule, filling the intermolecular space between complex units. Hydrogen bonding distances between the host and these water molecules are listed in Tables 4.30 and 4.31.

Two networks of water molecules form hydrogen bonds to primary and secondary hydroxyl groups [Figure 4.31]. Two water molecules, O(3WB) and O(6W), do not bond directly to a cyclodextrin molecule but are connected to other water molecules. The water molecules that interact with the O(6) rim of the cyclodextrin are O(2WA), O(2WB), O(3WA), O(4WA) and O(5W). They form bridges between adjacent dimers in the same layer. The water molecules that interact with the secondary rim are O(1W), O(4WB), O(7W), O(8W) and O(9W) which form part of an infinite sub-layer of water molecules that run between the cyclodextrin channels. The water molecules of crystallisation thereby form a hydrogen bonding network which facilitates the formation of the infinite dimer planes. The O(3WB)•••O(4WA) distance of 1.86 (5) Å indicates that these two water molecules will not be present simultaneously.

In addition to these O•••O hydrogen bond distances, two water molecules, namely O(2WA) and O(5W), are within hydrogen bonding contact of the host carbon atoms and these two contacts are listed in Table 4.30.

Table 4.30 C–H•••O hydrogen bonds between the host and the water molecules*

				Distance (Å)		Angle (°)
Donor(D)	H	Acceptor(A)	D–H	H•••A	D•••A	D–H•••A
C(6G2)	H(622) '	O(2WA) '	0.99	2.78	3.29 (4)	113 (2)
C(1G4)	H(141) "	O(5W) "	1.00	2.79	3.41 (2)	120 (1)

' Related by symmetry operation: $-^1/_2-x$, $^1/_2+y$, -z
" Related by symmetry operation -1-x, y, -z
* Hydrogen bonding parameters based on idealised hydrogen atom positions.

Table 4.31 Hydrogen bonding distances involving the water molecules

Interaction	Distance (A)	Symmetry operator for the second oxygen atom listed
O(1W) ••• O(2G3)	2.89 (4)	$^{1}/_{2}$+x, -$^{1}/_{2}$+y, z
O(1W) ••• O(3G5)	2.80 (3)	x, y, z
O(2WA) ••• O(6G5)	2.67 (3)	x, y, z
O(2WB) ••• O(6G5)	2.73 (5)	x, y, z
O(3WA) ••• O(66A)	2.79 (3)	1-x, y, 1-z
O(4WA) ••• O(63A)	2.77 (3)	x, y, z
O(4WB) ••• O(3G3)	2.88 (4)	-1-x, y, -z
O(5W) ••• O(6G1)	2.83 (2)	-$^{1}/_{2}$-x, -$^{1}/_{2}$+y, -z
O(7W) ••• O(2G2)	2.67 (2)	x, y, z
O(7W) ••• O(3G6)	2.81 (3)	-$^{1}/_{2}$+x, $^{1}/_{2}$+y, z
O(8W) ••• O(2G7)	2.79 (4)	x, y, z
O(9W) ••• O(2G4)	2.65 (5)	-x, y, 1-z
O(2WB) ••• O(6W)	2.48 (6)	x, y, z
O(3WA) ••• O(4WA)	2.76 (4)	1+x, y, 1+z
O(3WA) ••• O(5W)	2.62 (3)	1+x, y, 1+z
O(3WA) ••• O(9W)	2.58 (4)	x, y, z
O(3WB) ••• O(4WB)	2.93 (5)	1+x, y, 1+z
O(3WB) ••• O(5W)	2.82 (5)	1+x, y, 1+z
O(4WA) ••• O(6W)	2.89 (4)	-$^{1}/_{2}$-x, $^{1}/_{2}$+y, -z
O(4WB) ••• O(6W)	2.84 (4)	-$^{1}/_{2}$-x, $^{1}/_{2}$+y, -z
O(4WB) ••• O(8W)	2.62 (5)	-1+x, y, -1+z
O(7W) ••• O(8W)	2.85 (4)	-$^{1}/_{2}$+x, $^{1}/_{2}$+y, z
O(7W) ••• O(9W)	2.93 (4)	-$^{1}/_{2}$+x, $^{1}/_{2}$+y, z
O(8W) ••• O(8W) [§]	1.67 (6)	1-x, y, 1-z
O(8W) ••• O(9W)	2.43 (6)	x, y, z

[§] Two-fold related counterpart

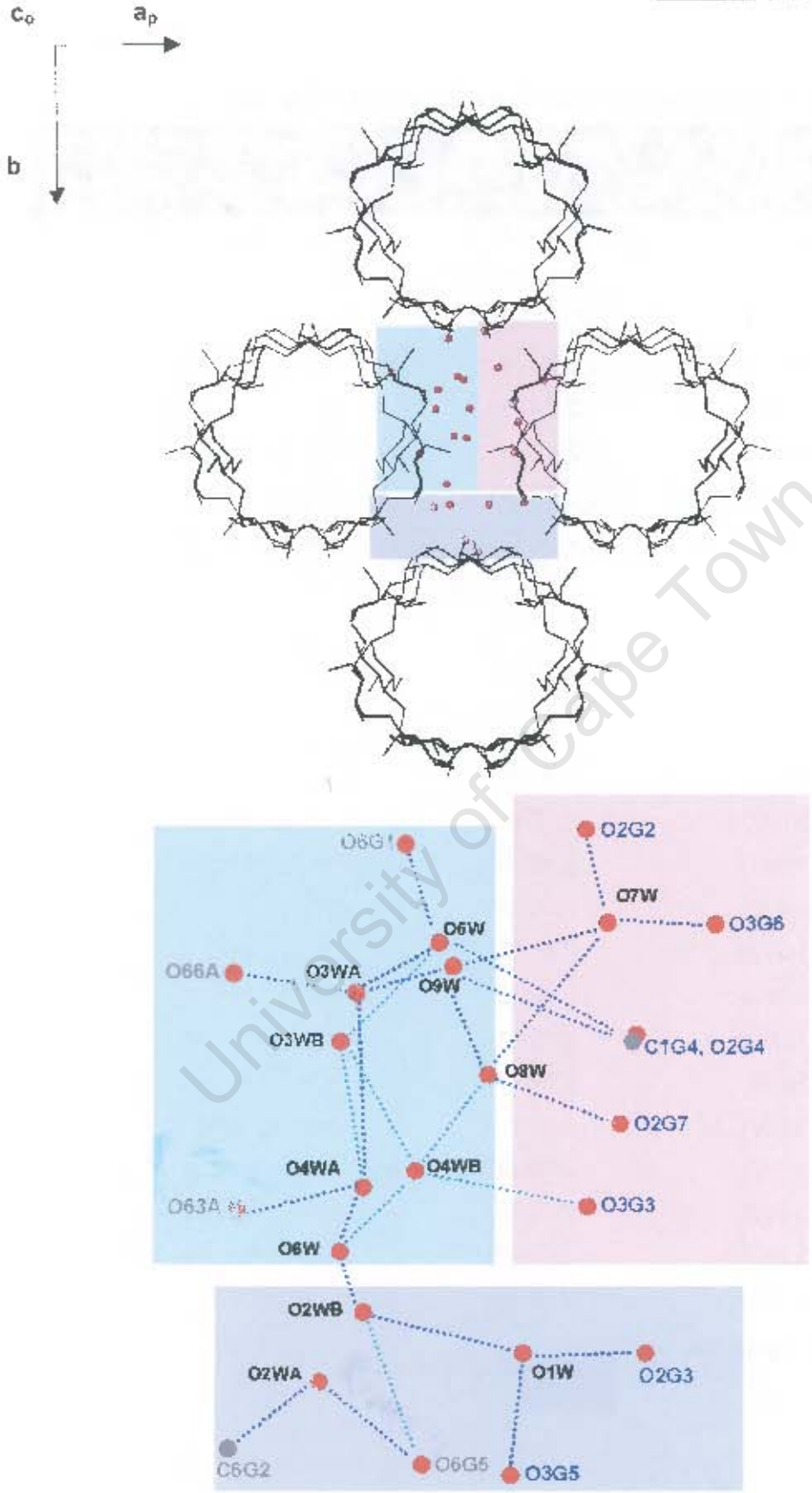

Figure 4.31 A schematic representation of the water molecules that connect adjacent host units

Crystal packing of the PPBCD structure

The PPBCD structure is characteristic of the channel type packing motif for β-CD dimers.[15-25] The dimers pack in a head-to-head manner and are arranged in C-centred layers which form channels parallel to the *xy*-plane of the structure. The relative average shift of consecutive dimers, when the dimers are viewed perpendicular to their mean O(4) planes, is reported as 2.7 (2) Å for the channel type structures crystallising in the space group C2.[4]

Figure 4.32 is a plot of the unit cell viewed down the *b*- and *c*-axes prepared using the Section program in X-Seed[39] and shows the "endless" channels formed by the dimer columns running parallel to the *c*-axis. This clearly illustrates the geometry of the cavities in which the guest molecules are accommodated.

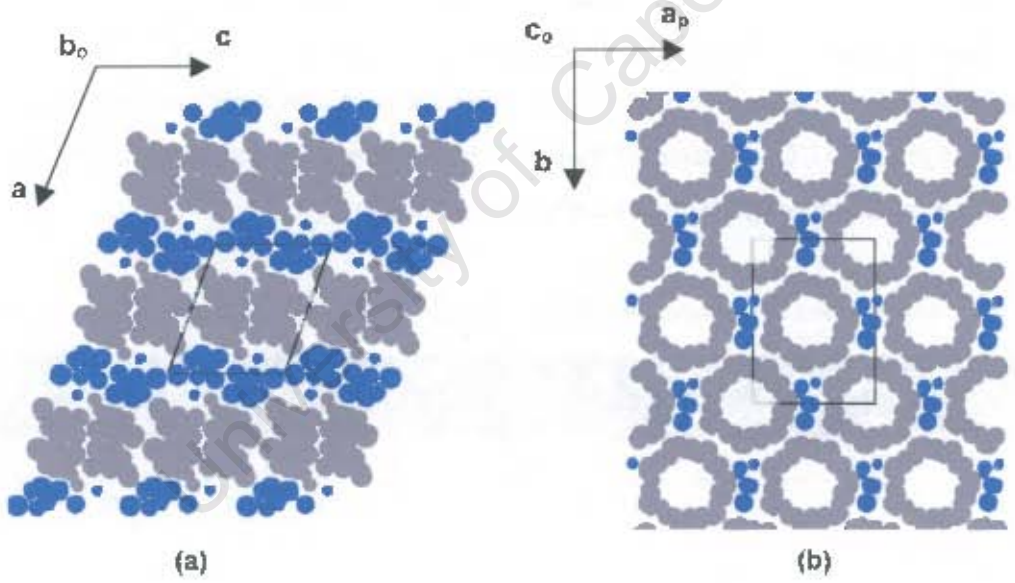

Figure 4.32 Section plot of PPBCD with the host positions represented in grey and water molecules in blue (a) viewed down [010] with the unit cell sectioned at y = 0.73 and (b) viewed down [001] with the unit cell sectioned at z = 0.26

DISCUSSION

A search of the CSD[40] showed data for 70 crystallographic structures of dimeric β-CD complexes, crystallising in the space groups P1, $P2_1$, C2 or $C222_1$. The molecules of a dimer pair are related by a crystallographic two-fold axis, strictly for space groups C2 and $C222_1$ and approximately for space groups P1 and $P2_1$. The stacking of these dimers is either collinearly to yield a channel type packing arrangement [CH] or the dimers are displaced sideways to different degrees forming intermediate [IM], chessboard [CB] and screw-channel [SC] type packing modes. Table 4.32 summarises the average unit cell dimensions for these different β-CD dimer packing types and their occurrence. The table shows that dimeric β-CD inclusion complexes prefer to crystallise in the space groups P1, IM and C2, CH.

It is worth mentioning that in this search of the CSD there was no occurrence of a cyclodextrin inclusion complex of a particular organic guest crystallising in more than one arrangement. The author is therefore unaware of a precedent in the literature of pseudo-polymophic CD inclusion complexes. Hence the inclusion complexes of β-CD with the methyl paraben guest represents a novel discovery.

Table 4.32 Average unit cell dimensions for different β-CD dimer packing types from the CSD

Space group	Packing type	Occurrence	a (Å)	b (Å)	c (Å)	α (°)	β (°)	γ (°)
P1	CH [a]	4	15.347	15.612	15.670	95.30	99.77	103.49
P1	IM [b]	26	18.266	15.432	15.412	103.21	113.69	99.97
$P2_1$	SC [c]	9	15.382	32.745	15.363	90	102.48	90
C2	CH [d]	24	18.630	23.391	15.903	90	108.03	90
$C222_1$	CB [e]	7	19.327	24.113	33.231	90	90	90

[a] CCD refcodes used: BCYDPR, CHANAO, FERCOU, XADHIT.
[b] CCD refcodes used: AGAZIR, AGAZOX, AGAZUD, BCDIPH, BCDMPH, BCDNPR, BIDMOQ, BOGCAB, BULFIX, CACPOM, CIDEXPR, CIDMUT, CIGXOF, DEVVAB, DIFHOP, DOGVUM, GESVUV, HEGXUM, LONGIE, MASBIR, MASBOX, TEJHAR, VOQDOU, VOQDOU, WISREV, WISRIZ.
[c] CCD refcodes used: CDETAN, CIVBUC, DUTLIN, GETPAW, GETPEA, KIFPAQ, NIZGUY, QAGXEX, SAJPIC.
[d] CCD refcodes used: BIBJEH, COCMIQ, CYDXTF, DEVTED, DEVTIH, DOQPOO, DOQPUU, GOSQOU, HAMBZB, HPAMIB, KOGLIB, KOGLOH, KUTJUE, MASBAJ, ODEJOW, PUKPIU, PUKPOA, SOBHUM, SOBJEY, TEMCIX, VIJXAN, XERTET, YOVVID, ZUZXOH.
[e] CCD refcodes used: DEVTON, DEVTUT, FASXUS, GIPFEQ, KOFJEU, MEGQUK, TECYIJ.

Over 70% of the products produced by the pharmaceutical industry are solids, which are mostly obtained by crystallisation, making them prone to the development of various polymorphs. Polymorphism is described as the ability of a compound [or of an element] to crystallise in more than one distinct crystal structure. The best-known example of polymorphism is that of carbon, which can exist in several forms: diamond, graphite, C_{60} and others. Polymorphism was possibly first observed by Klaproth in 1788 when he noticed that calcium carbonate existed in two different crystalline forms, calcite and aragonite.[41] The extent of polymorphism among pharmaceuticals was assessed by Kuhnert-Brandstätter in 1965, who reported that 67% of 48 steroids, 40% of 40 sulphonamides and 63% of 38 barbiturates studied, exhibited polymorphism.[42] In a more recent publication[43] the authors listed about 500 drugs for which polymorphism is known. One consequence of polymorphism is variation in solubility or dissolution rate [and hence bioavailability] and this could have serious implications, especially for drugs with a narrow therapeutic window. The potential impact is so great that the International Conference on Harmonisation [ICH] requires proper investigations [and analytical methods] for drug substances and drug products according to a decision tree.[44-45]

Many analytical techniques are used to monitor polymorphism in the pharmaceutical industry, thermal analysis being one of the more commonly used analytical techniques. In this study HSM proved to be a very useful and quick visual technique to observe the thermal differences between the two pseudo-polymorphic complexes. TGA results indicated that the P1 complex loses its waters of crystallisation more readily than the C2 complex. This corresponded to the DSC results, as the dehydration endotherm of the C2 complex was broader than that of the P1 complex. The DSC results also indicated that the P1 complex had a higher decomposition temperature than the C2 complex. This could be an indication that the P1 complex is the more stable form. In addition to dehydration and decomposition events, the DSC is capable of illustrating phase changes in polymorphs. However, endothermic or exothermic events that could have corresponded to a phase change were not observed in these complexes.

Another useful technique to monitor polymorphism is XRD, as polymorphs have different crystal packing arrangements. The XRD traces computed from the single crystal structure of the MPBCD and MPBCDP1 complexes are shown in Figure 4.33. From these XRD traces it is clear that two different forms of the β-CD-methyl paraben complex exist. X-ray photography and a comparison of these XRD traces with the reference traces of Caira[3] indicated that the β-CD-methyl paraben inclusion complex crystallises in the space groups P1 and C2 with packing modes IM and CH respectively.

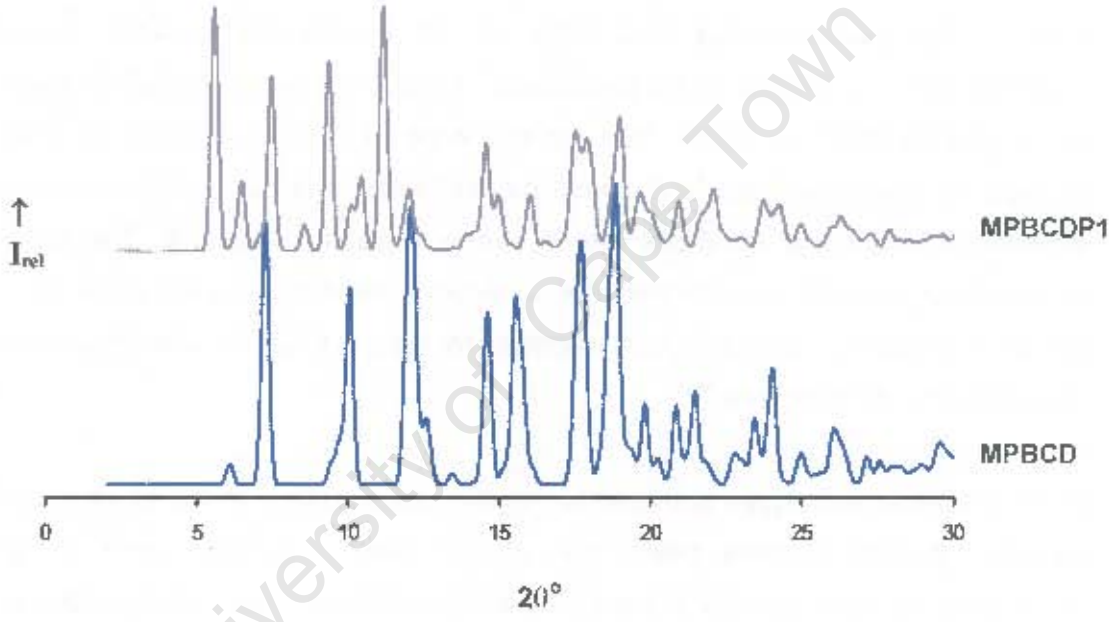

Figure 4.33 Calculated XRD traces of the MPBCD and MPBCDP1 complexes

Apart from polymorphic identification, XRD is a valuable tool in demonstrating isostructurality of CD complexes. In this study XRD showed that all the β-CD complexes prepared by co-precipitation and kneading methods [i.e. MPBCD, EPBCD, PPBCD and BPBCD] were isostructural to each other. This was very beneficial as X-ray intensity data were not collected for the EPBCD and BPBCD complexes but it can be expected, from the XRD results, that the crystal structures would be similar to those of the MPBCD and PPBCD complexes. The structures of the latter two complexes, crystallising in the space group C2 with Z = 4 and a host to guest ratio of 1:1, have been elucidated.

Conformation of the β-CD host molecule

In the complexes of this study, the β-CD molecules adopt a rather round and symmetrical structure as the variation in the radii of the heptagon and deviation of the O(4) atoms from the plane of the macrocycle are small. The average bond distances and angles are consistent with those of other β-CD structures. All the glucose units are orientated *syn*, and thus the O(2) and O(3) atoms of adjacent glucose units form seven intramolecular O(2)•••O(3') hydrogen bonds that maintain the conformation of the macrocycle. The tilt angles are all positive resulting in the β-CD molecule adopting a cone-like structure with the secondary rim wider than the primary rim.

Overall it has been found that in spite of the inclusion of a variety of guest molecules, the β-CD macrocycle is almost round, and the tilt angle is restricted to a relatively narrow range [-5° to 23°]. The average geometrical parameters that define the conformation of the cyclodextrin O(4) heptagon, the average O(2)•••O(3') distance and the average tilt angle [τ_1], were calculated from a number of dimeric structures in the CSD[41] [Table 4.33]. Comparison of the data for the MPBCD, MPBCDP1 and PPBCD structures showed them to lie within the ranges tabulated. For all three structures the geometric parameters occur over a relatively narrow range of values and this can be attributed to the fact that the formation of the β-CD dimers requires certain geometrical requirements to be met so that the important intra-dimeric O•••O hydrogen bond contacts can be made.

Negligible differences were observed in the geometric parameters of the MPBCD and PPBCD host structures [Table 4.33]. However, it was noticed that the O(4) heptagon in the MPBCDP1 structure was more symmetrical and undistorted than those in the C2 complexes. These differences were clearly expressed in the smaller deviations of the O(4) atoms from the mean O(4) plane and O(4) torsion angles. This suggests that the constraints that the two-fold symmetry places on the guest, in the space group C2, lead to a less favourable fit of the guest within the cavity and consequently a more distorted β-CD macrocyclic structure.

Table 4.33 The average values of the O(4) heptagon parameters, the O(2)•••O(3') distances and tilt angles for the MPBCD, PPBCD and MPBCDP1 structures, and the average values for a number of β-CD dimeric structures

Complex	*r* (Å)	*l* (Å)	*a* (°)	*d* (Å)	*t* (°)	O(2)•••O(3')	τ_1 (°)
MPBCD	5.04	4.38	128	0.06	2.8	2.82	6.0
PPBCD	5.10	4.43	129	0.07	3.2	2.81	4.4
MPBCDP1	5.03	4.36	129	0.02	1.4	2.79	5.1
β-CD dimeric structures	5.04	4.38	129	0.11	5.9	2.80	7.9

Paraben guest molecules

The orientation of a guest molecule within the CD cavity is dependent on a number of factors, such as the size and shape of the guest, dipole moments, hydrophobic interactions, hydrogen bonding and solvent interactions. The tendency to optimise the occurrence of hydrophobic and hydrophilic domains at the host-guest interface is thought to be important in orientating the guest in the cavity and determining the stability of the complex. In this regard Lichtenthaler *et al* [46,47] did a very comprehensive study in which they showed with computer aided visualisation of the molecular lipophilicity patterns [MLP] that the secondary rim of the β-CD molecule is relatively hydrophilic and its opposite primary rim is relatively hydrophobic. The bulk of the intensely hydrophobic regions is concentrated on the inner regions of the CD cavities. Additionally they showed that the sandwiched area between the secondary hydroxyls of a β-CD dimer is relatively hydrophilic. Figure 4.34 shows the MLPs for β-CD with the colour code ranging from dark blue for intensely hydrophilic portions to full yellow for the most hydrophobic regions. Their views are consistent with structures in the literature where water molecules of crystallisation are often found at the secondary hydroxyl interface of a β-CD dimer. From these studies they have suggested that the difference in the relative hydrophobicity of the two rims can be a determining factor in the orientation of the guest molecule within the cavity, as the hydrophilic portion of the guest will align with the hydrophilic secondary rim, and the hydrophobic portion of the guest will be located at the primary rim. These hydrophobic attractions are especially important in cases where the guest is devoid of polar groups. However, if polar groups are present, then dipole-dipole alignments and the need for solvation of polar groups may diminish the importance of hydrophobic attractions for orientating and stabilising a guest in a CD cavity.

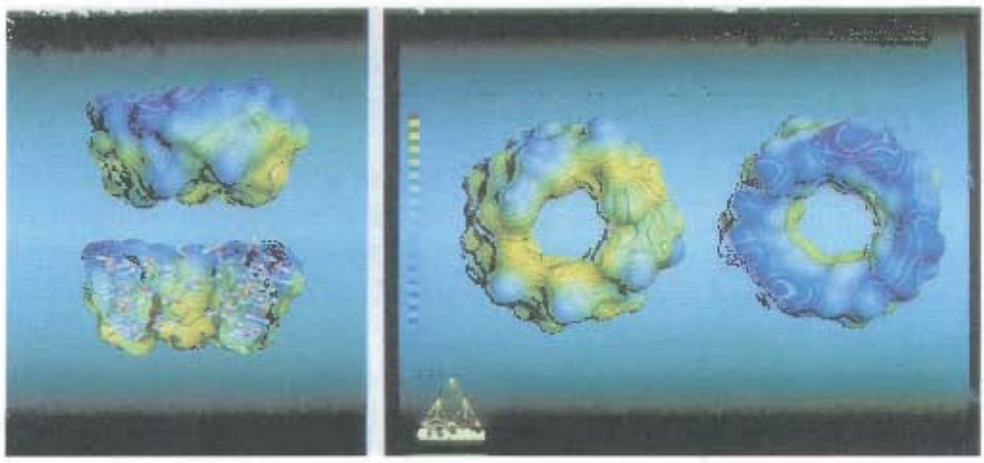

Figure 4.34 MLPs of β-CD: side views [left] in closed and bisected form each with secondary rim aligned upwards; views onto primary and secondary rims [right][42]

The mode of inclusion of the propyl paraben guest could not be determined due to the disordered nature of the guest within the CD cavity. The modes of guest inclusion for the MPBCD and MPBCDP1 complexes are comparable. In both complexes, two disordered guest molecules are included within the β-CD dimeric unit. The phenyl rings of the guest molecules are centralised in the cavities of the β-CD molecules with the hydroxyl group located at the primary rim and the ester moiety occupying the secondary rim. Figure 4.35 shows the orientation of the methyl paraben guest within the β-CD cavity as determined in this study. The relatively planar conformation of the uncomplexed methyl paraben guest, which is necessary for its close packing, is relaxed in the complexes.

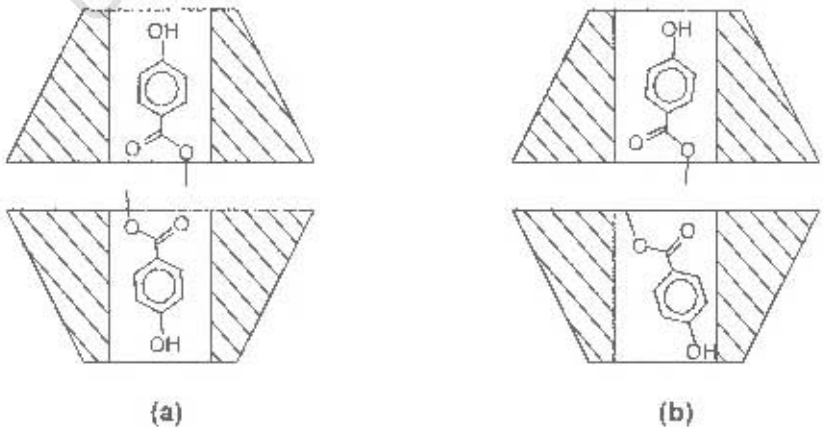

Figure 4.35 Orientation of the guest in the β-CD cavity (a) MPBCD and (b) MPBCDP1

Figure 4.36 illustrates how the guest is totally included within the CD dimer cavity in both of the methyl paraben inclusion complexes. This is achieved by tilting the guest molecules within the β-CD cavity. The tilt permits the guests to occupy most of the available space in the cavity and is necessary to avoid abnormally short contacts and steric clashes between the residues in the vicinity of the secondary hydroxyl dimer interface. The average tilt angles for the phenyl ring relative to the O(4) mean planes of the CD were 78° and 66° for the MPBCD and MPBCDP1 complexes respectively. Hence the guests included in the C2 complex have greater tilt angles than the guest included in the P1 complex. This may be a direct influence of the packing types, as the CH packing may allow for a more linear inclusion of the guest with respect to the β-CD dimer axis.

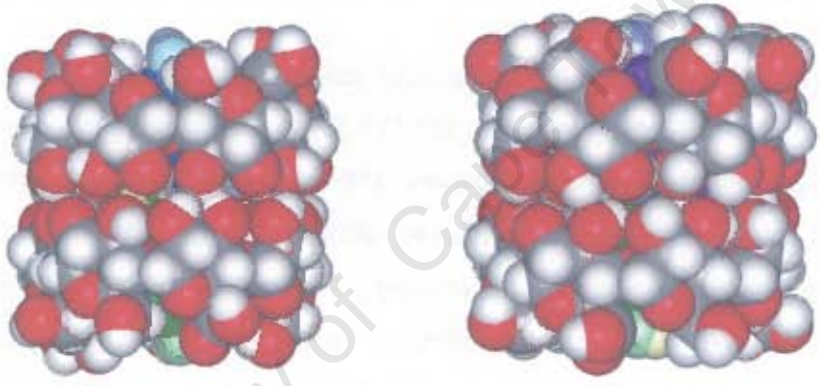

Figure 4.36 Space-filling diagrams of (a) MPBCD and (b) MPBCDP1 dimer structures

No direct hydrogen bonds are observed between the host and guest hydroxyl groups in the P1 complex, a weak association existing through water mediated hydrogen bonding. The opposite is true for the C2 complex in which the guest interacts with host O(6) hydroxyl oxygen atoms that are in the (+) *gauche* conformation and no direct interaction between the guest and the water molecules was observed.

From this analysis it is evident that the dominant factor in determining the orientation and positioning of the guest within the CD cavity is the solvation and hydrogen bonding of the guest hydroxyl group with water molecules and CD-hydroxyl groups respectively. This observation is in accordance with Bergeron *et al*[49] who state that the most important factor in the positioning and stability of the guest in the β-CD cavity is the solvation of the polar group.

For both complexes the orientation of the guest molecules, with the smaller hydroxyl substituent at the primary rim, also allows for more efficient inclusion. Additionally it allows the hydrophobic phenyl ring to be centralised within the cavity, which according to Lichtenthaler *et al* [46-47] is the most hydrophobic area of the CD. It is worth mentioning that the majority of the guest molecules of β-CD complexes found in the literature contain a hydrophobic moiety and a polar group and these are orientated in such a way that the polar group is found in the region of the primary rim or protruding from it.[4]

Hydroxyl-mediated hydrogen bonding interactions

Despite the different packing arrangements, the hydrogen bonding networks within the layers are very similar in different packing types.[50] The hydrogen bonding can be segregated into two sub-networks, one containing the primary -OH groups and the other containing the secondary hydroxyl groups. It has been observed in dimeric β-CD complexes studied thus far that the secondary hydroxyl groups are not influenced by the guest, but participate in an invariant network of hydrogen bonds connecting neighbouring dimers directly or through water molecules.[50] Primary hydroxyl groups also form a network of hydrogen bonds connecting dimers but they are influenced by the presence of the guest if the latter protrudes from those faces.[34]

With regard to the secondary hydroxyl network the host molecules are stabilised by seven intramolecular O(2)•••O(3') hydrogen bonds and these bonds contribute to the rigidity and highly symmetrical conformation of the cyclodextrin. This network was further extended by dimer formation through the association of the two β-CD monomers by hydrogen bonding of the secondary O(3) hydroxyl oxygen atoms. The mean distances of these contacts are 2.85, 2.81 and 2.86 Å [average e.s.d.s 0.01, 0.03, 0.02 Å] for the MPBCD, MPBCDP1 and PPBCD complexes respectively.

The primary hydroxyl groups form hydrogen bonds to adjacent dimers of the same layer, either directly or via water-mediated interactions. The O(2)•••O(2) and O(6)•••O(6) contacts, which are present in all three complexes, are the only direct CD-to-CD intra-layer interactions observed. In addition to these intra-layer interactions, inter-layer interactions were found between the primary -OH groups in the C2 complexes.

In these complexes, the minor position of the disordered hydroxyl group O(63B) forms a hydrogen bond to its symmetry related hydroxyl group on an adjacent dimer in the next layer of the channel. The relative weakness of this bond, due to the low site-occupancy of 0.19 and 0.37 in the MPBCD and PPBCD complexes respectively, may explain in part the instability of the crystal structure. This inter-layer interaction was not observed in the MPBCDP1 structure because of the distortion in the linearity of the dimeric columns. Finally, the analysis of the structure revealed a handful of weaker, partly electrostatic C-H•••O intermolecular interactions.

In addition to these host-host interactions, the O(2), O(3) and O(6) hydroxyl groups are involved in contacts with the solvent water molecules. Some of these primary and secondary hydroxyl groups are linked to parallel CD columns via hydrogen bonding to the water channel. The water molecules thus contribute to the overall stability of the crystal structure and crystallinity is reduced upon dehydration.

Water-mediated hydrogen bonding interactions

The DSC results indicated that water loss from the complexes is a multi-step process pointing to different populations of water molecules. This can be reconciled with the crystal structure, where some water molecules are involved in a complex network of hydrogen bonds.

The water molecules fill the interstitial space between the host molecules. Water-water type hydrogen bonding mediates many of the hydrogen bonds that have already been discussed and in many of the guest interactions, water molecules form a link between guest and guest or guest and host. Despite the seemingly intrinsic disorder of the water molecules, a quasi-invariant water network organised in layers has been shown to exist.[52] This network can be divided into two separate sub-networks, one involving hydrogen bonds with the primary hydroxyl groups and the other with the secondary hydroxyl groups.

None of the primary hydroxyl groups links a water site of the secondary sub-network. An important distinction between the two sub-networks is that in the secondary network, water molecules extend the intramolecular and intradimer hydrogen bonding system. However, the primary network constitutes an interface between two β-CD dimeric layers and it is therefore principally involved in -OH•••water and water•••water interactions. The water sub-layer constituting the interface between two adjacent dimeric layers is said to contribute to the cohesiveness of the crystal since direct hydrogen bonding between these dimers is rare.[4] Owing to this dense hydrogen bonding network the water molecules are held more tightly than the guest molecules.

Table 4.34 shows the normalised number of contacts and their mean O•••O contact distances for the various water interactions. The numbers of contacts were normalised for the purpose of comparison. The normalised number of contacts was calculated by multiplying the number of water molecules per dimer by the total site-occupancy factor of the water molecule which was then divided by the total number of positions over which the water molecules were found [Equation 1].

$$\text{Normalised number of contacts} = \frac{\text{Number of water molecules per dimer x s.o.f.}}{\text{Total number of positions of the water molecules}} \quad (1)$$

The number of secondary hydroxyl hydrogen bonds is limited by the dimerisation of the β-CD molecule. This tabulation shows that the IM structure has more O(6)•••water and water•••water contacts than the CH structures.

Table 4.34 Summary of the water interactions for the MPBCD, PPBCD and MPBCDP1 structures

Complex	O(2)•••Water		O(3)•••Water		O(6)•••W		Water•••Water	
	No.	Mean (Å)	No.	Mean (Å)	No.	Mean (Å)	No.	Mean (Å)
MPBCD	6	2.77	5	2.79	6	2.79	13	2.71
PPBCD	6	2.75	5	2.83	8	2.76	20	2.75
MPBCDP1	5	2.77	10	2.74	26	2.70	32	2.74

Crystal packing

Most complexes of native β-CD crystallise as dimers. The dimers are linked together in a head-to-head fashion into infinite two-dimensional layers by a dense network of hydrogen bonds involving primary and secondary hydroxyl groups as well as water molecules. These layers are approximately perpendicular to the dimer axis and are stacked with their seven-fold axes approximately parallel. All known β-CD dimeric crystal structures are generated from a superposition of these practically invariant layers. As mentioned earlier, β-CD dimers crystallise in four different packing types, which differ in the relative placement of the CD layers.[4] They are classified as: channel type [CH], intermediate type [IM], chessboard type [CB] and screw-channel type [SC]. An important feature of these packing types is that they present different environments for intermolecular interactions at the primary end of the β-CD dimers and thus any part of the guest that protrudes from the primary rim plays a crucial role in determining how the two-dimensional layers pack to form the crystal.[34] However, in the pseudo-polymorphic structures no, or very little, guest protrusion from the primary rim was observed.

In the MPBCD and PPBCD CH structures, the β-CD dimers stack parallel to the *c*-axis nearly directly on top of each other with only a slight shift of 2.7 Å between two dimers of successive layers along the channel. The guests therefore find themselves shielded from the water environment and interact only with the host O(6) hydroxyl groups.

In the MPBCDP1 IM structure, the packing mode falls between the CH and CB type packing modes as the lateral displacement of dimers in consecutive layers is 6.2 Å. In the CB type packing, the lateral displacement between two consecutive β-CD dimeric layers is 8.9 Å. Hence each dimer is isolated, so that the structure takes on the appearance of a three-dimensional chessboard with "squares" of water channels and β-CD dimers alternating throughout. This leaves the primary face and included guest fully exposed to water molecules and hydroxylic groups of neighbouring macrocycles.

The lateral shift of 6.2 Å in the IM mode puts the seven-fold axis of the dimer near the rim of the dimer below and results in the guest molecules finding themselves in a nearly "cage-like" environment. The primary hydroxylic sides are therefore partially closed by the β-CD atoms of adjacent layers. The IM packing is thought of as more open than the CH type packing and permits the entrance of water molecules between the primary faces of the dimers, allowing the guest to be fully hydrated.

The packing arrangement of the β-CD structures can be examined in terms of the volume per inclusion unit, which is defined as the cell volume required for a single β-CD molecule, its included guest and its associated water molecules, and these are given in Table 4.35 with the average volume per inclusion unit for the various types of β-CD packing types.

Mentzafos *et al* [4] suggest that the volume per inclusion unit probably reflects the extent of hydration over the primary faces of the dimers. In addition it is a measure of close packing, as it was noted that the monomeric herringbone structure, which has the smallest volume [average value 1530 (10) Å^3], is also the most compact packing type of all β-CD structures. For the dimeric structures it can be seen that a decrease in the linearity of the dimeric columns results in an increase in the volume per inclusion unit. The trend observed is CH < IM < SC < CB. This would suggest that the packing arrangement adopted by the β-CD structure correlates directly with the volume per inclusion unit.

Table 4.35 Volume per inclusion unit of the MPBCD, PPBCD and MPBCDP1 structures and the average asymmetric volumes of some structures from the literature

Complex	Packing type	Space group	V / Z (Å^3)
MPBCD	CH	C2	1683
PPBCD	CH	C2	1747
MPBCDP1	IM	P1	1828
Average literature values[27]	CH	P1	1763
	IM	P1	1843
	SC	$P2_1$	1899
	CH	C2	1761
	CB	$C222_1$	1943

The volume per inclusion unit therefore shows that the IM structure has a less compact packing arrangement than the CH structure. This is probably due to the extended hydration shell found around the primary rim. However, this still does not explain why two different packing arrangements occur. A possible explanation for this phenomenon is that the hydroxyl group of the guest forms a strong interaction with the water environment favouring the IM packing over the CH. If this interaction is purely electrostatic then the spatial fit of the guest to the cavity becomes important. If the guest does not provide a tight spatial fit [as suggested by the disorder observed in the guest position within the cavity], then the interaction with the water molecules will be destabilised and the CH type packing will form. At low temperature the degree of motion of the guest is reduced and the hydration shell is more ordered thereby preventing the CH type of packing from forming and thus favouring the IM packing mode.

Final remarks

In summary, the observed differences between the MPBCD and MPBCDP1 structures are that i) the P1 complex exhibits a more symmetrical macrocycle than the C2 complex, ii) the tilt angles of the guests in the C2 complex are greater than those for the guests included in the P1 complex, iii) the P1 complex is more extensively hydrated and consequently has a larger volume per inclusion unit than the C2 complex and iv) there are differences in the interactions of the guest with the host and water molecules. With regard to the latter point, when crystals of the methyl paraben inclusion complexes were grown at room temperature they display CH packing, which allows the guest to hydrogen bond to the CD primary hydroxyl groups and minimise contact with the waters of crystallisation. In contrast, when the crystals were grown at low temperature the inclusion complex crystallises in the IM type packing allowing the guest to interact with the hydrophilic water environment.

The results presented here provide support that detailed structural studies are essential in understanding the molecular interactions occurring in complex supramolecular systems. Additionally, this study shows the importance of the conditions of crystallisation. The observation of pseudo-polymorphism in CD inclusion complexes has to date not been reported in the literature and was therefore an unexpected and most significant finding. It can therefore be concluded that polymorphism of CD inclusion complexes is rare, but systematic variations in crystallisation conditions could increase the chances of its occurrence.

Part 2

SOLUTION STUDY

PROTON NUCLEAR MAGNETIC RESONANCE SPECTROSCOPY (NMR) OF THE β-CD PARABEN COMPLEXES

The present section describes a parallel study of the inclusion of the paraben drugs with the host β-CD, in solution. NMR spectroscopy is one of the most useful techniques for studying CD inclusion complexes in solution because of its sensitivity.[52-53] The interaction of a guest molecule with the CD is clearly reflected in changes in various NMR spectral parameters.[54-55] Lists of the chemical shifts of the pure compounds and of the equilibrium mixtures containing the β-CD-paraben complexes are presented in Appendix A. Partial 300 MHz ^{1}H NMR spectra of the pure compounds and of the equilibrium mixtures containing the β-CD-paraben complexes and the remaining reagents are displayed in Appendix B. The assignment of the β-CD protons was performed following those of Schneider *et al.*[56] For the alkylparabens, assignment of the protons was performed in accordance with Chan *et al.* [57] However, whereas Chan *et al* [57] used DMSO•d_6 as the solvent, in this study D_2O was used. In the present study, preliminary tests using DMSO•d_6 as solvent did not yield spectroscopic evidence for inclusion complex formation with the parabens. A probable reason for this is that the DMSO•d_6 becomes firmly fixed within the β-CD cavity, thus preventing the entry of the guest. The large peak at 4.8 ppm seen in each spectrum is due to residual HDO molecules in the D_2O solvent and was considered as an internal standard in the measurement of the chemical shifts of the peaks of β-CD in the presence and absence of the paraben drug. The numbering scheme of the β-CD protons is shown in Figure 4.37. In each of the β-CD-paraben spectra, the β-CD spectra showed significant shifts for the H3, H5 and H6 protons, whereas the H1, H2 and H4 protons were relatively unaffected [Figure 4.38].

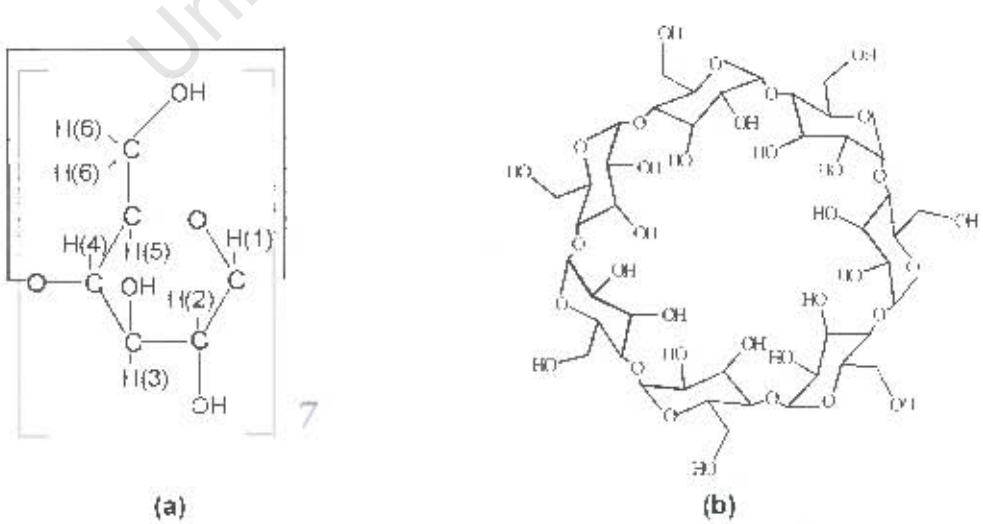

Figure 4.37 (a) The glucopyranose unit with the numbering scheme (b) β-CD

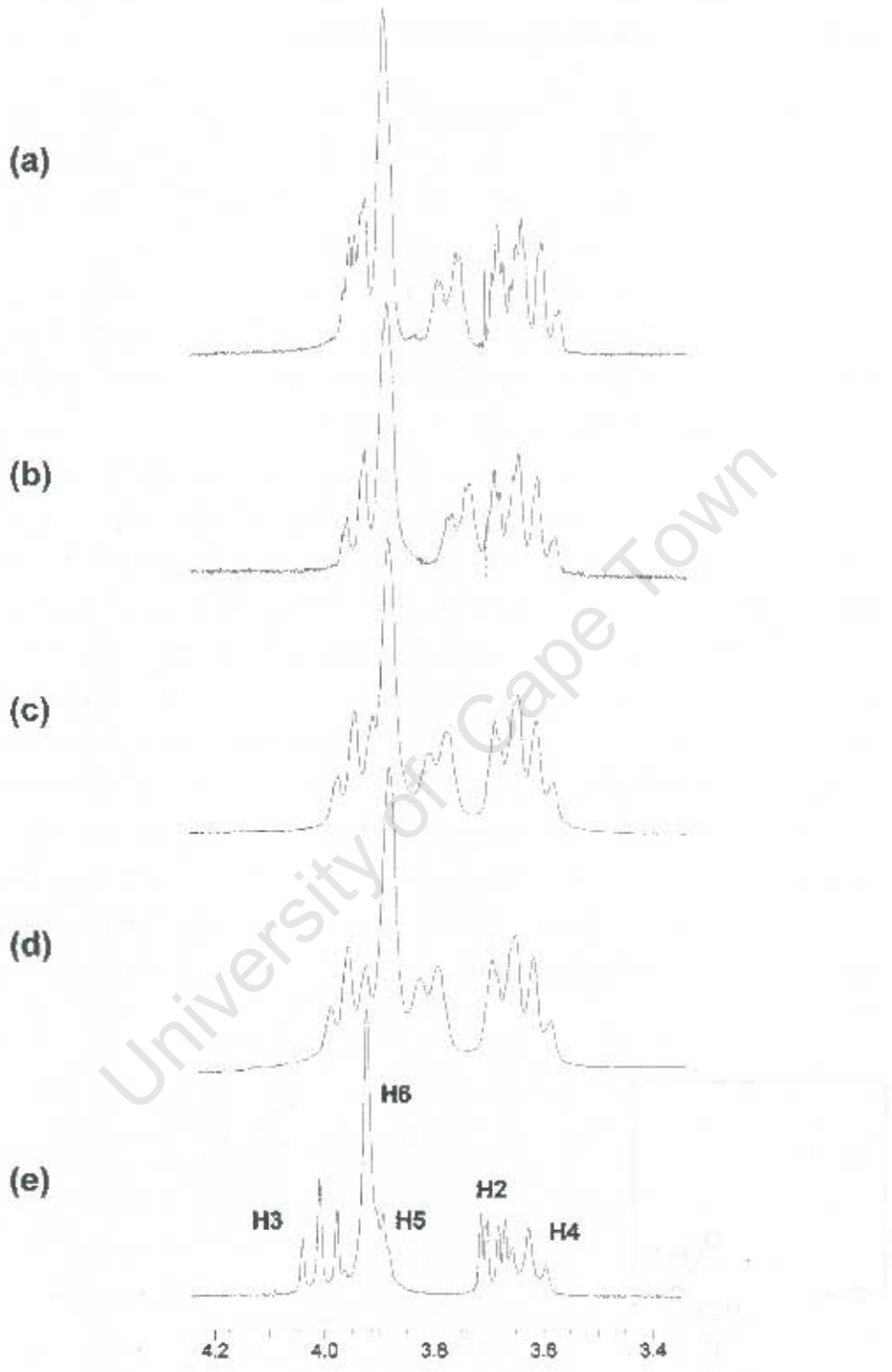

Figure 4.38 Partial ^{1}H NMR spectra (300 MHz) of [H]/[G] 1:1 of the (a) MPBCDS, (b) EPBCDS, (c) PPBCDS and (d) BPBCDS complexes and (e) the pure β-CD at 298 K

The H3 and H5 protons are located within the cavity, the H6 proton is located on the cavity rim at the narrow end of the molecule and the H1, H2 and H4 protons are located on the exterior of the β-CD torus. The up-field shifts of the H3, H5 and H6 protons verified that the parabens interact only with the inside of the cavity and therefore inclusion complexes form in solution. The complexes of β-CD with each paraben will be referred to as MPBCDS, EPBCDS, PPBCDS and BPBCDS.

A small dispersion of the chemical shift values of the H1 proton was noticed. This can be interpreted in terms of the small differences in the conformation around the glucosidic bond among the α(1,4)-linkages in the complexed state.[58]

Distinct peaks were not observed for a bound and a free form. This observation implied that complexation was a dynamic process, the included drug undergoing fast exchange [relative to the NMR time scale] between the free and bound states and only the shifts of the spectral lines were observed. Therefore the exchange rate between the free and bound states must exceed the reciprocal of the largest observed shift difference [in Hz] for any proton of the guest molecule.[59] The exchange rate, τ_{exch}, can be calculated from the equation given below[60] and was found to be less than or equal to 19, 12, 5 and 9 ms for the MPBCDS, EPBCDS, PPBCDS and BPBCDS complexes respectively.

$$\tau_{exch} \leq \frac{1}{2\pi \cdot \Delta\nu(\mathrm{Hz})} \qquad (2)$$

Stoichiometry

The stoichiometries of the complexes were determined using the continuous variation method,[61] as described in the *Experimental* section. Chapter 2, by following the changes in the chemical shifts of the host protons which showed the greatest variations *viz.* H3, H5 and H6. The Job's plot of the β-CD proton shifts is more accurate than that of the parabens, as the β-CD signals are strengthened by the seven identically positioned protons [one from each glucose monomer].

The Job's plots for the β-CD H3, H5 and H6 protons are presented in Figure 4.39 and have an almost symmetric appearance, indicating that only one type of complex had formed.[62,63] For each β-CD-paraben complex, the Job's plot shows a maximum at r = 0.5, indicating the existence of a complex with 1:1 stoichiometry within the range of concentrations investigated.

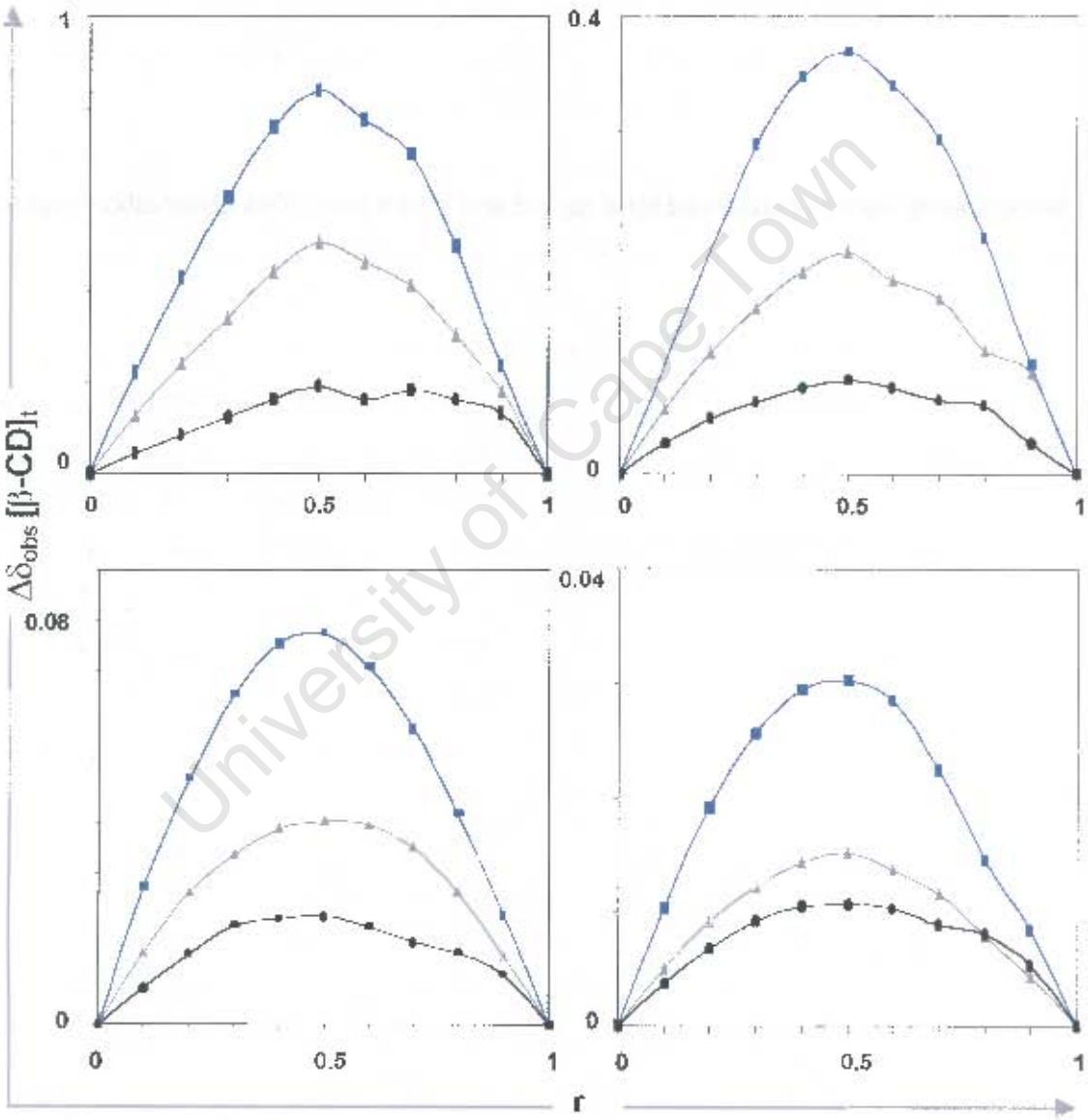

Figure 4.39 Job's plots for protons of β-CD [-▲- H3; -■- H5; -●- H6] in the (a) MPBCDS [10Mm], (b) EPBCDS [5Mm], (c) PPBCDS [1.5Mm] and (d) BPBCDS [0.7Mm] complexes

Association constant

The association constants for the 1:1 complexes were evaluated by a non-linear least-squares regression analysis of the observed chemical shift changes of the drug and β-CD NMR lines, as a function of β-CD concentration, Equation (3), where [X] is the concentration of the host or guest of a sample and $M = [G]_t + [H]_t$.

$$\Delta\delta_{obs}^{[X]} = \frac{\Delta\delta_c^{[X]}}{2[X]}\left[M - {}^1/_K - \left\{(M + {}^1/_K)^2 - 4[G]_t[H]_t\right\}^{1/2}\right] \quad (3)$$

For consistency, K was evaluated from the observed differences in chemical shifts for the H3, H5, and H6 protons of β-CD in each case. The overall association constants (K) obtained are listed in Table 4.36, along with the loss functions (E), the correlation factors (R) and the complexation-induced shifts ($\Delta\delta$).

The results show that $\Delta\delta$(H5) > $\Delta\delta$(H3), indicating a deeper penetration of the guest into the cavity and demonstrating that the primary side of the β-CD cavity is involved in complex formation. In addition these results indicate that the association constant generally decreases as the alkyl chain length increases, as this part of the guest finds itself outside the cavity in the hydrophilic water environment. However the BPBCDS complex is inconsistent with this trend and the calculated association constant suggests that this guest has the tightest fit within the CD cavity. As the stability of the complex in solution refers to the degree of association between the two species involved in a state of equilibrium, the overall stability follows the order BPBCDS > MPBCDS > EPBCDS > PPBCDS.

Table 4.36 K, E, R and $\Delta\delta_c$ of the β-CD complexes at 298 K.

		MPBCDS	EPBCDS	PPBCDS	BPBCDS
K	M^{-1}	1631	938	460	2022
E		5.198×10^{-4}	1.177×10^{-4}	1.459×10^{-4}	1.378×10^{-4}
R		0.9980	0.9991	0.9988	0.9984
$\Delta\delta$(H3)	ppm	0.1363	0.1421	0.2550	0.1298
$\Delta\delta$(H5)	ppm	0.2369	0.2768	0.4820	0.2687
$\Delta\delta$(H6)	ppm	0.0488	0.0629	0.1327	0.0975

In addition the association constant allows for the estimation of the percentage of the drug which will complex with the cyclodextrin at 298 K. For any mixture of host and guest, the concentration of the included drug [C] can be calculated from the association constant using Equations (4) and (5). If $[H]_t = [G]_t$, which corresponds to the mid-point of the Job's plot experiment, [C] can be calculated and its value indicates the percentage of the drug that was not included. From Table 4.37 it can be seen that as the association constant decreases so the percentage of the drug included in the CD decreases.

$$d = K[H]_t + K[G]_t + 1 \quad (4)$$

$$[C] = \left(d - \{d^2 - 4K^2[H]_t\,[G]_t\}^{1/2}\right)\left(2K\right)^{-1} \quad (5)$$

Table 4.37 Percentage of the drug not included in the CD cavity

	MPBCDS	EPBCDS	PPBCDS	BPBCDS
K (M^{-1})	1631	938	460	2022
$[H]_t = [G]_t$	5	2.5	0.75	0.35
[C]	3.53	1.32	0.16	0.11
% of drug not included	29 %	47 %	79 %	69 %

Determination of the structure

One source of structural information is the set of chemical shift changes relative to the free forms observed upon formation of the complex. This parameter is referred to as the complexation-induced shift ($\Delta\delta$) and is given in Table 4.38. Patterns in the magnitudes of these shifts might indicate possible complex geometries.

The signals of the included paraben are shifted by complexation to a variable extent and a similar trend for each of the guest proton resonances was observed, suggesting a comparable insertion of each paraben guest in the β-CD cavity. For each β-CD-paraben mixture an increase in the concentration of the CD caused down-field shifts of the alkyl chain and ester moiety signals and up-field shifts of the aromatic ring protons.

The shielding of the aromatic protons was interpreted as a consequence of their inclusion in the CD,[64] while the deshielding of the alkyl protons indicated that this part of the guest lies outside the cavity. The guest position is consistent with the up-field shifts of the β-CD cavity protons, as the β-CD protons experience anisotropic shielding attributed to the inclusion of the guest aromatic ring.[65-73]

The orientation of the guest within the CD is determined by dipole-dipole interaction between the guest and inner protons of the host, as well as by the formation of hydrogen bonds between the -OH group and the hydrophilic water environment. In the PPBCDS and BPBCDS complexes $\Delta\delta$(H3,H7) > $\Delta\delta$(H4,H6) suggesting that the guest hydroxyl groups are located at the primary rim. In the MPBCDS complex the shifts of the *meta* protons are larger than those of the *ortho* protons, i.e. the reverse of the PPBCDS and BPBCDS complexes. This suggests that the phenol moiety of the methyl paraben is located at the secondary rim of the CD. In the EPBCDS complex $\Delta\delta$(H3,H7) ~ $\Delta\delta$(H4,H6), i.e. both the aromatic protons show an approximately equal interaction with the CD and hence the orientation of the guest cannot be unequivocally determined.

A clearer geometrical relationship between the host CD and the guest in the inclusion complex could be attained by measuring the ^{1}H spectral enhancement due to the homonuclear Overhauser effect [NOE].[58, 74] In this case, the origin of the NOE is a host-guest intermolecular dipole-dipole interaction. The magnitude of the ^{1}H homonuclear NOE enhancement is small [max. 50 %] and depends critically on the mutual motion and the distances between relevant protons. NOE experiments were conducted and confirmed the orientation of the methyl paraben guest within the cavity, *viz.* that the hydroxyl group is located at the secondary rim. The NOE experiments of the ethyl-, propyl- and butyl paraben complexes showed that there was no interaction between the host and guest, suggesting that the intramolecular interactions between the two species were greater than 4 Å.

Table 4.38 Chemical shifts (ppm) of the alkylparabens in the free (experimental values) and complexed states (fitted values)

Parabens	Protons	δ_{free}	$\Delta\delta$	Effect
Methyl paraben	H3, H7	7.9863	0.006	Shielded (S)
	H4, H6	6.9987	0.028	Shielded (S)
	CH_3	3.9337	-0.024	Deshielded (D)
Ethyl paraben	H3, H7	8.0029	0.037	S
	H4, H6	7.0039	0.044	S
	CH_2	4.4004	-0.039	D
	CH_3	1.4116	-0.032	D
Propyl paraben	H3, H7	8.0037	0.126	S
	H4, H6	6.8900	0.052	S
	CH_2 (t)	4.3120	-0.098	D
	CH_2 (q)	1.8181	-0.027	D
	CH_3	1.0272	-0.032	D
Butyl paraben	H3, H7	7.9944	0.112	S
	H4, H6	6.9895	0.042	S
	CH_2 (t)	4.3764	-0.059	D
	CH_2 (q)	1.7963	-0.029	D
	CH_2 (st)	1.4982	-0.009	D
	CH_3	0.9894	-0.045	D

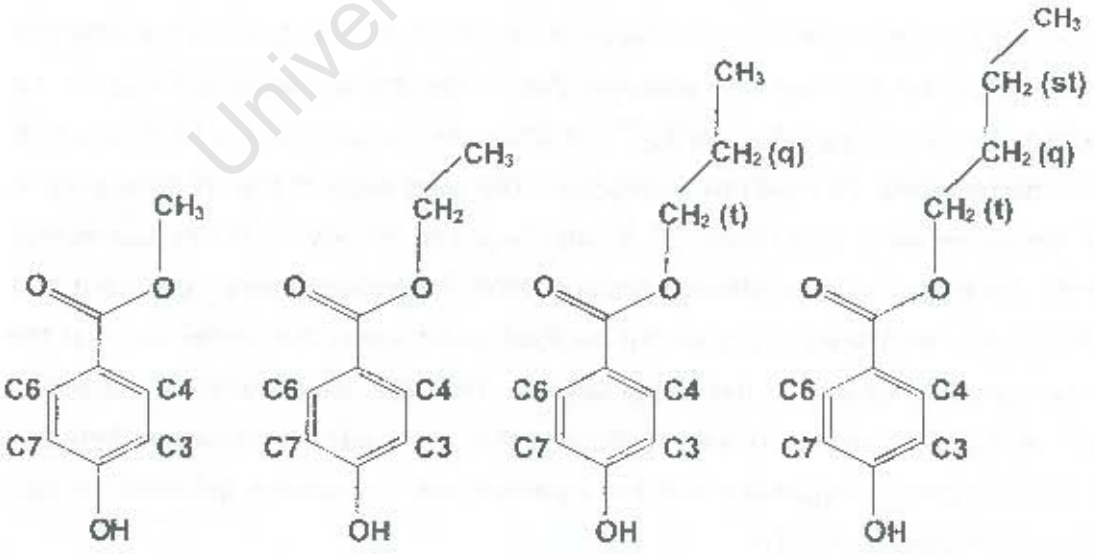

Figure 4.40 Chemical structure of methyl-, ethyl-, propyl- and butyl paraben. Numerals correspond to proton positions referred to in the NMR study.

DISCUSSION

Previous work by McDonald *et al* [75] reported the association constants for the inclusion complexes of 2-hydroxypropyl-β-CD (2-HP-β-CD) with parabens as 1099, 699, 1338 and 2495 M^{-1} for the methyl-, ethyl-, propyl- and butyl paraben complexes respectively. They found that the K value increased as the hydrophobicities of the esters increased, indicating a greater ability of the long chained parabens to compete for the hydrophobic core of the 2-HP-β-CD molecule. Later, Matsuda *et al* [76] postulated that the hydrophobic part of the paraben molecule entered the hydrophobic cavity of β-CD, with the phenol moiety located at the wider secondary rim. Chan *et al* [57] conducted ^{1}H NMR spectral studies and concluded that the phenyl ring was inserted into the hydrophobic cavity [as found in this study]. Additionally Chan *et al* [57] suggested that the steric strain due to longer chain length would be overcome by a convenient twist in the chain conformation, which favoured a compact accommodation of the guest molecule in the hydrophobic β-CD cavity.

In this study it was found that the values obtained for K did not show a uniform decrease as the length of the alkyl chain increased. This trend resembles the variation found by Chan *et al* [57] for the R and S parameters based on membrane dialysis results. They obtained a relatively high value for S for the β-CD-methyl paraben complex, indicating that the methyl group could be accommodated quite well in the β-CD hydrophobic cavity. However, the ethyl group showed a decrease in the S value while further increase in the size of the alkyl chain produced the opposite effect. This suggests that the increase in the hydrophobicity of the larger alkyl group leads to a greater interaction with β-CD. If this were the case, then there should have been a uniform increase in the extent of interaction as the alkyl chain length increased. However this was not observed, implying that not only the hydrophobic effect but also some other factors play a significant role in determining the formation of the complex [for instance the orientation of the preservatives within the β-CD cavity, van der Waals forces, London dispersion forces[77-78] and hydrogen bonding].

It is worth noting that in solution additional arrangements of the complex are possible, including inversion of the guest positions found in the crystal.[79] This is a consequence of the secondary hydroxyl end being open in solution and allowing solvation of the hydroxylic group at either end of the CD cavity.

REFERENCES

1) F. Giordano, R. Bettini, C. Donini, A. Gazzaniga, M. R. Caira, G. G. Z. Zhang, D. J. W. Grant, *J. Pharm. Sci.*, **1999**, 88, 11, 1210.
2) L. Szente, *In Comprehensive Supramolecular Chemistry*, (Vol. 3), J. L. Atwood, J. E. D. Davies, D. D. MacNicol, F. Vögtle (eds.), Pergamon, UK, **1996**, Ch 8, p. 253-278.
3) M. R. Caira, *Roum. Chim. Rev.*, **2001**, 46, 4, 371.
4) D. Mentzafos, I. M. Mavridis, G. le Bas, G. Tsoucaris, *Acta Crystallogr.*, **1991**, B47, 746.
5) F. H. Herbstein, R. E. Marsh, *Acta Crystallogr.*, **1998**, B54, 677.
6) F. H. Herbstein, *Acta Crystallogr.*,**1997**, B53, 968.
7) V. Schomaker, R. E. Marsh, *Acta. Crystallogr.*, **1979**, B35, 1933.
8) Paratone N oil (Exxon Chemical Co., TX, USA).
9) *Data Preparation and Reciprocal Space Exploration,* Version 5.1, (Copyright Bruker Analytical X-ray Systems, **1997**).
10) C. Giacovazzo, *Fundamentals of Crystallography*, ed. C. Giacovazzo, Oxford University Press, **1994**.
11) P. M. de Wolff, *International Tables for Crystallography*, T. Hahn (ed.), Vol. A, Boston: D. Reidel Publishing Co., Kluwer Academic Publishers, Dordrecht, p. 737-744, Table 9.3.1.
12) G. Brown, *MSc. Thesis, Cyclodextrin Inclusion Compounds with Non-steroidal Anti-inflammatory Drugs,* University of Cape Town, South Africa, **1997**.
13) G. M. Sheldrick, *SHELXL-97, Program for the Refinement of Crystal Structures*, University of Göttingen, Germany, **1997**.
14) X. Lin, *J. Struct. Chem.*, **1983**, 2, 213.
15) J. A. Hamilton, M. N. Sabesan, L. K. Steinrauf, A. Geddes, *Biochem. Biophys. Res. Commun.*, **1976**, 73, 659.
16) M. Noltemeyer, W. Saenger, *J. Am. Chem. Soc.*, **1980**, 102, 2710.
17) J. A. Hamilton, M. N. Sabesan, L. K. Steinrauf, *Carbohydr. Res.*, **1981**, 89, 33.
18) J. A. Hamilton, M. N. Sabesan, *Carbohydr. Res.*, **1982**, 102, 31.
19) C. Betzel, B. E. Hingerty, M. Noltemeyer, G. Weber, W. Saenger, J. A. Hamilton, *J. Incl. Phenom.*, **1983**, 1, 181.
20) G. le Bas, C. de Rango, N. Rysanek, G. Tsoucaris, *J. Incl. Phenom.*, **1984**, 2, 861.

21) I. M. Mavridis, E. Hadjoudis, G. Tsoucaris, *Mol. Cryst. Liq. Cryst.*, **1990**, 186, 185.

22) B. Klingert, G. Rihs, *J. Chem. Soc., Dalton Trans.*, **1991**, 2749.

23) I. M. Mavridis, E. Hadjoudis, G. Tsoucaris, *Carbohydr. Res.*, **1991**, 220, 11.

24) D. Mentzafos, I. M. Mavridis, M. B. Hursthouse, *Acta Crystallogr.*, **1996**, C52, 1220.

25) N. Rysanek, G. le Bas, F. Villain, G. Tsoucaris, *Acta Crystallogr.*, **1996**, C52, 2932.

26) G. A. Jeffery, *An Introduction to Hydrogen Bonding,* Oxford University Press, Oxford, **1997**, p. 50.

27) D. R. Dodds, *PhD Thesis, Physicochemical Study of Inclusion of Drug Molecules in Cyclodextrins,* University of Cape Town, South Africa, **1999**.

28) T. J. Brett, J. M. Alexander, J. L. Clark, C. R. Ross II, G. S. Harbison, J. J. Stezowski, *J. Chem. Soc., Chem. Comm.*, **1999**, 1275.

29) T. J. Brett, J. M. Alexander, J. J. Stezowski, *J. Chem. Soc., Perkin Trans 2,* **2000**, 1095.

30) A. Kokkinou, S. Makedonopoulou, *Carbohydr. Res.*, **2000**, 328, 135.

31) W. C. McCrone, *Physics and Chemistry of the Organic Solid State,* D. Fox, M. M. Labes, A. Weissberger (eds.), **1965**, New York, (Vol. 2), p. 726-767.

32) A. Rontoyianni, I. M. Mavridis, E. Hadjoudis, A. J. M. Duisenberg, *Carbohydr. Res.*, **1994**, 252, 19.

33) R. Bergeron, *Incl. Compd.*, **1984**, 3, 391.

34) W. Saenger, *J. Incl. Phenom.*, **1984**, 2, 445.

35) W. Saenger, *Isr. J. Chem.*, **1985**, 25, 43.

36) W. Saenger, C. Betzel, B. E. Hingerty, G. M. Brown, *Nature,* **1982**, 296, 581.

37) W. Saenger, C. Betzel, B. E. Hingerty, G. M. Brown, *Angew. Chem., Int. Ed. Engl.*, **1983**, 22, 883.

38) E. Mvula, *MSc. Thesis, Preparation and Solid State Properties of Cyclodextrin Complexes of Selected Drug Molecules,* University of Cape Town, South Africa, **1999**.

39) L. J. Barbour, *X-Seed, A Software Tool for Supramolecular Crystallography, Supramol. Chem.*, **2001**, 1, 189.

40) *Cambridge Structural Database and Cambridge Structural Database System,* Version 5.23, April **2002**, Cambridge Crystallographic Data Centre, University Chemical Laboratory, Cambridge, England.

41) J. Haleblain, W. C. McCrone, *J. Pharm. Sci.,* **1969**, 8, 58,911.

42) P. York, *Int. J. Pharm.,* **1983**, 14, 1.

43) L. Borka, J. K. Haleblian, *Acta Pharm. Yugoslavia,* **1990**, 40, 71.

44) International Conference on Harmonisation (ICH), Guild Line Specification Q6A, Step 3, Draft, 16 July **1997**, *Decision tree: Investigating the Need to Set Acceptance Criteria for Polymorphism in Drug Substances and Drug Products.*

45) *The Gold Sheet*, **1996**, 30, 1-4, F.D.C. Reports.

46) F. W. Lichtenthaler, S. Immel, *Starch*, **1996**, 48, 4, 145.

47) F. W. Lichtenthaler, S. Immel, *Starch*, **1996**, 48, 6, 225.

48) F. W. Lichtenthaler, S. Immel, *Liebigs Ann.,* **1996**, 27.

49) R. Bergeron, M. Channing, K. McGovern, W. Roberts, *Bioorg. Chem.,* **1979**, 8, 263.

50) G. le Bas, G. Tsoucaris, *Supramol. Chem.,* **1994**, 4, 13.

51) G. le Bas, G. Tsoucaris, *Mol. Cryst. Liq. Cryst.,* **1986**, 137, 287.

52) Y. Inoue, *JEOL NEWS*, **1987**, 23A, 36.

53) Y. Yamamoto, Y. Inoue, *Carbohydr. Chem.,* **1989**, 8, 29.

54) D. J. Wood, F. E. Hruska, W. Saenger, *J. Am. Chem. Soc.,* **1977**, 99, 1735.

55) Y. Yamamoto, Y. Kanda, Y. Inoue, R. Chûjô, S. Kobayashi, *Carbohydr. Res.,* **1987**, 166, 156.

56) H.-J. Schneider, F. Haket, V. Rüdiger, H. Ikeda, *Chem. Rev.*, **1998**, 98, 5, 1755.

57) L. W. Chan, T. R. R. Kurup, A. Muthaiah, J. C. Thenmozhiyal, *Int. J. Pharm.,* **2000**, 195, 71.

58) B. Casu, M. Reggiani, G. G. Gallo, A. Vigevani, *Tetrahedron,* **1968**, 24, 803.

59) F. Djedaini, S. Z. Lin, B. Perly, D. Wouessidjewe, *J. Pharm. Sci.,* **1987**, 79, 643.

60) J. A. Pople, W. G. Schneider, H. J. Bernstein, *High resolution NMR*, McGraw-Hill Book Co. Inc., **1959**, New York, Ch. 10.

61) P. Job, *Ann. Chim. Phys.,* **1928**, 9, 113.

62) F. Djedaini, B. Perly, *Minutes of the 5th Int. Symp. on Cyclodextrins,* Editions de Santé, Paris, **1990**, p. 124-129.

63) F. Djedaini, F. Lechat, D. Wouessidjewe, B. Perly, *Minutes of the 5th Int. Symp. on Cyclodextrins,* Editions de Santé, Paris, **1990**, p. 130-133.

64) M. E. Amato, F. Djedaini-Pilard, B. Pertly, G. Scarlatta, *J. Chem. Soc., Perkin Trans. 2*, **1992**, 2065.

65) H. Uede, T.Nagai, *Chem. Pharm. Bull.*, **1980**, 28, 1415.

66) H. Uede, T.Nagai, *Chem. Pharm. Bull.*, **1981**, 29, 2710.

67) D. Djedaïni, B. Perly, In *New Trends in Cyclodextrins and Derivatives*, Ch. 6, D. Duchene (ed.), Edition de Santé, France, **1991**.

68) P. V. Dermarco, A. L. Thakka, *J. Chem. Soc., Chem. Commun.*, **1970**, 2.

69) R. Fornassier, V. Lucchini, P. Srimin, U. Tonnelato, *J. Incl. Phenom.*, **1986**, 4, 292.

70) S. Li, W. C.Purdy, *Anal. Chem.*, **1992**, B4, 1405.

71) Z. Li, Q. Guo, T. Ren, X. Zhu, Y. Liu, *J. Incl. Phenom.*, **1993**, 15, 359.

72) M. E. Amato, G. A. Pappalardo, B. Pertly, *Magnetic Resonance in Chemistry*, **1993**, 31, 455.

73) S. G. Frank, M. J. Cho, *J. Pharm. Sci.*, **1978**, 67, 1665.

74) J. Inoue, *Annu. Rep. NMR Spectroscopy*, **1993**, 27, 59.

75) C. McDonald, L. Palmer, M. Boddy, *Drug Dev. Ind. Pharm.*, **1996**, 22, 1025.

76) H. Matsuda, K. Ito, Y. Sato, D. Yoshizawa, M. Tanaka, A. Taki, H. Sumiyoshi, T. Utsuki, F. Hirayama, K. Uekama, *Chem. Pharm. Bull.*, **1993**, 41, 8, 1448.

77) D. W. Griffiths, M. L. Bender, *Adv. Catal.*, **1973**, 23, 209.

78) E. A. Lewis, L. D. Hansen, *J. Chem. Soc., Perkin Trans. 2*, **1973**, 2081.

79) J. A. Hamilton, M. N. Sabesan, *Acta Crystallogr.*, **1982**, B38, 3063.

Chapter 5

DIMEB INCLUSION COMPLEXES

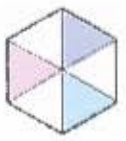

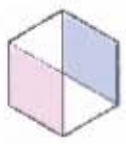

COMPLEX PREPARATION

Initially, powdered inclusion complexes of methyl-, ethyl-, propyl- and butyl paraben with DIMEB [heptakis(2,6–di–*O*–methyl)–β–cyclodextrin] were prepared by kneading. X-ray powder diffraction was used to determine if complexation had occurred. The diffraction patterns of the kneaded materials were compared with those of the physical mixtures [consisting of a 1:1 molar ratio of DIMEB with each drug]. In each instance, the patterns for the kneaded materials and physical mixtures were similar, indicating that complexation did not occur by kneading. The XRD patterns for the methyl-DIMEB, ethyl-DIMEB, propyl-DIMEB and butyl-DIMEB kneaded materials and their physical mixtures are shown in Figure 5.1.

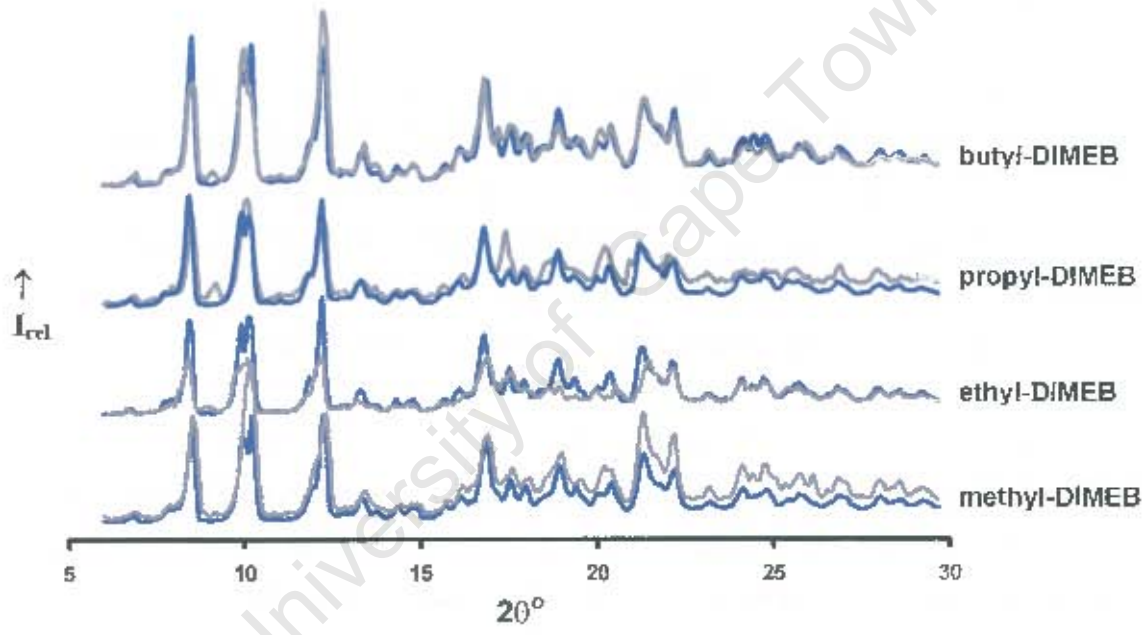

Figure 5.1 XRD patterns of the methyl-DIMEB, ethyl-DIMEB, propyl-DIMEB and butyl-DIMEB kneaded materials [grey] and 1:1 physical mixtures [blue]

Crystalline complexes were prepared by dissolving an equimolar amount of DIMEB with each drug in distilled water at room temperature. In the case of the methyl- and ethyl paraben, the resulting unfiltered dilute solutions were placed in the oven at 60°C. In the case of propyl- and butyl paraben the solutions were filtered and incubated at approximately 50°C. Crystals were obtained on standing for a period of 48 hours. The densities of the crystals were not measured due to the high solubility of the host in both aqueous solution and organic solvents. The complexes of DIMEB with each paraben will be referred to as MPDMB, EPDMB, PPDMB and BPDMB.

THERMAL ANALYSIS OF THE INCLUSION COMPLEXES

HSM results for the DIMEB complexes

HSM was used to analyse the thermal behaviour of the complexes upon heating at a constant rate of 10°C / min. The visual interpretations of the changes observed in the crystals upon heating are illustrated in Figures 5.2 and 5.3. Upon removal from the mother liquor the crystals were submerged in silicone oil, in order to prevent preliminary dehydration and to aid in the observation of dehydration upon heating. The MPDMB and EPDMB complexes crystallise as transparent rectangular blocks while the PPDMB and BPDMB crystals occur as long thin colourless needles.

Initial lateral cracking of the MPDMB crystals was observed from 32°C and this became more pronounced as the temperature increased to 65°C. Dehydration started at 87°C and continued at a steady flow until 108°C, at which point the crystals became opaque, and started to fragment. The crystals continued to fragment further and had a glue-like appearance at 115°C. No further observations were seen until 270°C, when the remaining material started to decompose and become brown in colour.

In the EPDMB complex, lateral cracking was observed from 41°C to 72°C, and very small bubbles were released as this cracking occurred. Larger bubbles were liberated by 91°C and continued in a steady stream until 112°C. This process of dehydration reduced the crystals to fragments and led to the crystals becoming opaque. By 134°C the crystals had a glue-like appearance, with poorly defined edges. The onset of decomposition was observed at 289°C.

In the PPDMB crystals, bubbling was initially seen at 45°C and continued to 96°C. Small cracks were observed as dehydration took place. The release of bubbles started to become more vigorous from 99°C and continued to 117°C, decelerating and finally stopping at 127°C. At this point the crystals were slightly opaque and had lost the sharpness of their edges. By 150°C the crystals were totally opaque and decomposition commenced at 267°C, evident by discolouration of the crystals. Between 350°C and 400°C the crystals show a pseudo-melt and liquefy somewhat. As decomposition continues the crystals become black and charred.

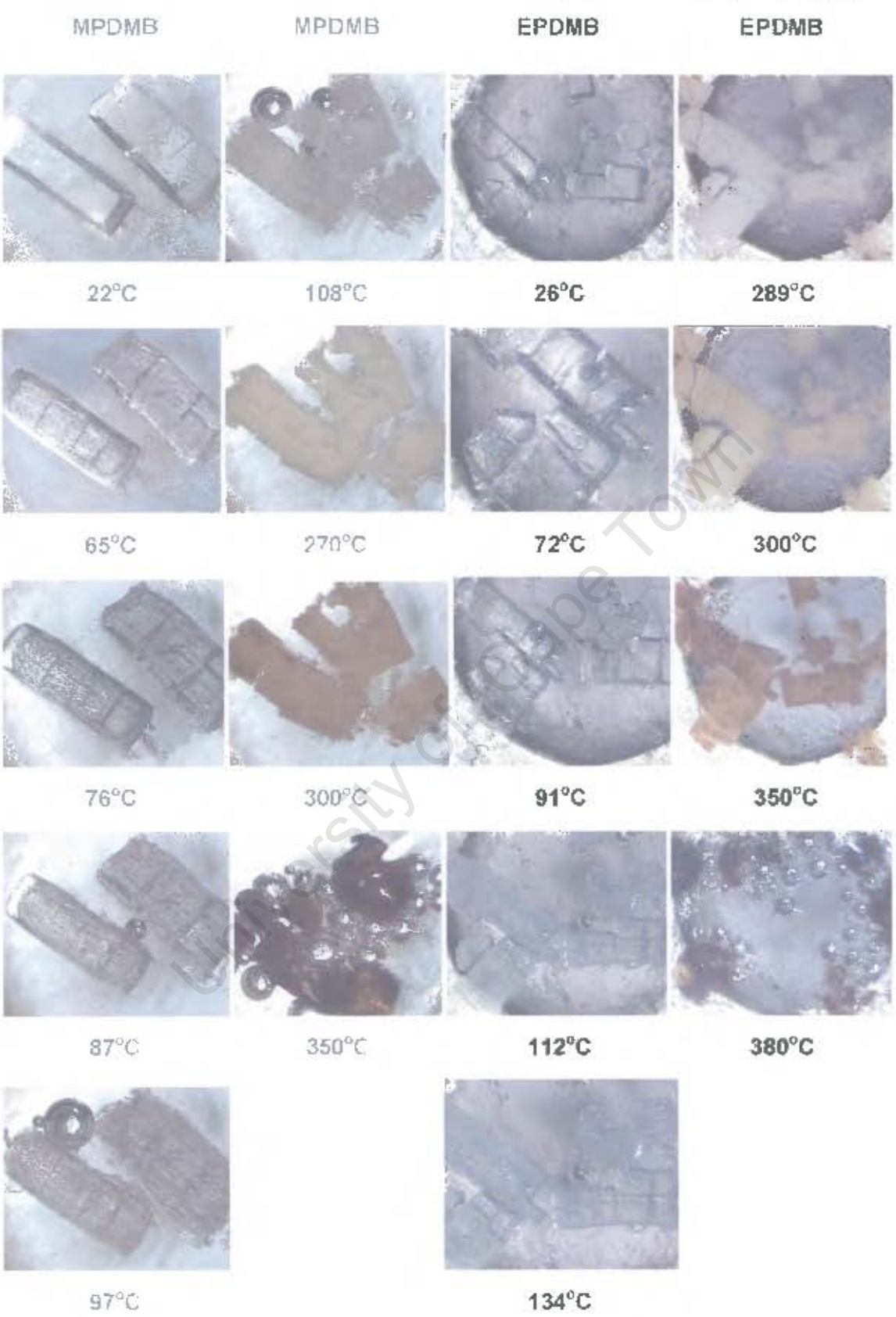

Figure 5.2 HSM photographs taken at various temperatures for crystals of the MPDMB and the EPDMB complexes

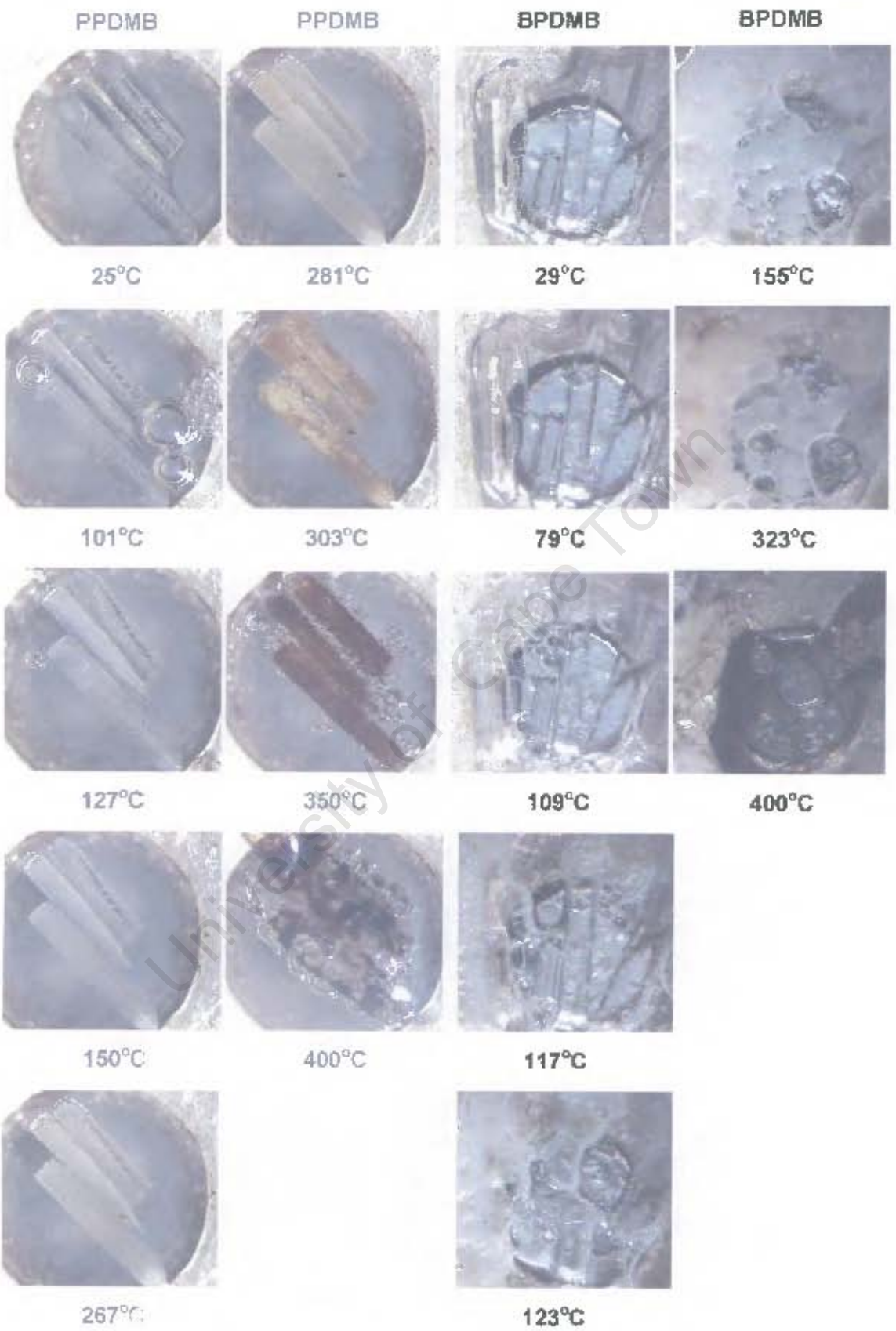

Figure 5.3 HSM photographs taken at various temperatures for crystals of the PPDMB and the BPDMB complexes

In the BPDMB crystals, bubbles were seen at 44°C, indicating the beginning of dehydration and continued in a slow steady stream to 86°C. The bubbling became more vigorous at 96°C and continued to 117°C. Thereafter, dehydration continued more slowly until 155°C, at which point the crystals were opaque and had a glue-like appearance. Thereafter no physical changes took place until decomposition at 323°C.

TGA results for the DIMEB complexes

The TGA traces for the MPDMB, EPDMB, PPDMB and BPDMB complexes are shown in Figure 5.4 (a), (b), (c) and (d) respectively. A summary of the observed percentage weight losses is presented in Table 5.1.

The four DIMEB complexes exhibit similar thermogravimetric events. Weight losses from ambient temperature up to 100°C represent water loss from the complexes. From 100 to 150°C no significant weight loss was observed. Thereafter, there was a weight loss step from 150°C to 250°C. This is interpreted as the dissociation of the guest molecule from the host, as the percentage weight loss corresponds to the molecular weight of the paraben in each case. Finally, the remaining sample decomposed at temperatures beyond 300°C. These thermal events correspond with those observed in HSM.

Table 5.1 The percentage weight losses for the DIMEB complexes

Temp (°C)	MPDMB		EPDMB		PPDMB		BPDMB	
	Sample weight (%)	Δ Weight loss (%) *	Sample weight (%)	Δ Weight loss (%) *	Sample weight (%)	Δ Weight loss (%) *	Sample weight (%)	Δ Weight loss (%) *
30	100	-	100		100	-	100	-
100	95.8	4.2	95.4	4.6	95.5	4.5	95.8	4.2
150	95.2	0.6	94.9	0.5	94.8	0.7	95.1	0.7
250	85.2	10.0	84.9	10.0	83.3	11.5	83.5	11.6
300	85.1	0.1	84.8	0.1	81.7	1.6	82.8	0.7
350	84.6	0.5	83.5	1.3	71.7	10	82.5	0.3
400	37.8	46.8	8.9	74.6	6.9	64.9	23.0	59.5
Average number of water molecules per H:G unit								
	3.7		4.0		3.9		3.7	

* Δ Weight loss (%) = [Sample weight (%) at temperature (n-1)] - [Sample weight (%) at temperature (n)]

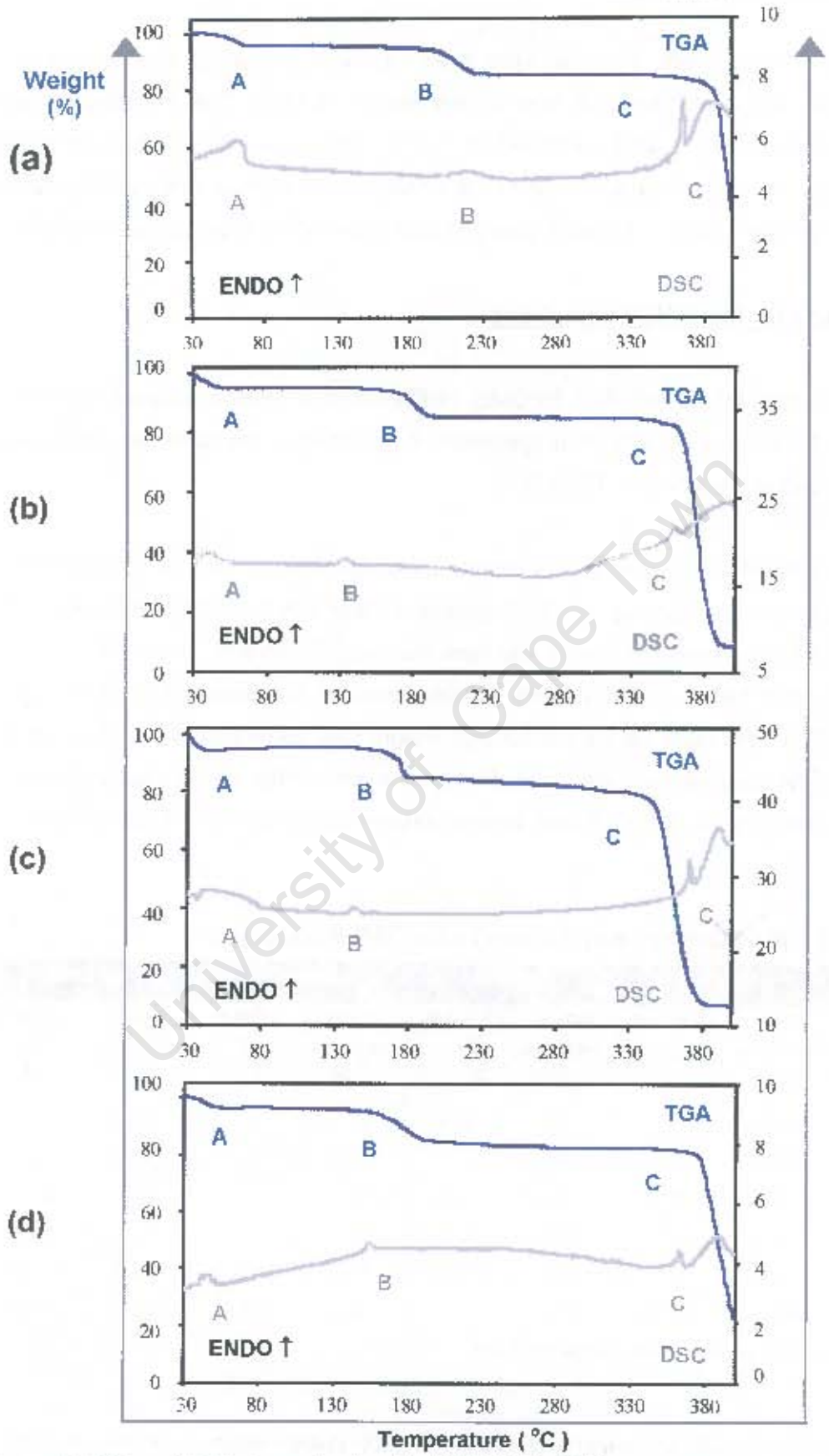

Figure 5.4 TGA and DSC traces for the (a) MPDMB (b) EPDMB (c) PPDMB and (d) BPDMB complexes

DSC results for the DIMEB complexes

The DSC results for the MPDMB, EPDMB, PPDMB and BPDMB complexes are shown in Figure 5.4 (a), (b), (c) and (d) respectively and the results are summarised in Table 5.2. The four DIMEB complexes show a broad endothermic event representing water loss in the range 30-100°C, which corresponds to an observed mass loss in the TGA traces [labelled A]. The asymmetric shapes of the dehydration endotherms suggest that water loss from these complexes was a multi-stage process, as was observed from HSM.

The anhydrous complex undergoes a smaller endothermic event in the range 150-230°C [labelled B], whose corresponding TGA weight loss is in each case consistent with a 1:1 host-guest stoichiometry. The separate losses of water and the guest can also be observed on the HSM. Figures 5.2 and 5.3 show how the crystals of the complexes crack as they lose water and then become completely opaque as they lose the guest molecule.

The final event, endotherm C, represents fusion of the host followed by decomposition and appears similar in each case. Fusion of pure DIMEB does not occur, but rather the host starts to decompose over the temperature range 277-294°C. The stability of the complexes was based on the analysis of the onset of guest loss for the complexes. The stability followed the order MPDMB > BPDMB ~ PPDMB > EPDMB.

Table 5.2 Summarised DSC results for the DIMEB complexes

			MPDMB	EPDMB	PPDMB	BPDMB
Temperature range	A	(°C)	30-84	30-70	30-90	30-80
Endotherm A	T_{on}	(°C)	30	30	30	30
	Peak	(°C)	61	43	51	42
Temperature range	B	(°C)	189-254	126-134	136-153	143-168
Endotherm B	T_{on}	(°C)	206	130	142	147
	Peak	(°C)	222	134	145	155
Temperature range	C	(°C)	347-400	321-400	357-400	347-400
Endotherm C	Peak 1	(°C)	366	360	371	364
	Peak 2	(°C)	386	389	393	388
			METHYL	**ETHYL**	**PROPYL**	**BUTYL**
Endotherm for fusion of pure paraben		(°C)	126	116	96	69

X-RAY CRYSTALLOGRAPHIC ANALYSIS OF THE MPDMB STRUCTURE

Data-collection

The preliminary unit cell parameters and space group for the MPDMB structure were determined by X-ray photographic techniques. The oscillation photograph displayed m_x symmetry indicating the monoclinic system or higher. The Weissenberg photography showed two central lattice rows, 90° apart, each of which was a mirror line. The overall symmetry of the reciprocal lattice [Laue symmetry] was thus determined as *mmm*, indicating that the crystal belonged to the orthorhombic system. The systematic absences are listed below, and these confirmed the space group $P2_12_12_1$.

hkl: none
h00: h = 2n + 1
0k0: k = 2n + 1
00l: l = 2n + 1

A single crystal was mounted on a glass fibre and covered in Paratone N oil[2] to prevent cracking due to loss of water of crystallisation and to provide a rigid mounting for the low-temperature data collection. X-ray intensity data-collection was performed at 173(2) K on the Nonius Kappa CCD diffractometer using graphite-monochromated MoKα radiation. Crystal data and data-collection parameters are listed in Table 5.3.

Structure determination and refinement

An initial search of the CSD did not locate any DIMEB complex structures with similar unit cell dimensions. Hence it was necessary to solve the structure *ab initio*. The structure was solved using the program *PATSEE*,[3,4] which uses Patterson and direct methods to orientate and position a fragment of known geometry in a unit cell. The search model consisted of the skeleton atoms of the host, DIMEB, from a previously solved DIMEB clofibric-acid complex,[5] as it was hoped that the conformation of the cyclodextrin would be similar. After 5000 random positions were refined for 1 000 000 random orientations, a starting model with favourable statistics was produced from the *PATSEE* run [*viz.* RFOM = 0.439; TPRSUM = 0.709; TFOM = 0.221; R_L = 0.207; CFOM = 0.815]. Full-matrix least-squares methods [*SHELX-97*][6] were used to refined the starting model. The difference electron density map based on this initial refinement revealed most of the remaining non-hydrogen atoms of the host. After further refinement it was found that the atom C(7) on O(2G4) and the atoms O(6) and C(8) on C(6G5) were disordered. Two alternative positions were found for each disordered atom. For a given pair, a fixed U_{iso} of 0.09 Å^2 [the mean of U_{iso} for the chemically equivalent ordered atoms] was assigned and site-occupancy factors [s.o.f.'s] of x and 1-x were assigned, with x variable.

Table 5.3 Details of the data collection and refinement parameters for the MPDMB structure

Empirical formula	$C_{56}H_{98}O_{35}\cdot C_8H_8O_2\cdot 3.7H_2O$
Formula weight	1550.2
Crystal system	Orthorhombic
Space group	$P2_12_12_1$
a / Å	10.6014 (1)
b / Å	15.4760 (2)
c / Å	48.2438 (6)
α / °	90
β / °	90
γ / °	90
Volume / Å^3	7915.2 (2)
Z	4
Density$_{calc}$ / g cm^{-3}	1.301
μ (MoKα) / mm^{-1}	0.109
F(000)	3324
Temperature of data collection / K	173 (2)
Crystal size / mm^3	0.27 x 0.38 x 0.35
Range scanned θ / °	$2 \leq \theta \leq 25$
Index ranges	h: -8,12 k: -18,10 l: -56, 55
ϕ scan angle / °	0.5
ϕ scan range, frames	131.5°, 263
ω scan angle / °	0.5
ω scan ranges, frames	100.5°, 201 and 75.5°, 151 and 97.5°, 195
Dx / mm	77.8
Total no. of reflections collected	14594
No. of independent reflections	9801
No. of reflections with $I > 2\sigma(I)$	7416
No. of parameters	826
R_{int}	0.0196
S	1.037
R_1 (for 6241 reflections)	0.0904
Reflections omitted	(0 1 3); (0 2 3); (0 2 5); (0 2 6); (0 4 4); (0 5 1); (2 1 0); (2 1 1); (-2 1 1)
wR_2	0.2407
Weighting scheme	a = 0.1546 b = 12.9325
$(\Delta / \sigma)_{mean}$	< 0.001
$\Delta\rho$ excursions / e.Å^{-3}	0.76 and -0.52

Distance constraints were placed on the bonds linking these disordered atoms to their parent atoms. All the non-hydrogen atoms on the host, except the disordered atoms and O(6G1), C(8G1), C(7G3), O(6G4), O(3G5), O(6G5) and C(8G5) were refined anisotropically. Once all the non-hydrogen atoms of the host had been placed, the cyclodextrin hydrogen atoms were geometrically fixed at idealised positions in a riding-model. All the methyl hydrogen atoms were assigned a common variable isotropic temperature factor and the remaining hydrogen atoms of each glucose moiety were assigned common variable isotropic temperature factors.

Refinement continued with the placement of the water oxygen atoms. Five positions were identified, with one water molecule, O(4W), disordered over two sites. The water oxygen atoms were each assigned a fixed isotropic temperature factor of 0.07 $Å^2$ and the s.o.f.'s were allowed to vary. The s.o.f.'s refined to 0.93, 0.78, 0.79, 0.64, 0.20 and 0.31 for O(1W), O(2W), O(3W), O(4WA), O(4WB) and O(5W) respectively. This led to a total of 3.7 water molecules in the asymmetric unit, which was comparable to the number of waters observed from the TGA results. The hydrogen atoms of the water molecules were not located.

From the remaining electron density map a fragment of the guest was discernible and after further refinement all the non-hydrogen atoms of the guest were located in the difference electron density map. The phenyl ring was constrained as a rigid hexagon using the AFIX 66 instruction. It became evident that the ester substituent was disordered over two positions. They were labelled with suffixes **A** and **B** and each of these disordered atoms was assigned a s.o.f. of x and 1-x, with x variable. These values refined to 0.57 for O(10A) and C(11A) and 0.43 for O(10B) and C(11B). A single isotropic temperature factor was used for the non-hydrogen atoms of the guest and this refined to a final value of 0.12 $Å^2$. The two positions of the ester substituent and the numbering scheme for the methyl paraben molecule can be seen in Figure 5.5.

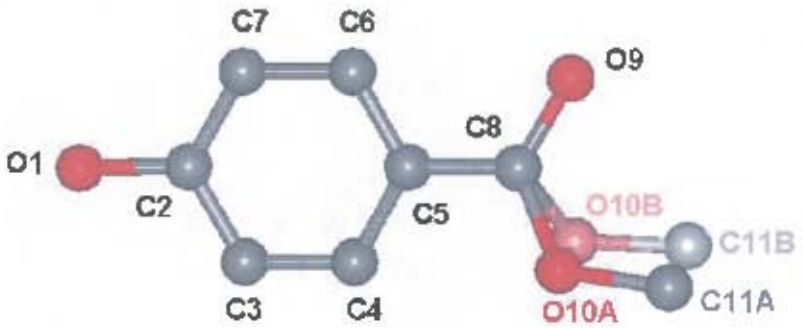

Figure 5.5 Structure of the methyl paraben guest molecule showing the two disordered positions of the ester substituent [**A** and **B**]

The hydrogen atoms attached to the carbon atoms of the guest were also inserted at idealised positions and assigned a common isotropic temperature factor. The hydrogen atom of the hydroxyl group was placed using the rotating group refinement strategy [AFIX 83]. Due to the abnormally long bond distances found in the guest molecule, distance constraints were placed on certain bonds, namely: C(5)–C(8) 1.469 Å; C(8)–O(9) 1.217 Å; C(8)–O(10A) 1.334 Å; and O(10B)–C(11B) 1.436 Å [all with σ = 0.005 Å]. The values chosen were taken from Lin.[7]

Geometrical analysis of the MPDMB structure

A single DIMEB molecule, its associated guest and 3.7 water molecules make up the asymmetric unit of the MPDMB structure. The glucose units will be referred to as G1, G2, G3, G4, G5, G6 and G7 and the structure and numbering scheme of the MPDMB complex and water molecules are shown in Figure 5.6. The geometrical data for the DIMEB molecule are listed in Tables 5.4 and 5.5 [e.s.d.s are in the range 0.007-0.012 Å for distances and 0.1-0.6° for angles].

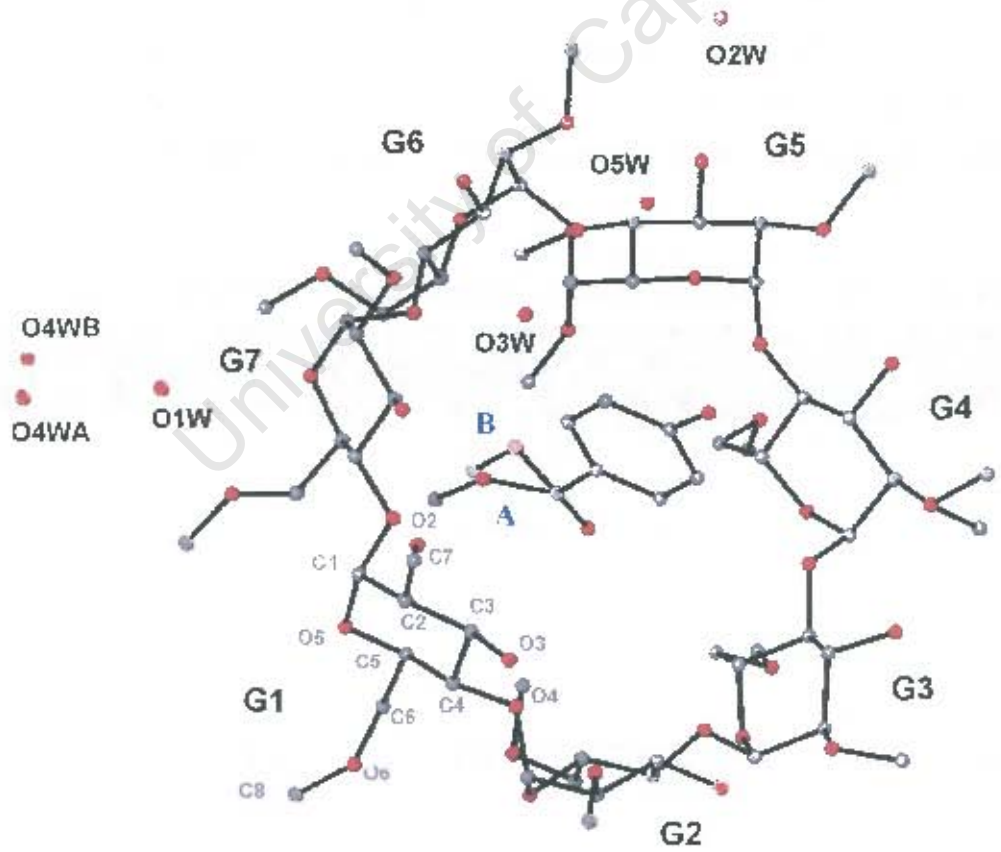

Figure 5.6 Macrocyclic structure and numbering scheme of glucose residues and water oxygen atoms, with the hydrogen atoms excluded. The host is viewed from the secondary face.

The DIMEB molecule has a round and rather symmetrical structure with all the glucopyranose residues in the $^4C_1$ chair conformation. Each of the glucose residues inclines with the O(6) side turned towards the inside of the macrocycle. The C(6)–O(6) bonds of the G1, G3, G4, G6, and G7 residues are directed away from the cavity and are in the (-) *gauche* conformation to the C(4)–C(5) and O(5)–C(5) bonds. The C(6)–O(6) bond of the G2 residue points towards the cavity in the (+) *gauche* conformation. The O(6) atoms of the G5 residue are disordered over two sites with the major position [O(65A)] adopting the (+) *gauche* conformation while the minor position [O(65B)] adopts the (-) *gauche* conformation. All the O(6)–C(6) bonds are *trans* to the respective C(5)–C(6) bonds, except in the G2 residue and in the case of the major position of the G5 residue, where the bond lies *gauche*. All the O(2)–C(7) bonds, including the disordered CH_3 on O(2) of the G4 residue, are directed away from the cavity.

The geometric parameters of the O(4) heptagon of the MPDMB structure are listed in Table 5.4. These include the radii, the O(4)•••O(4') distances, the O(4)•••O(4')•••O(4'') angles, the O(4)•••O(4')•••O(4'')•••O(4''') torsion angles and the deviations of each of the O(4) atoms from the mean O(4) plane. Table 5.5 lists the other important features of the macrocyclic structure such as the intersaccharidic bond angle (φ), the O(2)•••O(3') distance and the tilt angles [τ_1 and τ_2]. These parameters are defined in Chapter 1.

Table 5.4 Geometrical parameters of the O(4) heptagon for the MPDMB structure

Glucose unit	Radii (Å)	O(4)•••O(4') (Å)	O(4) angle (°)	Torsion angle (°)	Deviation (Å)
G1	5.16 (1)	4.28	127	3.2 (3)	0.02
G2	5.22 (1)	4.41	124	-4.1 (3)	-0.10
G3	4.83 (1)	4.48	134	-1.4 (3)	0.04
G4	5.05 (1)	4.38	128	3.9 (3)	0.10
G5	5.24 (1)	4.31	125	0.9 (3)	-0.07
G6	5.01 (1)	4.44	129	-6.3 (3)	-0.08
G7	4.85 (1)	4.41	133	3.4 (3)	0.11
Average	**5.05**	**4.39**	**129**	**|3.3|**	**|0.07|**

The average value of 5.05 Å for the radius of the heptagon is in good agreement with the radius of β-CD [5.04 Å].[8-9] The values calculated for these parameters compare favourably with those of the DIMEB-clofibric-acid complex.[5]

Table 5.5 φ, O(2)•••O(3') distance, τ for the MPDMB structure

Glucose unit	φ (°)	O(2)•••O(3') (Å)	τ_1 (°)	τ_2 (°)
G1	118	2.76	0.6 (2)	4.4 (3)
G2	118	2.86	12.5 (2)	15.0 (2)
G3	119	2.82	11.2 (1)	15.2 (2)
G4	120	2.82	7.8 (3)	13.7 (4)
G5	117	2.92	9.7 (1)	13.2 (2)
G6	119	2.93	14.5 (1)	17.1 (3)
G7	118	2.84	5.4 (2)	10.1 (2)
Average	**118**	**2.85**	**8.8**	**12.7**

The distances between the O(2) and O(3) atoms of the adjacent residues indicate that the O(3) hydroxyl group is hydrogen bonded to the O(2) atom of the adjacent residue. The intramolecular O(2)•••O(3') hydrogen bonds contribute to the rigidity and highly symmetrical conformation of DIMEB.

Guest geometry and interactions for the MPDMB structure

The conformation of the methyl paraben guest may be defined by three torsion angles. The torsion angles δ_1 [C(6)–C(5)–C(8)–O(9)], δ_{2A} [C(5)–C(8)–O(10A)–C(11A)] and δ_{2B} [C(5)–C(8)–O(10B)–C(11B)], will be used to describe rotation around the C(5)–C(8), C(8)–O(10A) and C(8)–O(10B) bonds respectively. These torsion angles were compared with the corresponding ones of the uncomplexed methyl paraben molecule[7] and were found to be similar in the case of δ_2 [Figure 5.7]. δ_1 of the complexed methyl paraben has a slightly larger out-of-plane twist than that of the uncomplexed MP, indicating that inclusion allows for more rotational freedom around the C(5)–C(8) bond.

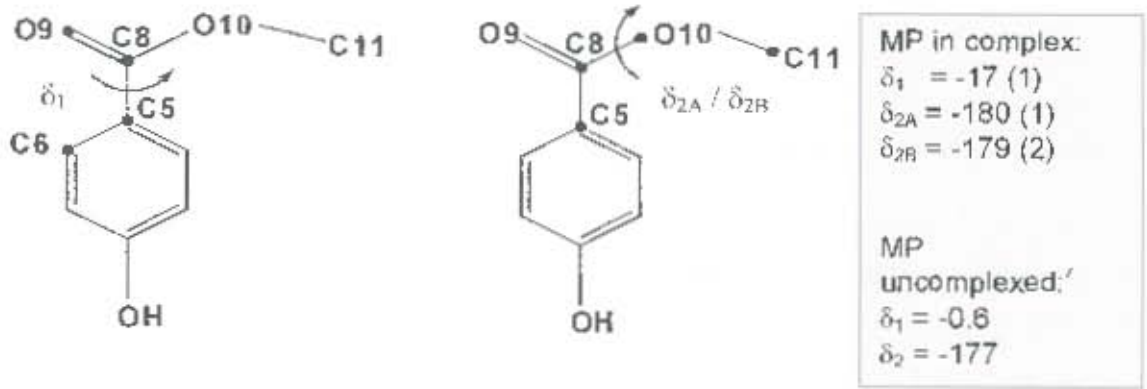

Figure 5.7 Torsion angles δ_1, δ_{2A} and δ_{2B} of the methyl paraben

The close contact distances for the re-evant interactions between the host and guest molecule are listed in Table 5.6. Most of the close contacts occur between the guest and the disordered C(85A) and C(85B) atoms and their related hydrogen atoms of the host. The ester oxygen atom, O(10B), is in close contact with C(85A) indicating that these two disordered atoms are not present at the same time. The last five contacts show how the disordered atom C(85B) of one host protrudes into the cavity of the host above it.

Table 5.6 Close contact distances for the MPDMB structure

Interaction	Distance (Å)
H(4) ··· H(561)	2.39
C(8) ··· H(851)	2.85 (1)
O(10B) ··· C(85A)	2.66 (3)
O(10B) ··· H(851)	1.95 (2)
H(11A) ··· C(85A)	2.77 (2)
C(11B) ··· C(85A)	2.33 (4)
C(11B) ··· H(851)	2.08 (4)
C(11B) ··· H(852)	2.25 (3)
C(11B) ··· H(853)	2.29 (3)
H(11D) ··· H(851)	1.59
H(11D) ··· H(852)	1.32
H(11D) ··· H(853)	1.89
H(11E) ··· C(85A)	2.59 (2)
H(11E) ··· H(853)	2.17
O(1) ··· C(85B)^{i}	3.09 (3)
C(7) ··· C(85B)^{i}	3.24 (2)
C(7) ··· H(858)^{i}	2.75 (1)
H(7) ··· C(85B)^{i}	2.58 (2)
H(7) ··· H(858)^{i}	1.96

^{i} Related by symmetry operation -1+x, y, z

The methyl paraben guest is almost completely enclosed in the cyclodextrin cavity, with its long axis orientated in the direction of the molecular axis of the host. The phenolic hydroxyl group is located at the secondary rim of the cyclodextrin, while the ester moiety of the guest molecule is located at the primary rim. The phenyl ring of the guest is almost perpendicular to the mean O(4) plane with an angle of 88.9 (2)° between the two. Figures 5.8 and 5.9 show CPK diagrams of the MPDMB structure.

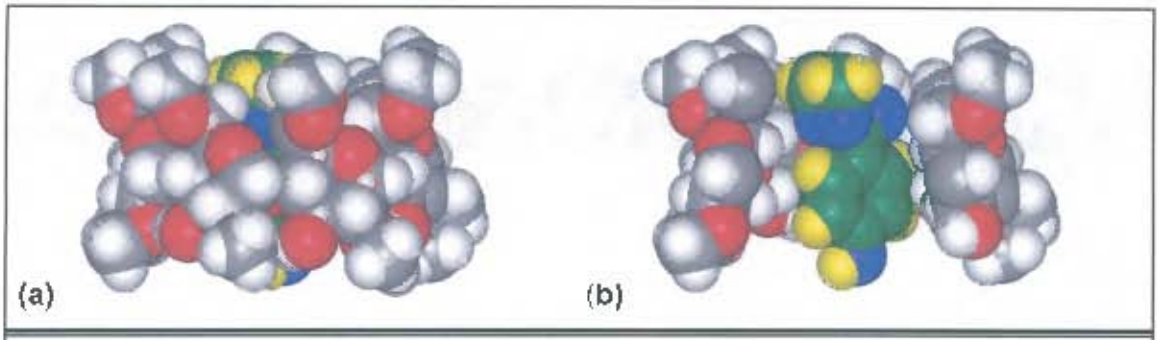

Figure 5.8 Space-filling diagram of the MPDMB structure (a) side view (b) sectioned view of the same orientation

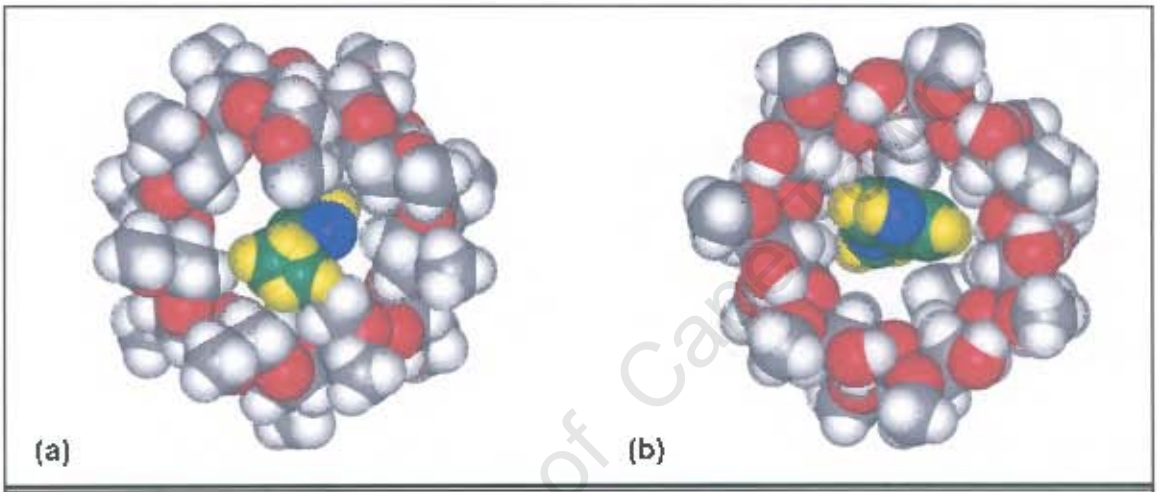

Figure 5.9 Space-filling diagram of the MPDMB structure (a) viewed from the primary rim (b) viewed from the secondary rim

Hydrogen bonding interactions of the MPDMB structure

Host interactions

Seven strong intramolecular O(2)•••O(3') hydrogen bonds, which are in the range 2.76-2.93 Å with a mean of 2.85 Å [Table 5.5], contribute to the "roundness" of the cyclodextrin structure. The conformation of the DIMEB molecule is stabilised by seven intramolecular C–H•••O hydrogen bonds [Table 5.7], a common interaction found in carbohydrate crystal structures.[10] The intramolecular hydrogen bonds consist of five C(6)–H•••O(5') hydrogen bonds, a C(7)–H•••O(3) hydrogen bond and a C(8)–H•••O(5') hydrogen bond. Three intermolecular C–H•••O hydrogen bonds stabilise the crystal structure and consist of a C(2)–H•••O(3) hydrogen bond, a C(8)–H•••O(3) hydrogen bond and a C(8)–H•••O(6) hydrogen bond. All the C•••O distances are in the range 3.2-3.5 Å.

Table 5.7 C–H•••O hydrogen bonds in the MPDMB structure*

			Distance (Å)			Angle (°)
C	H	O	C–H	H•••O	C•••O	C–H•••O
Intramolecular hydrogen bonds						
C(6G1)	H(612)	O(5G2)	0.99	2.60	3.34 (1)	131.5 (6)
C(6G3)	H(632)	O(5G4)	0.99	2.76	3.32 (1)	116.7 (5)
C(6G4)	H(642)	O(5G5)	0.99	2.63	3.36 (1)	131.2 (7)
C(6G6)	H(662)	O(5G7)	0.99	2.80	3.48 (1)	125.4 (5)
C(6G7)	H(672)	O(5G1)	0.99	2.70	3.45 (1)	132.6 (5)
C(7G1)	H(713)	O(3G1)	0.98	2.65	3.21 (1)	116.4 (7)
C(8G3)	H(833)	O(5G4)	0.98	2.90	3.44 (1)	115.8 (7)
Intermolecular hydrogen bonds						
C(2G1)	H(211)	O(3G4) [i]	1.00	2.61	3.350 (9)	130.5 (4)
C(8G3)	H(832)	O(3G2) [ii]	0.98	2.65	3.43 (1)	136.8 (7)
C(8G7)	H(873)	O(6G4) [i]	0.98	2.77	3.34 (1)	118.0 (6)

[i] Related by symmetry operation x, -1+y, z
[ii] Related by symmetry operation: 1-x, $^1/_2$+y, $^1/_2$-z
* Hydrogen bonding parameters based on idealised hydrogen atom positions.

Guest interactions

Hydrogen bonding distances involving the guest are listed in Table 5.8. The hydroxyl oxygen atom is involved in hydrogen bonding with one water oxygen atom and engages in three hydrogen bonds to the host molecules in symmetry related positions [Figure 5.10].

Table 5.8 Hydrogen bonding distances involving the guest in the MPDMB structure*

			Distance (Å)			Angle (°)
Donor(D)	H	Acceptor(A)	D–H	H•••A	D•••A	D–H•••A
O(1)	H(1)	O(2W) [i]	0.840	1.90	2.72 (1)	168.0 (7)
C(85B)	H(855)	O(1) [ii]	0.980	2.62	3.09 (3)	109 (1)
C(6G6)	H(661)	O(1) [ii]	0.990	2.76	3.43 (1)	125.9 (5)
C(7G6)	H(762)	O(1) [iii]	0.980	2.65	3.38 (2)	131.8 (9)
C(11A)	H(11C)	O(3G2) [iv]	0.980	2.62	3.30 (1)	127.0 (7)

[i] Related by symmetry operation: $^1/_2$+x, $^1/_2$-y, -z
[ii] Related by symmetry operation: 1+x, y, z
[iii] Related by symmetry operation: $^1/_2$+x, $^1/_2$-y, -z
* Hydrogen bonding parameters based on idealised hydrogen atom positions.

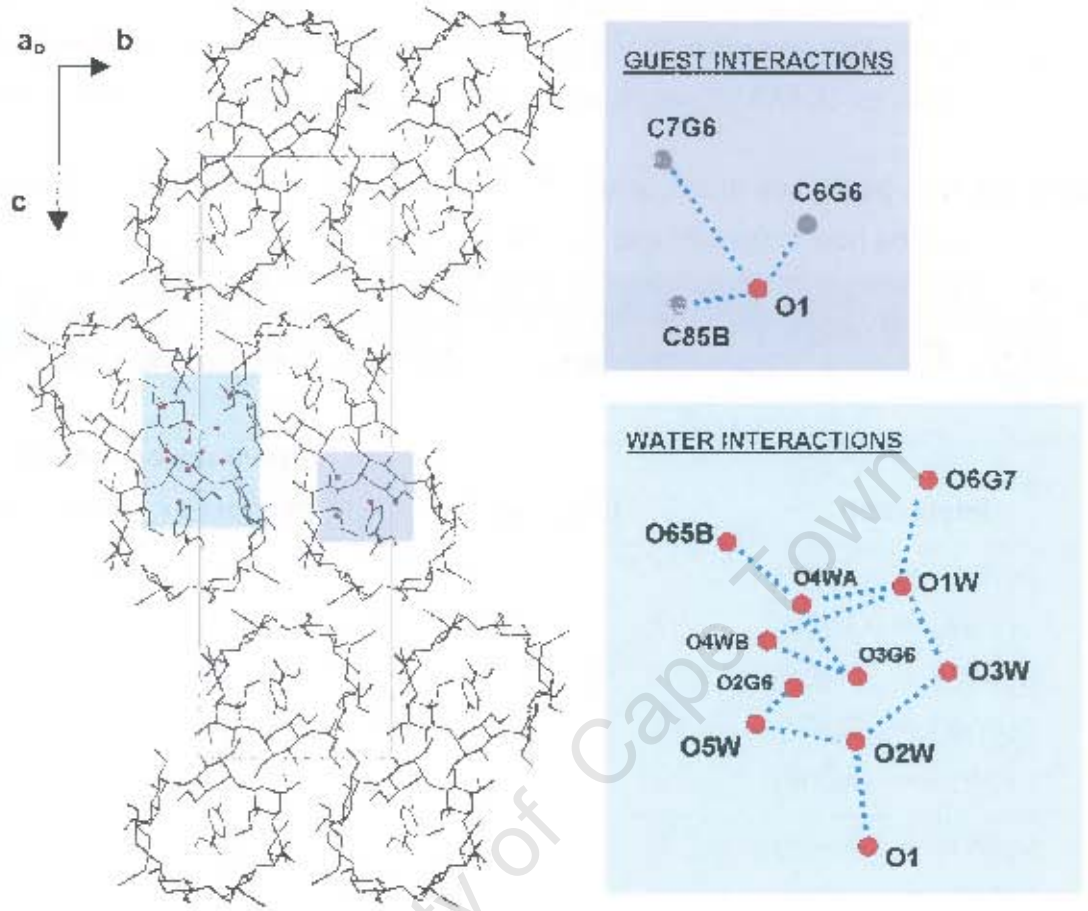

Figure 5.10 A schematic representation of guest and water interactions that connect adjacent host units

Water interactions

Thermogravimetric analysis gave a weight loss which corresponds to 3.7 water molecules per 1:1 complex unit. These water molecules were all accounted for in the crystallographic analysis by setting the common isotropic temperature factor to 0.07 $Å^2$. All the water molecules are situated at the periphery of the cyclodextrin molecule, filling the intermolecular space between complex units. Hydrogen bonding distances between the host and these water molecules are listed in Table 5.9.

All the water molecules are within hydrogen bonding distance of a host oxygen atom, except for O(2W) and O(3W). O(2W) is hydrogen bonded to the guest hydroxyl oxygen atom and is within hydrogen bonding distance of two water oxygen atoms, thus forming bridges with atoms of adjacent glucose units [Figure 5.10].

Both the O(4WA) and O(4WB) water atoms are in hydrogen bonding contact with the same host oxygen atom and water oxygen atom, namely O(3G6) and O(1W). O(4WB) is 2.28 Å from O(5W), indicating that these atoms will not be present simultaneously. The s.o.f. values for O(4WA), O(4WB) and O(5W) are 0.64, 0.20 and 0.31 respectively.

Table 5.9 Hydrogen bonds and hydrogen bonding distances between water molecules and the host in the MPDMB structure*

			Distance (Å)			Angle (°)
Donor(D)	H	Acceptor(A)	D–H	H•••A	D•••A	D–H•••A
C(3G6)	H(361)	O(5W)	1.00	2.70	3.36 (2)	124.3 (6)

Interaction	Distance (Å)	Symmetry operator for the host oxygen atoms
O(1W) ••• O(6G7)	2.84 (1)	x, y, z
O(4WA) ••• O(65B)	2.70 (2)	x, -1+y, z
O(4WA) ••• O(3G6)	2.80 (1)	$^1/_2$+x, $^1/_2$-y, -z
O(4WB) ••• O(3G6)	2.69 (3)	$^1/_2$+x, $^1/_2$-y, -z
O(5W) ••• O(2G6)	2.70 (2)	x, y, z
O(1W) ••• O(3W)	2.75 (1)	$^1/_2$+x, $^1/_2$-y, -z
O(1W) ••• O(4WA)	2.70 (1)	x, y, z
O(1W) ••• O(4WB)	2.74 (3)	x, y, z
O(2W) ••• O(3W)	2.85 (1)	$^1/_2$+x, 1$^1/_2$-y, -z
O(2W) ••• O(5W)	2.92 (2)	$^1/_2$+x, 1$^1/_2$-y, -z
O(4WB) ••• O(5W)	2.28 (4)	$^1/_2$+x, $^1/_2$-y, -z

* Hydrogen bonding parameters based on idealised hydrogen atom positions.

Crystal packing of the MPDMB structure

Figures 5.11 and 5.12 are extended stereo packing diagrams of the MPDMB structure showing projections as viewed down the *a*- and *b*-axes. Complex units stack in columns in a head-to-tail mode, forming what appear to be continuous channels along the *a*-axis. Figure 5.11 shows the "endless" channels while Figure 5.12 shows the columns running parallel to the *a*-axis. This style of packing is considered to be a modified herringbone type packing.

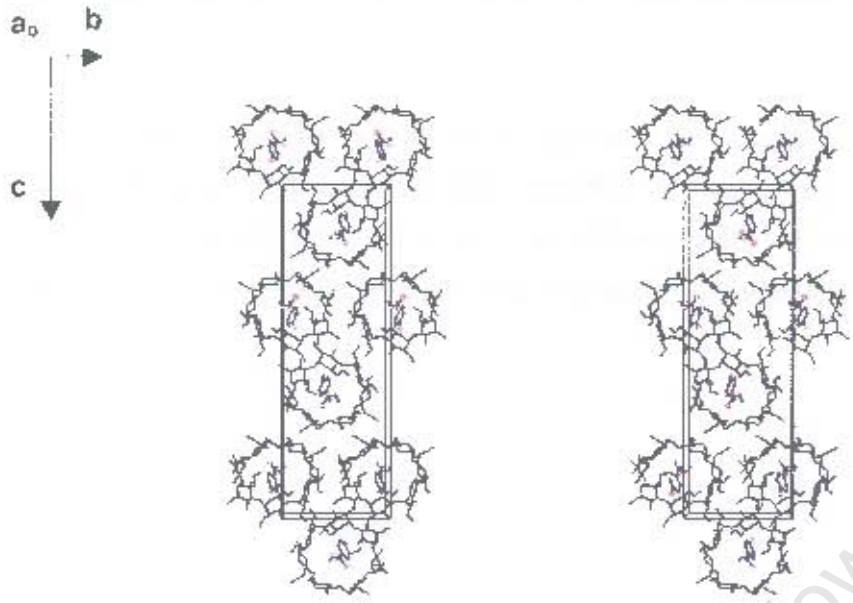

Figure 5.11 Stereo packing diagram of the MPDMB structure [*a*-axis projection]

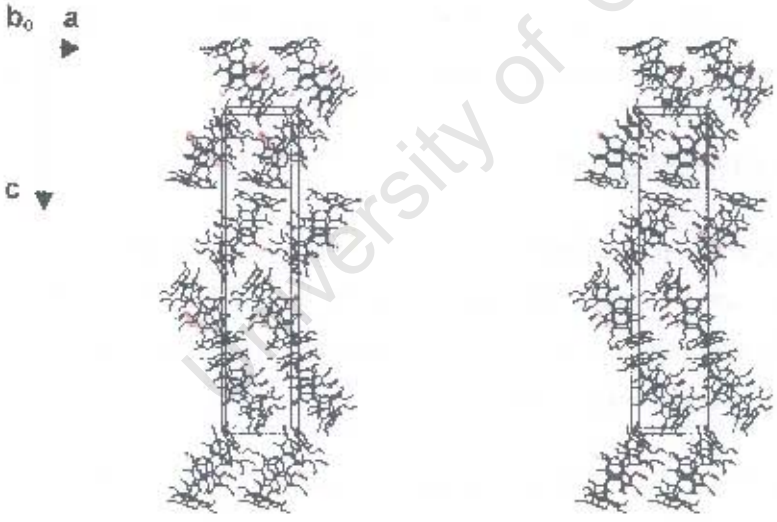

Figure 5.12 Stereo packing diagram of the MPDMB structure [*b*-axis projection]

X-RAY CRYSTALLOGRAPHIC ANALYSIS OF THE EPDMB STRUCTURE

Data-collection

Preliminary X-ray photography was used to determine the unit cell parameters, crystal system and space group of the EPDMB complex. Oscillation and Weissenberg photography indicated that the complex belongs to the orthorhombic system [*mmm* Laue symmetry]. The systematic absences are listed below, and these confirmed the space group $P2_12_12_1$.

hkl: none
h00: h = 2n + 1
0k0: k = 2n + 1
00l: l = 2n + 1

A single crystal was mounted on a glass fibre and covered in Paratone N oil.[2] This was done to prevent cracking due to loss of water of crystallisation and to provide a rigid mounting for the low-temperature data collection. X-ray intensity data-collection was performed on the Nonius Kappa CCD diffractometer using graphite-monochromated MoKα radiation [λ = 0.71073 Å], at 173(2) K. Crystal data, unit cell parameters, data-collection and final refinement parameters are listed in Table 5.10.

Structure determination and refinement

The crystal structure of EPDMB was solved by the isomorphous replacement method using co-ordinates of the non-hydrogen atoms [excluding the O(6), C(7), and C(8) atoms of each methylglucose residue] of the host cyclodextrin in the isomorphous DIMEB complex of MPDMB described previously.

The structure was refined by full-matrix least-squares refinement using the *SHELX-97* program[6] with subsequent location of the remaining non-hydrogen atoms from the electron density map. After further refinement the atom C(7) on O(2G4) and the atoms O(6) and C(8) on C(6G5) were found to be disordered. Two alternative positions were found for each disordered atom and for a given pair, a fixed U_{iso} of 0.08 Å^2 [the mean of U_{iso} for the chemically equivalent ordered atoms] was assigned. Site-occupancy factors of x and 1-x were assigned, with x variable. Distance constraints were placed on the bonds linking these disordered atoms. All the oxygen atoms on the host, except the disordered oxygen atoms O(2G4) and O(6G1) were refined anisotropically.

Table 5.10 Details of the data collection and refinement parameters for the EPDMB structure

Empirical formula	$C_{56}H_{90}O_{35}\cdot C_8H_{10}O_2\cdot 4.0H_2O$
Formula weight	1569.6
Crystal system	Orthorhombic
Space group	$P2_12_12_1$
a / Å	10.6560 (1)
b / Å	15.3073 (2)
c / Å	49.0417 (6)
α / °	90
β / °	90
γ / °	90
Volume / $Å^3$	7999.5 (2)
Z	4
$Density_{calc}$ / g cm^{-3}	1.303
μ (MoKα) / mm^{-1}	0.109
F(000)	3368
Temperature of data collection / K	173 (2)
Crystal size / mm^3	0.33 x 0.23 x 0.20
Range scanned θ / °	$1 \leq \theta \leq 22$
Index ranges	h: -11,11 k: -12,15 l: -48, 29
ϕ scan angle / °	0.5
ϕ scan range, frames	142.0°, 284 and 141.0°, 282
ω scan angle / °	0.5
ω scan ranges, frames	74.5°, 149 and 28.5°, 57
Dx / mm	99.0
Total no. of reflections collected	12680
No. of independent reflections	7013
No. of reflections with $I > 2\sigma(I)$	5766
No. of parameters	604
R_{int}	0.0186
S	1.026
R_1 (for 4391 reflections)	0.0857
Reflections omitted	(0 0 6); (0 1 2); (0 5 2); (1 0 5); (1 6 0); (1 1 1); (-1 1 1); (2 0 0); (2 1 0); (2 1 1); (-2 1 1)
wR_2	0.2122
Weighting scheme	a = 0.1109 b = 28.8084
$(\Delta / \sigma)_{mean}$	< 0.006
$\Delta\rho$ excursions / $e.Å^{-3}$	0.73 and -0.43

Hydrogen atoms bonded to the carbon atoms of the host were geometrically fixed at idealised positions in a riding-model. All the methyl hydrogen atoms were assigned a common variable isotropic temperature factor and the remaining hydrogen atoms of each glucose moiety were assigned common variable isotropic temperature factors. Once the refinement of the host was complete, water oxygen atoms were located and placed. Five positions were located, with one water molecule, O(4W), distributed over two sites. Each atom was assigned a fixed isotropic temperature factor of 0.08 $Å^2$, and the site-occupancy factors were allowed to vary. The s.o.f.'s refined to 0.93, 0.80, 0.73, 0.71, 0.17 and 0.28 for O(1W), O(2W), O(3W), O(4WA), O(4WB) and O(5W) respectively. The isotropic temperature factor of 0.08 $Å^2$ was chosen with the intention of allowing the total number of refined water oxygen atoms to equate to the total number of waters observed from the TGA results. The hydrogen atoms of the water molecules were not located.

Refinement continued with the placement of the guest atoms. Once the phenyl ring was located it was refined as a rigid hexagon using the AFIX 66 instruction. A single isotropic temperature factor was used for the non-hydrogen atoms of the guest and this refined to a final value of 0.12 $Å^2$. Upon further refinement it became evident that the ester substituent was disordered over two positions and these were labelled with suffixes **A** and **B**. The C(12) atom was located in one position, it was therefore duplicated and the position of **A** and **B** were kept the same using an EXYZ instruction. For each of these disordered atoms site-occupancy factors of x and 1-x were assigned, with x variable. The major position refined to a s.o.f. of 0.70. The two positions of the ester substituent and the numbering scheme for the ethyl paraben molecules can be seen in Figure 5.13. The hydrogen atoms attached to the carbon atoms of the guest were also inserted at idealised positions and assigned a common isotropic temperature factor. The hydrogen atom of the hydroxyl group was placed using the AFIX 83 instruction.

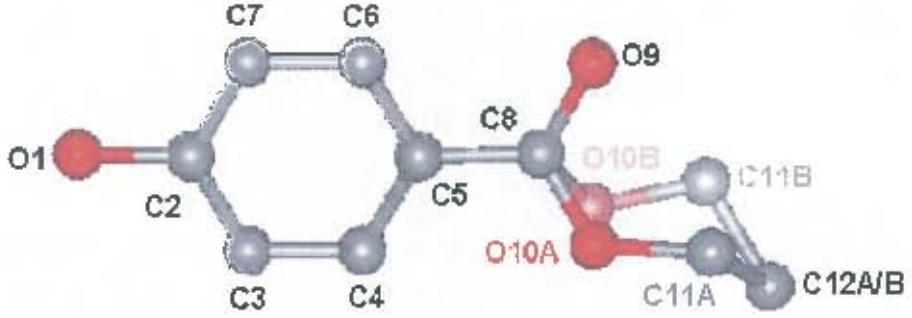

Figure 5.13 Structure of the ethyl paraben guest molecule showing the two disordered positions of the ester substituent [**A** and **B**]

Due to the abnormally long bond distances found in the guest molecule, distance constraints were placed on certain bonds, namely: O(1)–C(2) 1.351 Å; C(5)–C(8) 1.471 Å; C(8)–O(9) 1.207 Å; C(8)–O(10) 1.334 Å; O(10)–C(11) 1.448 Å; C(11)–C(12) 1.490 Å [all with σ = 0.005 Å]. The values chosen were taken from Lin.[11] Due to abnormally large bond angles, distance constraints were placed on non-bonded atoms to maintain the angles O(9)–C(8)–O(10), C(8)–O(10)–C(11) and O(10)–C(11)–C(12) close to the ideal value of 109.5°.

Geometrical analysis of the EPDMB structure

The structure and numbering scheme of the EPDMB complex are shown in Figure 5.14 and the geometrical data for the DIMEB molecule are listed in Tables 5.11 and 5.12 [e.s.d.s are in the range 0.008-0.013 Å for distances and 0.2-0.8° for angles]. The asymmetric unit of the EPDMB structure consists of a single DIMEB molecule, its associated guest and 4.0 water molecules. The glucose units will be referred to as G1, G2, G3, G4, G5, G6 and G7.

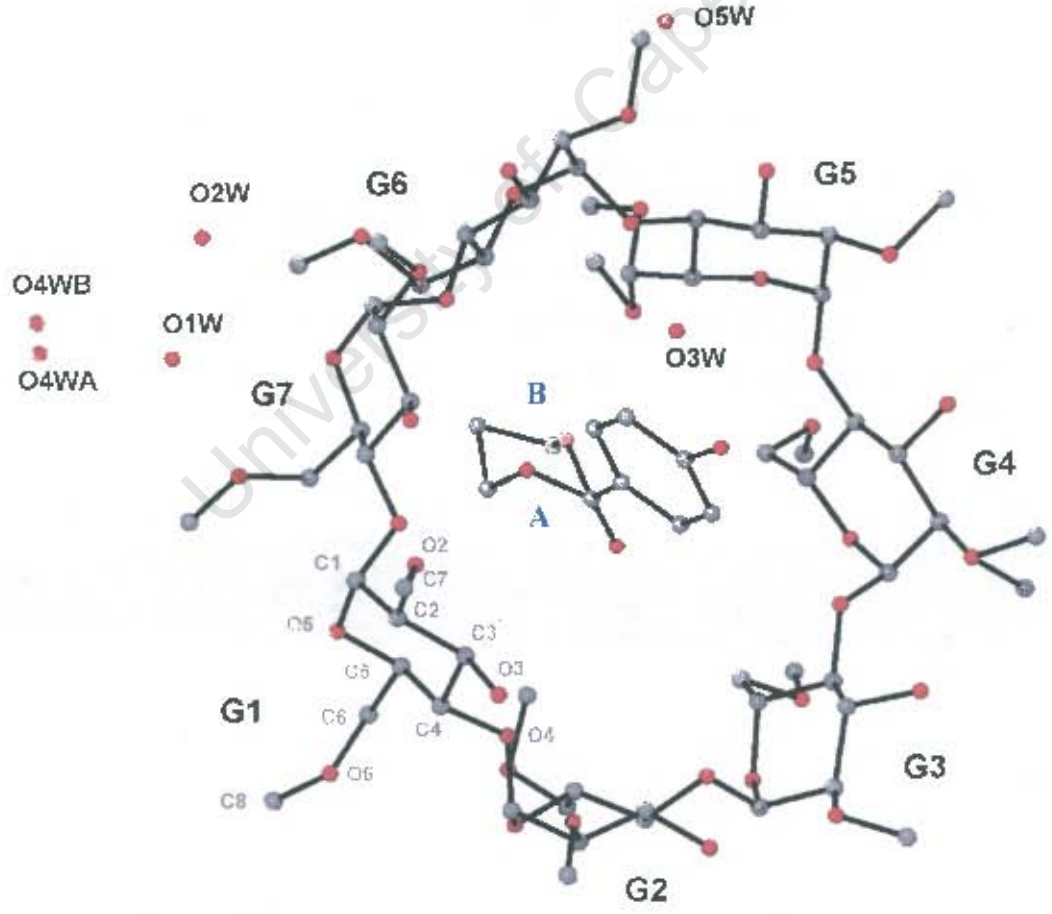

Figure 5.14 Macrocyclic structure and numbering scheme of glucose residues and water oxygen atoms, with the hydrogen atoms excluded. The host is viewed from the secondary face.

As shown in Figure 5.14 the DIMEB molecule has a round and rather symmetrical structure. Each glucose unit has the $^4C_1$ chair conformation and is connected to the next residue by the $\alpha(1,4)$-linkages. Each of the glucose residues inclines with the O(6) side turned towaeds the inside of the macrocycle. The tilt angles, τ_1 and τ_2, are in the range 0.5-16.9°, with the G6 residue having the largest tilt angle [Table 5.12].

The C(6)–O(6) bonds show two types of orientations, the (-) *gauche* conformation [to the C(4)–C(5) and O(5)–C(5) bonds] in the G1, G3, G4, G6, and G7 residues and the (+) *gauche* conformation in the G2 residue. The C(6)–O(6) bond in the G5 residue is disordered with the major position [O(65A)] adopting the (+) *gauche* conformation while the minor position [O(65B)] adopts the (-) *gauche* conformation. All the O(6)–C(8) bonds are *trans* to the respective C(5)–C(6) bonds, except in the G2 residue and the major position of the G5 residue, where the bond lies *gauche*.

The geometric parameters of the O(4) heptagon of the EPDMB structure are listed in Table 5.11. These include the radii, the O(4)•••O(4') distances, the O(4)•••O(4')•••O(4'') angles, the O(4)•••O(4')•••O(4'')•••O(4''') torsion angles and the deviations of each of the O(4) atoms from the mean O(4) plane. Table 5.12 lists the other important features of the macrocyclic structure such as the intersaccharidic bond angle (φ), the O(2)•••O(3') distance and the tilt angles [τ_1 and τ_2]. These parameters are defined in Chapter 1. The values calculated for these parameters compare favourably with those of the DIMEB-clofibric-acid complex[5] and the MPDMB complex previously described on pages 154-155.

Table 5.11 Geometrical parameters of the O(4) heptagon for the EPDMB structure

Glucose unit	Radii (Å)	O(4)•••O(4') (Å)	O(4) angle (°)	Torsion angle (°)	Deviation (Å)
G1	4.78 (1)	4.29	127	4.5 (3)	0.04
G2	5.06 (1)	4.36	123	-5.1 (4)	-0.13
G3	5.29 (1)	4.51	134	-1.9 (4)	0.04
G4	4.98 (1)	4.39	129	5.2 (3)	0.12
G5	4.82 (1)	4.27	124	0.2 (3)	-0.09
G6	5.28 (1)	4.45	128	-6.2 (4)	0.09
G7	5.15 (1)	4.44	134	2.8 (4)	0.12
Average	**5.05**	**4.39**	**128**	**|3.7|**	**|0.09|**

Table 5.12 φ, O(2)•••O(3') distance, τ for the EPDMB structure

Glucose unit	φ (°)	O(2)•••O(3') (Å)	τ_1 (°)	τ_2 (°)
G1	119	2.72	0.5 (2)	2.9 (3)
G2	118	2.86	13.8 (2)	16.3 (3)
G3	119	2.79	11.5 (2)	16.8 (3)
G4	120	2.81	9.3 (3)	14.4 (4)
G5	118	2.93	8.7 (2)	12.2 (2)
G6	118	2.87	14.1 (2)	16.9 (3)
G7	119	2.85	5.0 (2)	11.4 (3)
Average	**119**	**2.83**	**9.0**	**13.0**

The average radius of the heptagon, composed of seven glycosidic oxygen atoms, is 5.05 Å, which is in good agreement with the radius of the parent β-CD [5.04 Å].[8-0] The distances between the O(2) and O(3) atoms of the adjacent residues indicate that the O(3) hydroxyl group is hydrogen bonded to the O(2) atom of the adjacent residue. This indicates that the round shape of the macrocycle is maintained by the intramolecular O(2)•••O(3') hydrogen bonds. All the O(2)–C(7) bonds, including the disordered bonds on the G4 residue, are directed away from the cavity and therefore the methylation of the O(2)H hydroxyl group does not affect the formation of the intramolecular hydrogen bonds.

Guest geometry and interactions for the EPDMB structure

The conformation of the ethyl paraben guest may be defined by five torsion angles which are listed below and were used to describe the rotation around each of the corresponding bonds. They were compared with the conformation of the uncomplexed ethyl paraben molecule [Figure 5.15].[11] The close contact distances for the relevant interactions between the host and guest molecule are listed in Table 5.13.

The δ_{2A}, δ_{2B}, δ_{3A} and δ_{3B} torsion angles of the complexed ethyl paraben have a larger out-of-plane twist than those of the uncomplexed ethyl paraben, indicating that the complexation yields more rotational freedom around the C(8)–O(10) and O(10)–C(11) bonds.

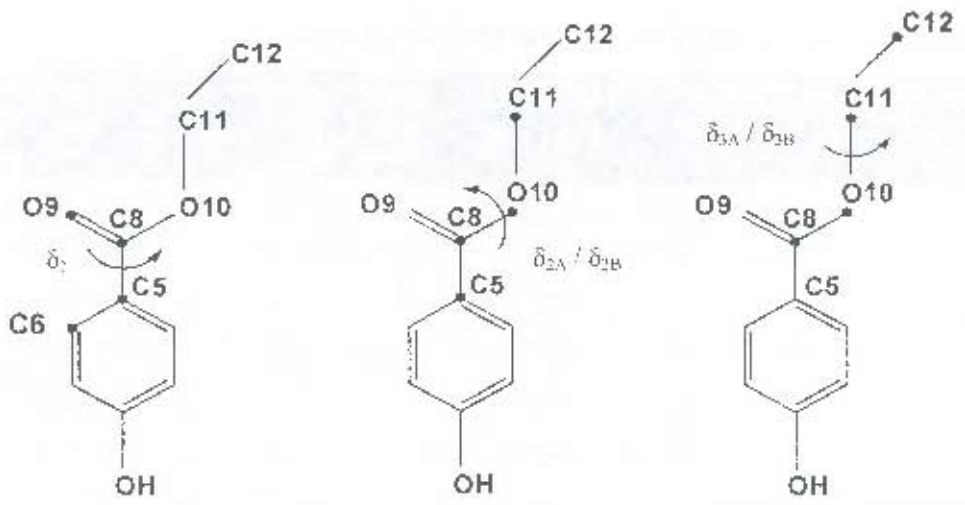

δ_1 C(6)–C(5)–C(8)–O(9)	➡	C(5)–C(8)
δ_{2A} C(5)–C(8)–O(10A)–C(11A)	➡	C(8)–O(10A)
δ_{2B} C(5)–C(8)–O(10B)–C(11B)	➡	C(8)–O(10B)
δ_{3A} C(8)–O(10A)–C(11A)–C(12A)	➡	O(10A)–C(11A)
δ_{3B} C(8)–O(10B)–C(11B)–C(12B)	➡	O(10B)–C(11B)

EP in complex:

δ_1 = -2 (1)
δ_{2A} = -172 (1)
δ_{2B} = +157 (1)
δ_{3A} = -117 (1)
δ_{3B} = +113 (1)

EP uncomplexed:

δ_1 = +5.6
δ_2 = -179.7
δ_3 = -179.4

Figure 5.15 Torsion angles δ_1, δ_{2A}, δ_{2B}, δ_{3A} and δ_{3B} of the ethyl paraben

Table 5.13 Close contact distances for the EPDMB structure

Interaction	Distance (Å)
H(4) ••• H(561)	2.22
C(11B) ••• C(6G5)	3.20 (2)
H(11D) ••• C(6G5)	2.33 (1)
H(11D) ••• O(65A)	1.87 (3)
H(12A) ••• C(6G6)	2.91 (1)
H(12A) ••• H(661)	2.17
O(1) ••• H(856)^{i}	2.57 (1)
C(7) ••• H(856)^{i}	2.82 (1)
H(7) ••• C(85A)^{i}	2.77 (3)
H(7) ••• H(851)^{i}	2.39
H(7) ••• H(852)^{i}	2.32
H(7) ••• H(856)^{i}	2.25
H(11C) ••• H(733)^{i}	2.44
H(12B) ••• H(321)^{i}	2.38

^{i} Related by symmetry operation: -1+x, y, z

The ester moiety of the guest molecule is located at the primary rim while the phenolic hydroxyl group is located at the secondary rim of the cyclodextrin. The phenyl ring of the guest is almost perpendicular to the mean O(4) plane with an angle of 87.3 (2)° between the two. The guest makes a number of van der Waals contacts with the inside wall of the cavity. Figures 5.16 and 5.17 show CPK diagrams of the EPDMB structure.

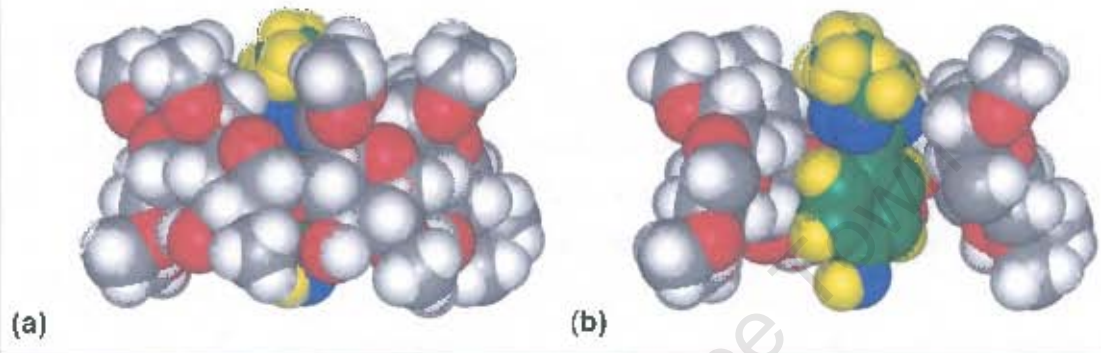

Figure 5.16 Space-filling diagram of the EPDMB structure (a) side view (b) sectioned view of the same orientation

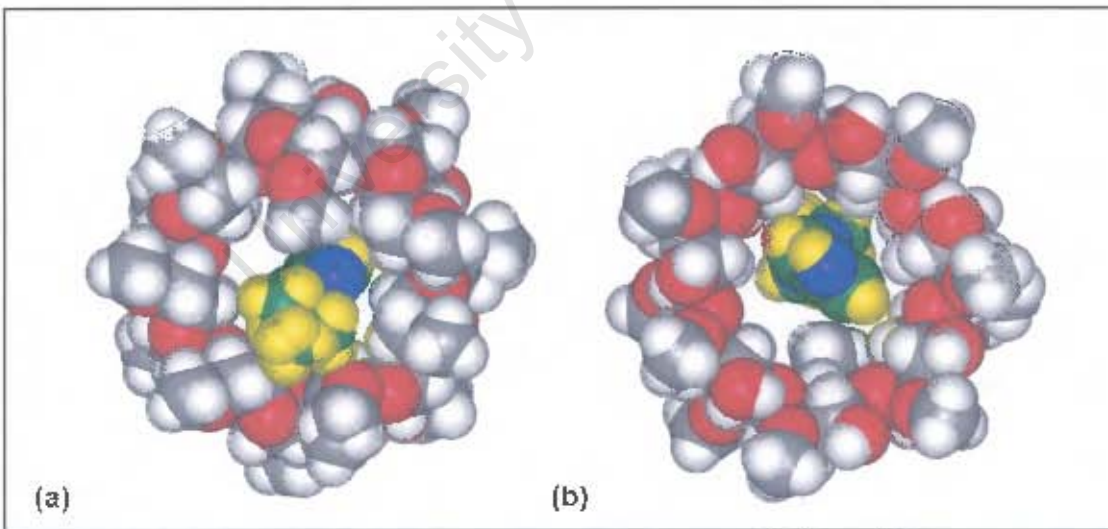

Figure 5.17 Space-filling diagram of the EPDMB structure (a) viewed from the primary rim (b) viewed from the secondary rim

Hydrogen bonding interactions of the EPDMB structure

Host interactions

There are seven intramolecular O(2)•••O(3') hydrogen bonds which contribute to the rigidity and highly symmetrical conformation of the cyclodextrin. These hydrogen bonds are in the range 2.72-2.93 Å, with a mean of 2.83 Å, Table 5.12. Additionally the conformation of the DIMEB molecule is stabilised by six intramolecular C–H•••O hydrogen bonds which consist of five C(6)–H•••O(5') hydrogen bonds and a C(8)–H•••O(5') hydrogen bond. The crystal structure is further stabilised by five intermolecular C–H•••O hydrogen bonds which consist of a C(2)–H•••O(3) hydrogen bond, a C(8)–H•••O(2) hydrogen bond, two C(8)–H•••O(3) hydrogen bonds and a C(8)–H•••O(6) hydrogen bond. This indicates that the disordered atoms C(85A) and C(85B) atoms add to the overall stability of the structure. These C–H•••O hydrogen bonds are listed in Table 5.14 and the C•••O distances are in the range 3.2-3.5 Å.

Table 5.14 C–H•••O hydrogen bonds in the EPDMB structure*

			Distance (Å)			Angle (°)
C	H	O	C–H	H•••O	C•••O	C–H•••O
Intramolecular hydrogen bonds						
C(6G1)	H(612)	O(5G2)	0.99	2.64	3.36 (1)	129.7 (7)
C(6G3)	H(632)	O(5G4)	0.99	2.70	3.29 (1)	118.9 (6)
C(6G4)	H(642)	O(5G5)	0.99	2.66	3.36 (1)	127.3 (6)
C(6G6)	H(662)	O(5G7)	0.99	2.78	3.44 (1)	124.4 (6)
C(6G7)	H(672)	O(5G1)	0.99	2.69	3.44 (1)	132.2 (6)
C(8G3)	H(833)	O(5G4)	0.98	2.76	3.40 (1)	123.5 (7)
Intermolecular hydrogen bonds						
C(2G1)	H(211)	O(3G4)^{i}	1.00	2.56	3.32 (1)	132.4 (6)
C(8G3)	H(832)	O(3G2)^{ii}	0.98	2.62	3.43 (1)	139.8 (8)
C(85A)	H(852)	O(2G4)^{iii}	0.98	2.67	3.22 (4)	115 (2)
C(85B)	H(854)	O(3G4)^{iii}	0.98	2.75	3.43 (2)	127 (1)
C(8G7)	H(873)	O(6G4)^{i}	0.98	2.73	3.32(1)	119.1 (7)

^{i} Related by symmetry operation: x, 1-y, z
^{ii} Related by symmetry operation: 1-x, $^{1}/_{2}$+y $^{1}/_{2}$-z
^{iii} Related by symmetry operation: 1+x, y, z
* Hydrogen bonding parameters based on idealised hydrogen atom positions

Guest interactions

The hydroxyl oxygen atom forms three hydrogen bonds to host molecules in symmetry related positions and a hydrogen bond with one water oxygen atom O(3W) [Figure 5.18]. The atom C(12A) forms a weak hydrogen bond to the atom O(65A). Hydrogen bonding distances involving the guest are listed in Table 5.15.

Table 5.15 Hydrogen bonding distances involving the guest in the EPDMB structure*

			Distance (Å)			Angle (°)
Donor(D)	H	Acceptor(A)	D–H	H•••A	D•••A	D–H•••A
O(1)	H(1)	O(3W)	0.84	1.89	2.72 (1)	169.4 (7)
C(85B)	H(856)	O(1)^{i}	0.98	2.57	3.30 (2)	132 (1)
C(6G6)	H(661)	O(1)^{i}	0.99	2.67	3.40 (1)	130.7 (6)
C(7G6)	H(762)	O(1)^{ii}	0.98	2.79	3.48 (2)	128 (1)
C(12A)	H(12C)	O(65A)	0.98	2.84	3.53 (4)	128 (1)

^{i} Related by symmetry operation: 1+x, y, z
^{ii} Related by symmetry operation: ½+x, 1½−y, -z
* Hydrogen bonding parameters based on idealised hydrogen atom positions.

Water interactions

Thermogravimetric analysis yielded a weight loss that corresponds to 4.0 water molecules per 1:1 complex unit and these were all accounted for in the crystallographic analysis. All the water molecules are situated at the periphery of the cyclodextrin molecule, filling the intermolecular space between complex units. Hydrogen bonding distances between the host and these water molecules are listed in Table 5.16.

All the water molecules are within hydrogen bonding distance of a host oxygen atom, except for O(3W). This water molecule is hydrogen bonded to the guest hydroxyl oxygen atom and is within hydrogen bonding distance of two water oxygen atoms forming bridges with atoms of adjacent glucose units [Figure 5.18].

Both the water oxygen atoms O(4WA) and O(4WB) are in hydrogen bonding contact with the same host oxygen atom and water oxygen atom, namely O(3G6) and O(1W). O(4WB) is 2.23 Å from O(5W), indicating that these atoms will not be present simultaneously. The s.o.f.'s of O(4WA), O(4WB) and O(5W) are 0.71, 0.17 and 0.28 respectively.

Table 5.16 Hydrogen bonds and hydrogen bonding distances between water molecules and the host in the EPDMB structure*

			Distance (Å)			Angle (°)
Donor(D)	H	Acceptor(A)	D–H	H···A	D···A	D–H···A
C(3G6)	H(361)	O(5W) [i]	1.00	2.69	3.36 (3)	124.0 (8)
C(7G7)	H(772)	O(2W) [ii]	0.98	2.89	3.46 (2)	117.9 (9)

Interaction	Distance (Å)	Symmetry operator for the host oxygen atoms
O(1W) ··· O(6G7)	2.89 (1)	x, y, z
O(4WA) ··· O(65B)	2.72 (1)	x, -1+y, z
O(4WA) ··· O(3G6)	2.77 (1)	$^{1}/_{2}$+x, $^{1}/_{2}$-y, -z
O(4WB) ··· O(3G6)	2.72 (5)	$^{1}/_{2}$+x, $^{1}/_{2}$-y, -z
O(5W) ··· O(2G6)	2.78 (3)	$^{1}/_{2}$+x, $1^{1}/_{2}$-y, -z
O(1W) ··· O(2W)	2.75 (1)	x, y, z
O(1W) ··· O(4WA)	2.69 (1)	x, y, z
O(1W) ··· O(4WB)	2.81 (5)	x, y, z
O(2W) ··· O(3W)	2.78 (1)	$^{1}/_{2}$+x, $^{1}/_{2}$-y, -z
O(3W) ··· O(5W)	2.89 (3)	-$^{1}/_{2}$+x, $1^{1}/_{2}$-y, -z
O(4WB) ··· O(5W)	2.23 (5)	x, 1-y, z

[i] Related by symmetry operation: -$^{1}/_{2}$+x, $1^{1}/_{2}$-y, -z
[ii] Related by symmetry operation: -$^{1}/_{2}$+x, $^{1}/_{2}$-y, -z
* Hydrogen bonding parameters based on idealised hydrogen atom positions.

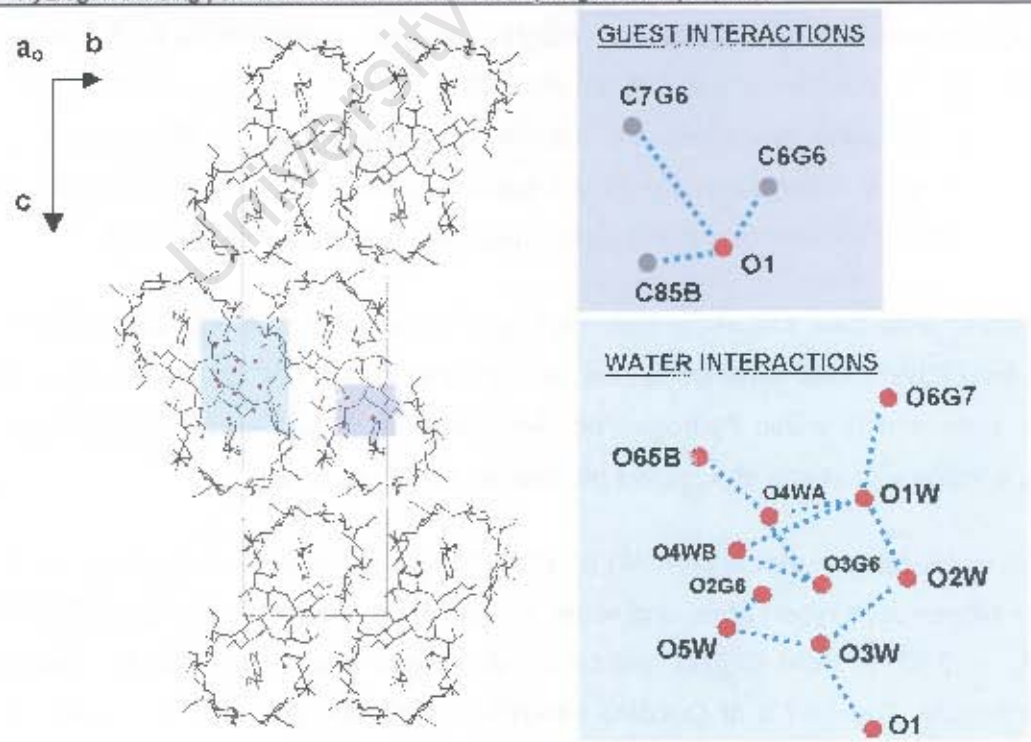

Figure 5.18 A schematic representation of guest and water interactions that connect adjacent host units

Crystal packing of the EPDMB structure

Figures 5.19 and 5.20 are extended stereo packing diagrams of the EPDMB structure showing projections as viewed down the *a*- and *b*-axes. Figure 5.19 shows the "endless" channels while Figure 5.20 shows the columns running parallel to the *a*-axis. The EPDMB molecules are stacked in columns in a head-to-tail mode, forming what appear to be continuous channels along the *a*-axis in a herringbone type pattern.

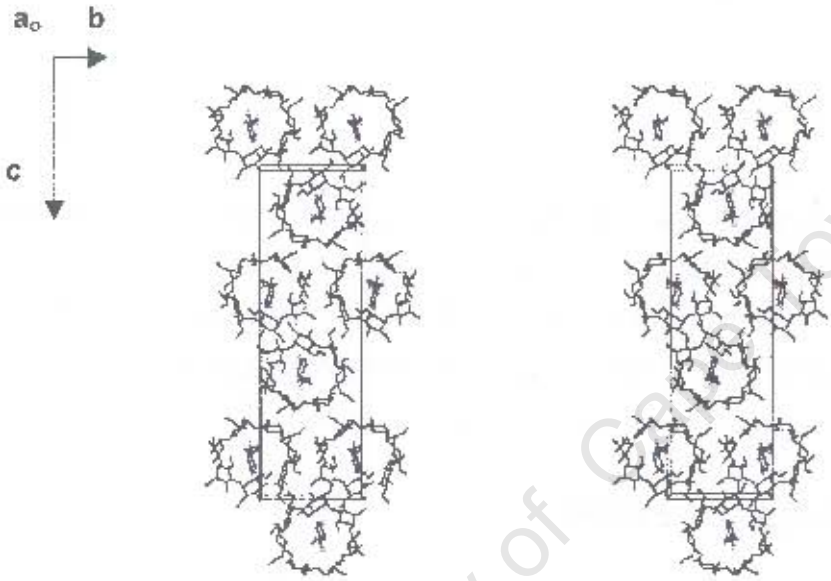

Figure 5.19 Stereo packing diagram of the EPDMB structure [*a*-axis projection]

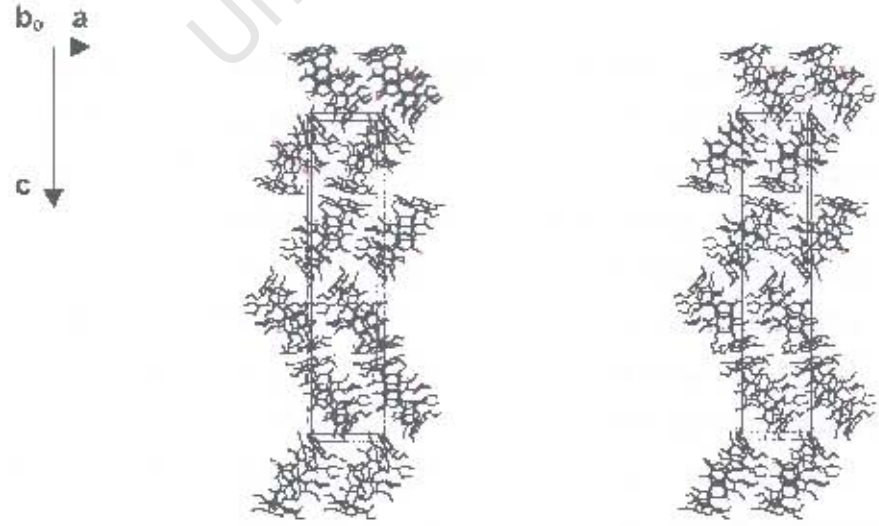

Figure 5.20 Stereo packing diagram of the EPDMB structure [*b*-axis projection]

X-RAY CRYSTALLOGRAPHIC ANALYSIS OF THE PPDMB STRUCTURE

Data-collection

X-ray photographic techniques were used to determine the preliminary unit cell parameters, crystal system and space group for the PPDMB structure. Oscillation and Weissenberg photography revealed Laue symmetry *mmm*, corresponding to the orthorhombic system. The systematic absences observed are listed below and these verified that the space group is $P2_12_12_1$.

hkl: none
h00: h = 2n + 1
0k0: k = 2n + 1
00l: l = 2n + 1

A single crystal of the complex was mounted on a glass fibre and covered in Paratone N oil[2] to prevent cracking due to loss of water of crystallisation and to provide a rigid mounting for the low-temperature data collection. Data were collected on the Nonius Kappa CCD diffractometer using graphite-monochromated MoKα radiation at 173(2) K. Crystal data and data-collection parameters are listed in Table 5.17.

Structure determination and refinement

The structure was solved using published co-ordinates for the non-hydrogen cyclodextrin atoms [excluding the O(6), C(7), and C(8) atoms of each methylglucose residue] of the isomorphous DIMEB-2-naphthoic acid trihydrate complex.[12-13] This skeletal structure was refined with SHELX-97[6] and the difference Fourier map showed the positions of most of the remaining non-hydrogen atoms.

As the refinement of the host proceeded, it become evident that the atom C(7) on O(2G3) was disordered. For each disordered atom two alternative positions were found and for a given pair of atoms a fixed U_{iso} of 0.08 Å^2 [the mean of U_{iso} for the chemically equivalent ordered atoms] was assigned and site-occupancy factors of x and 1-x were assigned, with x variable. The final site-occupancy from the major position refined to 0.57 for C(73A). Distance constraints were placed on the bonds involving these disordered atoms. All the non-hydrogen atoms on the host were refined anisotropically, except the disordered atoms, the atoms C(8) and O(6G2), C(7G2), C(1G3), O(3G3), C(3G3), C(4G3), C(5G3) and O(2G5). The hydrogen atoms of the host were geometrically constrained to their parent atoms and refined with linked temperature factors.

Table 5.17 Details of the data collection and refinement parameters for the PPDMB structure

Empirical formula	$C_{56}H_{88}O_{35}$•$C_{10}H_{12}O_3$•$3.9H_2O$
Formula weight	1581.8
Crystal system	Orthorhombic
Space group	$P2_12_12_1$
a / Å	15.1399 (2)
b / Å	18.8943 (3)
c / Å	28.4009 (5)
α / °	90
β / °	90
γ / °	90
Volume / Å^3	8124.3 (2)
Z	4
Density$_{calc}$ / g cm^{-3}	1.293
μ (MoKα) / mm^{-1}	0.108
F(000)	3396
Temperature of data collection / K	173 (2)
Crystal size / mm^3	0.45 x 0.39 x 0.17
Range scanned θ / °	$2 \leq \theta \leq 22$
Index ranges	h: -15,15 k: -19,19 l: -29, 29
ϕ scan angle / °	1.0
ϕ scan range, frames	181.0°, 181
ω scan angle / °	1.0
ω scan ranges, frames	42.0°, 42 and 47.0°, 47
Dx / mm	59.0
Total no. of reflections collected	19849
No. of independent reflections	9393
No. of reflections with $I > 2\sigma(I)$	6601
No. of parameters	819
R_{int}	0.0534
S	1.292
R- (for 5247 reflections)	0.1125
Reflections omitted	(0 0 2); (0 1 1); (0 2 1); (0 6 0); (2 0 0); (2 0 3); (2 2 0); (1 1 4); (-1 1 4); (4 0 1); (5 0 2)
wR_2	0.3080
Weighting scheme	a = 0.2000 b = 0.0000
$(\Delta / \sigma)_{mean}$	< 0.057
Δρ excursions / e.Å^{-3}	0.49 and -0.51

Refinement continued with the placement of the water molecules. Seven water molecule sites were located and each water molecule was refined isotropically and assigned a fixed isotropic temperature factor of 0.12 $Å^2$ while the site-occupancies were allowed to vary. The s.o.f.'s refined to 0.46, 0.29, 0.35, 0.47, 0.60, 0.48, 0.23, 0.50 and 0.32 for O(1WA), O(1WB), O(2WA), O(2WB), O(3W), O(4W), O(5W), O(6W) and O(7W) respectively. This temperature factor was chosen to equate the number of water molecules per asymmetric unit to the 3.9 waters found by the TGA experiment. The computed waters amounted to a total of 3.7 water molecules per asymmetric unit. The hydrogen atoms of the water molecules were not located.

Once the waters were accounted for, the remaining difference electron density map revealed the non-hydrogen atoms of the guest. Refinement proceeded with the placement of these atoms. The phenyl group of the guest molecule was treated as a regular hexagon with bond lengths of 1.390 Å. A single isotropic temperature factor was used for the non-hydrogen atoms of the guest and this refined to a final value of 0.23 $Å^2$. For the hydrogen atoms linked to the carbon atoms of the guest, calculated co-ordinates were used [C-H distance 0.95 Å] and the H atoms were assigned a common isotropic temperature factor. The hydrogen atom of the hydroxyl group was placed using the rotating group refinement strategy [AFIX 83]. Due to the abnormally long bond distances found in the guest molecule, distance constraints were placed on certain bonds, namely: O(1)–C(2) 1.351 Å; C(5)–C(8) 1.471 Å; C(8)–O(9) 1.207 Å; C(8)–O(10) 1.334 Å; O(10)–C(11) 1.448 Å, C(11)–C(12) 1.490 Å, and C(12)–C(13) 1.490 Å [all with σ = 0.005 Å]. The values chosen were taken from Lin.[11] A distance constraint was placed on the alkyl chain atoms of C(11)–C(12)–C(13) to maintain the angle close to the tetrahedral value. The largest remaining difference electron density peak $\Delta\rho$ = 0.5 $e.Å^{-3}$ is not indicative of appreciably populated atomic sites which might have been missed.

Geometrical analysis of the PPDMB structure

The asymmetric unit of the PPDMB structure contains a single DIMEB molecule, its associated guest and 3.9 water molecules. The numbering scheme adopted for the inclusion complex is given in Figure 5.21.

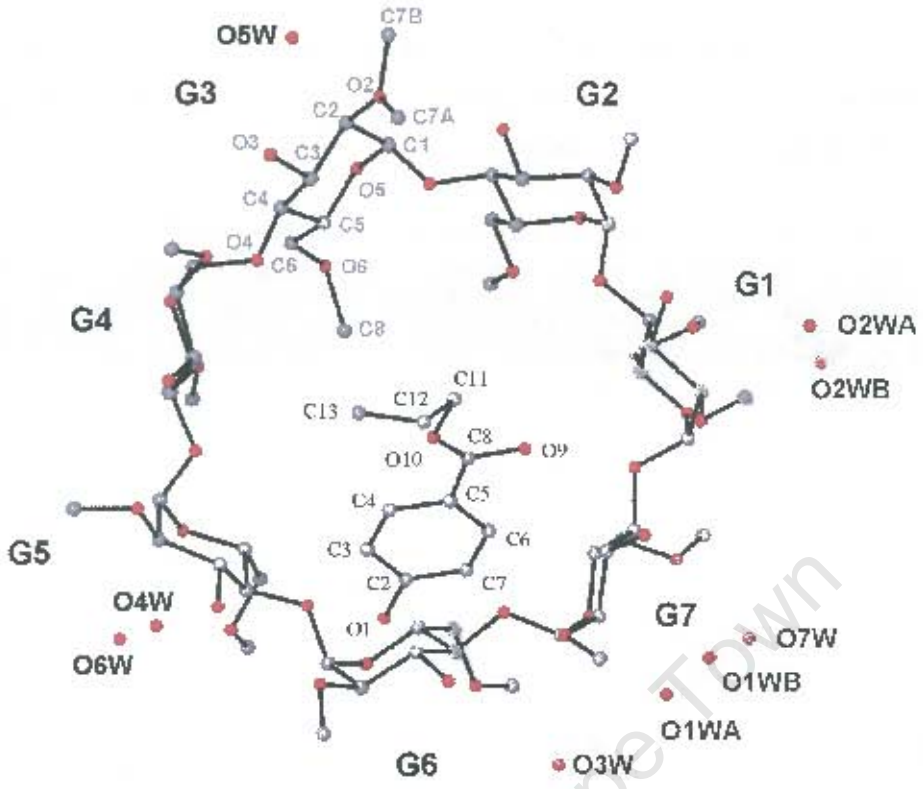

Figure 5.21 Macrocyclic structure and numbering scheme of glucose residues, water oxygen atoms and guest molecule, with the hydrogen atoms excluded. The host is viewed from the secondary face.

The glucose units will be referred to as G1, G2, G3, G4, G5, G6 and G7. The geometrical data for the DIMEB molecule are listed in Tables 5.18 and 5.19 [e.s.d.s are in the range 0.008-0.015 Å for distances and 0.2-0.9° for angles]. Figure 5.21 shows that the DIMEB molecule has a round and symmetrical structure with each of the glucopyranose residues in the $^4C_1$ chair conformation. The C(6)–O(6) bonds of the G1, G5, G6 and G7 residues are directed away from the cavity in the (-) *gauche* conformation to the C(4)–C(5) and O(5)–C(5) bonds. The C(6)–O(6) bonds of the G2 residue and the G4 residue point towards the cavity in the (+) *gauche* conformation. The C(6)–O(6) bond of the G3 residue is in a *trans* conformation. All the O(6)–C(8) bonds, including the O(6G5)–C(85A) and O(6G5)–C(85B) bonds, are *trans* with respect to the C(5)–C(6) bonds, except the O(6)–C(8) bond of the G3 residue which is *cis*. All the O(2)–C(7) bonds, including the O(2G3)–C(73A) and O(2G3)–C(73B) bonds, are directed away from the cavity.

The geometric parameters of the O(4) heptagon of the PPDMB structure are listed in Table 5.18. These include the radii, the O(4)•••O(4') distances, the O(4)•••O(4')•••O(4'') angles, the O(4)•••O(4')•••O(4'')•••O(4''') torsion angles and the deviations of each of the O(4) atoms from the mean O(4) plane.

Table 5.19 lists the other important features of the macrocyclic structure such as the intersaccharidic bond angle (φ), the O(2)•••O(3') distance and the tilt angles [τ_1 and τ_2]. These parameters are defined in Chapter 1.

Table 5.18 Geometrical parameters of the O(4) heptagon for the PPDMB structure

Glucose unit	Radii (Å)	O(4)•••O(4') (Å)	O(4) angle (°)	Torsion angle (°)	Deviation (Å)
G1	5.00 (1)	4.43	131	6.7 (4)	-0.03
G2	5.13 (1)	4.25	125	-11.0 (4)	-0.23
G3	4.94 (1)	4.55	132	2.1 (4)	0.13
G4	5.09 (1)	4.30	127	6.7 (4)	0.14
G5	5.10 (1)	4.43	128	-2.3 (4)	-0.12
G6	5.00 (1)	4.38	130	-6.5 (4)	-0.04
G7	5.06 (1)	4.36	127	4.3 (4)	0.17
Average	**5.05**	**4.38**	**129**	**5.6**	**0.13**

Table 5.19 φ, O(2)•••O(3') distance,τ for the PPDMB structure

Glucose unit	φ (°)	O(2)•••O(3') (Å)	τ_1 (°)	τ_2 (°)
G1	118	2.88	7.1 (2)	10.1 (3)
G2	118	2.80	14.5 (2)	16.6 (4)
G3	118	2.89	14.7 (3)	21.8 (4)
G4	120	2.87	4.8 (2)	1.7 (4)
G5	118	2.97	15.6 (3)	17.8 (4)
G6	118	2.88	16.0 (2)	19.6 (3)
G7	120	2.82	7.0 (2)	11.7 (4)
Average	**118**	**2.87**	**11.4**	**14.2**

The radii of the heptagon are in the range 4.94-5.13 Å and the average value of 5.05 Å is in good agreement with the radius of native β-CD [5.04 Å].[8-9] The side lengths of the heptagon are in the range 4.25-4.55 Å. Each glucose residue inclines with the O(6) side turning to the inside of the macrocycle. The tilt angles are in the range 1.7-21.8°, with the G3 and G6 residues being the most inclined. The distances between the O(2) and O(3) atoms of the adjacent residues [in the narrow range 2.80-2.97 Å] indicate that the O(3) hydroxyl group is hydrogen bonded to the O(2) atom of the adjacent residue. The values calculated for these parameters compare favourably with those of the DIMEB-2-naphthoic acid trihydrate complex.[12-13]

Guest geometry and interactions for the PPDMB structure

The conformation of the propyl paraben guest may be defined by four torsion angles and the torsion angles listed below are used to describe the rotation around each of the corresponding bonds [Figure 5.22]. The close contact distances for the relevant interactions between the host and guest molecule are listed in Table 5.20. This table shows that the hydroxyl oxygen atom is in close contact to the O(2WB) water oxygen atom while it is at a distance of 3.04 Å from its disordered counterpart.

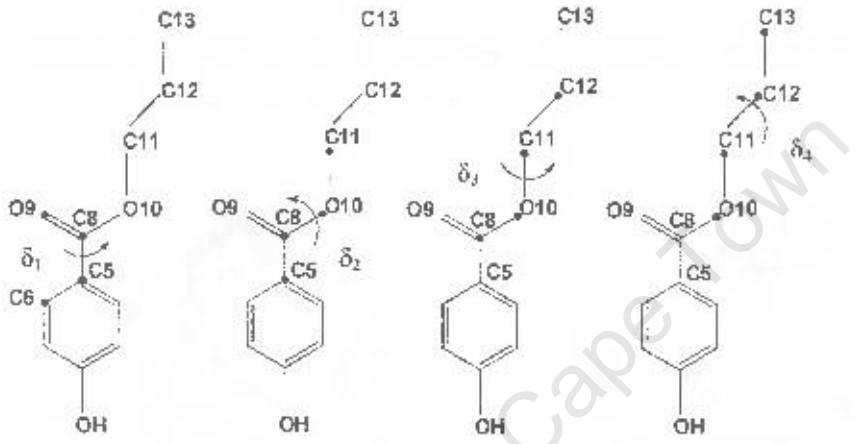

δ_1 C(6)–C(5)–C(8)–O(9)	➡	C(5)–C(8)
δ_2 C(5)–C(8)–O(10)–C(11)	➡	C(8)–O(10)
δ_3 C(8)–O(10)–C(11)–C(12)	➡	O(10)–C(11)
δ_4 O(10)–C(11)–C(12)–C(13)	➡	C(11)–C(12)

PP in complex:
δ_1 = +1 (2)
δ_2 = -170 (1)
δ_3 = -139 (1)
δ_4 = -63 (2)

Figure 5.22 Torsion angles δ_1, δ_2, δ_3 and δ_4 of the propyl paraben

Table 5.20 Close contact distances for the PPDMB structure

Interaction	Distance (Å)
H(3) ••• H(853)	2.21
H(11B) ••• H(511)	2.36
O(1) ••• C(7G7) [i]	3.09 (2)
O(1) ••• O(2WA) [ii]	3.04 (4)
O(1) ••• O(2WB) [ii]	2.18 (3)
H(1) ••• H(772) [i]	2.33
H(3) ••• O(5W) [iii]	2.58 (4)
C(4) ••• H(742) [iii]	2.81 (1)

[i] Relatoc by symmetry operation: -1+x, y, z
[ii] Related by symmetry operation: -1/2+x, 1/2-y, 1-z
[iii] Related by symmetry operation -1/2+x, 1 1/2-y, 1-z

Although the contact distance between O(2WB) and O(1) was abnormally close, spurious electron peaks of a low density were found in the vicinity of the water oxygen atom, suggesting either further disorder or a higher anisotropic thermal motion.

Figures 5.23 and 5.24 show CPK diagrams of the PPDMB structure. The phenolic hydroxyl group and the aromatic ring extend well beyond the primary rim of the host while the ester moiety occupies the centre of the host cavity. This can be ascribed to the hydrophilic nature of the hydroxyl group and the hydrophobic nature of the alkyl group. The phenyl ring of the guest forms an angle of 55.9 (2)° with the mean O(4) plane. This represents a significantly different mode of guest inclusion from that observed for the MPDMB and EPDMB complexes described earlier.

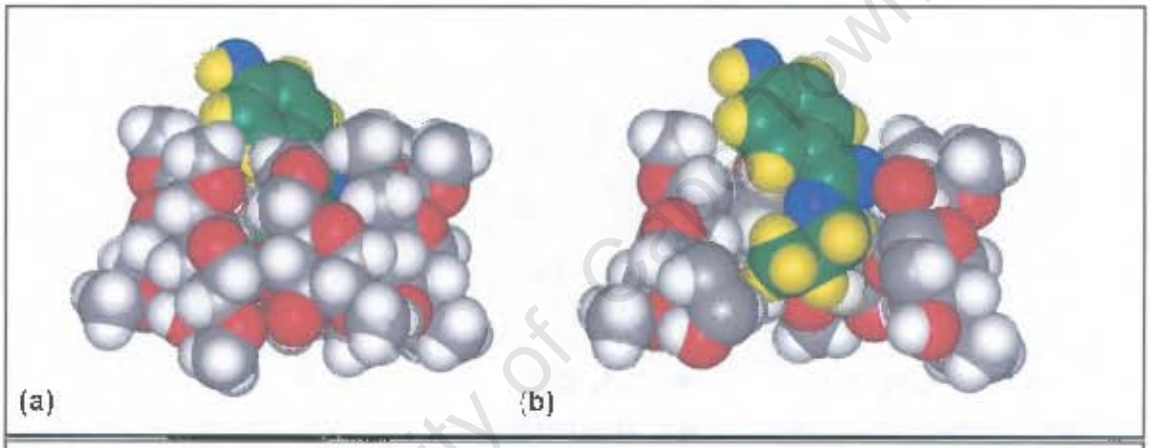

Figure 5.23 Space-filling diagram of the PPDMB structure (a) side view (b) sectioned view of the same orientation

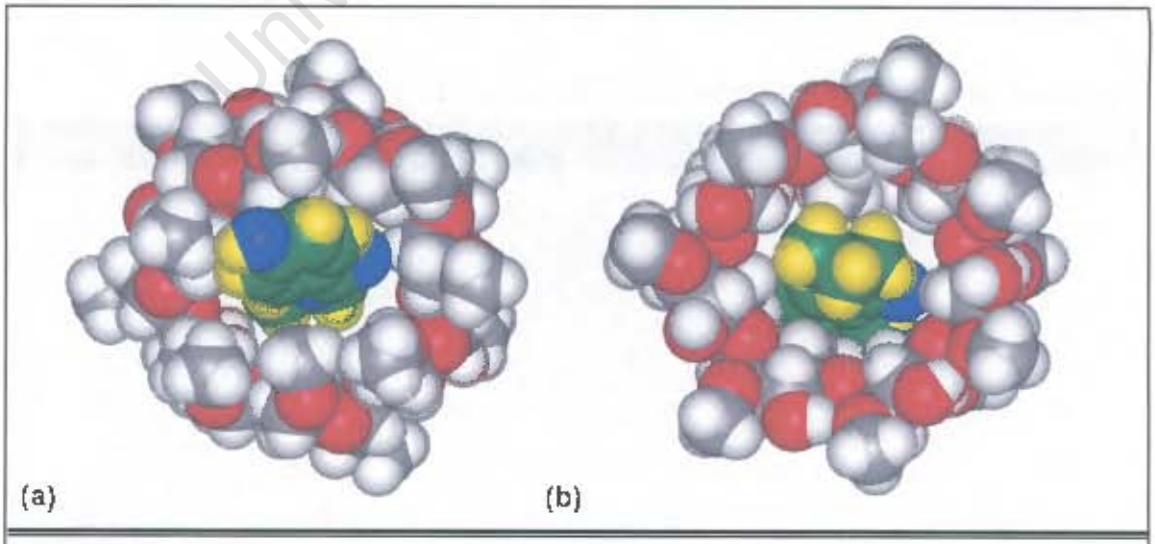

Figure 5.24 Space-filling diagram of the PPDMB structure (a) viewed from the primary rim (b) viewed from the secondary rim

Hydrogen bonding interactions of the PPDMB structure

Host interactions

In addition to the O(2)•••O(3') intramolecular hydrogen bonds [Table 5.19] which contribute to the roundness of the DIMEB molecule, the conformation of the DIMEB molecule is stabilised by eight intramolecular hydrogen bonds. These consist of four C(6)–H•••O(5') hydrogen bonds and four C(7)–H•••O(3) hydrogen bonds. Furthermore the crystal structure is stabilised by three intermolecular hydrogen bonds. These comprise one C(2)–H•••O(3) hydrogen bond, one C(7)–H•••O(3) hydrogen bond and a C(8)–H•••O(3) hydrogen bond to adjacent glucose units. All the C•••O distances are in the range 3.0-3.4 Å.

Table 5.21 C–H•••O hydrogen bonds in the PPDMB structure*

				Distance (Å)		Angle (°)
C	H	O	C–H	H•••O	C•••O	C–H•••O
Intramolecular hydrogen bonds						
C(6G1)	H(612)	O(5G2)	0.99	2.55	3.35 (1)	138.2 (8)
C(6G5)	H(652)	O(5G6)	0.99	2.66	3.37 (1)	128.5 (7)
C(6G6)	H(662)	O(5G7)	0.99	2.72	3.39 (1)	124.9 (6)
C(6G7)	H(672)	O(5G1)	0.99	2.64	3.36 (1)	129.1 (8)
C(7G1)	H(713)	O(3G1)	0.98	2.60	3.20 (2)	119.0 (8)
C(7G4)	H(743)	O(3G4)	0.98	2.48	3.09 (2)	120 (1)
C(7G6)	H(762)	O(3G6)	0.98	2.49	3.12 (2)	122 (1)
C(7G7)	H(773)	O(3G7)	0.98	2.59	3.17 (2)	118.3 (8)
Intermolecular hydrogen bonds						
C(2G4)	H(241)	O(3G7)^{i}	1.00	2.72	3.39 (1)	124.4 (6)
C(7G7)	H(772)	O(3G3)^{ii}	0.98	2.72	3.30 (2)	118.1 (8)
C(8G7)	H(871)	O(3G7)^{iii}	0.98	2.62	3.28 (2)	124 (1)

^{i} Related by symmetry operation: $-\frac{1}{2}+x$, $1\frac{1}{2}-y$, 1-z
^{ii} Related by symmetry operation: $\frac{1}{2}+x$, $1\frac{1}{2}-y$, 1-z
^{iii} Related by symmetry operation: $-\frac{1}{2}+x$, $\frac{1}{2}-y$, 1-z
* Hydrogen bonding parameters based on idealised hydrogen atom positions.

Guest interactions

The hydroxyl oxygen atom of the guest is hydrogen bonded to the water oxygen atom O(5W) and forms a weak hydrogen bond to two of the host C(7) atoms. The C(7G7)•••O(1)•••C(7G2) angle is 139°. In addition the O(5W) water atom is hydrogen bonded to C(3) of the guest. The carbonyl oxygen is in hydrogen bonding contact with two C(6) carbon atoms of the host

The carbon atom C(7) of the guest is hydrogen bonded to one of the disordered water oxygen atoms, namely O(2WB). By forming an integrated network the water molecules add to the stability of the complex. Hydrogen bonds and hydrogen bonding distances are listed in Table 5.22 and are illustrated in Figure 5.25.

Table 5.22 C–H···O hydrogen bonds and hydrogen bonding distances involving the guest in the PPDMB structure*

				Distance (A)		Angle (°)
Donar (D)	H	Acceptor (A)	D–H	H···A	D···A	D–H···A
O(1)	H(1)	O(5W) [i]	0.84	1.75	2.58 (1)	179 (2)
C(3)	H(3)	O(5W) [i]	0.95	2.58	3.24 (1)	127 (1)
C(7)	H(7)	O(2WB) [ii]	0.95	2.67	3.22 (1)	117 (1)
C(7G2)	H(722)	O(1) [iii]	0.98	2.69	3.21 (1)	114 (1)
C(7G7)	H(772)	O(1) [iv]	0.98	2.68	3.10 (1)	105.8 (8)
C(6G1)	H(611)	O(9)	0.99	2.71	3.39 (1)	126.0 (8)
C(6G7)	H(672)	O(9)	0.99	2.71	3.31 (1)	118.7 (8)

[i] Related by symmetry operation -½+x, 1½-y, 1-z
[ii] Related by symmetry operation: -½+x, ½-y, 1-z
[iii] Related by symmetry operation ½-x, 1-y, -½+z
[iv] Related by symmetry operation 1+x, y, z
* Hydrogen bonding parameters based on idealised hydrogen atom positions.

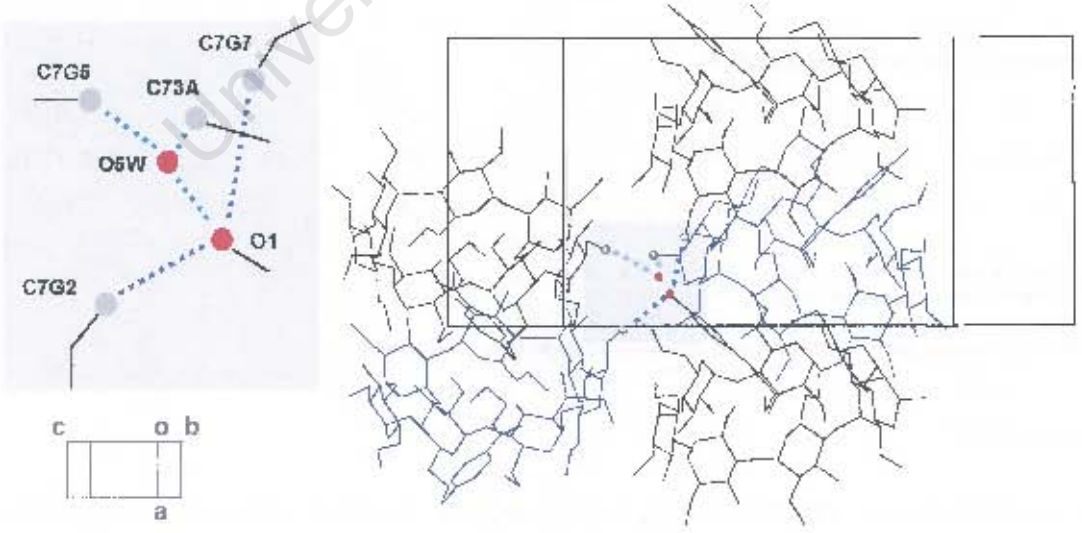

Figure 5.25 The hydrogen bond scheme involving the guest hydroxyl group in the PPDMB complex

Water interactions

TGA showed a weight loss that corresponds to 3.9 water molecules per 1:1 complex unit. Crystallographic analysis revealed that all the water molecules are located at the periphery of the cyclodextrin molecule, and fill the small intermolecular space between complex units. C–H•••O hydrogen bonds between the host and these water molecules are listed in Table 5.23 and hydrogen bonding distances between the host and these water molecules are listed in Table 5.24. Two water molecules [O(1W) and O(2W)] are found over two positions with the s.o.f. of these positions, A and B, being almost equivalent in each instance. All the water molecules are within hydrogen bonding distance of a host oxygen atom, except for O(1WA), O(2WB) and O(5W). The O(1WA) and O(2WB) water molecules are involved in hydrogen bonding to other water molecules, forming bridges with atoms of adjacent glucose units [Figure 5.26].

The O(5W) water molecule is hydrogen bonded to the guest hydroxyl and is also found to form a C(7G5)–H753•••O(5W) hydrogen bond to the host. Additionally this water molecule is within hydrogen bonding distance of C(73A) at a distance of 3.03 (4) Å and with C(73B) at a distance of 3.13 (5) Å [Figure 5.25].

The O(3W) and O(4W) water molecules are within hydrogen bonding distance of O(6G6) and O(6G5) respectively. This places these water molecules in a close contact distance of 3.21 (2) Å to C(8G6) and of 3.03 (4) Å to C(8G5) respectively.

Table 5.23 C–H•••O hydrogen bonds between the host and the water molecules*

				Distance (Å)		Angle (°)
Donor(D)	H	Acceptor(A)	D–H	H•••A	D•••A	D–H•••A
O(3G5)	H(352)	O(6W)	0.84	2.19	2.76 (2)	125.6 (8)
C(7G2)	H(723)	O(4W) [i]	0.98	2.43	3.17 (3)	132 (1)
C(73B)	H(734)	O(5W)	0.98	2.33	3.13 (5)	138 (1)
C(7G5)	H(753)	O(5W) [ii]	0.98	2.38	3.13 (4)	133 (1)

[i] Related by symmetry operation: $^1/_2$+x, $1^1/_2$–y, 1-z
[ii] Related by symmetry operation: $^1/_2$-x, 2-y, $^1/_2$+z
* Hydrogen bonding parameters based on idealised hydrogen atom positions.

Table 5.24 Hydrogen bonding distances involving the water molecules

Interaction	Distance (Å)	Symmetry operator for the host oxygen atoms
O(1WB) ••• O(6G7)	2.65 (4)	x, y, z
O(2WA) ••• O(6G1)	2.60 (3)	x, y, z
O(3W) ••• O(6G6)	2.89 (2)	x, y, z
O(4W) ••• O(3G2)	2.95 (2)	$-^{1}/_{2}$+x, $1^{+}/_{2}$-y, 1-z
O(4W) ••• O(6G5)	2.52 (2)	x, y, z
O(6W) ••• O(3G5)	2.77 (2)	x, y, z
O(1WA) ••• O(7W)	2.99 (4)	x, y, z
O(2WA) ••• O(4W)	2.21 (3)	$^{+}/_{2}$-x, 1-y, $-^{+}/_{2}$+z
O(2WB) ••• O(4W)	2.75 (3)	$^{+}/_{2}$-x, 1-y, $-^{+}/_{2}$+z
O(3W) ••• O(6W)	2.61 (3)	1-x, $-^{1}/_{2}$+y, $1^{1}/_{2}$-z

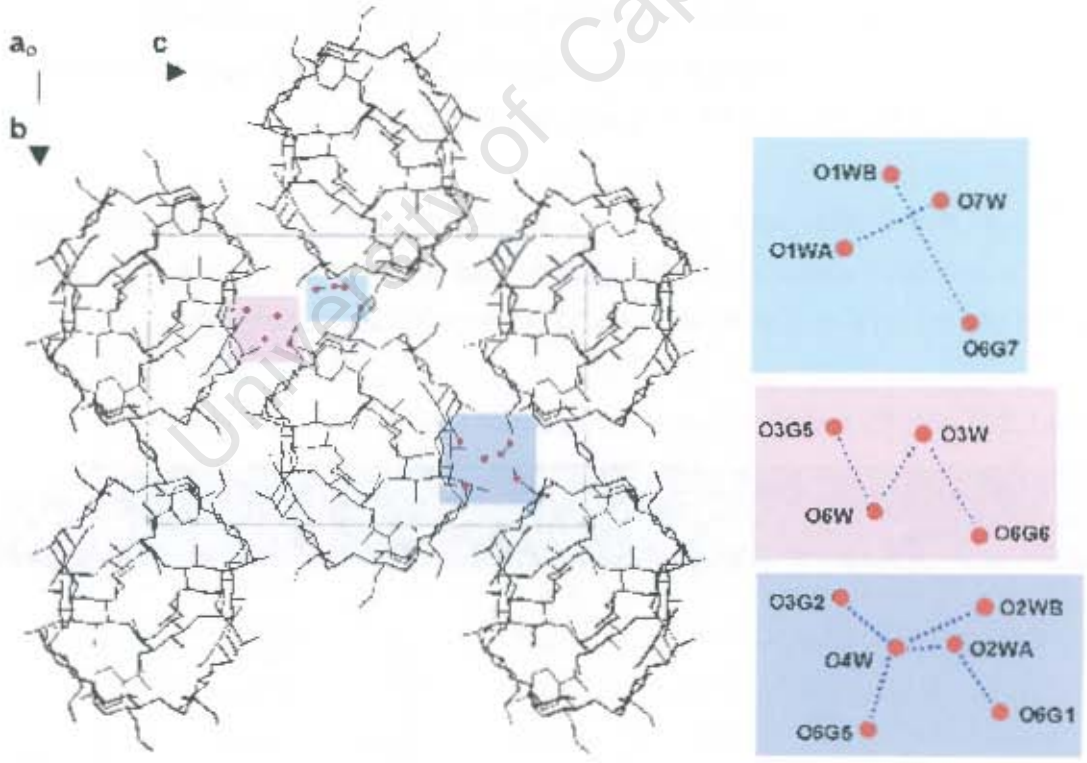

Figure 5.26 A schematic representation of the water molecules that connect adjacent host units

Crystal packing of the PPDMB structure

The extended stereo packing diagrams of the PPDMB structure showing projections as viewed down the *a*- and *c*-axes are given in Figures 5.27 and 5.28. These figures show the PPDMB molecules packing along the *a*-axis in a zigzag type pattern. The O(2), O(3) side of the PPDMB cavity is blocked by the O(6) side of the adjacent PPDMB molecule which is related by the two-fold screw axis along the *a*-axis. An inclusion of the primary $-OCH_3$ group on the G4 residue into the secondary side of the 2_1 related CD occurs. However this does not occur on the G3 residue as the O(6)–O(8) bond is in the *cis* conformation. The O(6) side of the cavity is open to the intermolecular space, where the guest is located.

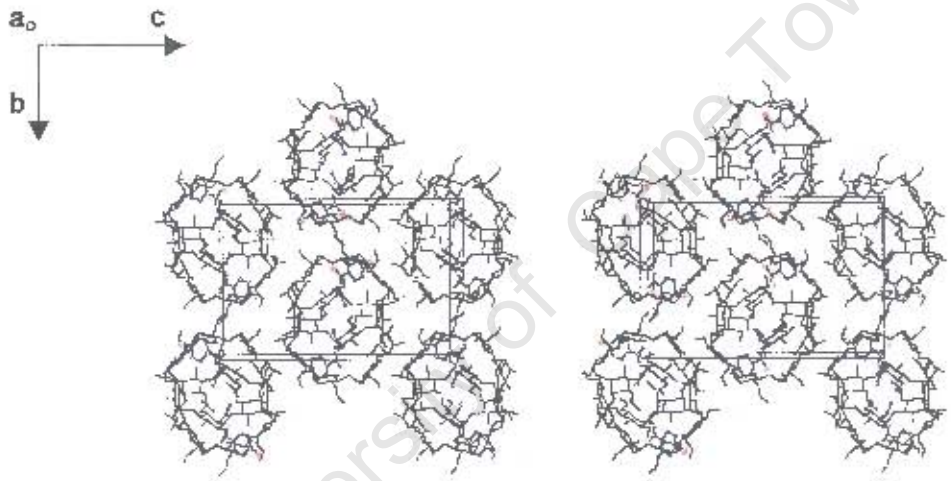

Figure 5.27 Stereo packing diagram of the PPDMB structure [*a*-axis projection]

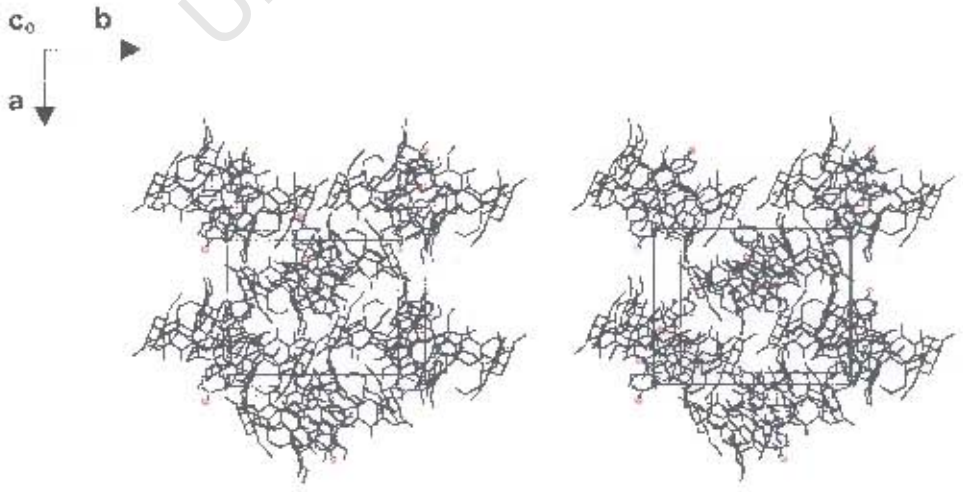

Figure 5.28 Stereo packing diagram of the PPDMB structure [*c*-axis projection]

X-RAY CRYSTALLOGRAPHIC ANALYSIS OF THE BPDMB STRUCTURE

Data-collection

A single crystal was mounted on a glass fibre and covered in Paratone N oil.[2] The crystal is prone to dehydration; contact with the atmosphere leads within seconds to cracking and subsequent disintegration. X-ray photographic techniques were used to determine the unit cell parameters, crystal system and space group for the BPDMB structure. Oscillation and Weissenberg photography revealed Laue symmetry *mmm* indicating that the system belonged to the orthorhombic system. The unit cell parameters for BPDMB determined from the photographs are a = 15.0, b = 19.1 and c = 28.3 Å. The systematic absences are listed below, and these confirmed the space group $P2_12_12_1$.

hkl:	none
h00:	h = 2n + 1
0k0:	k = 2n + 1
00l:	l = 2n + 1

X-ray intensity data-collection was performed on the Nonius Kappa CCD diffractometer using graphite-monochromated MoKα radiation [λ = 0.71073 Å] at 173(2) K. Crystal data and data-collection parameters are listed in Table 5.25.

Structure determination and refinement

As for PPDMB, the structure was solved using published co-ordinates for the non-hydrogen cyclodextrin atoms [excluding the O(6), C(7), and C(8) atoms of each methylglucose residue] of the isomorphous DIMEB-2-naphthoic acid trihydrate complex.[12-13] Initially isotropic refinement of this skeletal structure was performed using SHELX-97[6] and the difference Fourier map showed the positions of all the remaining non-hydrogen atoms.

Table 5.25 Details of the data collection and refinement parameters for the BPDMB structure

Empirical formula	$C_{56}H_{98}O_{35}{\cdot}C_{11}H_{14}O_3{\cdot}3.7H_2O$
Formula weight	1592.2
Crystal system	Orthorhombic
Space group	$P2_12_12_1$
a / Å	15.3735 (2)
b / Å	18.8114 (2)
c / Å	28.3989 (4)
α / °	90
β / °	90
γ / °	90
Volume / Å^3	8213.0 (2)
Z	4
Density$_{calc}$ / g cm^{-3}	1.288
μ (MoKα) / mm^{-1}	0.107
F(000)	3420
Temperature of data collection / K	173 (2)
Crystal size / mm^3	0.60 x 0.50 x 0.40
Range scanned θ / °	$2 \leq \theta \leq 21$
Index ranges	h: -13,15 k: -18,12 l: -28, 25
ϕ scan angle / °	1.0
ϕ scan range, frames	181.0°, 181
ω scan angle / °	1.0
ω scan ranges, frames	52.0°, 52 and 68.0°, 68
Dx / mm	58.3
Total no. of reflections collected	19801
No. of independent reflections	8750
No. of reflections with $I > 2\sigma(I)$	7503
No. of parameters	845
R_{int}	0.0295
S	1.028
R_1 (for 4903 reflections)	0.1007
Reflections omitted	(0 1 3); (0 6 0); (1 0 2); (1 1 1); (-1 1 1); (2 0 0); (2 2 0); (2 4 0); (4 0 2); (8 0 0)
wR_2	0.2668
Weighting scheme	a = 0.1736 b = 24.0473
$(\Delta / \sigma)_{mean}$	< 0.002
$\Delta\rho$ excursions / e.Å^{-3}	0.57 and -0.95

Further refinement indicated that the atom C(8) on O(6G5) was disordered over two positions. Two alternative positions were found for each disordered atom. The atom O(6) on each of C(6G3) and C(6G4) was also disordered over two positions labelled A and B. The C(8) atom on these disordered O(6) atoms was located in one position. The C(8) atom was therefore duplicated and the position was kept the same using an EXYZ instruction. For a given pair of atoms, a fixed U_{iso} of 0.08 Å^2 [the mean of U_{iso} for the chemically equivalent ordered atoms] was assigned and site-occupancy factors of x and 1-x were assigned, with x variable. The final site-occupancies from the major positions [A] refined to 0.55 for C(85A), 0.64 for O(63A) and C(83A) and 0.69 for O(64A) and C(84A). Distance constraints were placed on the bonds involving these disordered atoms. Anisotropic displacement parameters were assigned to all the non-hydrogen atoms on the host, except the disordered atoms and C(7G2), O(2G3), C(6G3), C(7G3), C(6G4) and O(6G5) which were refined isotropically. Hydrogen atoms were calculated for the C atoms of the host using a riding model with U_{eq}(H) equal to 1.2 U_{eq} or 1.5 U_{eq} of the parent primary and secondary or tertiary C atoms respectively.

After many successive refinements, six positions were located for the water molecules. Each water molecule was refined isotropically and assigned a fixed isotropic temperature factor of 0.10 Å^2 while the site-occupancies were allowed to vary. The s.o.f.'s refined to 0.39, 0.31, 0.43, 0.67, 0.58, 0.72, and 0.61 for O(1WA), O(1WB), O(2W), O(3W), O(4W), O(5W) and O(6W) respectively. The site-occupancies accounted for 3.7 water molecules per asymmetric unit, which is equivalent to the expected number of water molecules observed from the TGA results. The hydrogen atoms of the water molecules were not located.

Refinement continued with the placement of the non-hydrogen atoms of the guest. The guest phenyl ring was refined as a rigid hexagon. The hydrogen atoms attached to the carbon atoms of the guest were also inserted at idealised positions and assigned a common isotropic temperature factor. The hydrogen atom of the hydroxyl group was placed using the AFIX 83 instruction. A single isotropic temperature factor was used for the non-hydrogen atoms of the guest and this refined to a final value of 0.14 Å^2. Due to the abnormally long bond distances found in the guest molecule, distance constraints were placed on certain bonds, namely O(1)–C(2) 1.351 Å; C(5)–C(8) 1.471 Å; C(8)–O(9) 1.207 Å; C(8)–O(10) 1.334 Å; O(10)–C(11) 1.448 Å, C(11)–C(12) 1.490 Å, C(12)–C(13) 1.490 Å, C(13)–C(14) 1.490 Å [all with σ = 0.005 Å]. The values chosen were taken from Lin.[11] Due to abnormally large bond angles, distance constraints were placed on the alkyl chain atoms to maintain the angles C(11)–C(12)–C(13) and C(12)–C(13)–C(14) close to the tetrahedral values.

Geometrical analysis of the BPDMB structure

The BPDMB asymmetric unit consists of a single DIMEB molecule, 3.7 water molecules and its associated guest. The seven glucosidic residues have been assigned the Gn notation and the structure and numbering scheme of the BPDMB complex and water molecules are shown in Figure 5.29. The geometrical data for the DIMEB molecule are listed in Tables 5.26 and 5.27 [e.s.d.s are in the range 0.008-0.011 Å for distances and 0.2-0.7° for angles].

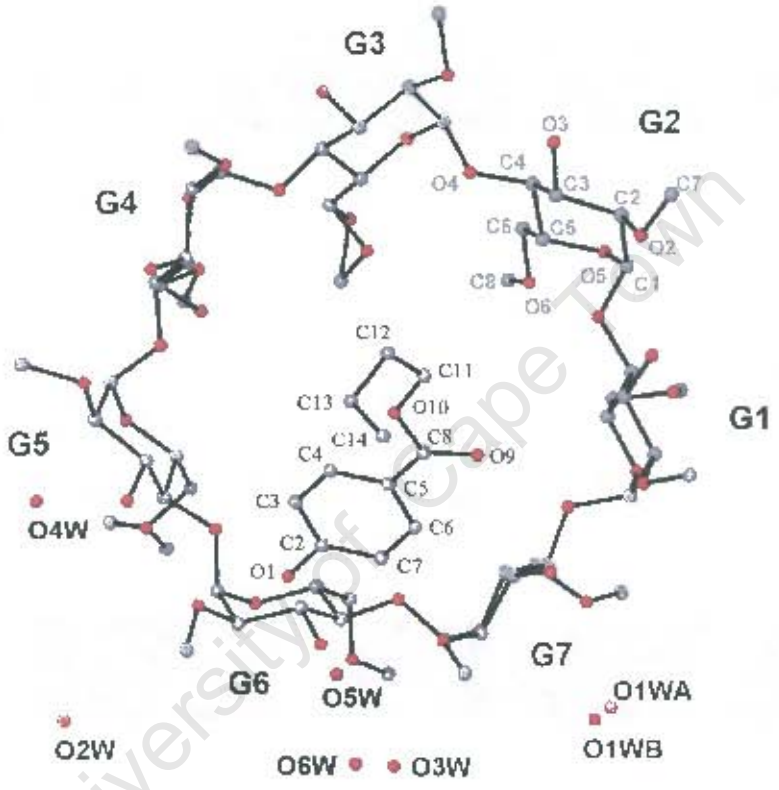

Figure 5.29 Macrocyclic structure and numbering scheme of glucose residues, water oxygen atoms and guest molecule, with the hydrogen atoms excluded. The host is viewed from the secondary face.

All glucose residues have the $^4C_1$ chair conformation with the O(6) side turning to the inside of the macrocycle. The C(6)–O(6) bonds of the G1, G5, G6 and G7 residues are in the (-) *gauche* conformation to the C(4)–C(5) and O(5)–C(5) bonds. The C(6)–O(6) bond of the G2 residue points towards the cavity in the (+) *gauche* conformation. The O(6) atoms of the G3 and G4 residues are disordered over two sites. Both the major and minor positions of the atoms of the G4 residue are in the (+) *gauche* conformation. The major position of the G3 residue assumes the (+) *gauche* conformation while the minor position assumes the (-) *gauche* conformation. All the O(6)–C(8) bonds, including the disordered CH_3 on O(6) of the G5 residue are *trans* with respect to the C(5)–C(6) bonds. All the O(2)–C(7) bonds are directed away from the cavity.

The geometric parameters of the O(4) heptagon of the BPDMB structure are listed in Table 5.26. These include the radii, the O(4)•••O(4') distances, the O(4)•••O(4')•••O(4'') angles, the O(4)•••O(4')•••O(4'')•••O(4''') torsion angles and the deviations of each of the O(4) atoms from the mean O(4) plane. Table 5.27 lists the other important features of the macrocyclic structure such as the intersaccharidic bond angle (φ), the O(2)•••O(3') distance and the tilt angles [τ_1 and τ_2]. These parameters are defined in Chapter 1.

Table 5.26 Geometrical parameters of the O(4) heptagon for the BPDMB structure

Glucose unit	Radii (Å)	O(4)•••O(4') (Å)	O(4) angle (°)	Torsion angle (°)	Deviation (Å)
G1	5.03 (1)	4.41	130	6.2 (3)	-0.02
G2	5.12 (1)	4.34	125	-10.6 (4)	-0.21
G3	4.91 (1)	4.41	133	3.4 (4)	0.12
G4	5.11 (1)	4.33	126	4.4 (3)	0.09
G5	5.08 (1)	4.44	128	-1.0 (3)	-0.10
G6	4.99 (1)	4.35	130	-6.1 (3)	-0.05
G7	5.07 (1)	4.38	127	3.7 (3)	0.15
Average	**5.04**	**4.38**	**128**	**5.1**	**0.11**

Table 5.27 ω, O(2)•••O(3') distance,τ for the BPDMB structure

Glucose unit	φ (°)	O(2)•••O(3') (Å)	τ_1 (°)	τ_2 (°)
G1	118	2.91	7.9 (2)	10.9 (3)
G2	119	2.80	15.1 (2)	17.3 (3)
G3	118	2.87	16.4 (2)	20.0 (3)
G4	120	2.87	5.3 (2)	2.4 (4)
G5	116	2.95	14.9 (1)	17.5 (4)
G6	118	2.86	16.1 (2)	19.5 (3)
G7	119	2.78	6.3 (2)	10.3 (3)
Average	**118**	**2.86**	**11.7**	**14.0**

The average value of 5.04 Å for the radius of the heptagon is in good agreement with the radius of β-CD [5.04 Å].[8,5] The distances between the O(2) and O(3) atoms of the adjacent residues indicate that the O(3) hydroxyl group is hydrogen bonded to the O(2) atom of the adjacent residue. The values calculated for these parameters compare favourably with those of the DIMEB-2-naphthoic acid trihydrate complex[12-13] and PPDMB, previously described on page 178.

Guest geometry and interactions for the BPDMB structure

The conformation of the butyl paraben guest may be defined by five torsion angles. The torsion angles listed below will be used to describe the rotation around each of the corresponding bonds [Figure 5.30]. The close contact distances for the relevant interactions between the host and guest molecule are listed in Table 5.28.

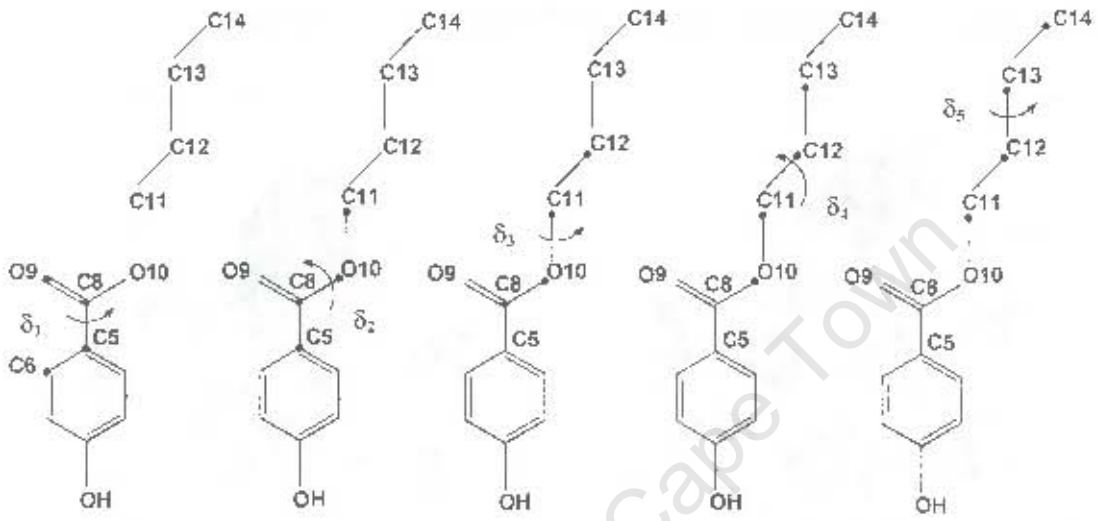

δ_1 C(6)–C(5)–C(8)–O(9)	➡	C(5)–C(8)
δ_2 C(5)–C(8)–O(10)–C(11)	➡	C(8)–O(10)
δ_3 C(8)–O(10)–C(11)–C(12)	➡	O(10)–C(11)
δ_4 O(10)–C(11)–C(12)–C(13)	➡	C(11)–C(12)
δ_5 C(11)–C(12)–C(13)–C(14)	➡	C(12)–C(13)

BP in complex:
δ_1 = +18 (1)
δ_2 = -176 (1)
δ_3 = -153 (1)
δ_4 = +45 (1)
δ_5 = +85 (1)

Figure 5.30 Torsion angles δ_1, δ_2, δ_3, δ_4 and δ_5 of the butyl paraben

Table 5.28 Close contact distances for the BPDMB structure

Interaction	Distance (A)
H(3) ••• H(851)	2.21
H(14A) ••• H(561)	2.33
O(1) ••• C(7G7)'	3.10 (2)
C(4) ••• H(742)''	2.81 (1)
H(12A) ••• H(845)'''	2.33

' Related by symmetry operation: -1+x, y, z
'' Related by symmetry operation: -1/2+x, 1 1/2-y, 1-z
''' Related by symmetry operation: 1/2+x, 1 1/2-y, 1-z

Figures 5.31 and 5.32 show CPK diagrams of the BPDMB structure. The phenolic hydroxyl group and the aromatic ring extend well beyond the primary rim of the host while the alkyl moiety occupies the centre of the host cavity. The orientation of the guest can be ascribed to the hydrophilic and hydrophobic nature of the hydroxyl group and alkyl moiety respectively. The phenyl ring of the guest forms an angle of 53.0 (2)° with the mean O(4) plane. This mode of guest inclusion is analogous to that found for propyl paraben in the isomorphous complex PPDMB described earlier.

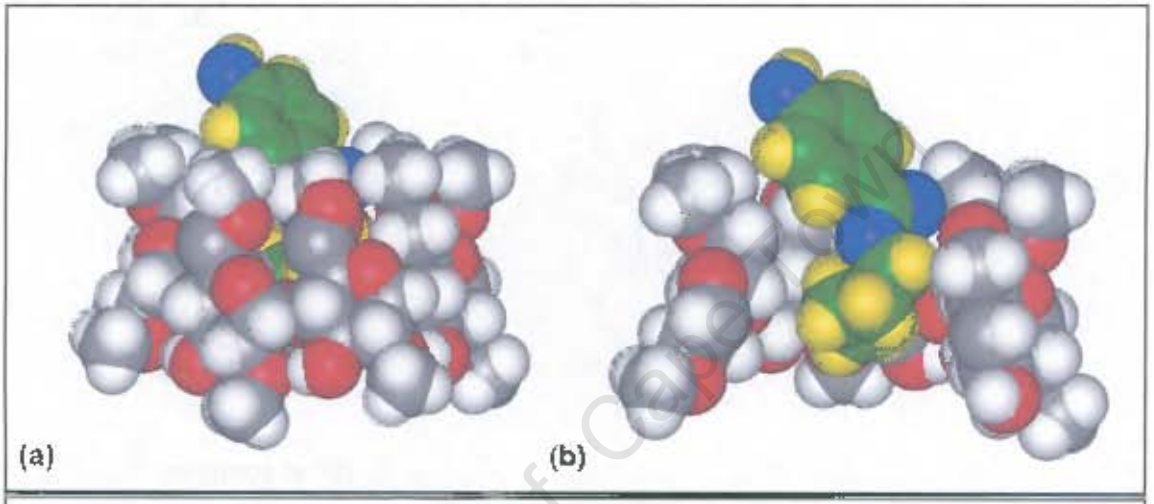

Figure 5.31 Space-filling diagram of the BPDMB structure (a) side view (b) sectioned view of the same orientation

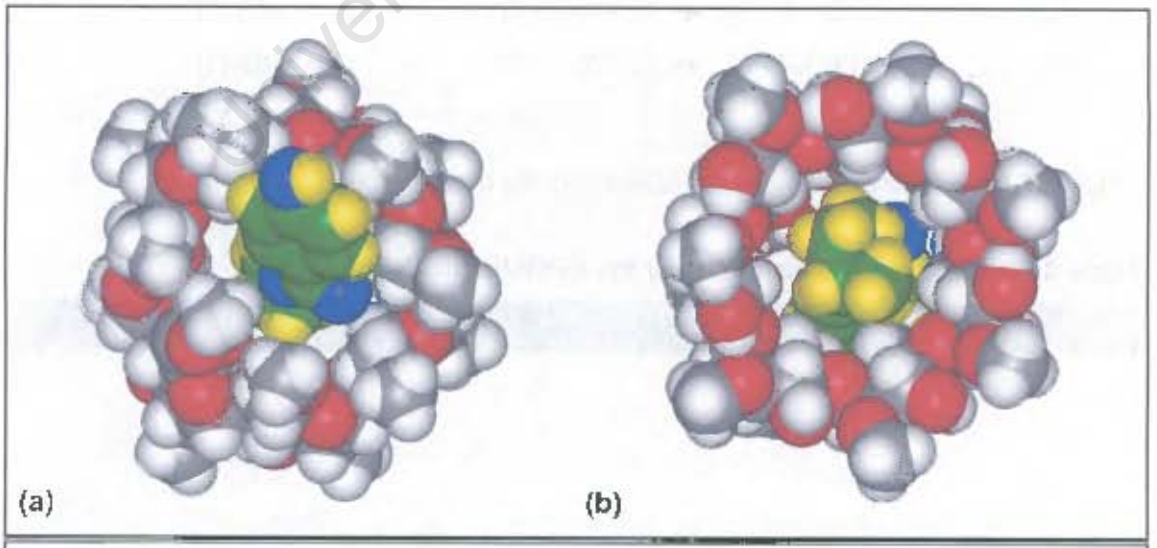

Figure 5.32 Space-filling diagram of the BPDMB structure (a) viewed from the primary rim (b) viewed from the secondary rim

Hydrogen bonding interactions of the BPDMB structure

Host interactions

Owing to the seven intramolecular O(2)•••O(3') hydrogen bonds which are in the range 2.78-2.95 Å, with a mean of 2.86 Å [Table 5.27], the CD structure has a highly symmetrical shape. The conformation of the DIMEB molecule is further stabilised by nine intramolecular C–H•••O hydrogen bonds [Table 5.29]. These encompass four C(6)–H•••O(5') hydrogen bonds, four C(7)–H•••O(3) hydrogen bonds and a C(8)–H•••O(6') hydrogen bond. The crystal structure is stabilised by four intermolecular C–H•••O hydrogen bonds. These comprise one C(2)–H•••O(3) hydrogen bond and three C(8)–H•••O(3) hydrogen bonds to adjacent glucose units. All the C•••O distances are in the range 3.0-3.4 Å.

Table 5.29 C–H•••O hydrogen bonds in the BPDMB structure*

				Distance (Å)		Angle (°)
C	H	O	C–H	H•••O	C•••O	C–H•••O
Intramolecular hydrogen bonds						
C(6G1)	H(612)	O(5G2)	0.99	2.59	3.36 (1)	135.1 (6)
C(6G5)	H(652)	O(5G6)	0.99	2.63	3.35 (1)	130.4 (7)
C(6G6)	H(662)	O(5G7)	0.99	2.78	3.43 (1)	123.8 (6)
C(6G7)	H(672)	O(5G1)	0.99	2.64	3.30 (1)	123.9 (7)
C(7G1)	H(713)	O(3G1)	0.98	2.53	3.15 (2)	121.7 (8)
C(7G4)	H(743)	O(3G4)	0.98	2.41	3.03 (2)	121.0 (8)
C(7G6)	H(761)	O(3G6)	0.98	2.41	3.08 (2)	125.2 (9)
C(7G7)	H(773)	O(3G7)	0.98	2.63	3.17 (1)	115.3 (8)
C(83B)	H(836)	O(64A)	0.98	2.51	3.36 (2)	144.5 (7)
Intermolecular hydrogen bonds						
C(2G4)	H(241)^{i}	O(3G7)^{i}	1.00	2.70	3.36 (1)	123.5 (6)
C(8G2)	H(821)^{i}	O(3G4)^{i}	0.98	2.82	3.37 (2)	116.4 (8)
C(83B)	H(835)^{i}	O(3G4)^{i}	0.99	2.56	3.37 (1)	140.0 (7)
C(8G7)	H(871)^{ii}	O(3G7)^{ii}	0.99	2.69	3.31 (2)	121.4 (9)

^{i} Related by symmetry operation: $-^{1}/_{2}+x$, $1^{1}/_{2}-y$, 1-z
^{ii} Related by symmetry operation: $-^{1}/_{2}+x$, $^{1}/_{2}-y$, 1-z
* Hydrogen bonding parameters based on idealised hydrogen atom positions.

Guest interactions

The hydroxyl oxygen atom of the guest is hydrogen bonded to one water oxygen atom O(5W) and to two of the host C(7) carbon atoms. The C(7G7)•••O(1)•••C(7G2) angle is 152°. In addition, the O(5W) water atom is hydrogen bonded to C(7) of the guest. The carbonyl oxygen is in hydrogen bonding contact with O(1WA) and is hydrogen bonded to a C(6) host carbon atom. The carbon atom C(11) of the guest forms a weak hydrogen bond to one of the disordered oxygen atoms on C(6G3). Hydrogen bonds and hydrogen bonding distances are listed in Table 5.30 and a simplified hydrogen bonding scheme is illustrated in Figure 5.33.

Table 5.30 C–H•••O hydrogen bonds and hydrogen bonding distances involving the guest in the BPDMB structure*

				Distance (Å)		Angle (°)
Donar (D)	H	Acceptor (A)	D–H	H•••A	D•••A	D–H•••A
O(1)	H(1)	O(5W)	0.84	1.87	2.67 (2)	157.3 (9)
C(7)	H(7)	O(5W)	0.95	2.83	3.46 (2)	124.7 (6)
O(9)		O(1W)^{iii}			2.85 (2)	
C(11)	H(11A)	O(63A)	0.99	2.88	3.50 (1)	121.1 (6)
C(7G2)	H(723)	O(1)^{i}	0.98	2.63	3.16 (2)	114 (1)
C(7G7)	H(772)	O(1)^{ii}	0.98	2.65	3.10 (2)	108.7 (7)
C(6G7)	H(672)	O(9)	0.99	2.83	3.41 (2)	118.2 (8)

^{i} Related by symmetry operation: $^{1}/_{2}$-x, 1-y, -$^{1}/_{2}$+z
^{ii} Related by symmetry operation: 1+x, y, z
^{iii} Related by symmetry operation -$^{1}/_{2}$+x, $^{1}/_{2}$-y, 1-z
* Hydrogen bonding parameters based on idealised hydrogen atom positions.

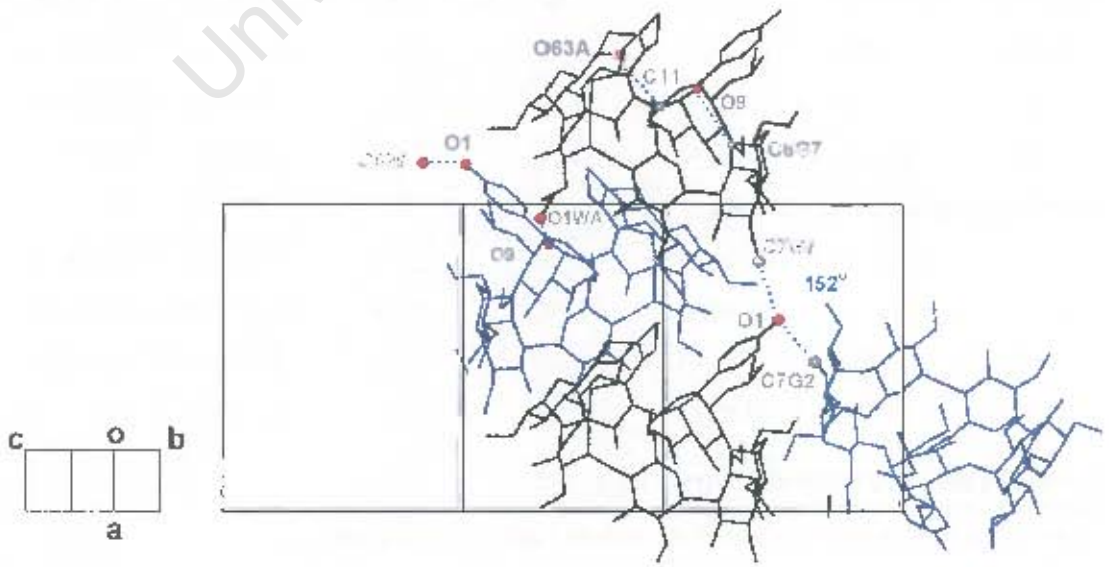

Figure 5.33 The hydrogen bond scheme in the BPDMB complex

Water interactions

Thermogravimetric analysis gave a weight loss which corresponds to 3.7 water molecules per 1:1 complex unit, and these were all accounted for in the crystallographic analysis. All the water molecules are located at the periphery of the cyclodextrin molecule, filling a small intermolecular space between complex units. C–H•••O hydrogen bonds between the host and these water molecules are listed in Table 5.31 and hydrogen bonding distances between the host and these water molecules are listed in Table 5.32. The hydrogen bonding scheme is illustrated in Figure 5.34.

All the water molecules are within hydrogen bonding distance of a host oxygen atom, except for the disordered O(1W). As seen in Table 5.30, the O(1WA) water molecule with a s.o.f. of 0.39, is involved in hydrogen bonding to the guest. The O(1WB) counterpart, with a s.o.f. of 0.31, is within hydrogen bonding distance of O(6G7). This O(1WB) atom is also in close proximity to the O(2W) water molecule [at a distance of 1.89 (4) Å by the symmetry operation 1-x, $-^1/_2$+y, $1^1/_2$-z], indicating that these two atoms are not present concurrently. The s.o.f. of the O(2W) water molecule is 0.43.

The O(3W) and O(4W) water molecules are within hydrogen bonding distance of O(6G6) and O(6G5) respectively. This places these water molecules in a close contact distance of 3.18 (2) Å to C(8G6) and of 3.21 (3) Å to C(85A) respectively. In addition the O(4W) water molecule is at a distance of 3.22 (2) Å to a symmetry related C(7G2) atom [$-^1/_2$+x,$1^1/_2$-y,1-z].

Table 5.31 C–H•••O hydrogen bonds between the host and the water molecules*

			Distance (Å)			Angle (°)
Donor(D)	H	Acceptor(A)	D–H	H•••A	D•••A	D–H•••A
O(3G5)	H(352)	O(6W)'	0.84	2.39	2.83 (2)	113.0 (7)
C(4G6)	H(461)	O(6W)	1.00	2.68	3.46 (2)	138.6 (6)

' Related by symmetry operation: 1-x, $^1/_2$+y, $1^1/_2$-z
* Hydrogen bonding parameters based on idealised hydrogen atom positions.

Table 5.32 Hydrogen bonding distances involving the water molecules

Interaction	Distance (Å)	Symmetry operator for the host oxygen atoms
O(1WB) ••• O(6G7)	3.04 (3)	x, y, z
O(2W) ••• O(5G7)	2.95 (2)	1-x, $^1/_2$+y, 1$^1/_2$-z
O(3W) ••• O(6G6)	2.89 (2)	x, y, z
O(4W) ••• O(3G2)	2.91 (2)	-$^1/_2$+x, 1$^1/_2$-y, 1-z
O(4W) ••• O(6G5)	2.61 (2)	x, y, z
O(5W) ••• O(6G1)	2.76 (1)	-$^1/_2$+x, $^1/_2$-y, 1-z
O(6W) ••• O(3G5)	2.82 (2)	1-x, -$^1/_2$+y, 1$^1/_2$-z
O(1WA) ••• O(2W)	3.00 (3)	1-x, -$^1/_2$+y, 1$^1/_2$-z
O(3W) ••• O(6W)	2.70 (2)	x, y, z
O(4W) ••• O(5W)	2.50 (2)	-x, $^1/_2$+y, 1$^1/_2$-z

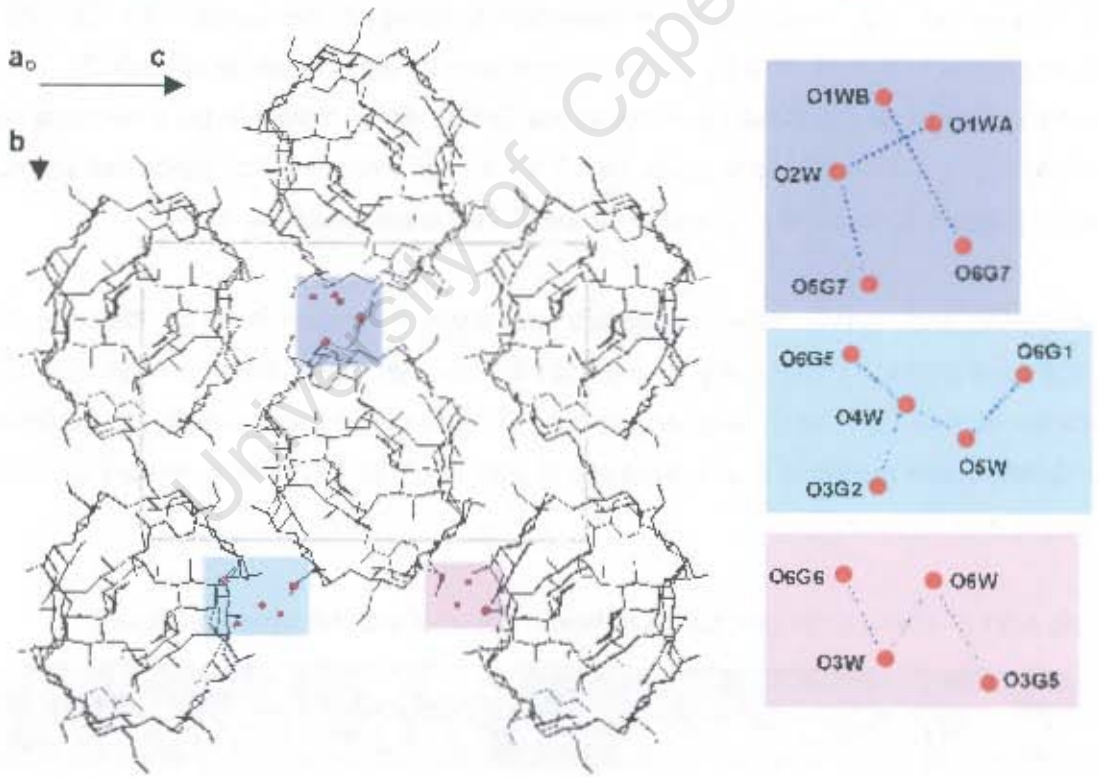

Figure 5.34 A schematic representation of the water molecules that connect adjacent host units

Crystal packing of the BPDMB structure

Figures 5.35 and 5.36 are extended stereo packing diagrams of the BPDMB structure showing projections as viewed down the *a*- and *c*-axes and illustrate the packing features in the crystal. The BPDMB molecules are stacked along the *a*-axis in a zigzag type pattern. An inclusion of the primary O(6)–CH_3 group on the G3 and G4 residues into the secondary side of the BPDMB molecule, which is related by the two-fold screw axis along the *a*-axis, occurs. The O(6) side of the cavity is open to the intermolecular space, where the guest is located.

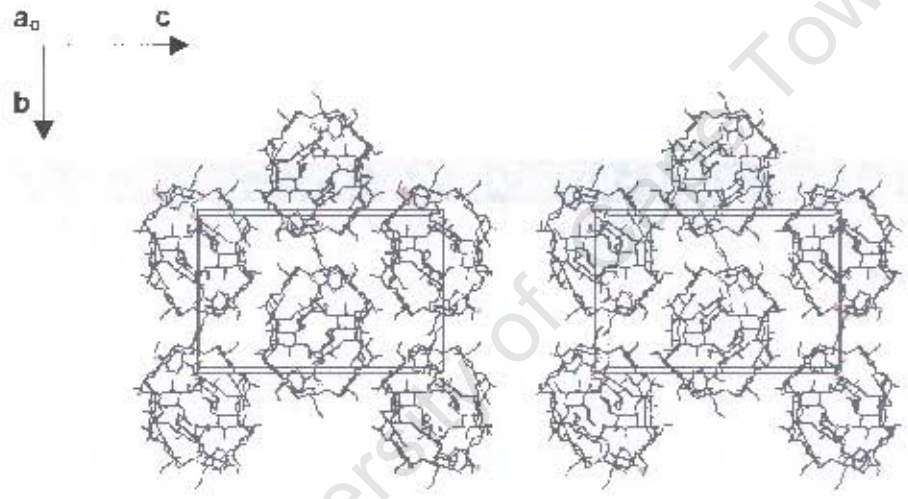

Figure 5.35 Stereo packing diagram of the BPDMB structure [*a*-axis projection]

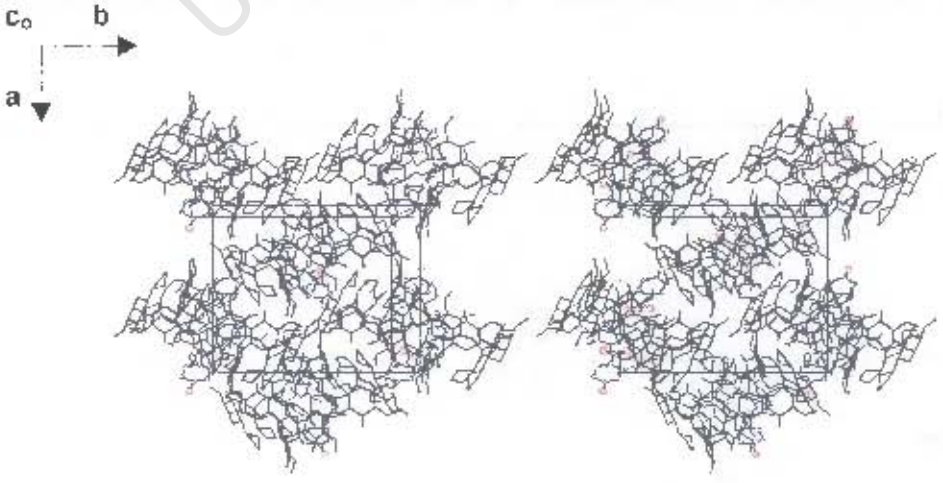

Figure 5.36 Stereo packing diagram of the BPDMB structure [*c*-axis projection]

DISCUSSION

Heptakis-(2,6-di-*O*-methyl)-β-cyclodextrin is attractive for the formation of inclusion complexes owing to its good solubility in water and organic solvents.[14] However only a few crystal structures have been reported thus far. The CSD[15] houses fifteen DIMEB structures, which include an anhydrous form, three hydrated forms and eleven inclusion complexes. DIMEB and its complexes crystallise in both the monoclinic space group $P2_1$ as well as the orthorhombic space group $P2_12_12_1$ and various packing modes are observed [Table 5.33]. The guest molecules can be either included in the cyclodextrin cavity, as with 2-naphthoic acid,[12-13] and adamantanol[16] or can be located in the interstitial sites while the cavity is occupied by water molecules, as with *p*-iodophenol and *p*-nitrophenol.[17-18] In some instances such as the carmofur complex, the guest being disordered over two sites, is found to be both included in the cavity [when in the major position] and located in the intermolecular space [when in the minor position].[19]

Table 5.33 DIMEB structures from the CSD

Guest	H:G:W	a (Å)	b (Å)	c (Å)	α (°)	β (°)	γ (°)	Refcode	Ref.
Space group – $P2_1$									
Herringbone type									
hydrate	1 : 0 : 2	10.639	15.242	23.324	101.80	90	90	CFQCUW	20
acetic acid	2 : 1 : 3	10.613	15.165	23.188	102.02	90	90	NITSIS	21
Zigzag type									
carmofur	1 : 1 : 3	15.697	15.947	18.533	90	90	106.64	SAJPCI	19
Channel type									
isobornylacrylate	1 : 1 : 4	9.668	15.603	29.036	90	90	99.39	QAZYIZ	22
Space group – $P2_12_12_1$									
Herringbone type									
m-cresol acetate	1 : 1 : 0	11.080	14.932	44.906	90	90	90	COFLOY	23,24
n-butylacrylate	1 : 1 : 1	10.776	15.108	49.029	90	90	90	QAZYEV	22
Zigzag type									
hydrate	1 : 0 . 15	14.163	20.828	29.261	90	90	90	BOYFOK	24-27
prostaglandin	1 : 1 : 0	14.163	23.096	27.641	90	90	90	BOYGAX	25
p-nitrophenol	1 : 1 : 2-3	14.779	18.965	28.741	90	90	90	DEZMIC	17-19
p-iodophenol	1 : 1 : 2-3	14.796	18.853	28.989	90	90	90	DEZMOK	17-18
hydrate	1 : 0 : 0.8	13.328	17.410	29.760	90	90	90	QIYKEC	24-26
2-naphthoic acid	1 : 1 : 3	15.463	18.922	27.852	90	90	90	WAGHAN	12-13
heptasaccharide	1 : 0 : 0	13.871	17.424	29.610	90	90	90	ZULQAY	28
Channel type									
adamantanol	1 : 1 : 12	24.210	19.333	18.266	90	90	90	BEFJOI	16
Layer type									
bislactam	1 : 1 : 1	14.989	23.147	31.254	90	90	90	YAPSEN	29-30

In the present study the structures of the inclusion complexes MPDBM, EPDMB, PPDMB and BPDMB have been solved and analysed. Each inclusion complex crystallises in the space group $P2_12_12_1$ with Z = 4 and a host to guest ratio of 1:1. Comparison of the morphology and cell dimensions of the four structures shows that there are two isostructural pairs *viz.*, MPDMB and EPDMB as one isostructural pair [hereon in denoted $\mathbf{A_{iso}}$] and PPDMB and BPDMB as the other [hereon in denoted $\mathbf{B_{iso}}$]. This could be confirmed by comparison of the single crystal XRD traces, Figure 5.37. The term "isostructural" signifies that the two complexes of one isostructural pair will exhibit a similar internal arrangement of molecules, have a comparable hydrogen bonding network and will have an analogous crystal packing motif.[31-32]

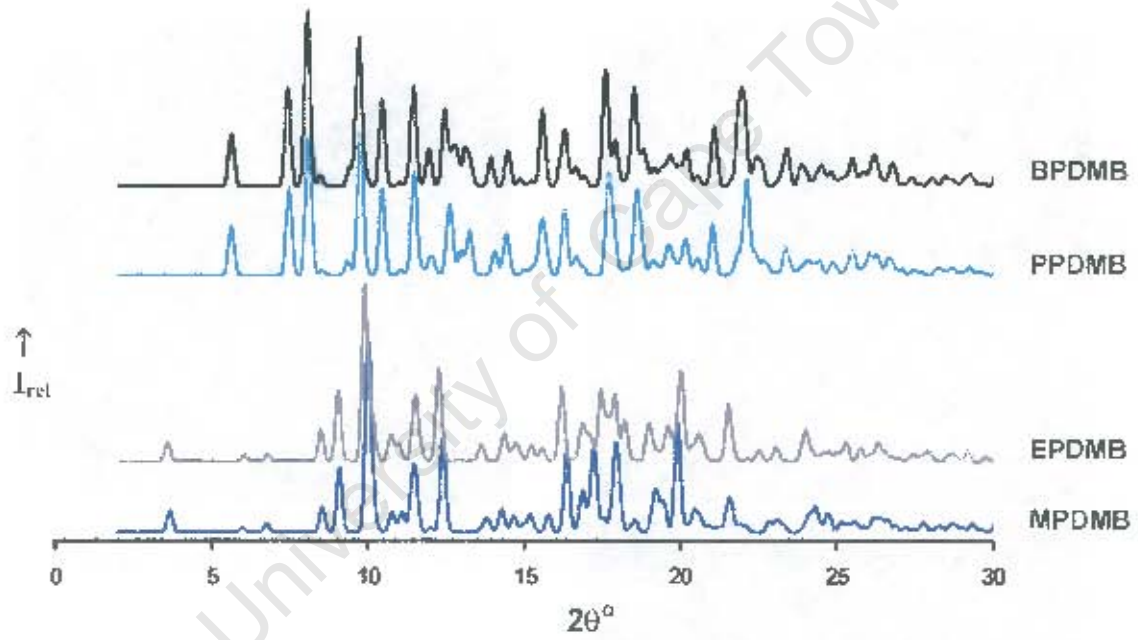

Figure 5.37 Calculated XRD traces of the MPDMB, EPDMB, PPDMB and BPDMB complexes

Conformation of the DIMEB host molecule

The average DIMEB conformational parameters of the four inclusion complexes appear to be similar and except for the orientation of the methyl groups, the macrocyclic conformation does not differ significantly from that of the β-CD observed in Chapter 4. The DIMEB molecules adopt a rather round and symmetrical structure as the variations in the radii of the heptagon and the deviations of the O(4) atoms from the plane of the macrocycle are small. The average bond distances and angles are in the usual range for the glucopyranose residues.

All the glucose units are orientated *syn*, and thus the O(2) and O(3) atoms of adjacent glucose units form seven intramolecular O(2)•••O(3') hydrogen bonds which contribute to the conformational stability of the CD macrocycle. Additionally a series of intramolecular C–H•••O hydrogen bonds maintains the conformation of the DIMEB molecule. The cohesion of the structure is ensured by intermolecular C•••O contacts involving the O(2), O(3) and O(6) groups of the macrocycle.

Figure 5.38 illustrates the similar internal arrangement of the host for both the isostructural pairs. Additionally it shows how the $\mathbf{A}_{iso}$ complexes differ slightly in their spatial arrangement of host atoms from those of the $\mathbf{B}_{iso}$ complexes and demonstrates the slight adjustment in the shape of the host as the alkyl chain length increases.

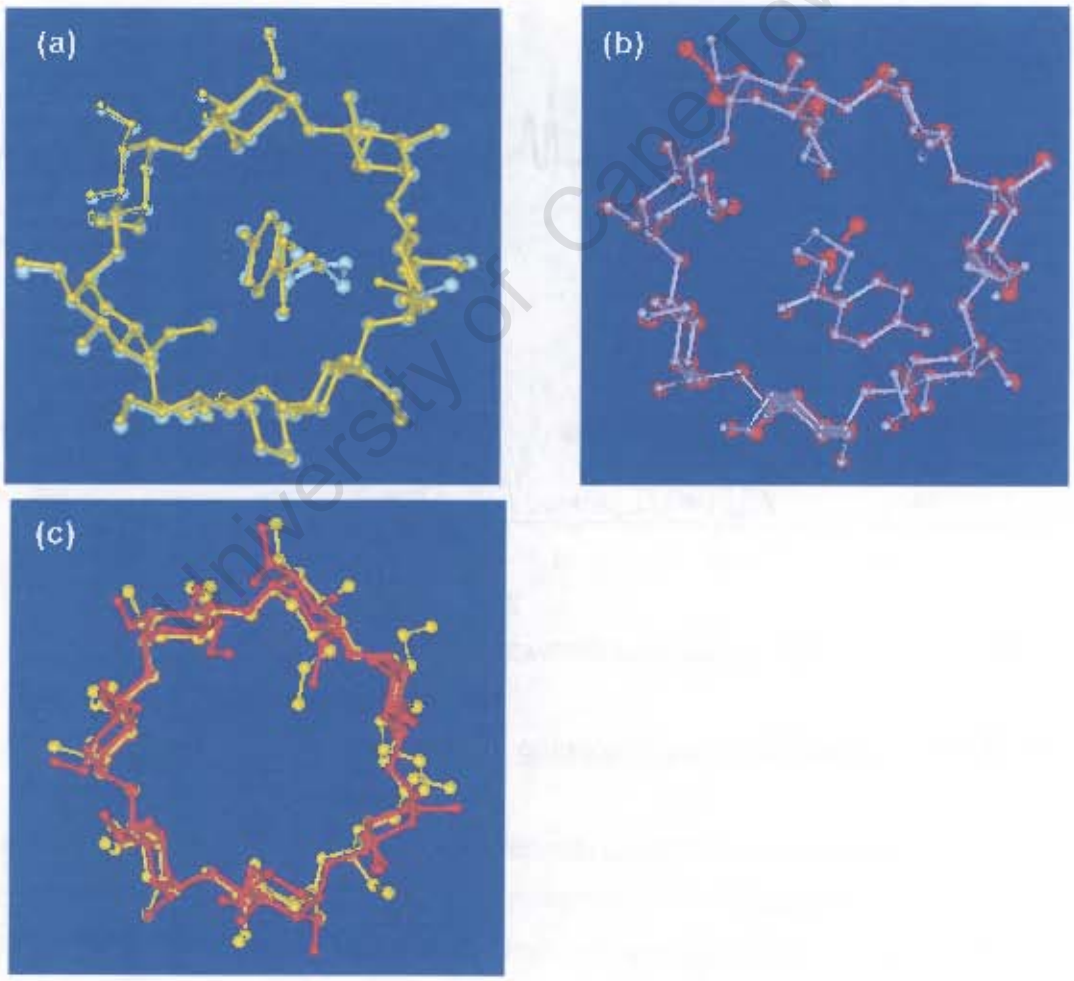

Figure 5.38 Conformation of the DIMEB inclusion complexes **(a)** MPDMB [yellow] and EPDMB [blue]; **(b)** PPDMB [red] and BPDMB [purple] **(c)** $\mathbf{A}_{iso}$ [yellow] and $\mathbf{B}_{iso}$ [red]

Paraben guest molecules

Many factors determine the mode of inclusion of a particular guest within the CD cavity. These include geometric compatibility, hydrophobicity and polarity. The geometry of the CD is such that the O(2), O(3) side is wider than the O(6) side as the CD glucose residues incline with the O(6) side turned to the inside of the macrocycle. The volume of the O(6) side is further reduced by the rotation of the O(6)–CH_3 groups inwards [two in the A_{ISO} structures and three in the B_{ISO} structures]. To reduce the van der Waals contacts the larger substituent of the guest would be located at the secondary rim. However in some cases the difference in relative hydrophobicity can be a determining factor in the orientation of the guest molecule in the CD cavity.

Lichtenthaler *et al* [33-34] have shown in their computer aided visualisation of the molecular lipophilicity patterns that the primary rim of the DIMEB molecule is relatively hydrophilic and its opposite, secondary rim is relatively hydrophobic.

Another factor to consider in the extent of complexation is the polarity of the guest molecule. If a polar group is present the dipole-dipole alignment and the need for solvation of the polar group may diminish the importance of the hydrophobic attractions for orientation.

Figure 5.38 (a) and (b) illustrate how the aromatic ring of the guest is located in almost identical positions in the A_{ISO} and B_{ISO} structures respectively, while Figure 5.39 illustrates how the orientation and mode of inclusion of the guests are significantly different between the A_{ISO} and B_{ISO} structures. As the guests of the B_{ISO} structures protrude well out of the cavity, the number of close contacts was found to be fewer in these complexes.

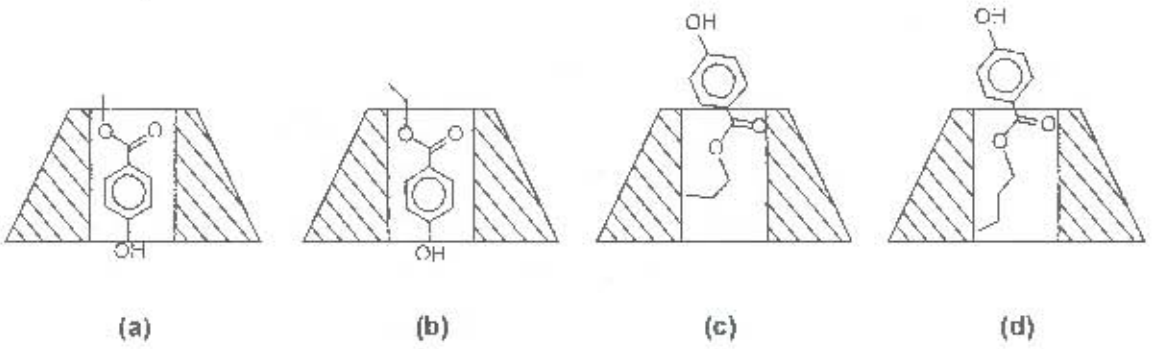

Figure 5.39 Orientation of the guest in the DIMEB cavity (a) MPDMB, (b) EPDMB, (c) PPDMB and (b) BPDMB

In the A_{iso} structures, the methyl- and ethyl paraben molecules are positioned approximately at the centre of the macrocycle with the guest almost perpendicular to the mean O(4) plane. The ester moiety is located at the narrower primary rim and in both structures is found to be disordered over two positions. This leads to a number of short contacts between the guest molecules and the host atoms but these are minimised by the "vertical" position of the guest within the cavity. This orientation allows more efficient inclusion of the guest and closer packing of the host molecules.

In the B_{iso} structures the phenolic hydroxyl group and the aromatic ring extend well beyond the primary rim of the host. The phenyl ring of the guest forms an angle of 53-56° relative to the macrocyclic ring axes. This allows the hydrophobic alkyl chain to be located at the hydrophobic inner surface of the CD cavity while the relatively more hydrophilic ester and polar hydroxyl group are positioned at the primary rim and in the polar environment respectively. This orientation corresponds to Lichtenthaler's *et al* [33-34] study in that the hydrophilic and hydrophobic portions of the guest align with the hydrophilic and hydrophobic portions of the host respectively.

Water molecules

Hydrogen bonds involving water molecules mediate many of the interactions between the host and guest. The hydrogen bonding network forms a spiral running down the channels. In this manner the hosts and guests are re-linked to each other and hence crystallinity is lost on dehydration. The four complexes have certain similarities: (i) all the water molecules are situated on the periphery of the CD molecules, filling the intermolecular space between complex units and (ii) the guest hydroxyl oxygen atom is hydrogen bonded to a water molecule. Since the water molecules act as a "filler" in the CD structure, this may be an indication that the guest might play a critical role in the determination of the packing arrangement of the complexes. The main difference, besides the spatial arrangement of the water molecules, is that the A_{iso} complexes have two water molecules that are not hydrogen bonded to the host, while all the water molecules are hydrogen bonded to the host in the B_{iso} complexes.

REFERENCES

1) F. Giordano, R. Bettini, C. Donini, A. Gazzaniga, M. R. Caira, G. G. Z. Zhang, D. J. W. Grant, *J. Pharm. Sci.*, **1999**, 88, 11, 1210.
2) Paratone N oil (Exxon Chemical Co., TX, USA).
3) E. Egert, *Acta Crystallogr.*, **1983**, A39, 936.
4) E. Egert, G. M. Sheldrick, *Acta Crystallogr.*, **1985**, A41, 262.
5) E. Mvula, *MSc. Thesis, Preparation and Solid State Properties of Cyclodextrin Complexes of Selected Drug Molecules*, University of Cape Town, South Africa. **1999**.
6) G. M. Sheldrick, *SHELXL-97, Program for the Refinement of Crystal Structures*, University of Göttingen, Germany. **1997**.
7) X. Lin, *J. Struct. Chem.*, **1983**, 2, 213.
8) K. Lindner, W. Saenger, *Carbohydr. Res.*, **1982**, 99, 103.
9) K. Harata, *Bull. Chem. Soc. Jpn.*, **1982**, 55, 2315.
10) T. Steiner, W. Saenger, *J. Am. Chem. Soc.*, **1992**, 114, 10146.
11) X. Lin, *J. Struct. Chem.*, **1986**, 5, 281.
12) K. Harata, *J. Chem. Soc., Chem. Commun.*, **1993**, 546.
13) K. Harata, *J. Chem. Soc., Chem. Commun.*, **1999**, 191.
14) K. Harata, *Inclusion Compounds*, (Vol. 5). J. L. Atwood, J. E. D. Davies, D. D. MacNicol (eds.), Oxford University Press, **1991**, p. 312-344.
15) *Cambridge Structural Database and Cambridge Structural Database System*, Version 5.23, April **2002**. Cambridge Crystallographic Data Centre, University Chemical Laboratory, Cambridge, England.
16) M. Czugler, E. Eckler, J. J. Stezowski, *J. Chem. Soc., Chem. Commun.*, **1981**, 1291.
17) K. Harata, *Bull. Chem. Soc. Jpn.*, **1988**, 61, 1939.
18) K. Harata, *Chem. Lett.*, **1984**, 1644.
19) K. Harata, F. Hiryama, K. Uekama, G. Tsoucaris, *Chem. Lett.*, **1988**, 1585.
20) T. Aree, W. Saenger, P. Leinbnitz, H. Hoier, *Carbohydr. Res.*, **1999**, 315, 199.
21) M. Selkti, A. Navaza, F. Villain, P. Charpin, C. de Rango, *J. Incl. Phenom.*, **1997**, 27, 1.
22) P. Glockner, H. Ritter, D. Schollmeyer, *Private Commun.*, **2000**.

Crystal packing

The unit cell parameters and XRD traces of the A_{ISO} complexes were in close agreement with each other indicating an analogous packing arrangement of the two complexes. A similar phenomenon was seen for the B_{ISO} complexes. In the A_{ISO} complexes, the complex units stack in infinite chains in a head-to-tail mode in a modified herringbone scheme. The herringbone chains form sheets parallel to the *bc*-plane which are stacked along the *a*-axis. However, the two-fold screw axis parallel to the *a*-axis does not pass through the host cavity and therefore complex units related by the 2_1-axis in this direction are members of adjacent columns. The consequence of this is a much shorter cell length *a* than the cell lengths *b* in the B_{ISO} complexes and therefore successive complex units within a column are related by a unit cell translation rather than by a two-fold screw axis as in other complexes.

In the B_{ISO} complexes, the molecules pack along the *a*-axis in a zigzag type pattern and the two-fold screw axis parallel to this direction passes through the host cavity. In the case of PPDMB, the O(6) side is partially blocked as the primary methoxy moiety of the G3 residue is in the *cis* conformation, while on the G4 residue it protrudes into the cavity "above" it. In the BPDMB structure, the primary O(6)–CH_3 group on both the G3 and G4 residues protrudes into the CD cavity "above" it. Thus the cavity is partially filled by the guest and the O(6)-CH_3 group of an adjacent molecule related by the two-fold screw axis parallel to *a* ["self-inclusion", Figure 5.40]. It was found that the cell volume increases by approximately 1 % as the alkyl chain length increased.

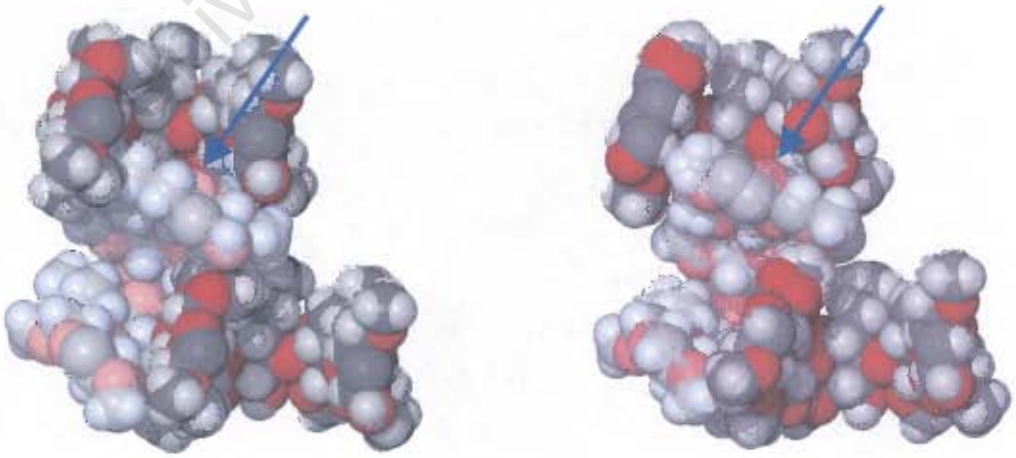

(a) (b)

Figure 5.40 A sectioned space-filling diagram of the (a) PPDMB and (b) BPDMB structures showing the "self inclusion" aspect, indicated by an arrow. To differentiate the hosts, one host molecule is represented in a lighter shade.

23) T. Steiner, W. Saenger. *Angew. Chem., Int. Ed. Engl.*, **1998**, 37, 3404.

24) H. Pohlmann, M. Gdaniec, E. Eckle, G. Geiger, J. J. Stezowski, *Acta Crystallogr.*, **1984**, A40, C276.

25) J. J. Stezowski, M. Czugler, E. Eckle, *Proc. I.S. Cyclodextrins*, **1981**, 151.

26) J. J. Stezowski, W. Parker, S. Hilgenkamp, M. Gdaniec, *J. Am. Chem. Soc.*, **2001**, 123, 3919.

27) T. Aree, H. Hoier, B. Schulz, G. Reck, W. Saenger, *Angew. Chem., Int. Ed. Engl.*, **2000**, 39, 897.

28) T. Steiner, W. Saenger, *Carbohydr. Res.*, **1995**, 275, 73.

29) D. Armspach, P. R. Ashton, C. P. Moorse, N. Spencer, J. F. Stoddart, T. J. Wear, D. J. Williams, *Angew. Chem., Int. Ed. Engl.*, **1993**, 32, 854.

30) D. Armspach, P. R. Ashton, R. Ballardini, V. Balzani, A. Godi, C. P. Moorse, L. Prodi, N. Spencer, J. F. Stoddart, M. S. Tolley, T. J. Wear, D. J. Williams, *Chemistry – A European Journal*, **1995**, 1, 33.

31) L. Fábián, A. Kálmán, *Acta Crystallogr.*, **1999**, B55, 1039.

32) A. Kálmán, L. Párkányi, *Advances in Molecular Structure Research*, (Vol. 3), M. Hargittai, I. Hargittai (eds.), JAI Press, Greenwich, CT., **1997**, p. 206.

33) F. W. Lichtenthaler, S. Immel, *Starch*, **1996**, 48, 4, 145.

34) F. W. Lichtenthaler, S. Immel, *Starch*, **1996**, 48, 6, 225.

Chapter 6

TRIMEB INCLUSION COMPLEXES

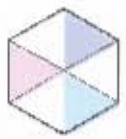

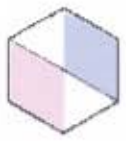

COMPLEX PREPARATION

Crystalline complexes were prepared by dissolving an equimolar amount of TRIMEB and each of the four parabens in distilled water at room temperature. The resulting dilute solutions were filtered and incubated at approximately 50°C. Crystals were obtained on standing for a period of 48 hours and were colourless needles. The density of the crystals was not measured due to the high solubility of the host in both aqueous solution and organic solvents. The complexes of TRIMEB with methyl-, ethyl-, propyl- and butyl paraben will be referred to as MPTMB, EPTMB, PPTMB and BPTMB respectively.

MICROANALYSIS

The host to guest ratios of the TRIMEB complexes were determined by carbon and hydrogen microanalysis and the results are given as the average of duplicate determinations. Each of the MPTMB, EPTMB, PPTMB and BPTMB complexes contains 1:1 stoichiometric amounts of host to guest. The water content present in each complex was calculated from the initial mass loss obtained from the TGA traces and the results are reported in Table 6.1. UV spectrophotometry was used to confirm these results.

Table 6.1 Carbon and hydrogen microanalysis results for the TRIMEB complexes

COMPLEX	CALCULATED (%)		EXPERIMENTAL (%)	
	C	H	C	H
MPTMB • 2.6 H_2O	52.36	7.75	52.21	8.06
EPTMB • 5.0 H_2O	51.29	7.89	51.59	7.82
PPTMB • 5.2 H_2O	51.45	7.95	51.30	7.70
BPTMB • 5.6 H_2O	51.52	8.02	51.81	7.80

THERMAL ANALYSIS

HSM results for the TRIMEB complexes

The HSM results for MPTMB, EPTMB, PPTMB and BBTMB are presented in Figure 6.1. Loss of water from the complexes is visible by a slow release of bubbles. Water loss occurred over the range 73 to 92°C for the MPTMB complex, from 76 to 101°C for the EPTMB complex, from 85 to 114°C for the PPTMB complex and from 72 to 103°C for the BPTMB complex.

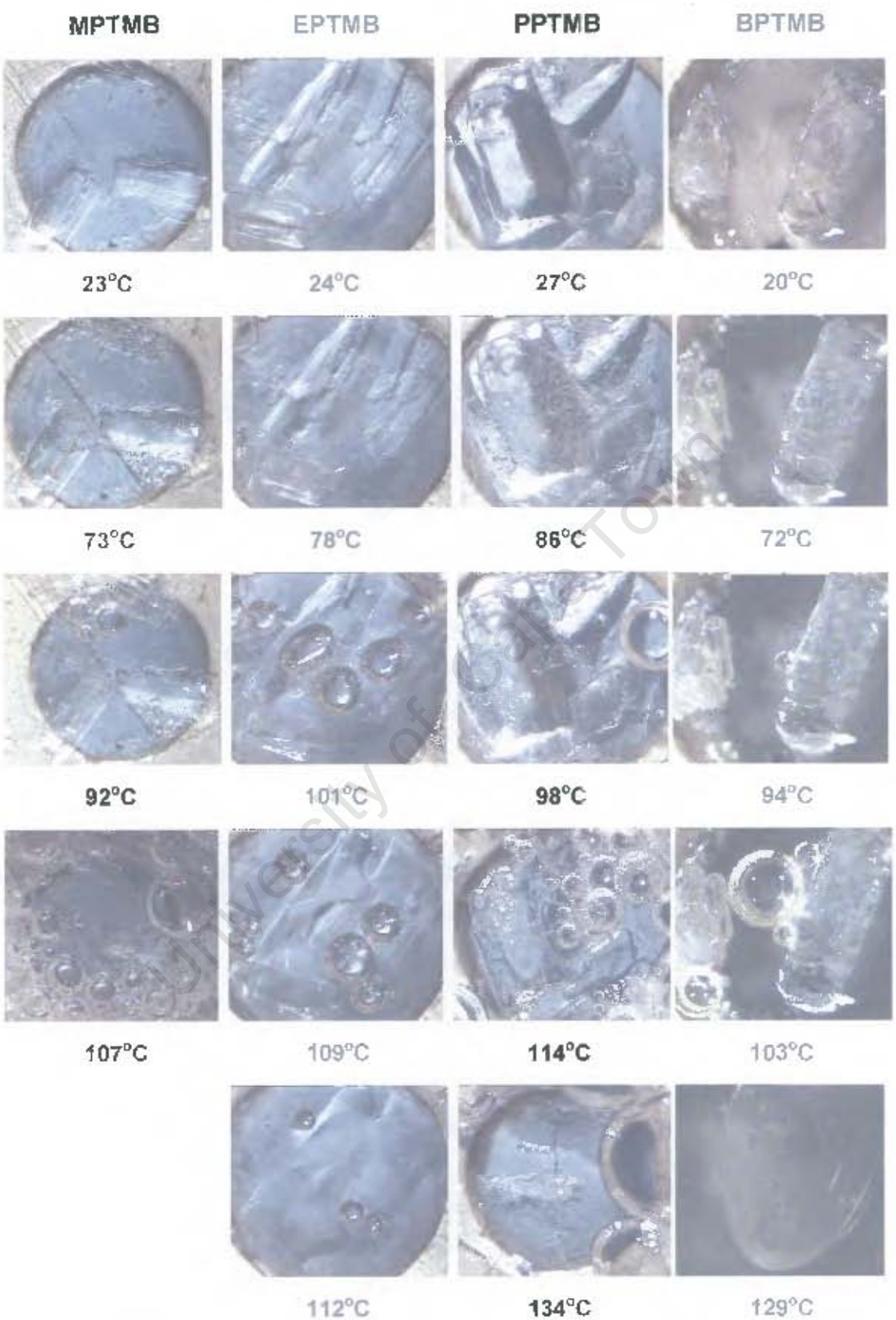

Figure 6.1 HSM photographs taken at various temperatures for crystals of the MPTMB, EPTMB, PPTMB and BPTMB complexes

The temperature range of water loss is also evident from the TGA traces [Figures 6.2 (a), (b), (c) and (d)]. In the case of the PPTMB complex, smaller crystallites appear to form on the outside of the crystal at 55°C and continue to do so till 85°C.

After water loss the crystals remain visibly unchanged up to the onset of decomposition, which is observed from 97 to 107°C for the MPTMB complex, from 109 to 112°C for the EPTMB complex, from 122 to 134°C for the PPTMB complex and from 120 to 127°C for the BPTMB complex. Decomposition of the complexes is observed by further mass losses in the TGA traces.

TGA results for the TRIMEB complexes

The TGA results for the MPTMB, EPTMB, PPTMB and BPTMB complexes are shown in Figure 6.2 (a), (b), (c) and (d) respectively. A summary of the observed percentage weight losses is presented in Table 6.2. Weight losses from 30 to 100°C represent water loss from the complexes. From 100 to 160°C a small weight loss is observed. From 160°C onwards weight losses due to decomposition are observed.

Table 6.2 The percentage weight losses for the TRIMEB complexes

Temp (°C)	MPTMB		EPTMB		PPTMB		BPTMB	
	Sample weight (%)	Δ Weight loss (%) *	Sample weight (%)	Δ Weight loss (%) *	Sample weight (%)	Δ Weight loss (%) *	Sample weight (%)	Δ Weight loss (%) *
30	100	-	100	-	100	-	100	-
100	97.1	2.9	94.7	5.3	94.5	5.5	94.1	5.9
110	96.9	0.2	94.6	0.1	94.4	0.1	94.0	0.1
120	96.8	0.1	94.5	0.1	94.3	0.1	94.0	0.0
130	96.8	0.0	94.3	0.2	94.2	0.1	94.0	0.0
140	96.7	0.1	94.2	0.1	94.2	0.0	94.0	0.0
150	96.6	0.1	94.0	0.2	94.1	0.1	93.8	0.2
160	96.5	0.1	94.0	0.0	94.1	0.0	93.7	0.1
180	95.5	1.0	93.9	1.5	93.9	0.1	93.4	0.3
200	93.5	2.0	91.4	2.5	93.7	0.2	93.1	0.3
Average number of water molecules per H:G unit								
	2.6		5.0		5.2		5.6	

* Δ Weight loss (%) = [Sample weight (%) at temperature (n-1)] - [Sample weight (%) at temperature (n)]

DSC results for the TRIMEB complexes

The DSC results for the MPTMB, EPTMB, PPTMB and BPTMB complexes are shown in Figure 6.2 (a), (b), (c) and (d) respectively and the results are summarised in Table 6.3.

All the complexes show endothermic events corresponding to water loss in the range 30-86°C, which correspond to an observed mass loss in the TGA traces [labelled A]. Each of the complexes shows an asymmetric endotherm [C] representing fusion of the complex.

The DSC trace of PPTMB shows a small endothermic peak [B] at 116°C before the sharper asymmetric endotherm of fusion is observed. This is also seen in the BPTMB complex, where the endotherm due to fusion [C] is split, the first peak occuring at 120°C with a shoulder at 124°C [B]. When the crystals of these two complexes were grown with an excess of the drug present it was noticed that this peak B increased. This suggests that this peak is produced on melt of the uncomplexed drug.

The onset of fusion occurs at 107, 94, 122 and 116°C for the MPTMB, EPTMB, PPTMB and BPTMB complexes respectively. The thermal stability of the inclusion complexes was based on the analysis of the onset of decomposition for the complexes. The stability follows the order of PPTMB > BPTMB > MPTMB > EPTMB.

The much lower melting point in comparison with the "melting points" of complexes of unsubstituted cyclodextrins is indicative of the weaker intermolecular interactions and is expected since methylation of the hydroxyl groups precludes host-host intermolecular hydrogen bonding.

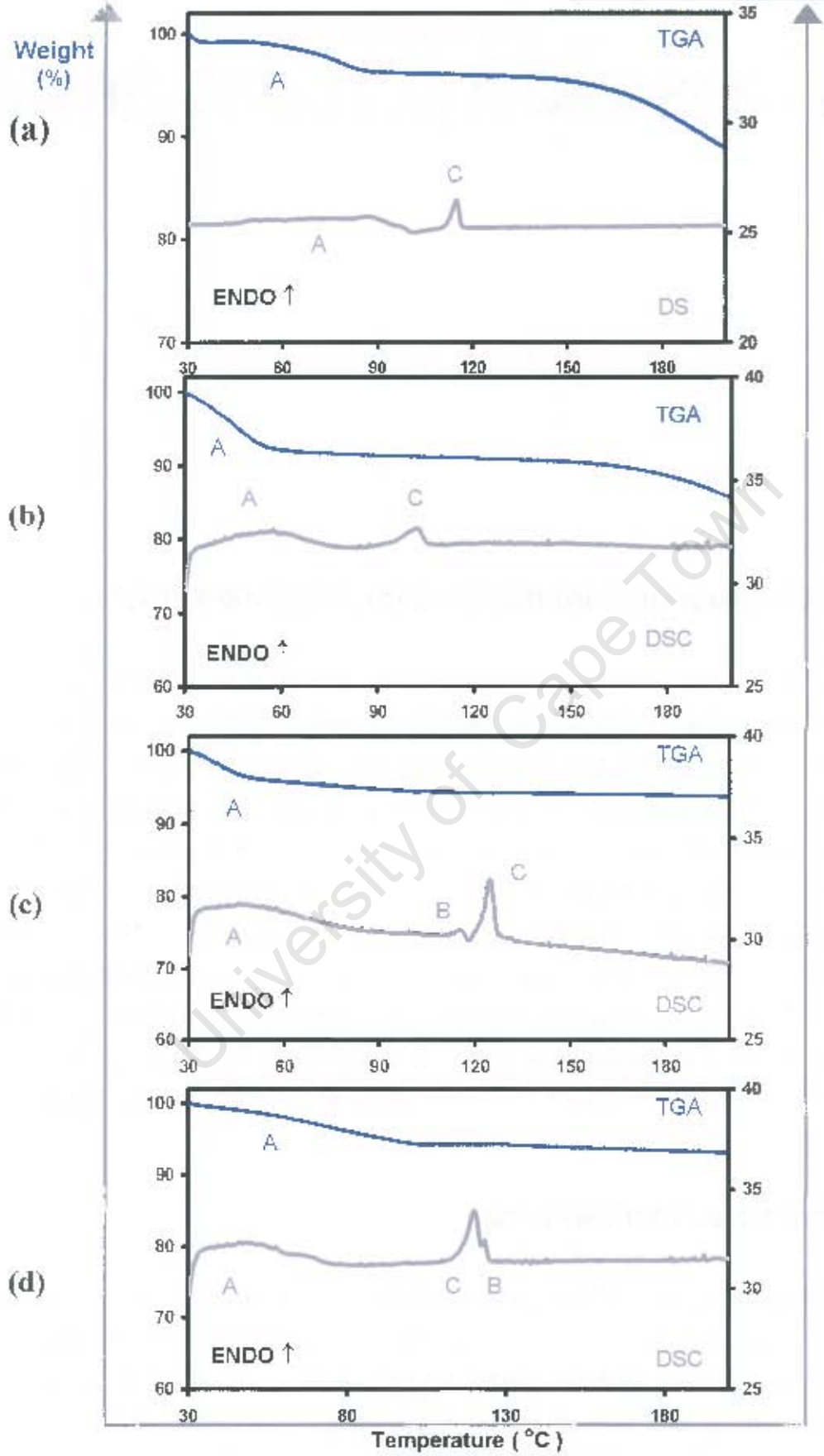

Figure 6.2 TGA and DSC traces for the (a) MPTMB (b) EPTMB (c) PPTMB and (d) BPTMB complexes

Table 6.3 Summarised DSC results for the TRIMEB complexes

		MPTMB	EPTMB	PPTMB	BPTMB
Temperature range	A (°C)	30-90	30-80	30-90	30-80
Temperature range	B (°C)			108-119	
Endotherm B	T_{on} (°C)			111	
	Peak (°C)			116	124
Temperature range	C (°C)	100-119	88-111	119-138	110-128
Endotherm C	T_{on} (°C)	107	94	122	116
	Peak (°C)	115	102	125	120
		METHYL	ETHYL	PROPYL	BUTYL
Endotherm of pure paraben	(°C)[1]	126	116	96	69

FOURIER TRANSFORM INFRARED SPECTROSCOPY (FTIR)

FTIR spectroscopy was used to determine how the carbonyl stretching frequency was affected by complexation. The C=O stretching frequency of the complexed methyl paraben is displaced to 1712 cm^{-1} from the measured value of 1679 cm^{-1} for the drug itself. In the EPTMB complex the C=O stretching frequency is displaced from the measured value of 1672 cm^{-1} for the drug itself to 1711 cm^{-1} in the complex. In PPTMB the stretching frequency is displaced from 1675 cm^{-1} in the pure drug to 1712 cm^{-1}. For the BPTMB complex the C=O stretching frequency is displaced from 1678 cm^{-1} in the pure drug to 1710 cm^{-1}. The FTIR spectra for the four paraben complexes are represented in Figure 6.3. This significant frequency shift also indicates that the guest is included in the host. Furthermore, this is consistent with the known presence of strong hydrogen bonding (C=O•••H–O) in the crystals of the guest and the absence of hydrogen bonding of this type in the CD complex.[1]

EXPERIMENTAL XRD ANALYSIS

The XRD patterns for the MPTMB, EPTMB, PPTMB and BPTMB powder complexes are shown in Figures 6.4, 6.5, 6.6 and 6.7 respectively together with the XRD patterns of the physical mixture of TRIMEB with the appropriate drug. The diffraction pattern of the kneaded material was compared with those of the physical mixture [consisting of a 1:1 molar ratio of drug and TRIMEB].

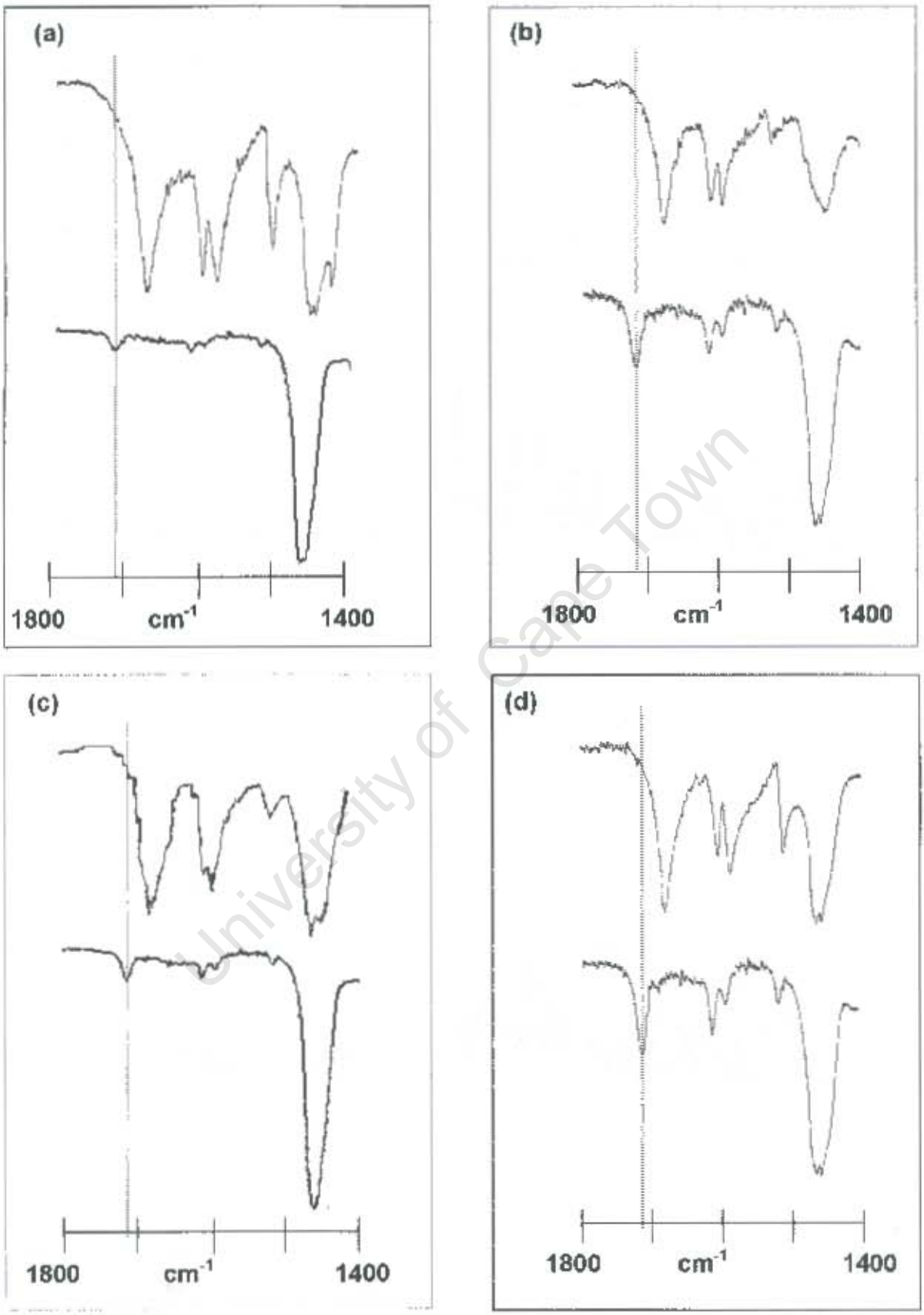

Figure 6.3 FTIR spectra (a) MP and MPTMB, (b) EP and EPTMB, (c) PP and PPTMB, (d) BP and BPTMB. The top spectrum is that of the pure paraben.

The appearance of new peaks and the disappearance of old peaks in the XRD traces of the physical mixture indicated that complexation had occurred. The XRD traces of EPTMB, PPTMB and BPTMB are closely matched and they can therefore be considered as isomorphous structures. The XRD pattern for the MPTMB complex is similar to those of the other three complexes of TRIMEB, but the 2θ positions are slightly different, and hence this complex may have a similar packing arrangement, but will have different cell dimensions [Figure 6.8].

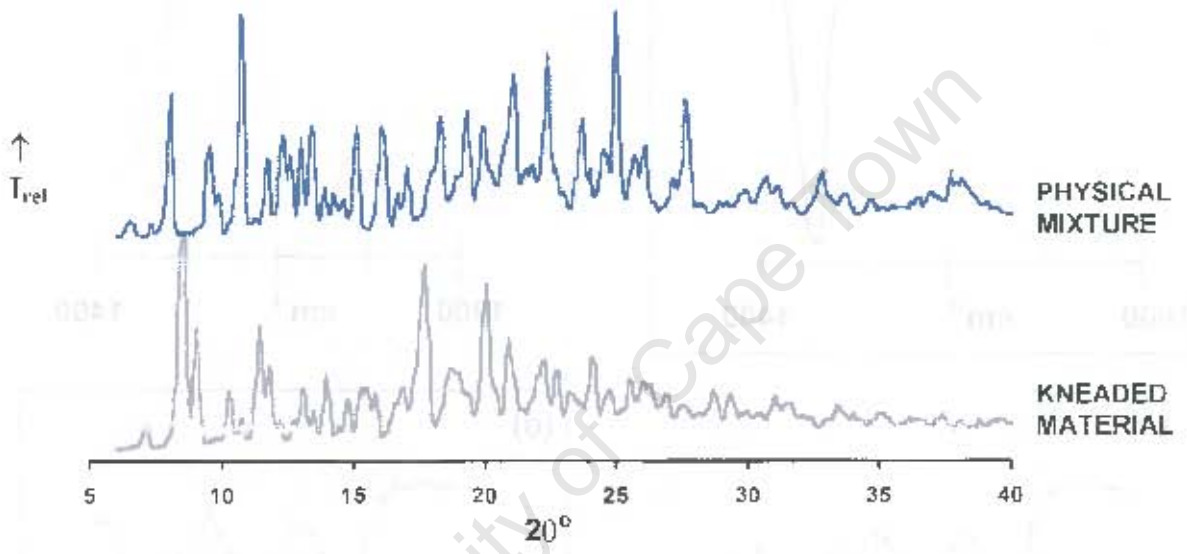

Figure 6.4 XRD patterns of the MPTMB complex and a 1:1 physical mixture

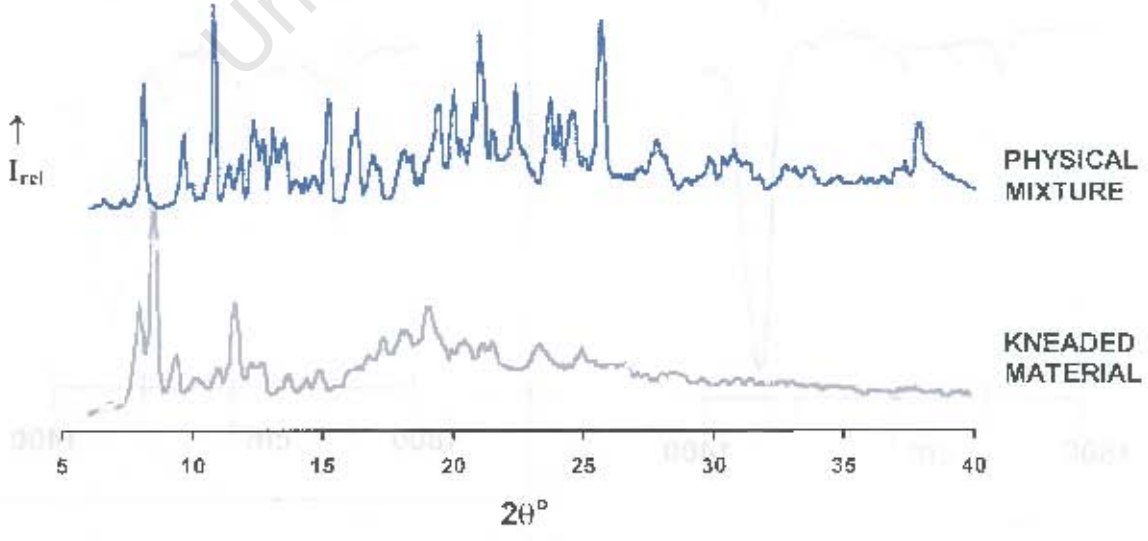

Figure 6.5 XRD patterns of the EPTMB complex and a 1:1 physical mixture

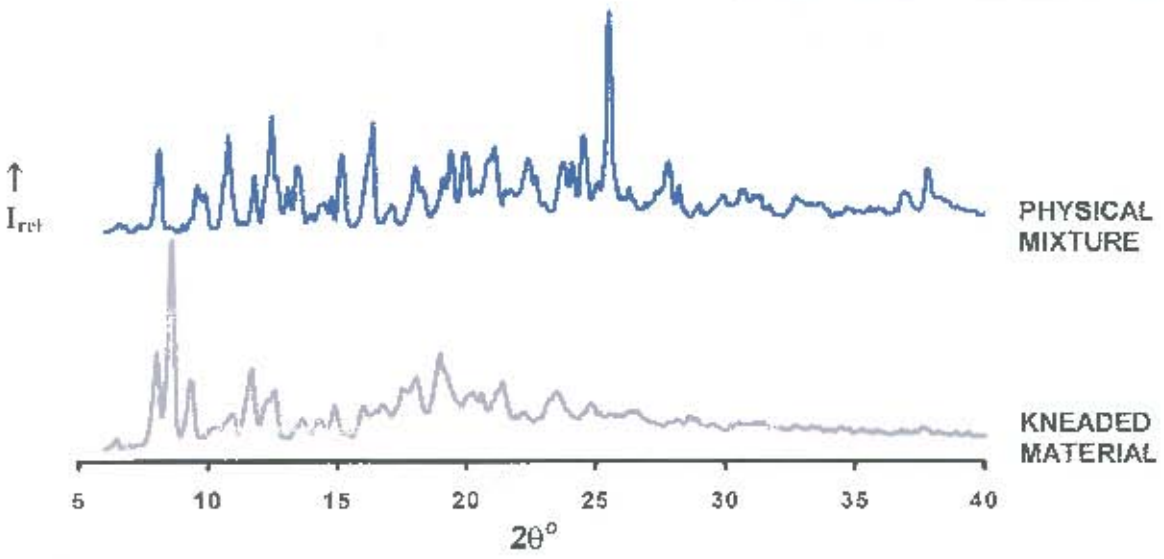

Figure 6.6 XRD patterns of the PPTMB complex and a 1:1 physical mixture

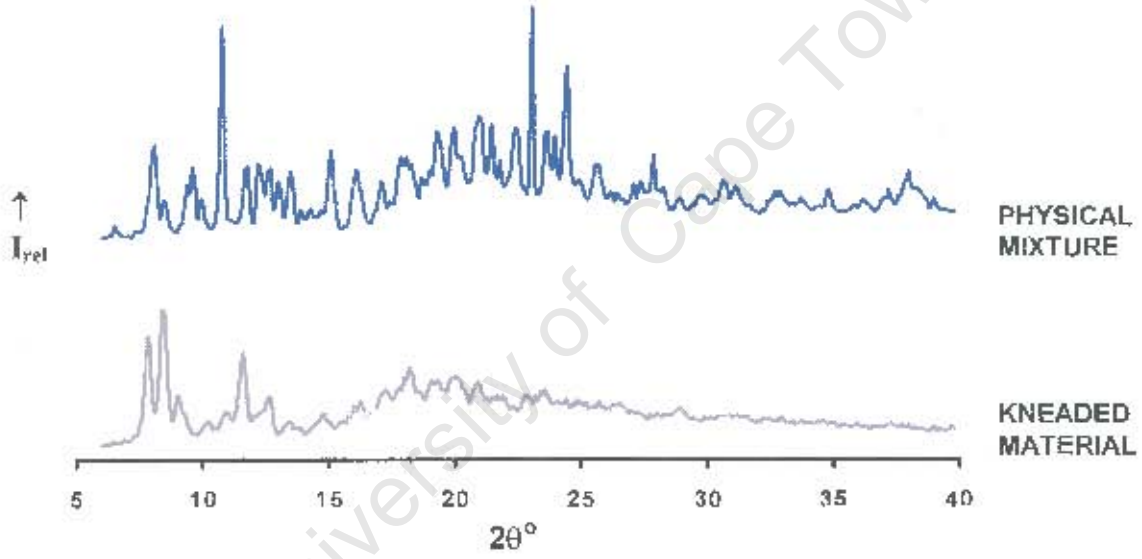

Figure 6.7 XRD patterns of the BPTMB complex and a 1:1 physical mixture

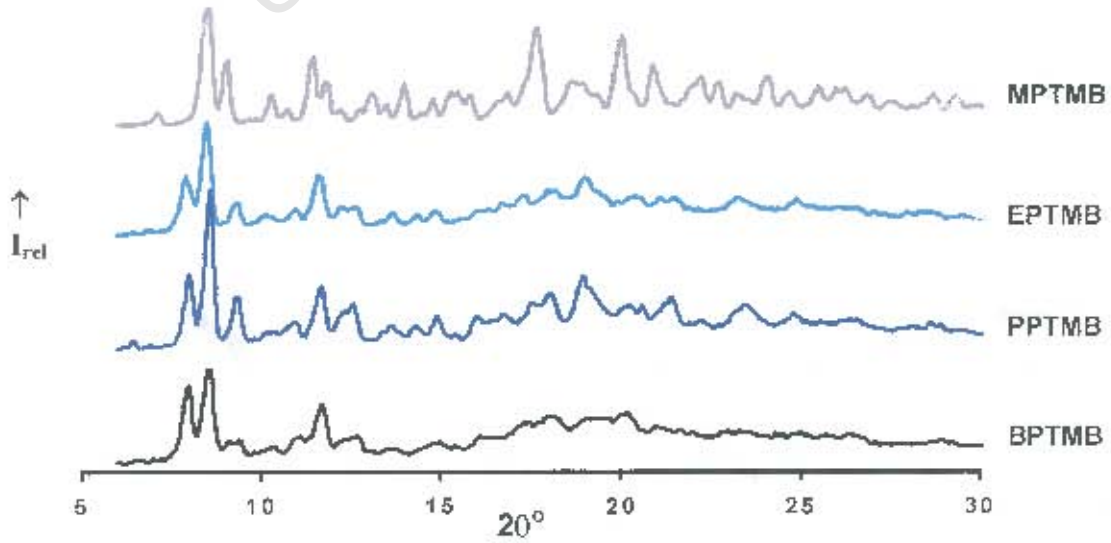

Figure 6.8 XRD patterns of the MPTMB, EPTMB, PPTMB and BPTMB complexes

X-RAY CRYSTALLOGRAPHIC ANALYSIS OF THE MPTMB STRUCTURE

Data-collection

The preliminary unit cell parameters and space group for the MPTMB structure were determined by X-ray photographic techniques. The oscillation photograph displayed m_x symmetry indicating the monoclinic system or higher. The Weissenberg photography showed two central lattice rows, 90° apart, of which each was a mirror line. The overall symmetry of the reciprocal lattice [Laue symmetry] was thus determined as *mmm*. indicating the crystal belonged to the orthorhombic system. The systematic absences are listed below, and these confirmed the space group $P2_12_12_1$.

hkl: none
h00: h = 2n + 1
0k0: k = 2n + 1
00l: l = 2n + 1

A single crystal was mounted on a glass fibre and covered in Paratone N oil[2] to prevent cracking due to loss of water of crystallisation and to provide a rigid mounting for the low-temperature data-collection. X-ray intensity data-collection was performed at 173(2) K on the Nonius Kappa CCD diffractometer using graphite-monochromated MoKα radiation. Crystal data and data-collection parameters are listed in Table 6.4.

Structure determination and refinement

Solving the MPTMB structure represented a difficult challenge in view of the fact that the cell parameters did not directly match any of the known TRIMEB structures reported in the Cambridge Structural Database[3] and the structure solution required the location of a large number of non-hydrogen atoms. The structure was solved using the program *PATSEE*,[4,5] which uses a Patterson vector search and direct methods to position a fragment of known geometry in a unit cell. The search model consisted of the skeleton atoms of a previously solved TRIMEB molecule,[6] as it was hoped that the conformation of the cyclodextrin would be similar. After many attempts, 1100 random positions were refined for 50 000 random orientations producing a starting model with favourable statistics from the *PATSEE* run [*viz.* RFOM = 0.477; TPRSUM = 0.465; TFOM = 0.215; R_E = 0.381; CFOM = 0.276].

Table 6.4 Details of the data collection and refinement parameters for the MPTMB structure

Empirical formula	$C_{63}H_{112}O_{35}{\bullet}C_6H_6O_3{\bullet}2.6H_2O$
Formula weight	1628.5
Crystal system	Orthorhombic
Space group	$P2_12_12_1$
a / Å	10.718 (1)
b / Å	26.353 (1)
c / Å	30.018 (2)
α / °	90
β / °	90
γ / °	90
Volume / c	8478.6 (1)
Z	4
$Density_{calc}$ / g cm^{-3}	1.276
μ (MoKα) / mm^{-1}	0.104
F(000)	3504
Temperature of data collection / K	173 (2)
Crystal size / mm^3	0.44 x 0.20 x 0.17
Range scanned θ / °	$2 < \theta < 22$
Index ranges	h: -10,11 k: ± 25 l: -31, 25
ϕ scan angle / °	0.6
ϕ scan range, frames	111.6°, 186
ω scan angle / °	0.6
ω scan ranges, frames	79.8°, 133 and 49.8°, 83
Dx / mm	66.1
Total no. of reflections collected	17039
No. of independent reflections	9240
No. of reflections with $I > 2\sigma(I)$	6987
No. of parameters	764
R_{int}	0.0320
S	1.043
R_1 (for 5598 reflections)	0.0755
Reflections omitted	(0 1 1); (0 1 7); (0 2 1); (0 2 3); (0 4 0); (0 5 3); (2 0 0)
wR_2	0 1825
Weighting scheme	a = 0.1038 b = 14.7997
$(\Delta / \sigma)_{mean}$	< 0.008
$\Delta\rho$ excursions / $e.Å^{-3}$	0.88 and -0.48

This model was refined isotropically by full-matrix least-squares methods [*SHELX-97*].[7] Difference electron density maps based on initial refinements revealed most of the remaining non-hydrogen atoms of the host and many of the non-hydrogen atoms for the guest. Once all the non-hydrogen atoms of the host and the water molecules had been located from subsequent difference electron density maps, all the cyclodextrin hydrogen atoms were placed. These hydrogen atoms were geometrically fixed at idealised positions in a riding-model. All the methyl hydrogen atoms were assigned a common variable isotropic temperature factor and the remaining hydrogen atoms of each glucose moiety were assigned common variable isotropic temperature factors. The O-methyl, methylene and methine groups [except C(9G7)] on the host were assigned anisotropic temperature factors. After many successive refinements, two water molecules with full site-occupancy were placed, O(1W) having a final temperature factor of U_{eq} = 0.08 Å^2 and O(2W) having a final isotropic temperature factor of 0.16 Å^2. The other water molecule with a site-occupancy of less then one was assigned a fixed isotropic temperature factor of 0.07 Å^2 [the mean of the preceding U values] and the s.o.f. was allowed to vary [final value 0.32]. The total occupancy of 2.3 for the water molecules compared favourably with the 2.6 water molecules observed from the TGA results. The hydrogen atoms of the water molecules were not located.

Eventually all the non-hydrogen atoms of the guest were located in the difference electron density map. All three oxygen atoms of the guest were refined with anisotropic temperature factors. The hydrogen atoms attached to the carbon atoms of the guest were also inserted at idealised positions and assigned a common isotropic temperature factor. The hydrogen atom of the hydroxyl group was placed using the rotating group refinement strategy [AFIX 147]. Due to the abnormally long bond distances found in the guest molecule, distance constraints were placed on certain bonds, namely: O(1)–C(2) 1.354 Å; C(5)–C(8) 1.469 Å; C(8)–O(9) 1.217 Å; C(8)–O(10) 1.334 Å; O(10)–C(11) 1.436 Å [all with σ = 0.005 Å]. The values chosen were taken from Lin.[8]

At the end of the refinement there was still one significant electron density peak unaccounted for with a height of 0.88 e.Å^{-3}, located at a distance of 0.8 Å from C(6G1). Hydrogen atoms were placed on C(6G1) before and after anisotropic temperature refinement, but the remaining electron density was still not accounted for. The possibility that this electron density peak represented a disordered carbon atom was rejected on the basis of the unfavourable geometric position relative to those atoms already placed.

Geometrical analysis of the MPTMB structure

The asymmetric unit of the MPTMB structure contains a single TRIMEB molecule, its associated guest and 2.6 water molecules. The glucose units will be referred to as G1, G2, G3, G4, G5, G6 and G7 and the structure and numbering scheme of the MPTMB complex and water molecules are shown in Figure 6.9. The geometrical data for the TRIMEB molecule are listed in Tables 6.5 and 6.6 [e.s.d.s are in the range 0.001-0.005 A for distances and 0.1-0.6° for angles].

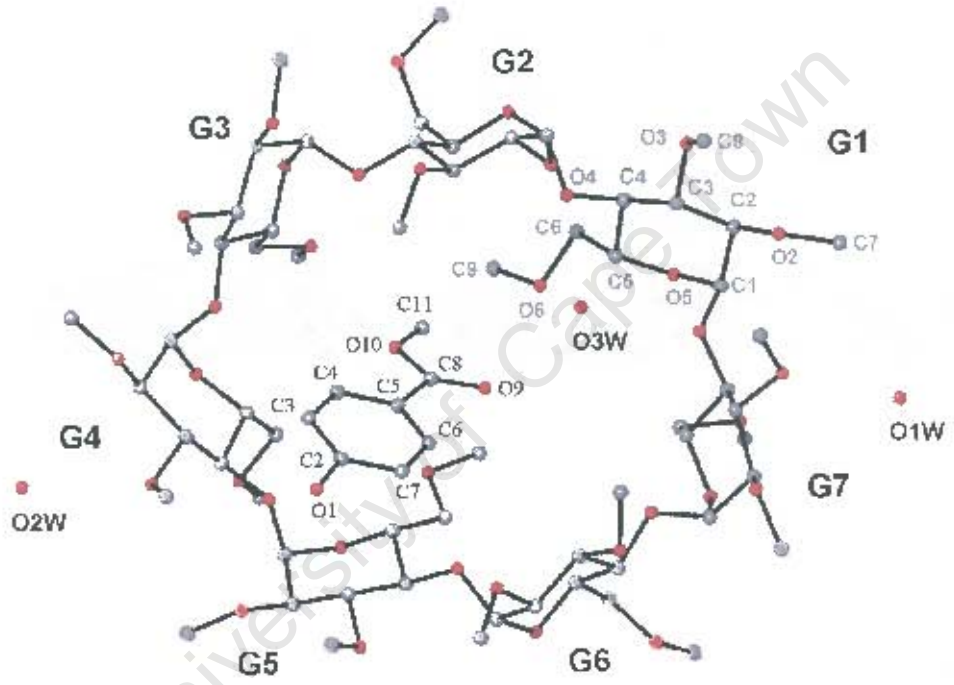

Figure 6.9 Macrocyclic structure and numbering scheme of glucose residues, water oxygen atoms and guest molecule, with the hydrogen atoms excluded. The host is viewed from the secondary face.

The glucopyranose residues are all in the $^4C_1$ chair conformation and the macrocycle is in the shape of an elliptically-distorted and truncated cone. The O(2)–C(7) bonds are directed away from the cavity and the O(3)–C(8) bonds are directed towards the cavity, as is observed in most TRIMEB complexes.[6, 9-12] The C(6)–O(6) bonds of the G2, G4, G6 and G7 residues are directed away from the cavity and are in the (-) *gauche* conformation, while those of the G1, G3 and G5 residues are pointed towards the cavity in the (+) *gauche* conformation. All the O(6)–C(9) bonds are *trans* to the respective C(5)–C(6) bonds, except in the G2 residue where the bond lies *gauche*.

The O(6)–C(9) groups of the G1 and G5 residues, which have the largest tilt angles, act as a "lid", closing off the O(6) side of the TRIMEB cavity, making it cup shaped. The G3, G4 and G7 residues also contribute to this effect. Hence TRIMEB assumes a cup-shape, in contrast to structures with β-CD and DIMEB where the cavity conforms to a more annular shape.

The geometric parameters of the O(4) heptagon of the MPTMB structure are listed in Table 6.5. These include the radii, the O(4)•••O(4') distances, the O(4)•••O(4')•••O(4'') angles, the O(4)•••O(4')•••O(4'')•••O(4''') torsion angles and the deviations of each of the O(4) atoms from the mean O(4) plane. Table 6.6 lists the other important features of the macrocyclic structure such as the intersaccharidic bond angle (ω), the O(2)•••O(3') distance and the tilt angles [τ_1 and τ_2]. These parameters are defined in Chapter 1.

Table 6.5 Geometrical parameters of the O(4) heptagon for the MPTMB structure

Glucose unit	Radii (Å)	O(4)•••O(4') (Å)	O(4) angle (°)	Torsion angle (°)	Deviation (Å)
G1	4.49 (1)	4.57	140	-6.6 (3)	-0.01
G2	4.80 (1)	4.25	131	11.4 (2)	-0.43
G3	5.52 (1)	4.39	117	12.8 (2)	0.11
G4	5.04 (1)	4.55	125	-32.9 (3)	0.50
G5	4.45 (1)	4.40	140	8.6 (3)	-0.45
G6	5.26 (1)	4.31	120	21.8 (2)	-0.28
G7	5.33 (1)	4.16	118	-21.5 (3)	0.64
Average	**4.98**	**4.38**	**127**	**|16.5|**	**|0.34|**

Table 6.6 φ, O(2)•••O(3') distance, τ for the MPTMB structure

Glucose unit	φ (°)	O(2)•••O(3') (Å)	τ_1 (°)	τ_2 (°)
G1	118	3.26	32.3 (2)	39.4 (2)
G2	117	3.54	-21.5 (1)	-19.0 (2)
G3	120	3.44	13.0 (1)	15.0 (2)
G4	118	3.46	31.2 (2)	32.6 (3)
G5	114	3.39	34.2 (1)	45.0 (2)
G6	118	3.68	-7.8 (2)	-6.6 (2)
G7	118	3.41	22.7 (2)	26.7 (2)
Average	**117**	**3.45**	**23.2**	**26.3**

Usually in TRIMEB complexes two glucose moieties have a negative tilt angle, while the others have positive tilt angles[6, 9-12] and this is also seen in the MPTMB complex. Thus far, only steric repulsion and the absence of O(2)•••O(3') hydrogen bonds have been invoked to explain the unusually large tilt angles found in TRIMEB structures.[6, 9-10] The values calculated for these parameters compare favourably with those of the TRIMEB-*p*-iodophenol tetrahydrate complex,[6] as this TRIMEB molecule was used as the search fragment in the Patterson search.

Guest geometry and interactions for the MPTMB structure

The conformation of the methyl paraben guest may be defined by two torsion angles. The torsion angles δ_1 [C(6)–C(5)–C(8)–O(9)] and δ_2 [C(5)–C(8)–O(10)–C(11)], will be used to describe rotation around the C(5)–C(8) and C(8)–O(10) bonds respectively. They were compared with the conformation of the uncomplexed methyl paraben molecule[8] and were found to be similar [Figure 6.10]. δ_2 of the complexed methyl paraben has a slightly larger out-of-plane twist than that of the uncomplexed MP, indicating that inclusion allows for more rotational freedom around the C(8)–O(10) bond. There are few close contacts between the host and guest molecule and the relevant interactions are listed in Table 6.7.

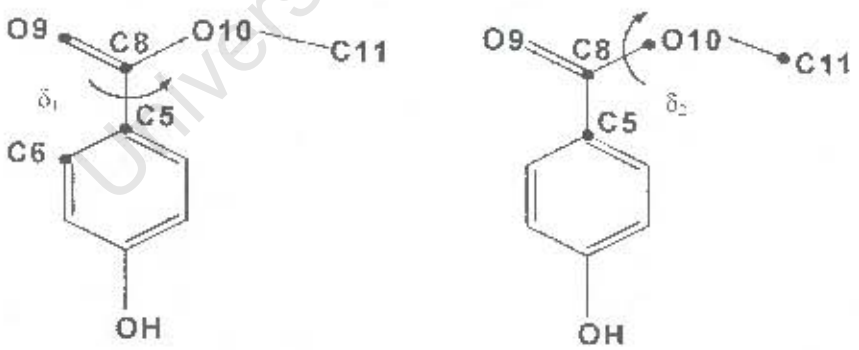

MP in complex :	δ_1 = 0 (2)	δ_2 = -171 (1)
MP uncomplexed:[8]	δ_1 = -0.6	δ_2 = -177

Figure 6.10 Torsion angles δ_1 and δ_2 of the methyl paraben

Table 6.7 Close contact distances for the MPTMB structure

Interaction	Distance (Å)
H(1) ••• H(651)'	2.19
H(11B) ••• H(531)	2.27

' Related by symmetry operation: -1+x, y, z

The phenolic hydroxyl group protrudes from the O(2), O(3) face of the host, while the ester moiety of the guest molecule occupies the centre of the host cavity. The phenyl ring of the guest forms an angle of 50.4 (2)° with the mean O(4) plane. The tilting permits the guest to occupy most of the available space in the cavity. Figures 6.11 and 6.12 show CPK diagrams of the MPTMB structure and include the O(3W) water oxygen atom [which is light blue in colour].

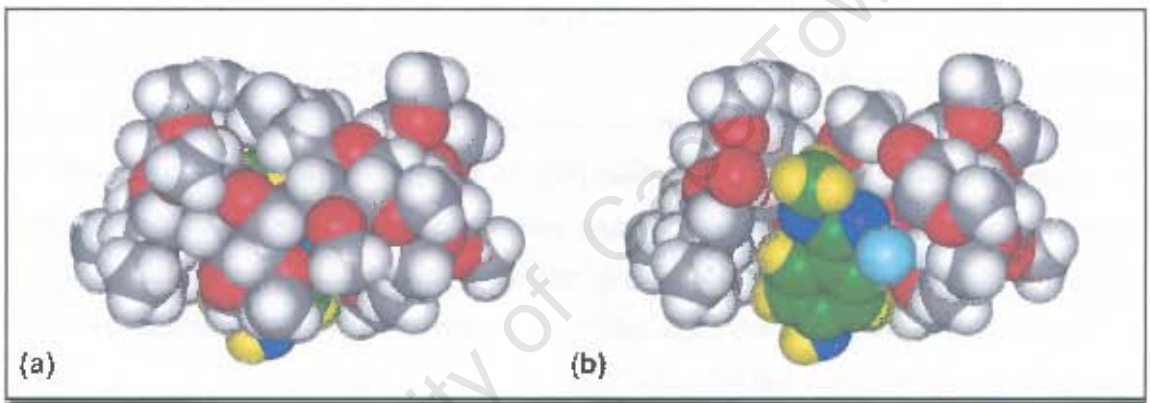

Figure 6.11 Space-filling diagram of the MPTMB structure (a) side view (b) sectioned view of the same orientation

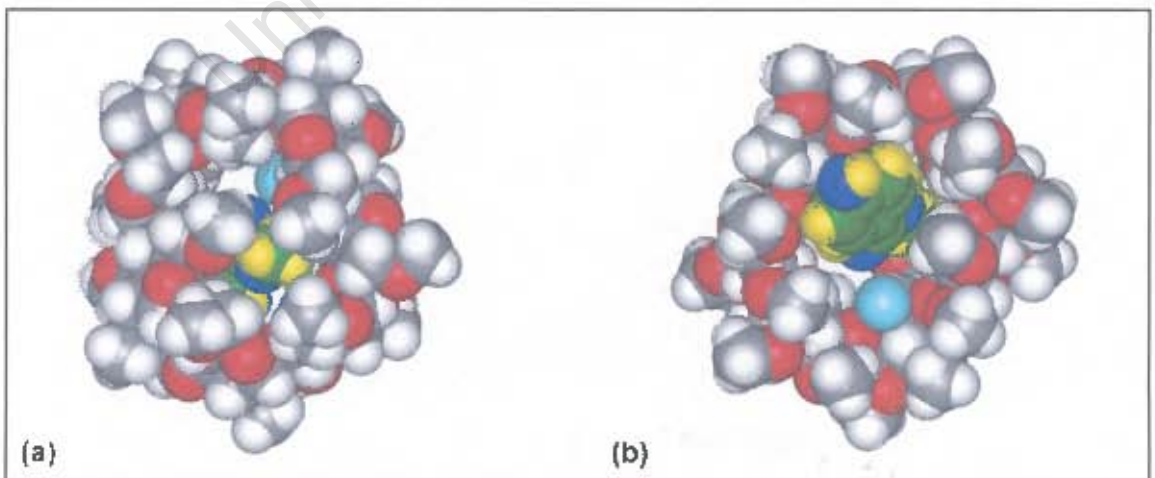

Figure 6.12 Space-filling diagram of the MPTMB structure (a) viewed from the primary rim (b) viewed from the secondary rim

Hydrogen bonding interactions of the MPTMB structure

Host interactions

The distorted conformation of the TRIMEB molecule relative to the conformation observed for the parent β-cyclodextrin molecule is stabilised by numerous intramolecular C–H•••O hydrogen bonds [Table 6.8], a common interaction found in carbohydrate crystal structures.[13]

The conformation of the TRIMEB molecule is stabilised by nine intramolecular C–H•••O hydrogen bonds, four of which are of the type C(6)–H•••O(5'), as observed in the TRIMEB monohydrate structure.[14] In addition, there are two C(1)–H•••O(3') hydrogen bonds and a C(1)–H•••O(6') hydrogen bond. Furthermore there are stabilising intramolecular hydrogen bonds within some of the glucose units, namely a C(7)–H•••O(3) hydrogen bond and one C(8)–H•••O(2) hydrogen bond. All the C•••O distances are in the range 3.0-3.4 Å.

Table 6.8 Intramolecular C–H•••O hydrogen bonds in the MPTMB structure*

			Distance (A)			Angle (°)
C	H	O	C–H	H•••O	C•••O	C–H•••O
C(1G2)	H(121)	O(3G1)	0.98	2.44	3.114 (9)	125.3 (5)
C(1G3)	H(131)	O(6G2)	0.98	2.60	3.243 (9)	123.5 (4)
C(1G6)	H(161)	O(3G5)	0.98	2.46	3.084 (9)	121.6 (5)
C(6G2)	H(622)	O(5G3)	0.97	2.45	3.198 (9)	133.2 (5)
C(6G4)	H(642)	O(5G5)	0.97	2.47	3.158 (8)	127.3 (5)
C(6G6)	H(662)	O(5G7)	0.97	2.43	3.16 (1)	132.0 (5)
C(6G7)	H(672)	O(5G1)	0.97	2.66	3.37 (1)	130.3 (6)
C(7G2)	H(723)	O(3G2)	0.96	2.47	3.08 (1)	121.0 (7)
C(8G5)	H(853)	O(2G5)	0.96	2.33	2.97 (1)	123.7 (5)

* Hydrogen bonding parameters based on idealised hydrogen atom positions.

Guest interactions

The hydroxyl oxygen atom is in hydrogen bonding contact with one water O(1W) oxygen atom while the carbonyl oxygen is in hydrogen bonding contact with O(3W). The water oxygen atoms in turn form hydrogen bonds with the atoms on the host molecule. Hydrogen bonding distances involving these water molecules are listed in Table 6.9.

Table 6.9 Hydrogen bonding distances involving the guest in the MPDMB structure*

			Distance (Å)			Angle (°)
Donor(D)	H	Acceptor(A)	D–H	H···A	D···A	D–H···A
O(1)	H(1)	O(1W)	0.82	2.07	2.68 (1)	130.4 (6)
C(3)	H(3)	O(2G6)	0.93	2.64	3.31 (1)	129.7 (7)
O(9)		O(3W)			3.05 (2)	

' Related by symmetry operation: 2-x, $^1/_2$+y, $1^1/_2$-z
* Hydrogen bonding parameters based on idealised hydrogen atom positions

Water interactions

Thermogravimetric analysis gave a weight loss which corresponds to 2.6 water molecules per 1:1 complex unit, of which 2.3 water molecules were accounted for in the crystallographic analysis. Two of the water molecules [O(1W) and O(2W)] are situated at the periphery of the cyclodextrin molecule, filling a small intermolecular space between complex units. The other water molecule [O(3W), s.o.f. 0.32] was located within the TRIMEB cavity and does not interact with the CD host. Hydrogen bonding distances between the host and these water molecules are listed in Table 6.10 and a schematic representation of these interactions is presented in Figure 6.13.

Table 6.10 Hydrogen bonding distances involving the water molecules

Interaction	Distance (Å)	Symmetry operator for the host oxygen atoms
O(1W) ••• O(5G5)	2.81 (1)	1-x, $-^1/_2$+y, $1^1/_2$-z
O(1W) ••• O(3G7)	2.79 (1)	x, y, z
O(2W) ••• O(3G4)	2.86 (1)	x, y, z
O(2W) ••• O(5G4)	3.16 (1)	$^1/_2$+x, $1^1/_2$-y, 1-z

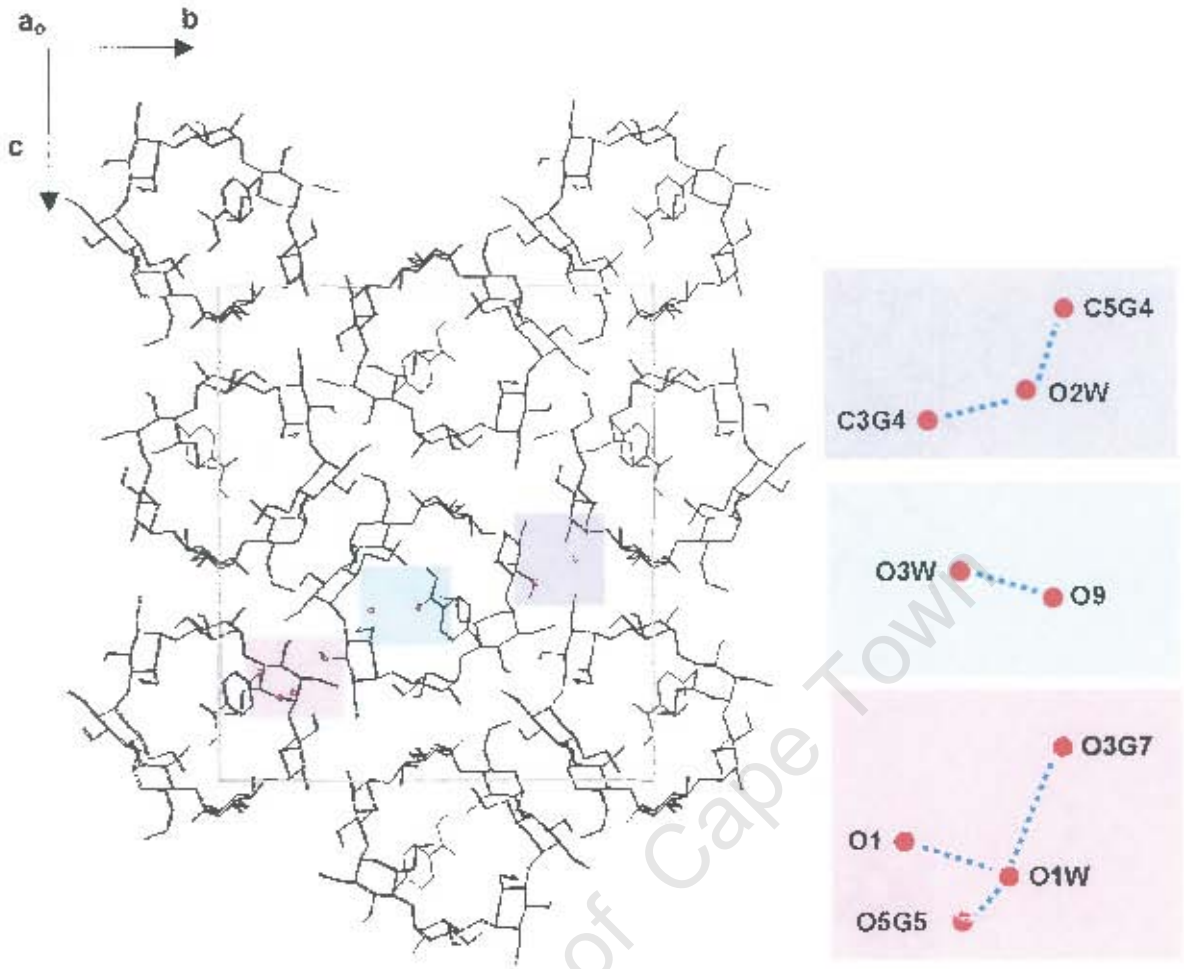

Figure 6.13 A schematic representation of guest and water interactions that connect adjacent host units

Crystal packing of the MPTMB structure

Figures 6.14 and 6.15 are extended stereo packing diagrams of the MPTMB structure showing projections as viewed down the *a*- and *c*-axes. Complex units stack in columns in a head-to-tail mode, forming what appear to be continuous channels along the *a*-axis.

Figure 6.14 shows the "endless" channels while Figure 6.15 shows that the phenolic group does not protrude into the cavity of the CD above it in the channel and also shows the columns running parallel to the *a*-axis.

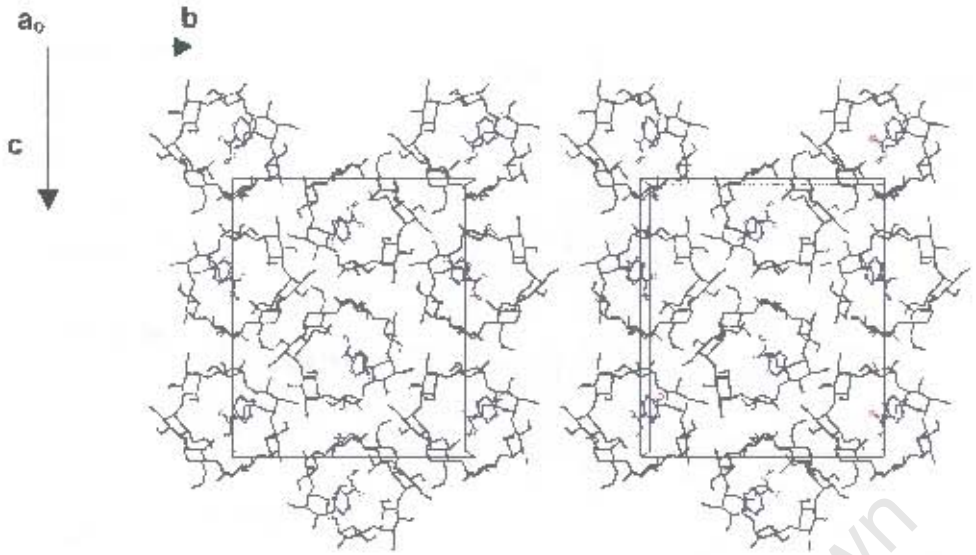

Figure 6.14 Stereo packing diagram of the MPTMB structure [a-axis projection]

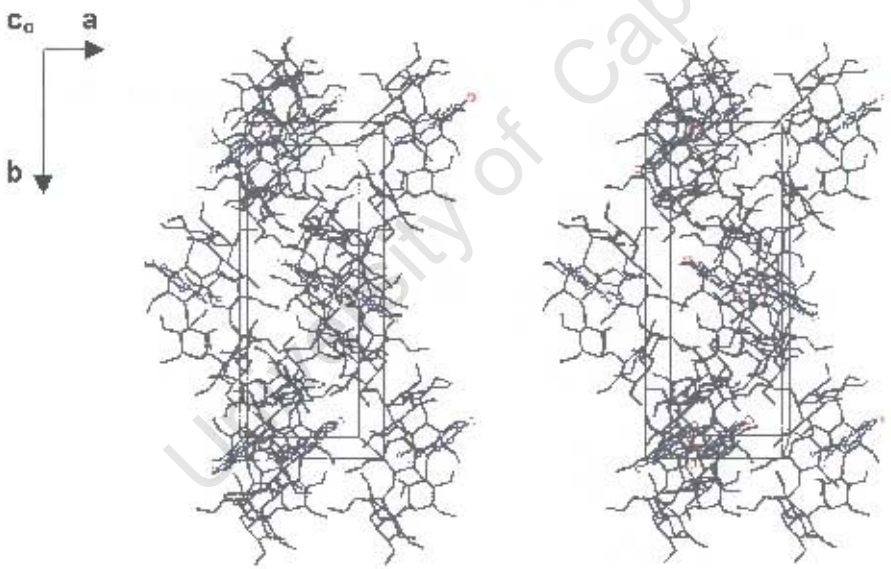

Figure 6.15 Stereo packing diagram of the MPTMB structure [c-axis projection]

Comparative XRD

The experimental X-ray powder diffraction pattern of MPTMB was successfully matched with that calculated from the single crystal structure data [Figure 6.16]. The very close match in peak positions (2θ) indicates that the sample giving rise to the experimental pattern is a homogeneous preparation of the MPTMB complex. The calculated pattern can be used in future as a fingerprint to identify that an inclusion complex has been obtained during complex preparation. The differences in relative intensities between the calculated and the experimental patterns are due to preferred orientation of the crystallites.

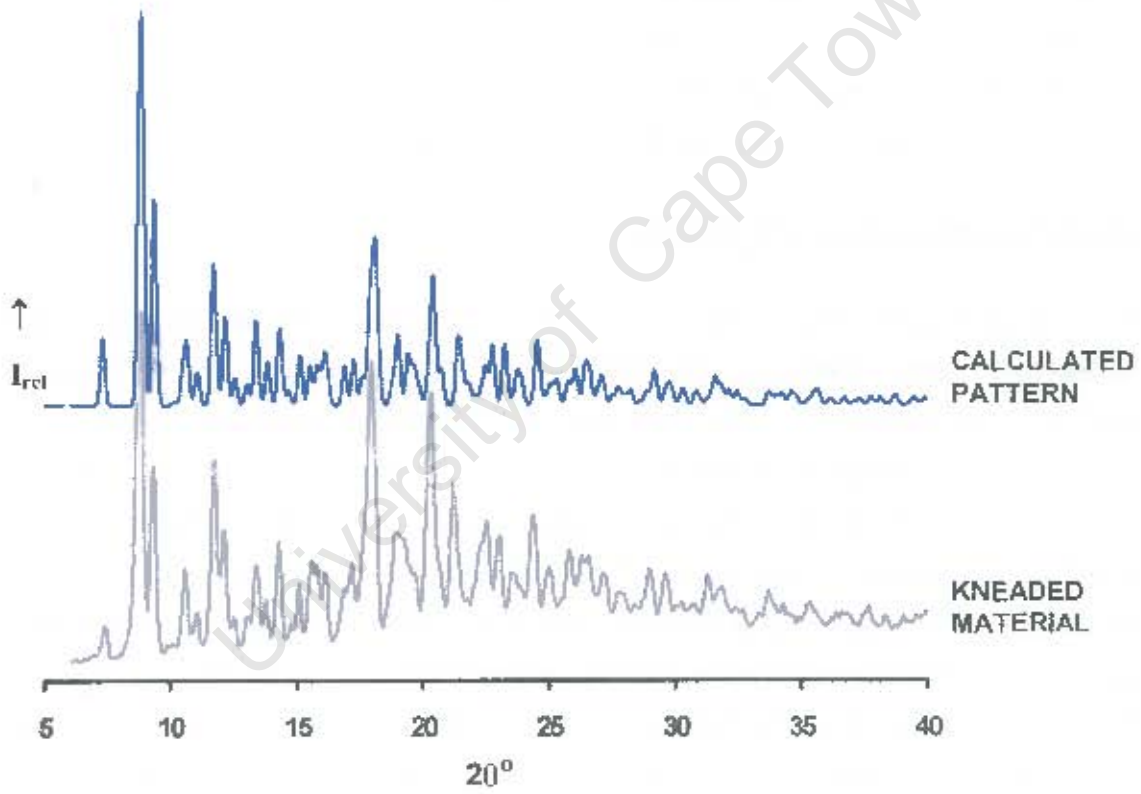

Figure 6.16 Experimental and calculated XRD traces for the MPTMB structure

X-RAY CRYSTALLOGRAPHIC ANALYSIS OF THE EPTMB STRUCTURE

Data-collection

The preliminary unit cell parameters and space group for the EPTMB structure were determined by X-ray photographic techniques. The latter revealed Laue *mmm* symmetry, with the systematic absences listed below. This corresponds to the orthorhombic system, space group $P2_12_12_1$.

hkl: none
h00: h = 2n + 1
0k0: k = 2n + 1
00l: l = 2n + 1

A crystal of the complex was mounted on a glass fibre and covered in Paratone N oil[2] to prevent cracking due to loss of water of crystallisation. Data were collected at 173(2) K on the Nonius Kappa CCD diffractometer using graphite-monochromated MoKα radiation. Crystal data and data-collection parameters are listed in Table 6.11.

Structure determination and refinement

The structure was solved using published co-ordinates for the non-hydrogen cyclodextrin atoms [excluding the O(6), C(7), C(8) and C(9) atoms of each methylglucose residue] of the isomorphous TRIMEB-*p*-iodophenol tetrahydrate complex.[6] After refinement in SHELX-97,[7] the difference Fourier map revealed the positions of most of the remaining non-hydrogen atoms. After further refinement it was found that the atoms C(7) and C(8) on O(2G3) and O(3G5) were disordered as well as the atom O(6) on C(6G2) and C(6G5), leading to disorder in the C(9) atoms. Two alternative positions were found for each disordered atom. For a given pair, a fixed U_{iso} of 0.07 Å^2 [the mean of U_{iso} for the chemically equivalent ordered atoms] was assigned and site-occupancy factors [s.o.f.'s] of x and 1-x were assigned, with x variable. Some of the bonds on these disordered atoms were either abnormally long or too short and thus distance constraints were placed on them. All the non-hydrogen atoms on the host, except the disordered atoms and C(6G2), C(6G5), C(7G5), C(8G1), C(8G3), C(8G6) and C(9G6) were refined anisotropically. Refinement continued with the placement of the water oxygen atoms. Six positions were located for the water molecules of which four could be assigned a full s.o.f. O(1W), O(2W) and O(3W) were refined anisotropically with a final temperature factor of U_{eq} in the range 0.10–0.12 Å^2, while O(5W) was refined isotropically with a final temperature factor of 0.16 Å^2.

Table 6.11 Details of the data collection and refinement parameters for the EPTMB structure

Empirical formula	$C_{63}H_{112}O_{35}{\cdot}C_9H_{10}O_3{\cdot}5.0H_2O$
Formula weight	1685.8
Crystal system	Orthorhombic
Space group	$P2{\cdot}2_12_1$
a / Å	14.886 (2)
b / Å	22.024 (3)
c / Å	27.602 (1)
α / °	90
β / °	90
γ / °	90
Volume / Å^3	9049.3 (2)
Z	4
Density$_{calc}$ / g cm^{-3}	1.237
μ (MoKα) / mm^{-1}	0.102
F(000)	3632
Temperature of data collection / K	173 (2)
Crystal size / mm^3	0.70 x 0.60 x 0.50
Range scanned θ / °	$2 \leq \theta \leq 23$
Index ranges	h: -14, 15 k: -23, 18 l: -28, 30
ϕ scan angle / °	0.6
ϕ scan range, frames	159.6°, 266
ω scan angle / °	0.6
ω scan ranges, frames	72.6°, 121 and 25.8°, 43
Dx / mm	65.1
Total no. of reflections collected	20520
No. of independent reflections	10390
No. of reflections with $I > 2\sigma(I)$	8942
No. of parameters	914
R_{int}	0.0212
S	1.345
R_1 (for 6107 reflections)	0.1020
Reflections omitted	(0 1 1); (0 1 3); (0 1 5); (0 5 3); (1 0 2); (2 0 1); (2 0 2);
wR_2	0.2830
Weighting scheme	a = 0.2 b = 0.0
$(\Delta / \sigma)_{mean}$	< 0.000
$\Delta\rho$ excursions / e.Å^{-3}	0.96 and -0.56

The remaining water molecules, with a site-occupancy of less than one, were assigned a fixed isotropic temperature factor of 0.12 $Å^2$ [the mean of the preceding U values] while the site-occupancies were allowed to vary. The site-occupancies of these two water molecules [O(4W) and O(6W)] are 0.57 and 0.41 respectively, amounting to an additional 1.0 water molecule per asymmetric unit. This amounted to a total of 5.0 water molecules per asymmetric unit, which was equivalent to the number of water molecules observed from the TGA results presented earlier in this chapter. The hydrogen atoms of the water molecules were not located.

Once all the non-hydrogen atoms of the host and the water molecules had been located from the subsequent difference electron density map, the positions of the hydrogen atoms attached to methine and methylene groups on the CD were calculated. These hydrogen atoms were geometrically fixed at idealised positions in a riding model and were included in the refinement with the isotropic temperature factor of 1.2 times that of the attached carbon atom.

After further refinement, all the non-hydrogen atoms of the guest were located in the difference electron density map. The guest phenyl ring was modelled as a regular hexagon. The hydrogen atoms attached to the carbon atoms of the guest were also inserted at idealised positions and assigned a common isotropic temperature factor. The hydrogen atom of the hydroxyl group was placed using the rotating group refinement strategy [AFIX 83]. Placement of the C(12) atom was challenging as the electron density was low and diffuse. Numerous positions were refined and it was found that the *cis*-conformation of the C(11)–C(12) bond to the C(8)–O(10) bond, which is energetically the most favourable, was the most suitable position. Due to the abnormally long bond distances found in the guest molecule, distance constraints were placed on certain bonds, namely: O(1)–C(2) 1.351 Å; C(5)–C(8) 1.471 Å; C(8)–O(9) 1.207 Å; C(8)–O(10) 1.334 Å; O(10)–C(11) 1.448 Å; C(11)–C(12) 1.490 Å [all with σ = 0.005 Å]. The values chosen were taken from Lin.[15] Due to abnormally large bond angles, distance constraints were placed on non-bonded atoms to maintain the angles O(9)–C(8)–O(10), C(8)–O(10)–C(11) and O(10)–C(11)–C(12), close to the tetrahedral value of 109.5°. At the end of the refinement there were still three significant electron density peaks unaccounted for with heights of 0.96, 0.81 and 0.74 $e.Å^{-3}$, the highest electron density being located at a distance of 0.9 Å from C(6G2) while the lower electron density of 0.81 $e.Å^{-3}$ was located at a distance of 0.7 Å from C(6G5).

The possibility that these electron density peaks represented a disordered carbon atom was rejected on the basis of the unfavourable geometric position relative to those atoms already placed. The 0.74 e.Å^{-3} electron density was initially refined as water, with a s.o.f. of less than one, as it was at a favourable hydrogen bonding distance from O(5W). However this led to a short contact distance to the atom C(12) and thus this electron density was not accounted for in the final refinement.

Geometrical analysis of the EPTMB structure

The asymmetric unit of the EPTMB structure contains a single TRIMEB molecule, its associated guest and 5.0 water molecules. The glucose units will be referred to as G1, G2, G3, G4, G5, G6 and G7 and the structure and numbering scheme of the EPTMB complex and water molecules are shown in Figure 6.17. The geometrical data for the TRIMEB molecule are listed in Tables 6.12 and 6.13 [e.s.d.s are in the range 0.006-0.010 Å for distances and 0.1-0.6° for angles].

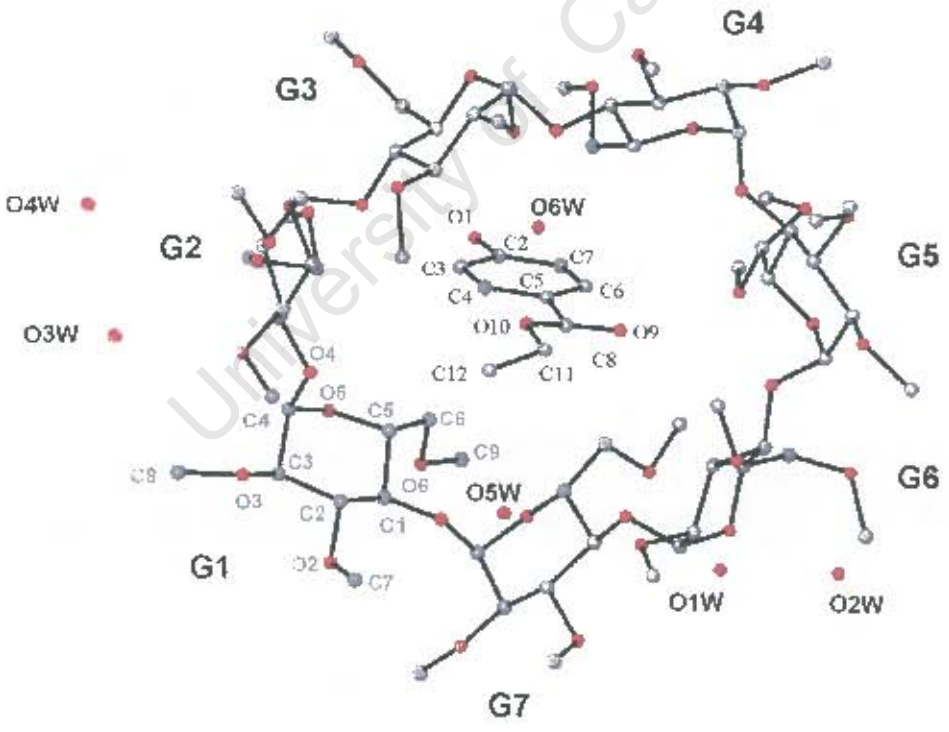

Figure 6.17 Macrocyclic structure and numbering scheme of glucose residues, water oxygen atoms and guest molecule, with the hydrogen atoms excluded. The host is viewed from the secondary face.

All seven methylglucose moieties of the TRIMEB molecule are in the $^4C_1$ chair conformation and the macrocycle is in the shape of an elliptically-distorted and truncated cone. The atoms C(7) and C(8) on O(2G3) and O(3G5) were disordered over two sites as well as the atom O(6) on C(6G2) and C(6G5), leading to disorder in the C(9) atoms. Methyl groups are located at the edge of the torus-shaped molecule. The O(2)–C(7) bonds point away from the centre of the macrocycle and are mostly *gauche* to the C(1)–C(2) bond. The O(3)–C(8) bonds are directed towards the cavity and are orientated roughly parallel to the molecular axis that is perpendicular to the plane through the seven O(4) atoms. The C(6)–O(6) bonds on all the glucose units are directed away from the cavity and are in the (-) *gauche* conformation, except for the C(6G5)–O(65A) bond which is pointed towards the cavity in the (+) *gauche* conformation. All the O(6)–C(9) bonds are *trans* to the respective C(5)–C(6) bonds, except in the G6 residue where the bond lies *gauche*. The O(6)–C(9) groups of the G5 residue [specifically O(65A)–C(95A)] and the G7 residue act as a "lid", closing off the O(6) side of the TRIMEB cavity, making it cup shaped.

The geometric parameters of the O(4) heptagon of the EPTMB structure are listed in Table 6.12. These include the radii, the O(4)•••O(4') distances, the O(4)•••O(4')•••O(4'') angles, the O(4)•••O(4')•••O(4'')•••O(4''') torsion angles and the deviations of each of the O(4) atoms from the mean O(4) plane. Table 6.13 lists the other important features of the macrocyclic structure such as the intersaccharidic bond angle (φ), the O(2)•••O(3') distance and the tilt angles [τ_1 and τ_2]. These parameters are defined in Chapter 1.

Table 6.12 Geometrical parameters of the O(4) heptagon for the EPTMB structure

Glucose unit	Radii (Å)	O(4)•••O(4') (Å)	O(4) angle (°)	Torsion angle (°)	Deviation (Å)
G1	5.74 (1)	4.42	122	10.9 (2)	0.51
G2	6.13 (1)	4.26	123	14.3 (3)	0.14
G3	5.41 (1)	4.57	127	-8.2 (3)	-0.51
G4	4.29 (1)	4.28	139	-22.5 (3)	-0.03
G5	4.56 (1)	4.32	116	26.1 (2)	0.67
G6	4.48 (1)	4.46	122	5.1 (3)	-0.37
G7	4.51 (1)	4.34	140	-31.0 (3)	-0.44
Average	5.02	4.37	127	|16.8|	|0.38|

Table 6.13 φ, O(2)•••O(3') distance, τ for the EPTMB structure

Glucose unit	φ (°)	O(2)•••O(3') (Å)	τ_1 (°)	τ_2 (°)
G1	117	3.21	29.3 (2)	16.4 (1)
G2	120	3.14	3.3 (2)	7.6 (2)
G3	118	3.35	-12.1 (2)	-18.7 (2)
G4	117	3.39	33.1 (1)	29.5 (3)
G5	119	3.80	33.1 (2)	19.9 (2)
G6	118	3.75	-17.2 (2)	-15.3 (1)
G7	116	3.45	33.0 (2)	47.3 (3)
Average	**118**	**3.44**	**23.0**	**22.1**

Generally, the bond lengths and bond angles conform to those of other known cyclodextrin complexes except in the case of some of the disordered atoms, as already mentioned. Usually in TRIMEB complexes two glucose moieties have a negative tilt angle, while the others have positive tilt angles[8, 9-12] and this is also seen in the EPTMB complex. The calculated parameters are in agreement with the corresponding ones in the TRIMEB-*p*-iodophenol complex,[6] whose host was used for the present structure solution by the isomorphous replacement technique.

Guest geometry and interactions for the EPTMB structure

The conformation of the ethyl paraben guest may be defined by three torsion angles. The torsion angles δ_1 [C(6)–C(5)–C(8)–O(9)], δ_2 [C(5)–C(8)–O(10)–C(11)] and δ_3 [C(8)–O(10)–C(11)–C(12)], will be used to describe rotation around the C(5)–C(8), C(8)–O(10) and O(10)–C(11) bonds respectively. They were compared with the conformation of the uncomplexed ethyl paraben molecule [Figure 6.18].[15]

The δ_1, δ_2, δ_3 torsion angles of the complexed ethyl paraben have a larger out-of-plane twist than those of the uncomplexed EP, indicating that inclusion allows for more rotational freedom around the C(5)–C(8), C(8)–O(10) and O(10)–C(11) bonds. The close contact distances for the relevant interactions between the host and guest molecule are listed in Table 6.14.

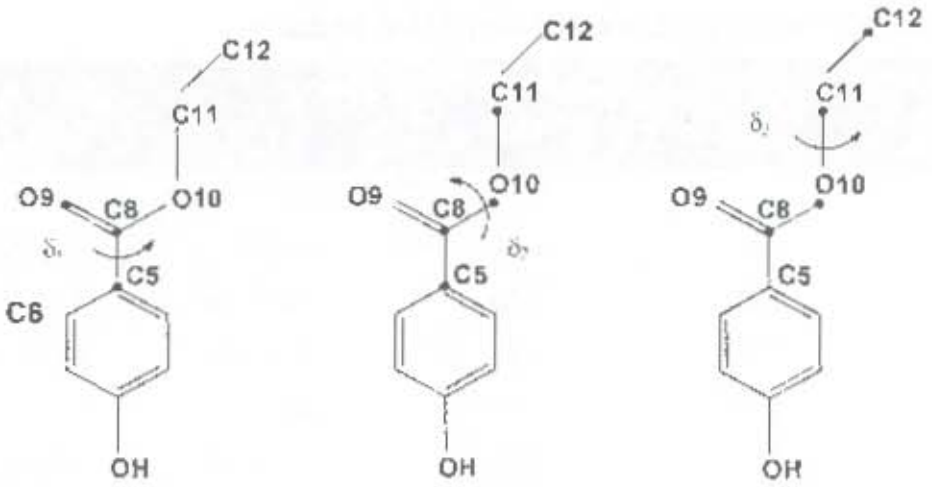

EP in complex :	δ_1 = +13 (2)	δ_2 = -179 (1)	δ_3 = -153 (1)
EP uncomplexed:[15]	δ_1 = +5.6	δ_2 = -179.7	δ_3 = -179.4

Figure 6.18 Torsion angles δ_1, δ_2 and δ_3 of the ethyl paraben

Table 6.14 Close contact distances for the EPTMB structure

Interaction	Distance (A)
C(3) ••• C(6G2)	3.17 (2)
C(3) ••• H(611)	2.83 (1)
H(3) ••• C(6G2)	2.27 (2)
H(3) ••• O(62B)	2.62 (1)
H(4) ••• H(521)	2.35
C(6) ••• C(6G4)	3.41 (2)
C(6) ••• H(641)	2.59 (1)
C(6) ••• H(671)	2.84 (1)
H(6) ••• O(65A)	2.43 (1)
H(6) ••• C(95A)	2.77 (1)
C(8) ••• H(672)	2.84 (1)
O(9) ••• H(551)	2.47 (1)
O(9) ••• H(672)	2.57 (1)
C(12) ••• H(831)	2.81 (2)
H(12C) ••• C(8G3)	2.46 (2)
H(12C) ••• H(831)	1.83
H(12C) ••• H(833)	2.31

The ethyl paraben guest molecule is held in the TRIMEB cavity by hydrophobic forces and is inserted from the O(2), O(3) side of the cyclodextrin molecule. The phenolic hydroxyl group protrudes from the primary rim of the host, while the ester moiety of the guest molecule is situated at the secondary face. The phenyl ring of the guest forms an angle of 87.6 (3)° with the mean O(4) plane. The tilting permits the guest to occupy most of the available space in the cavity. The guest makes a number of van der Waals contacts with the inside wall of the cavity. Figures 6.19 and 6.20 show CPK diagrams of the EPTMB structure, and include the O(5W) and O(6W) water oxygen atoms [which are light blue in colour].

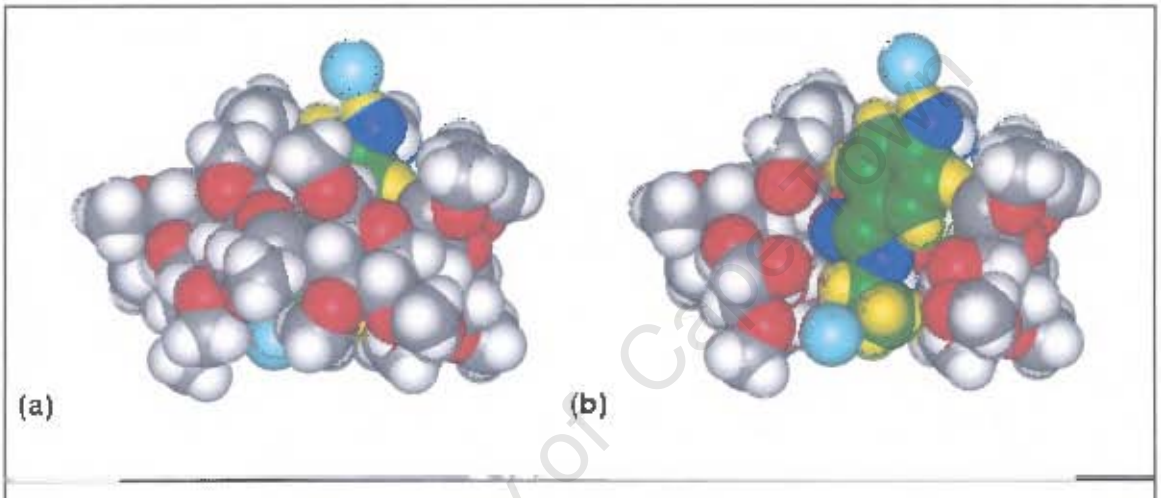

Figure 6.19 Space-filling diagram of the EPTMB structure (a) side view (b) sectioned view of the same orientation

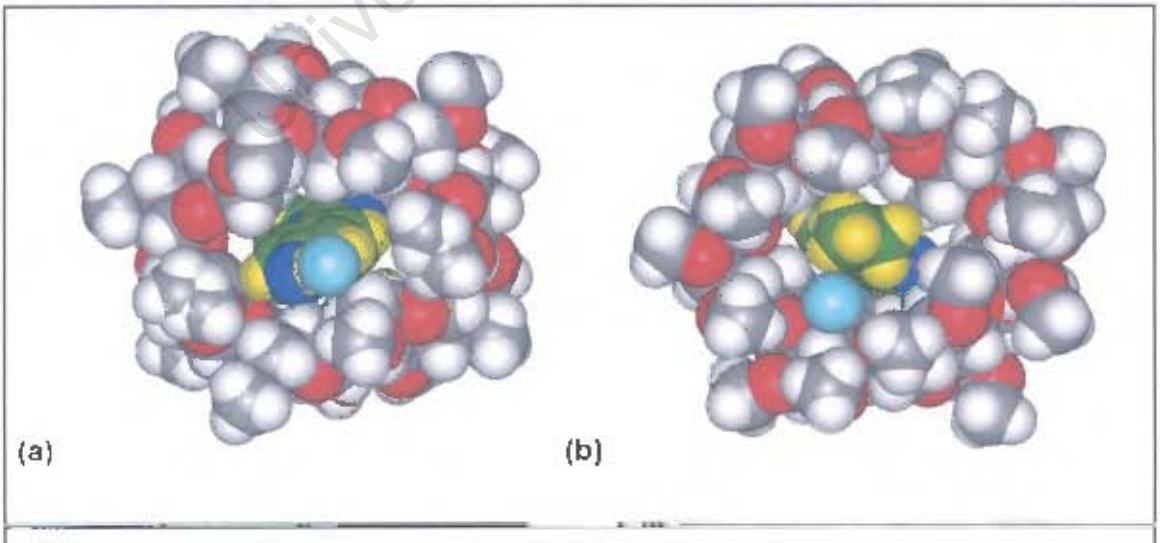

Figure 6.20 Space-filling diagram of the EPTMB structure (a) viewed from the primary rim (b) viewed from the secondary rim

Hydrogen bonding interactions of the EPTMB structure

Host interactions

The distorted conformation of the TRIMEB molecule relative to the conformation observed for the parent β-cyclodextrin molecule is stabilised by numerous intramolecular C–H•••O hydrogen bonds [Table 6.15].

The conformation of the TRIMEB molecule is stabilised by eleven intramolecular C–H•••O hydrogen bonds, three of which are of the type C(6)–H•••O(5'). In addition, there are two C(1)–H•••O(3') hydrogen bonds and a C(1)–H•••O(6') hydrogen bond [which stabilise the negative tilt angles of the G3 and G6 residues] and three C(8)–H•••O(2') hydrogen bonds, bonding adjacent glucose residues in the TRIMEB molecule. Furthermore there are stabilising intramolecular hydrogen bonds within some of the glucose units, namely a C(7)–H•••O(3) hydrogen bond and a C(8)–H•••O(2) hydrogen bond. The existence of these bonds has been confirmed by previous reports in other TRIMEB complexes and in uncomplexed TRIMEB.[3-14] All the C•••O distances are in the range 3.0-3.4 Å.

Table 6.15 Intramolecular C–H•••O hydrogen bonds in the EPTMB structure*

			Distance (Å)			Angle (°)
C	H	O	C–H	H•••O	C•••O	C–H•••O
C(1G3)	H(131)	O(3G4)	1.00	2.54	3.134 (9)	118.0 (4)
C(1G5)	H(151)	O(6G6)	1.00	2.44	3.174 (8)	130.2 (4)
C(1G6)	H(161)	O(3G7)	1.00	2.40	3.103 (9)	126.6 (5)
C(6G1)	H(612)	O(5G7)	0.99	2.49	3.12 (1)	121.4 (5)
C(6G3)	H(632)	O(5G2)	0.99	2.55	3.30 (1)	131.8 (5)
C(6G6)	H(662)	O(5G5)	0.99	2.33	3.099 (9)	134.1 (5)
C(7G6)	H(763)	O(3G6)	0.98	2.57	3.17 (1)	119.0 (7)
C(8G1)	H(811)	O(2G7)	0.98	2.73	3.32 (1)	119.9 (7)
C(8G2)	H(821)	O(2G1)	0.98	2.58	3.14 (1)	116.1 (6)
C(85A)	H(852)	O(2G4)	0.98	2.79	3.37 (2)	119 (1)
C(8G7)	H(873)	O(2G7)	0.98	2.60	3.16 (1)	116.6 (5)

* Hydrogen bonding parameters based on idealised hydrogen atom positions

Guest interactions

The guest hydroxyl oxygen atom is involved in hydrogen bonding with one water oxygen atom O(6W). The latter is also involved in hydrogen bonding to a symmetry related C(11), while C(12) is hydrogen bonded to the water oxygen atom of O(5W). The water oxygen atoms in turn form hydrogen bonds with the atoms on the host molecule. Hydrogen bonding contacts involving these water molecules are listed in Table 6.16.

Table 6.16 Hydrogen bonding contacts involving the guest*

			Distance (Å)			Angle (°)
Donor(D)	H	Acceptor(A)	D–H	H•••A	D•••A	D–H•••A
O(1)	H(1)	O(6W)	0.84	1.79	2.59 (3)	158 (1)
C(11)^{i}	H(11A)^{i}	O(6W)	0.99	2.17	3.12 (3)	160 (1)
C(12)	H(12B)	O(5W)	0.98	2.64	3.19 (2)	115 (1)

^{i} Related by symmetry operation: 2-x, $-\frac{1}{2}$+y, $\frac{1}{2}$-z

* Hydrogen bonding parameters based on idealised hydrogen atom positions.

Water interactions

Thermogravimetric analysis gave a weight loss which corresponds to 5.0 water molecules per 1:1 complex unit and these were all accounted for in the crystallographic analysis. Four of the water molecules [O(1W), O(2W), O(3W) and O(4W)] are situated at the periphery of the cyclodextrin molecule, filling a small intermolecular space between complex units. The oxygen atoms O(1W) and O(2W) are within hydrogen bonding distance of each other and they hydrogen bond to the host atoms O(5G3) and O(6G4) thus forming a bridge. The other two water molecules are located near the TRIMEB cavity, with O(5W) near the secondary rim and O(6W) near the primary rim [illustrated in Figure 6.19(b)]. The O(6W) water molecule is within hydrogen bonding contact to the guest as well as the host and therefore acts as a bridging atom. The contact distances of these intra-cavity water oxygen atoms are slightly longer than the sum of the van der Waals radii of two oxygen atoms, suggesting that these atoms are weakly hydrogen bonded to the host. Hydrogen bonding distances between the host and these water molecules are listed in Table 6.17.

Table 6.17 Hydrogen bonding distances involving the water molecules

Interaction	Distance (Å)	Symmetry operator for the second oxygen atom listed
O(1W) ••• O(5G3)	2.86 (1)	-1+x, y, z
O(1W) ••• O(6G7)	2.78 (1)	x, y, z
O(2W) ••• O(6G4)	2.76 (1)	-1+x, y, z
O(3W) ••• O(3G2)	2.82 (1)	x, y, z
O(4W) ••• O(5G4)	2.99 (2)	$2^1/_2$-x, 1-y, $^1/_2$+z
O(6W) ••• O(2G3)	2.98 (2)	2-x, $^1/_2$+y, $^1/_2$-z
O(1W) ••• O(2W)	2.67 (1)	x, y, z
O(2W) ••• O(3W)	2.75 (1)	$1^1/_2$-x, 1-y, $-^1/_2$+z
O(3W) ••• O(4W)	2.96 (2)	x, y, z
O(3W) ••• O(5W)	2.86 (1)	$^1/_2$+x, $^1/_2$-y, 1-z

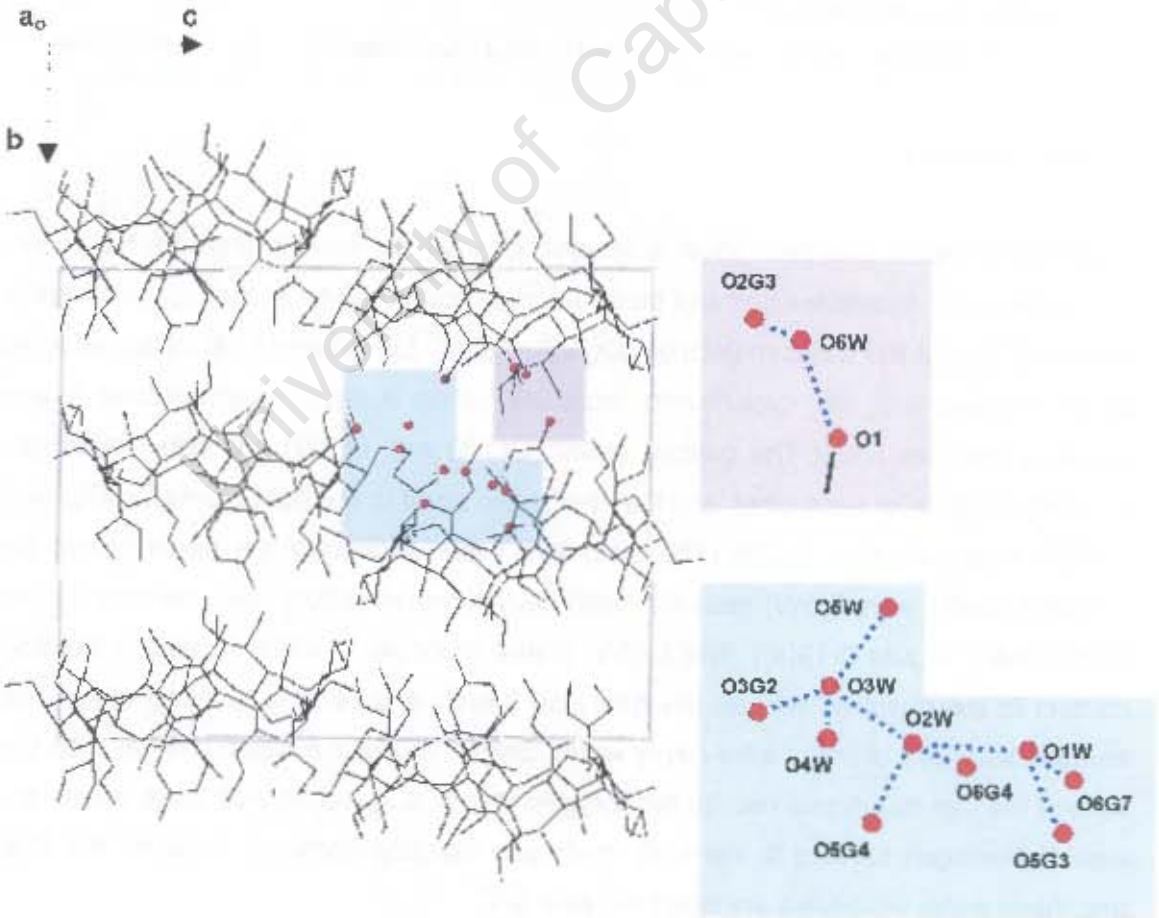

Figure 6.21 A schematic representation of guest and water interactions that connect adjacent host units

Crystal packing of the EPTMB structure

Figures 6.22 and 6.23 are extended stereo packing diagrams of the EPTMB structure showing projections as viewed down the *a*- and *b*-axes. Complex units pack in a screw-channel mode in a head-to-tail fashion with their axes almost parallel to the *b*-axis and the TRIMEB molecules are nearly parallel to the *ac*-plane. Two adjacent TRIMEB molecules, which are related by the two-fold screw axis parallel to *b*, are laterally shifted with respect to one another. As a result the channel does not run straight, but zigzags. This enables the guest molecule to have contact with the water molecules.

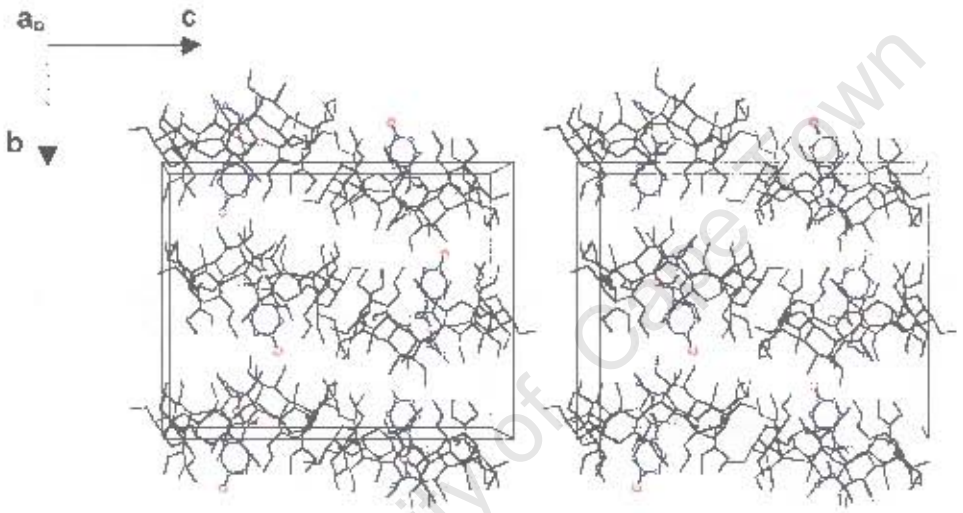

Figure 6.22 Stereo packing diagram of the EPTMB structure [*a*-axis projection]

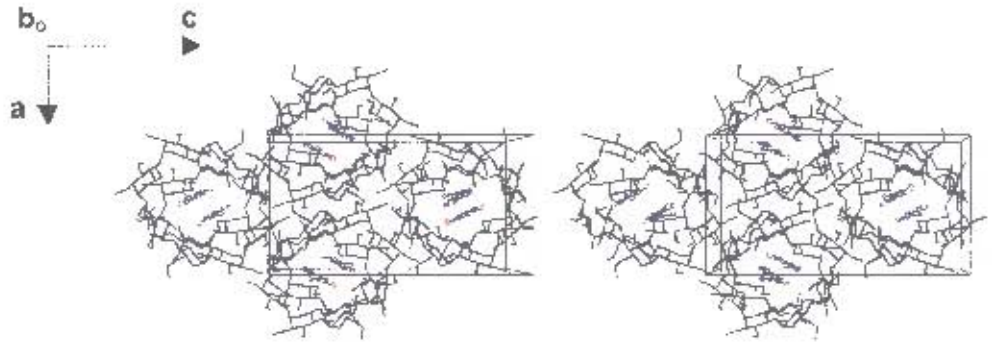

Figure 6.23 Stereo packing diagram of the EPTMB structure [*b*-axis projection]

Comparative XRD

The calculated and experimental XRD patterns for the EPTMB complex were successfully matched and are shown in Figure 6.24. The very close match in peak positions (2θ) show the high purity of the sample. The differences in relative intensities between the two patterns are due to preferred orientation of the crystallites.

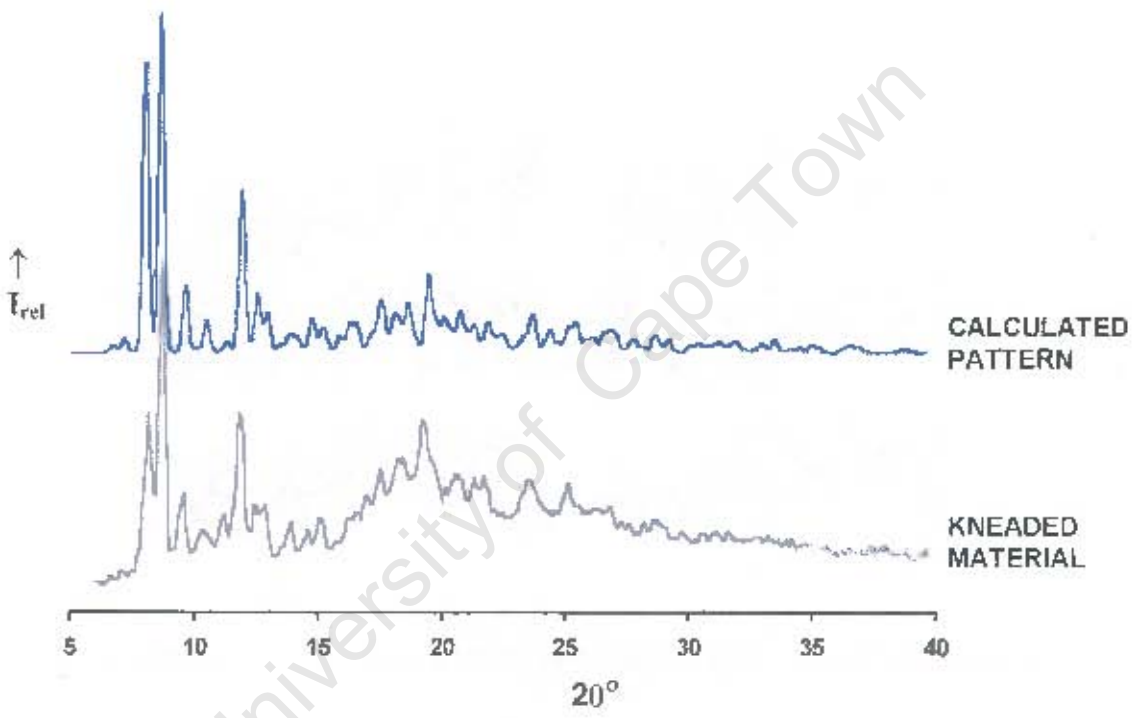

Figure 6.24 Experimental and calculated XRD traces for the EPTMB structure

X-RAY CRYSTALLOGRAPHIC ANALYSIS OF THE PPTMB STRUCTURE

Data-collection

The preliminary unit cell parameters and space group for the PPTMB structure were determined by X-ray photographic techniques. Oscillation and Weissenberg photography revealed Laue symmetry *mmm* corresponding to the orthorhombic system. The systematic absences observed are listed below and these confirmed the space group as $P2_12_12_1$.

hkl: none
h00: h = 2n + 1
0k0: k = 2n + 1
00l: l = 2n + 1

A crystal of the complex was mounted on a glass fibre and covered in Paratone N oil[2] to prevent cracking due to loss of water of crystallisation. Data were collected on the Nonius Kappa CCD diffractometer using graphite-monochromated MoKα radiation at 173(2) K. Crystal data and data-collection parameters are listed in Table 6.18.

Structure determination and refinement

The structure was solved using published co-ordinates for the non-hydrogen cyclodextrin atoms [excluding the O(6), C(7), C(8) and C(9) atoms of each methylglucose residue] of the isomorphous TRIMEB-*p*-iodophenol tetrahydrate complex.[6] The difference electron density map based on initial refinement in SHELX-97,[7] revealed the positions of most of the remaining non-hydrogen atoms. After further refinement it was found that the atoms O(6) on C(6G2) and C(6G5) were disordered, leading to disorder in the C(9) atoms. Two alternative positions were found for each disordered atom. For a given pair, a fixed U_{iso} of 0.07 Å^2 [the mean of U_{iso} for the chemically equivalent ordered atoms] was assigned and site-occupancy factors [s.o.f.'s] of x and 1-x were assigned, with x variable. Some of the bonds on these disordered atoms were either abnormally long or too short and thus distance constraints were placed on them. The O(2), O(3) and O(4) oxygen atoms on the host were refined anisotropically, as well as all the O(6) oxygen atoms that were not disordered. Refinement proceeded with the placement of water oxygen atoms, addition of geometrically fixed hydrogen atoms to CD carbon atoms and the placement of all CD methyl hydrogen atoms using the rotating group refinement [AFIX 137] strategy.

Table 6.18 Details of the data collection and refinement parameters for the PPTMB structure

Empirical formula	$C_{63}H_{112}O_{35}\cdot C_{10}H_{12}O_3\cdot 5.2H_2O$
Formula weight	1703.4
Crystal system	Orthorhombic
Space group	$P2_12_12_1$
a / Å	14.863 (1)
b / Å	21.862 (2)
c / Å	27.627 (3)
α / °	90
β / °	90
γ / °	90
Volume / Å^3	8977.0 (1)
Z	4
$Density_{calc}$ / g cm^{-3}	1.260
μ (MoKα) / mm^{-1}	0.104
F(000)	3672
Temperature of data collection / K	173 (2)
Crystal size / mm^3	0.58 x 0.25 x 0.25
Range scanned θ / °	$2 \leq \theta \leq 20$
Index ranges	h: -13, 9 k: -14, 19 l: -24, 23
ϕ scan angle / °	0.5
ϕ scan range, frames	119.5°, 239
ω scan angle / °	0.5
ω scan ranges, frames	56.0°, 112
Dx / mm	62.7
Total no. of reflections collected	12271
No. of independent reflections	6006
No. of reflections with $I > 2\sigma(I)$	5023
No. of parameters	609
R_{int}	0.0327
S	1.074
R_1 (for 3571 reflections)	0.1176
Reflections omitted	(0 0 4); (0 2 0); (0 2 1); (1 0 1); (1 0 2); (1 1 1); (-1 1 1)
wR_2	0.3037
Weighting scheme	a = 0.1738 b = 56.5160
$(\Delta / \sigma)_{mean}$	< 0.000
$\Delta\rho$ excursions / e.Å^{-3}	0.74 and -0.60

All the methyl hydrogen atoms were assigned a common variable isotropic temperature factor and the remaining hydrogen atoms of each glucose moiety were assigned common variable isotropic temperature factors.

After many successive refinements, three water molecules [O(1W), O(2W) and O(3W)] with full site-occupancy were placed and refined anisotropically with a final temperature factor U_{eq} in the range 0.12–0.17 $Å^2$. A further three water molecules [O(4W), O(5W) and O(6W)] with a site-occupancy of less than one were refined with a fixed isotropic temperature factor of 0.14 $Å^2$ [the mean of the preceding U values] and varying site-occupancy. The site-occupancies of these water molecules are 0.76, 0.69 and 0.46 respectively, and they amounted to a further 1.9 water molecules per asymmetric unit. A total of 4.9 water molecules per asymmetric unit were accounted for, which compared favourably with the 5.2 water molecules expected from the TGA results. The hydrogen atoms of the water molecules were not located.

Refinement continued with the placement of the non-hydrogen atoms of the guest. The guest phenyl ring was modelled as a regular hexagon and hydrogen atoms attached to the carbon atoms of the guest were also inserted at idealised positions and assigned a common isotropic temperature factor. The hydrogen atom of the hydroxyl group was placed using the rotating group refinement strategy [AFIX 83]. Due to the abnormally long bond distances found in the guest molecule, distance constraints were placed on certain bonds, namely: O(1)–C(2) 1.351 Å; C(5)–C(8) 1.471 Å; C(8)–O(9) 1.207 Å; C(8)–O(10) 1.334 Å; O(10)–C(11) 1.448 Å; C(11)–C(12) 1.490 Å, C(12)–C(13) 1.490 Å [all with σ = 0.005 Å]. The values chosen were taken from Lin.[15] Due to abnormally large bond angles, distance constraints were placed on non-bonded atoms to maintain the angles O(9)–C(8)–O(10), C(8)–O(10)–C(11), O(10)–C(11)–C(12) and C(11)–C(12)–C(13) close to the tetrahedral value of 109.5°.

The anomaly seen in the MPTMB and EPTMB structures of the high density electron peaks being located in the vicinity of the disordered O(6) was also seen in this structure, although the electron density was not significant. An electron density of 0.73 $e.Å^{-3}$ was located at a distance of 0.8 Å from C(6G2).

Geometrical analysis of the PPTMB structure

The asymmetric unit of the PPTMB structure contains a single TRIMEB molecule, its associated guest and 5.2 water molecules. The glucose units will be referred to as G1, G2, G3, G4, G5, G6 and G7 and the structure and numbering scheme of the PPTMB complex and water molecules are shown in Figure 6.25. The geometrical data for the TRIMEB molecule are listed in Tables 6.19 and 6.20 [e.s.d.s are in the range 0.013-0.020 Å for distances and 0.3-1.3° for angles].

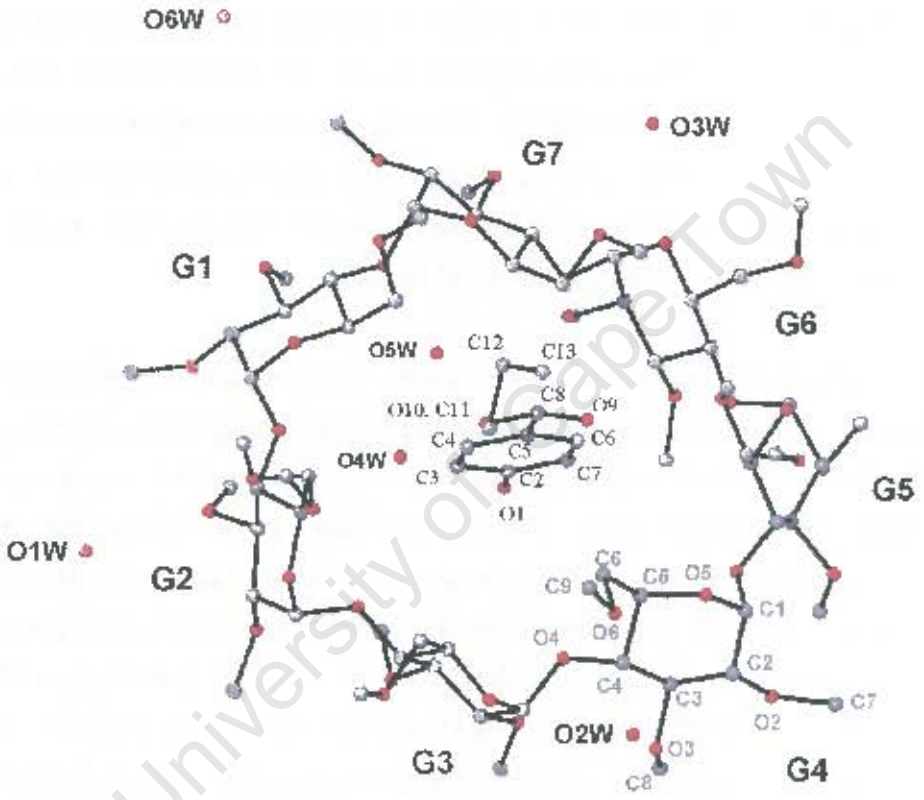

Figure 6.25 Macrocyclic structure and numbering scheme of glucose residues, water oxygen atoms and guest molecule, with the hydrogen atoms excluded. The host is viewed from the primary face.

All seven methylglucose moieties of the TRIMEB molecule are in the $^4C_1$ chair conformation, with the O(2)–C(7) bonds directed away from the cavity and the O(3)–C(8) bonds directed towards the cavity. The atoms O(6) on C(6G2), C(6G5) were disordered over two sites each leading to disorder in the C(9) atoms. The C(6)–O(6) bonds on all the glucose units are in the (-) *gauche* conformation and are directed away from the cavity, except for the C(6G5)–O(65A) bond which is pointed towards the cavity in the (+) *gauche* conformation. All the O(6)–C(9) bonds are *trans* to the respective C(5)–C(6) bonds, except in the G6 residue where the bond lies *gauche*.

The O(6)–C(9) groups of the G5 residue [specifically O(65A)–C(95A)] and the G7 residue act as a "lid", closing off the O(6) side of the TRIMEB cavity, making it cup shaped.

The geometric parameters of the O(4) heptagon of the PPTMB structure are listed in Table 6.19. These include the radii, the O(4)•••O(4') distances, the O(4)•••O(4')•••O(4'') angles, the O(4)•••O(4')•••O(4'')•••O(4''') torsion angles and the deviations of each of the O(4) atoms from the mean O(4) plane. Table 6.20 lists the other important features of the macrocyclic structure such as the intersaccharidic bond angle (φ), the O(2)•••O(3') distance and the tilt angles [τ_1 and τ_2]. These parameters are defined in Chapter 1. The calculated parameters show good agreement with those for the complex of TRIMEB with *p*-iodophenol[6] and are comparable to those for the complex formed with ethyl paraben, pages 232-233.

Table 6.19 Geometrical parameters of the O(4) heptagon for the PPTMB structure

Glucose unit	Radii (A)	O(4)•••O(4') (A)	O(4) angle (°)	Torsion angle (°)	Deviation (A)
G1	5.70 (1)	4.40	122	12.2 (5)	0.53
G2	6.05 (1)	4.22	123	12.8 (5)	0.12
G3	5.30 (1)	4.57	128	-8.3 (6)	-0.47
G4	4.28 (2)	4.28	139	-21.1 (6)	0.01
G5	4.64 (1)	4.31	116	25.4 (5)	0.67
G6	4.54 (1)	4.48	123	4.4 (7)	-0.35
G7	4.54 (2)	4.31	140	-30.6 (6)	-0.40
Average	**5.01**	**4.37**	**127**	**16.4**	**0.36**

Table 6.20 φ, O(2)•••O(3') distance, τ for the PPTMB structure

Glucose unit	φ (°)	O(2)•••O(3') (A)	τ_1 (°)	τ_2 (°)
G1	117	3.17	29.5 (3)	15.9 (3)
G2	115	3.16	4.7 (4)	7.6 (3)
G3	120	3.35	-13.4 (4)	-18.0 (4)
G4	117	3.36	32.4 (3)	29.1 (8)
G5	120	3.79	32.4 (4)	18.6 (4)
G6	118	3.72	-18.0 (4)	-15.4 (3)
G7	115	3.47	31.5 (3)	46.1 (5)
Average	**117**	**3.42**	**23.1**	**21.5**

Guest geometry and interactions for the PPTMB structure

The conformation of the propyl paraben guest may be defined by four torsion angles. The torsion angles listed below will be used to describe the rotation around each of the corresponding bonds [Figure 6.26]. This conformation is favoured as it reduces the width of the paraben molecule. The close contact distances for the relevant interactions between the host and guest molecule are listed in Table 6.21.

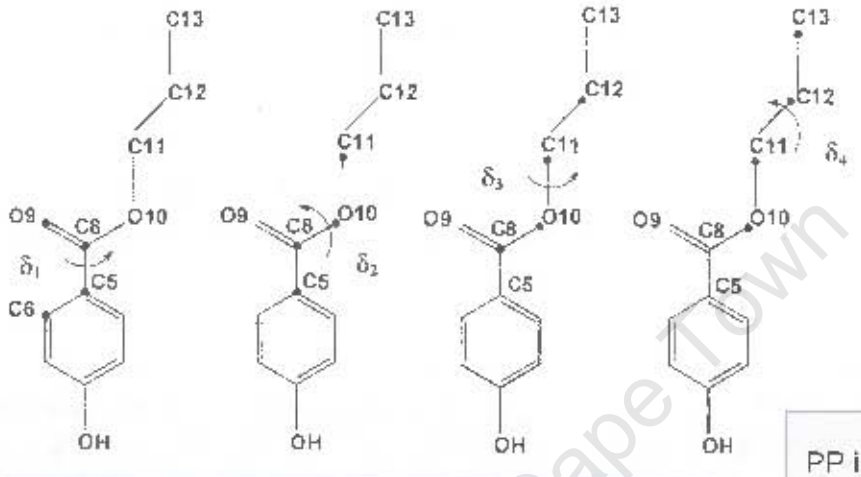

δ_1 C(6)–C(5)–C(8)–O(9)	➡	C(5)–C(8)
δ_2 C(5)–C(8)–O(10)–C(11)	➡	C(8)–O(10)
δ_3 C(8)–O(10)–C(11)–C(12)	➡	O(10)–C(11)
δ_4 O(10)–C(11)–C(12)–C(13)	➡	C(11)–C(12)

PP in complex:
δ_1 = -23 (2)
δ_2 = +159 (2)
δ_3 = +69 (2)
δ_4 = -140 (2)

Figure 6.26 Torsion angles δ_1, δ_2, δ_3 and δ_4 of the propyl paraben

Table 6.21 Close contact distances for the PPTMB structure

Interaction	Distance (Å)
H(4) ••• H(521)	2.38
C(5) ••• H(671)	2.95 (1)
C(6) ••• C(6G7)	3.37 (3)
C(6) ••• H(672)	2.77 (2)
H(6) ••• O(65A)	2.48 (2)
H(7) ••• H(551)	2.37
H(11A) ••• H(941)	2.28
H(11B) ••• C(8G6)^{i}	2.81 (3)
H(12B) ••• H(732)^{i}	2.27
C(13) ••• O(2G3)^{i}	2.98 (4)
H(13A) ••• O(2G3)^{i}	2.16 (1)

^{i}Related by symmetry operation: 2-x, $^{1}/_{2}$+y, $^{1}/_{2}$-z

The phenolic hydroxyl group is situated at the secondary rim of the host, while the ester moiety of the guest molecule protrudes from the primary face. The phenyl ring of the guest forms an angle of 89.9 (4)° with the mean O(4) plane. Figures 6.27 and 6.28 show CPK diagrams of the PPTMB structure, and include the O(4W) and O(5W) water oxygen atoms [which are light blue in colour].

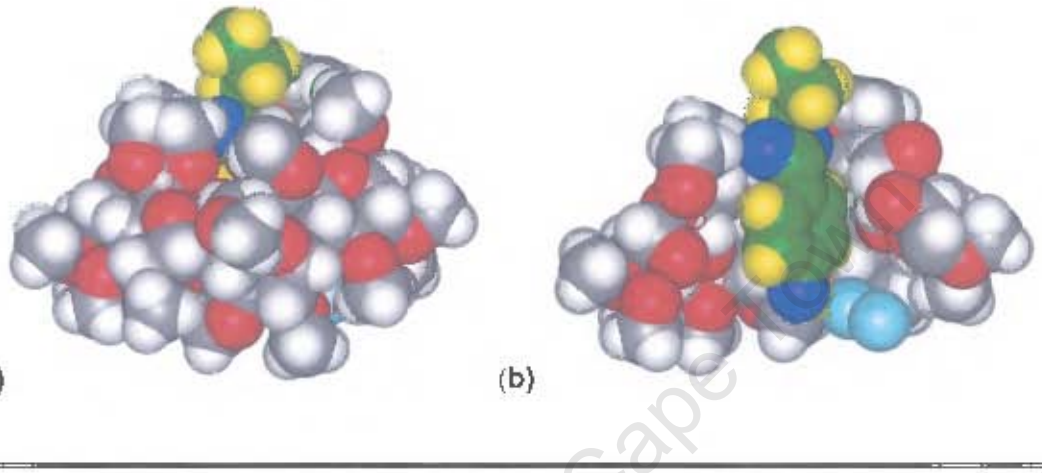

Figure 6.27 Space-filling diagram of the PPTMB structure (a) side view (b) sectioned view of the same orientation

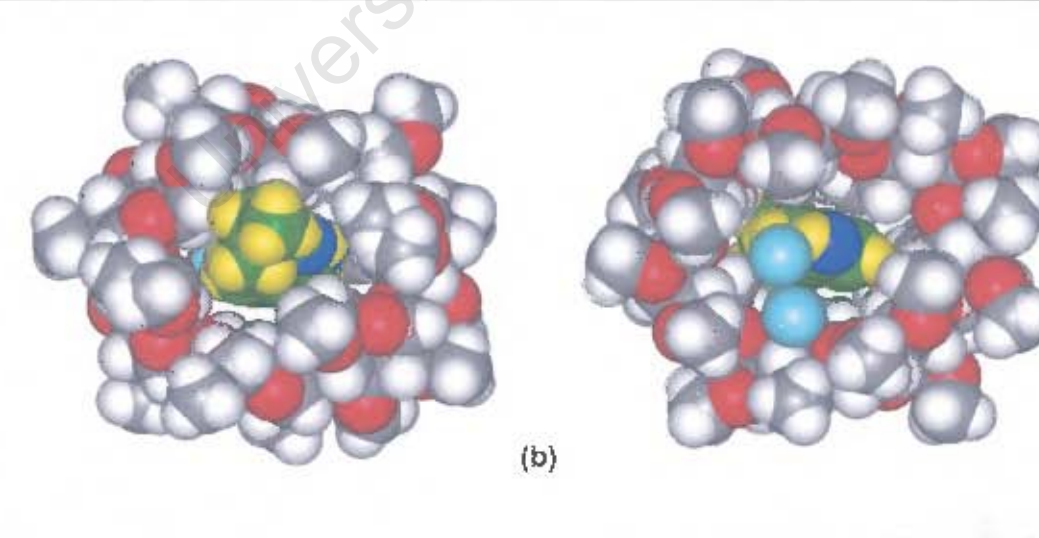

Figure 6.28 Space-filling diagram of the PPTMB structure (a) viewed from the primary rim (b) viewed from the secondary rim

Hydrogen bonding interactions of the PPTMB structure

Host interactions

The conformation of the TRIMEB molecule is stabilised by twelve intramolecular C–H•••O hydrogen bonds [Table 6.22], three of which are of the type C(6)–H•••O(5'). In addition, there are two C(1)–H•••O(3') hydrogen bonds, a C(1)–H•••O(6') hydrogen bond [which stabilise the negative tilt angles of the G3 and G6 residues], two C(8)–H•••O(2') hydrogen bonds and a C(9)–H•••O(5') hydrogen bond. Furthermore there are stabilising intramolecular hydrogen bonds within some of the glucose units, namely a C(7)–H•••O(3) hydrogen bond and two C(8)–H•••O(2) hydrogen bonds. All the C•••O distances are in the range 3.0-3.3 Å.

Table 6.22 Intramolecular C–H•••O hydrogen bonds in the PPTMB structure*

			Distance (Å)			Angle (°)
C	H	O	C–H	H•••O	C•••O	C–H•••O
C(1G3)	H(131)	O(3G4)	1.00	2.60	3.17 (2)	116.9 (9)
C(1G5)	H(151)	O(6G6)	1.00	2.37	3.10 (2)	130 (1)
C(1G6)	H(161)	O(3G7)	1.00	2.43	3.13 (2)	126 (1)
C(6G1)	H(612)	O(5G7)	0.99	2.43	3.08 (2)	123 (1)
C(6G3)	H(632)	O(5G2)	0.99	2.57	3.31 (2)	132 (1)
C(6G6)	H(662)	O(5G5)	0.99	2.36	3.09 (2)	130 (1)
C(7G3)	H(733)	O(3G3)	0.98	2.55	3.16 (3)	120 (2)
C(8G2)	H(821)	O(2G1)	0.98	2.39	3.11 (2)	130 (1)
C(8G3)	H(832)	O(2G2)	0.98	2.33	3.06 (3)	131 (2)
C(8G5)	H(853)	O(2G5)	0.98	2.59	3.18 (3)	119 (2)
C(8G7)	H(873)	O(2G7)	0.98	2.58	3.15 (2)	117 (1)
C(9G1)	H(913)	O(5G7)	0.98	2.72	3.34 (3)	122 (1)

* Hydrogen bonding parameters based on idealised hydrogen atom positions.

Guest interactions

The guest hydroxyl oxygen atom is involved in hydrogen bonding with one water oxygen atom O(4W). The atom C(13) of the propyl moiety is involved in hydrogen bonding to an oxygen atom on the secondary rim. Hydrogen bonding contacts with these water molecules are listed in Table 6.23. The O(1)–H•••O(4W) bond may be classified as a strong hydrogen bond from the O•••O distance of 2.51(4) Å.[16]

Table 6.23 Hydrogen bonding contacts involving the guest*

			Distance (A)			Angle (°)
Donor(D)	H	Acceptor(A)	D–H	H•••A	D•••A	D–H•••A
O(1)	H(1)	O(4W)	0.84	1.83	2.51 (4)	137 (2)
C(13)^{i}	H(13C)^{i}	O(1)^{i}	0.98	2.64	3.01 (5)	107 (2)
C(13)^{i}	H(13A)^{i}	O(2G3)^{i}	0.98	2.16	2.98 (4)	141 (2)

^{i} Related by symmetry operation: 2-x, $^{1}/_{2}$+y, $^{1}/_{2}$-z

* Hydrogen bonding parameters based on idealised hydrogen atom positions.

Water interactions

The distribution of the water molecules is such that four of the water molecules [O(1W), O(2W), O(3W) and O(6W)] are situated at the periphery of the cyclodextrin molecule, filling a small intermolecular space between complex units. The other two water molecules [O(4W) and O(5W)] are located within the TRIMEB cavity near the secondary rim [illustrated in Figure 6.28(b)]. These water molecules do not bond directly to a cyclodextrin molecule but are connected to the other intra-cavity water molecule. Hydrogen bonding distances between the host and these water molecules are listed in Table 6.24 and are illustrated in Figure 6.29.

Table 6.24 Hydrogen bonding distances involving the water molecules

Interaction	Distance (A)	Symmetry operator for the second oxygen atom listed
O(1W) ••• O(3G2)	2.84 (2)	x, y, z
O(2W) ••• O(6G4)	2.75 (2)	x, y, z
O(3W) ••• O(5G3)	2.87 (2)	-1+x, y, z
O(3W) ••• O(6G7)	2.74 (2)	x, y, z
O(6W) ••• O(5G4)	2.97 (4)	$1^{1}/_{2}$-x, 1-y, $^{1}/_{2}$+z
O(1W) ••• O(2W)	2.69 (3)	$2^{1}/_{2}$-x, 1-y, $^{1}/_{2}$+z
O(1W) ••• O(5W)	2.82 (3)	$^{1}/_{2}$+x, $^{1}/_{2}$-y, 1-z
O(1W) ••• O(6W)	2.90 (4)	1+x, y, z
O(2W) ••• O(3W)	2.75 (3)	1+x, y, z
O(4W) ••• O(5W)	2.62 (4)	x, y, z

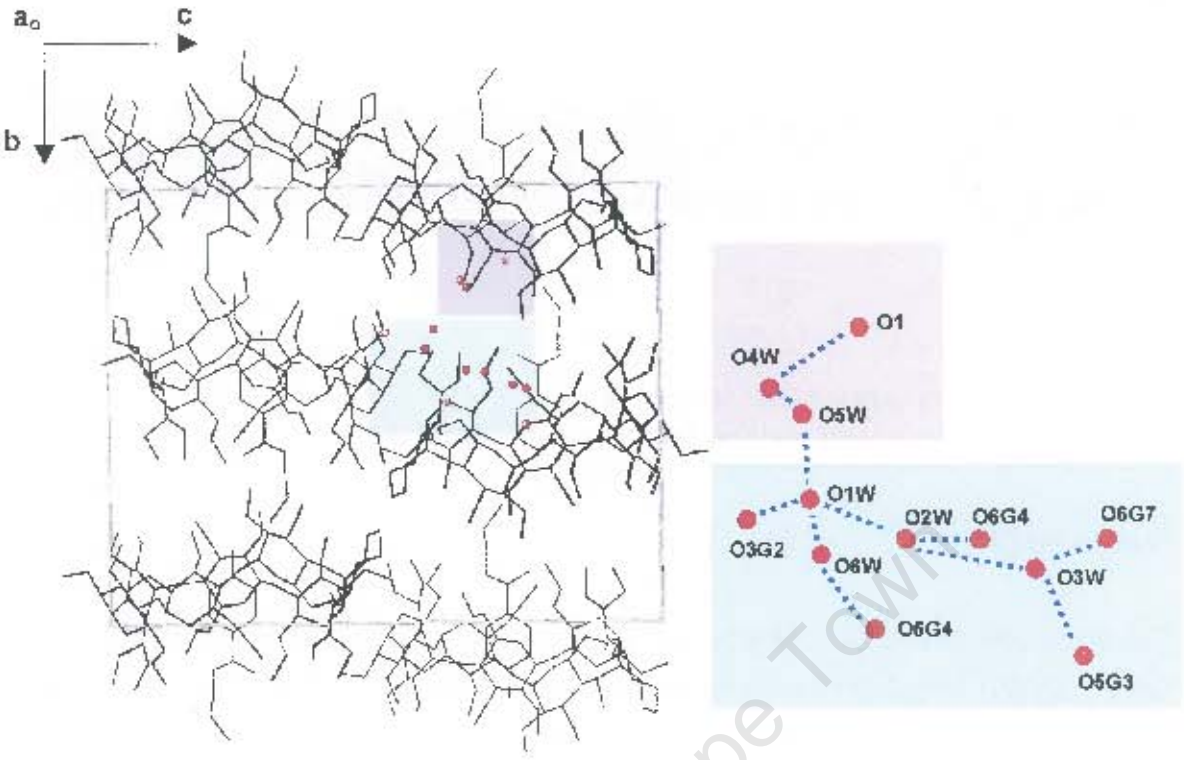

Figure 6.29 A schematic representation of guest and water interactions that connect adjacent host units

Crystal packing of the PPTMB structure

Figures 6.30 and 6.31 are extended stereo packing diagrams of the PPTMB structure showing projections as viewed down the *a*- and *b*-axes. Complex units pack in a screw-channel mode in a head-to-tail fashion with their axes almost parallel to the *b*-axis. This type of packing allows for the penetration of the alkyl chain into the secondary side of the CD "above" it.

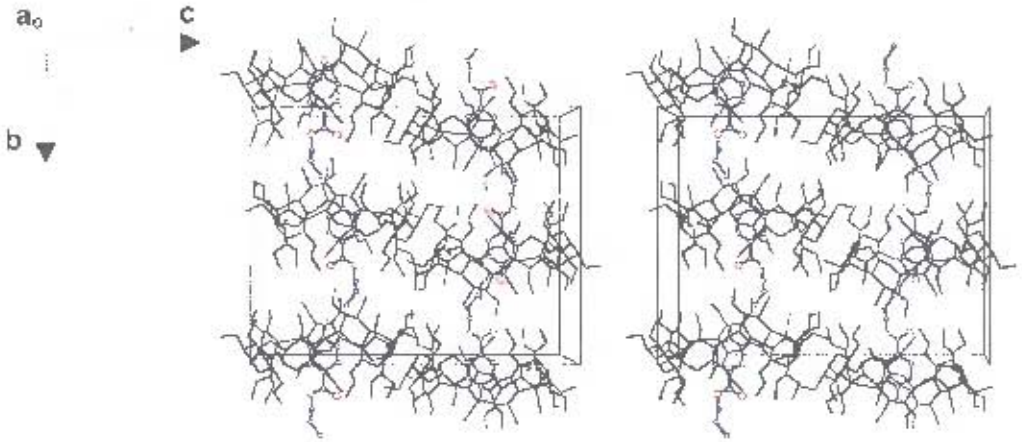

Figure 6.30 Stereo packing diagram of the PPTMB structure [*a*-axis projection]

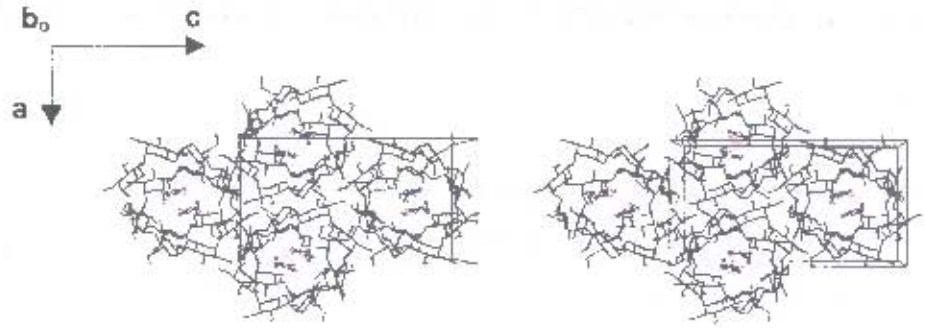

Figure 6.31 Stereo packing diagram of the PPTMB structure [*b*-axis projection]

Comparative XRD

The calculated and experimental XRD patterns for the PPTMB complex were successfully matched and are shown in Figure 6.32. The very close match in peak positions (2θ) is evidence for the high purity of the sample. The differences in relative intensities between the two patterns are due to preferred orientation of the crystallites.

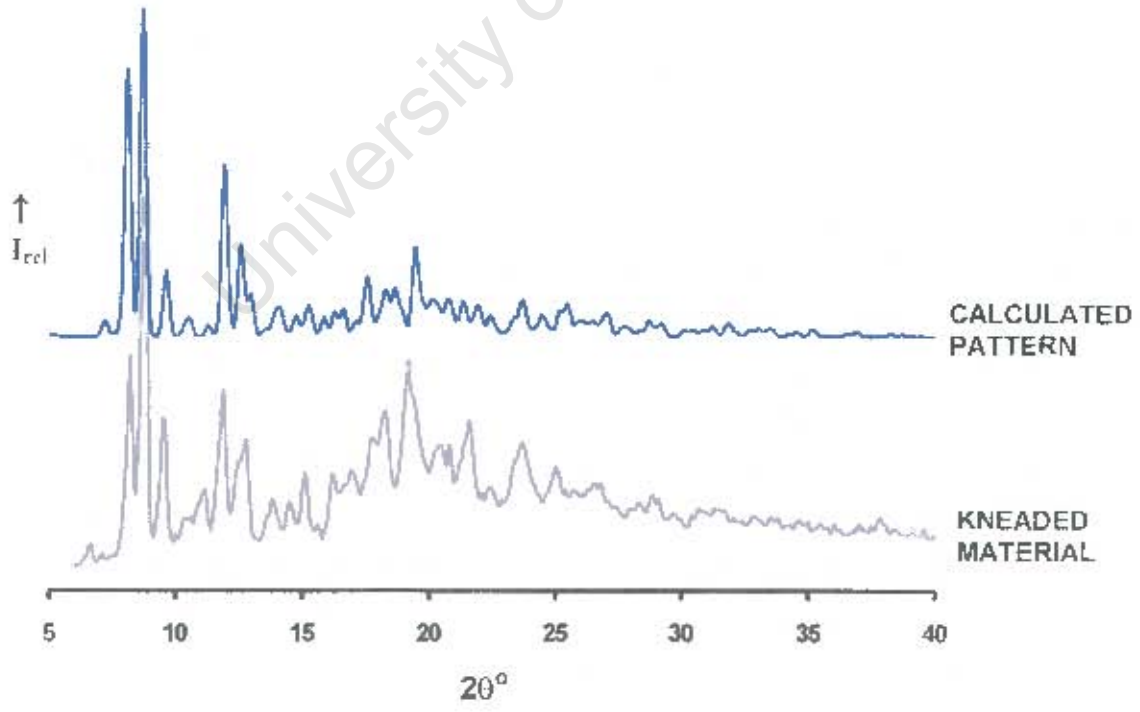

Figure 6.32 Experimental and calculated XRD traces for the PPTMB structure

X-RAY CRYSTALLOGRAPHIC ANALYSIS OF THE BPTMB STRUCTURE

Data-collection

The preliminary unit cell parameters and space group for the BPTMB structure were determined by X-ray photographic techniques. Oscillation and Weissenberg photography revealed Laue symmetry *mmm*, corresponding to the orthorhombic system. The systematic absences observed are listed below and these confirmed the space group as $P2_12_12_1$.

hkl: none
h00: h = 2n + 1
0k0: k = 2n + 1
00l: l = 2n + 1

A crystal of the complex was mounted on a glass fibre and covered in Paratone N oil[7] to prevent cracking due to loss of water of crystallisation. Data were collected at 173 K on the Nonius Kappa CCD diffractometer using graphite-monochromated MoKα radiation. Crystal data and data-collection parameters are listed in Table 6.25.

Structure determination and refinement

The structure was solved using published co-ordinates for the non-hydrogen cyclodextrin atoms [excluding the O(6), C(7), C(8) and C(9) atoms of each methylglucose residue] of the isomorphous TRIMEB-*p*-iodophenol tetrahydrate complex.[6] After refinement in SHELX-97,[7] the difference Fourier map revealed the positions of most of the remaining non-hydrogen atoms. After further refinement it was found that the atoms C(7) and C(8) on O(2G3) and O(3G5) were disordered as well as the atom O(6) on C(6G2), C(6G5), leading to disorder in the C(9) atoms. The atoms that showed disorder were assigned a fixed isotropic temperature factor of 0.07 Å^2 [the mean of the preceding U values] and the s.o.f.'s were allowed to vary. Some of the bonds on these disordered atoms were either abnormally long or too short and thus distance constraints were placed on these bonds. All the non-hydrogen atoms on the host, except the disordered atoms, C(6G2), C(7G5), C(7G6), C(8G1), C(8G6) and C(9G6) were refined anisotropically. Refinement continued with the placement of the water oxygen atoms, for which six positions were located. O(1W), O(2W) and O(3W) were assigned a full site-occupancy factor and refined anisotropically with a final temperature factor of U_{eq} in the range 0.10–0.14 Å^2.

Table 6.25 Details of the data collection and refinement parameters for the BPTMB structure

Empirical formula	$C_{63}H_{112}O_{35}$•$C_{11}H_{14}O_3$•$5.6H_2O$
Formula weight	1724.6
Crystal system	Orthorhombic
Space group	$P2_12_12_1$
a / Å	14.866 (2)
b / Å	21.967 (2)
c / Å	27.635 (4)
α / °	90
β / °	90
γ / °	90
Volume / $Å^3$	9024 (2)
Z	4
$Density_{calc}$ / g cm^{-3}	1.269
μ (MoKα) / mm^{-1}	0.104
F(000)	3720
Temperature of data collection / K	173 (2)
Crystal size / mm^3	0.45 x 0.40 x 0.35
Range scanned θ / °	$2 \leq \theta \leq 22$
Index ranges	h: -15, 15 k: -22, 23 l: -18, 29
ϕ scan angle / °	0.9
ϕ scan range, frames	180.0°, 200
ω scan angle / °	0.9
ω scan ranges, frames	57.6°, 64 and 73.8°, 82
Dx / mm	60.0
Total no. of reflections collected	22421
No. of independent reflections	11006
No. of reflections with $I > 2\sigma I$	8811
No. of parameters	924
Rint	0.0243
S	1.040
R_1 (for 6247 reflections)	0.0993
Reflections omitted	(0 0 2); (0 0 4); (0 1 3); (0 2 0); (1 0 2); (1 1 0); (1 0 1); (1 1 1); (-1 1 1)
wR_2	0.2658
Weighting scheme	a = 0.1903 b = 13.3291
$(\Delta / \sigma)_{mean}$	< 0.001
$\Delta\rho$ excursions / $e.Å^{-3}$	0.99 and -0.62

The remaining water molecules, with a site-occupancy of less than one, were assigned a fixed isotropic temperature factor of 0.14 $Å^2$ [the mean of the preceding U values] while the site-occupancies were allowed to vary. The site-occupancies of O(4W), O(5W) and O(6W) are 0.51, 0.65 and 0.64 respectively, amounting to an additional 1.8 water molecules per asymmetric unit. This amounted to a total of 4.8 water molecules per asymmetric unit which were accounted for, as compared to the 5.6 water molecules expected from the TGA results presented earlier in this chapter. The hydrogen atoms of the water molecules were not located. Once all the non-hydrogen atoms of the host and the water molecules had been located from subsequent difference electron density maps, all the cyclodextrin hydrogen atoms were placed. These hydrogen atoms were geometrically fixed at idealised positions in a riding-model. The thermal parameters of the primary, secondary and tertiary hydrogen atoms were kept constant at 0.15, 0.15 and 0.12 $Å^2$ respectively.

After further refinement all the non-hydrogen atoms of the guest [except C(14)] were located in the difference electron density map. The guest phenyl ring was modelled as a rigid hexagon. The hydrogen atoms attached to the carbon atoms of the guest were also inserted at idealised positions and assigned a common isotropic temperature factor. The hydrogen atom of the hydroxyl group was placed using the rotating group refinement strategy [AFIX 83]. Placement of the C(14) atom was challenging as the electron density was low and diffuse. Using WebLab Viewer,[17] the C(14) atom was rotated around the bond C(12)–C(13) and the most suitable position, that minimised the number of abnormally close contacts, was attained. Due to the abnormally long bond distances found in the guest molecule, distance constraints were placed on certain bonds, namely: O(1)–C(2) 1.351 Å; C(5)–C(8) 1.471 Å; C(8)–O(9) 1.207 Å; C(8)–O(10) 1.334 Å; O(10)–C(11) 1.448 Å; C(11)–C(12) 1.490 Å, C(12)–C(13) 1.490 Å, C(13)–C(14) 1.490 Å [all with σ = 0.005 Å]. The values chosen were taken from Lin.[15] Due to abnormally large bond angles distance constraints were placed on non-bonded atoms to maintain the angles O(9)–C(8)–O(10), C(8)–O(10)–C(11), O(10)–C(11)–C(12), C(11)–C(12)–C(13) and C(12)–C(13)–C(14) close to the tetrahedral value [109.5°]. At the end of the refinement there was still one significant electron density peak unaccounted for with a height of 0.99 $e.Å^{-3}$ at a distance of 0.8 Å from C(6G2). The possibility that this electron density peak represented a disordered carbon atom was rejected on the basis of the unfavourable geometric position relative to those atoms already placed.

Geometrical analysis of the BPTMB structure

The asymmetric unit of the BPTMB structure contains a single TRIMEB molecule, its associated guest and 5.6 water molecules. The seven glucosidic residues have been assigned the Gn notation and the structure and numbering scheme of the BPTMB complex and water molecules are shown in Figure 6.33. The geometrical data for the TRIMEB molecule are listed in Tables 6.26 and 6.27 [e.s.d.s are in the range 0.007-0.010 Å for distances and 0.1-0.6° for angles].

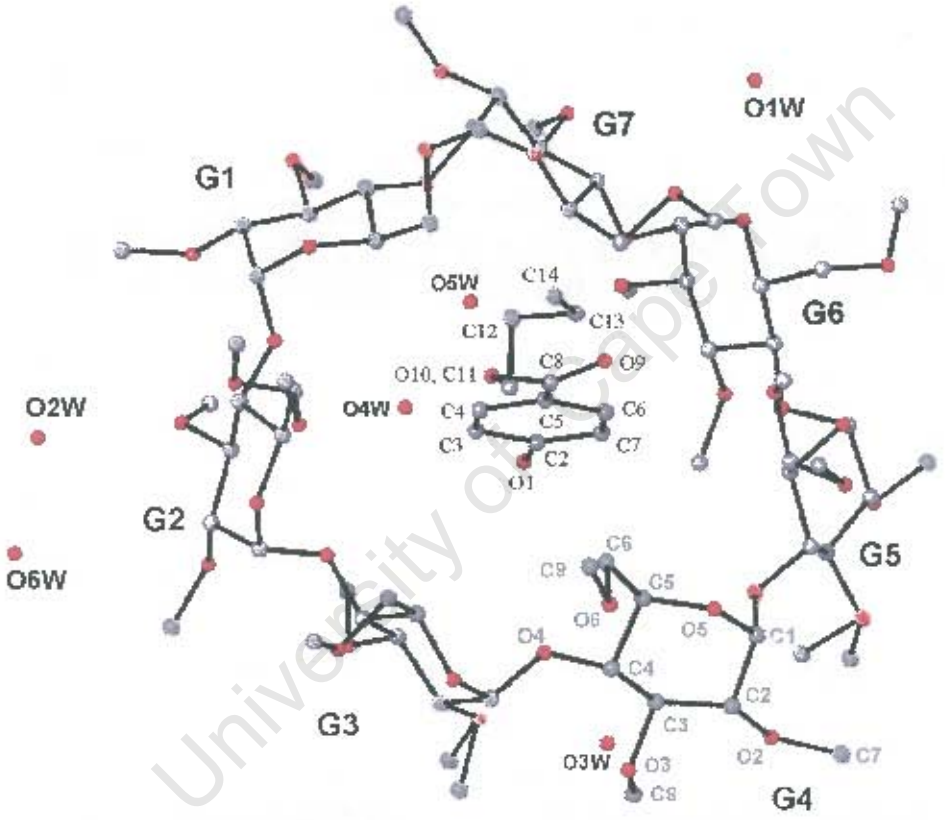

Figure 6.33 Macrocyclic structure and numbering scheme of glucose residues, water oxygen atoms and guest molecule, with the hydrogen atoms excluded. The host is viewed from the primary face.

The macrocycle is in the shape of an elliptically-distorted and truncated cone and all the glucopyranose residues are in the $^4C_1$ chair conformation. The atoms O(2G3), O(3G5), C(6G2), C(6G5) are each disordered over two sites A and B. As is normally the case for TRIMEB, the O(2)–C(7) bonds point outwards from the cavity, while the O(3)–C(8) bonds point towards the cavity.[9-11] The O(6)–C(9) groups of the G5 residue [specifically O(65A)–C(95A)] and the G7 residue, which have the large tilt angles, act as a "lid", closing off the O(6) side of the TRIMEB cavity, making it cup shaped.

The C(6)–O(6) bonds on all the glucose units are directed away from the cavity and are in the (-) *gauche* conformation, except for the C(6G5)–O(65A) bond which is pointed towards the cavity in the (+) *gauche* conformation. All the O(6)–C(9) bonds are *trans* to the respective C(5)–C(6) bonds, except in the G6 residue where the bond lies *gauche*.

The geometric parameters of the O(4) heptagon of the BPTMB structure are listed in Table 6.26. These include the radii, the O(4)•••O(4') distances, the O(4)•••O(4')•••O(4'') angles, the O(4)•••O(4')•••O(4'')•••O(4''') torsion angle and the deviations of each of the O(4) atoms from the mean O(4) plane. Table 6.27 lists the other important features of the macrocyclic structure such as the intersaccharidic bond angle (φ), the O(2)•••O(3') distance and the tilt angles [τ_1 and τ_2]. These parameters are defined in Chapter 1.

Table 6.26 Geometrical parameter of the O(4) heptagon for the BPTMB structure

Glucose unit	Radii (Å)	O(4)•••O(4') (Å)	O(4) angle (°)	Torsion angle (°)	Deviation (Å)
G1	5.08 (1)	4.42	122	11.8 (3)	0.51
G2	5.34 (1)	4.25	122	13.4 (3)	0.12
G3	4.89 (1)	4.58	128	-7.3 (3)	-0.51
G4	4.58 (1)	4.27	139	-23.3 (3)	-0.05
G5	5.36 (1)	4.32	116	26.6 (2)	0.66
G6	5.15 (1)	4.45	123	4.5 (3)	-0.39
G7	4.49 (1)	4.35	139	-31.2 (3)	-0.46
Average	**4.98**	**4.38**	**127**	**|16.9|**	**|0.39|**

Table 6.27 φ, O(2)•••O(3') distance, τ for the BPTMB structure

Glucose unit	φ (°)	O(2)•••O(3') (Å)	τ_1 (°)	τ_2 (°)
G1	119	3.25	29.6 (2)	16.8 (2)
G2	120	3.17	4.4 (2)	-7.0 (2)
G3	119	3.36	-12.4 (2)	17.9 (2)
G4	117	3.35	32.5 (1)	30.2 (3)
G5	120	3.82	32.9 (2)	20.2 (2)
G6	118	3.72	-17.4 (2)	-15.9 (1)
G7	115	3.43	32.4 (1)	46.3 (3)
Average	**118**	**3.44**	**23.1**	**22.0**

Unlike the situation in β-CD, the seven-fold symmetry is not well maintained. This fact is reflected in the geometrical parameters of the glycosidic O(4) heptagon ring. This conformation is attributed to the absence of the O(2)•••O(3') hydrogen bonds that exist in the β-CD dimer complexes and which lock the macrocycle into a round shape. Two of the glucose moieties in the BPTMB complex have a negative tilt angle, while the others have positive tilt angles[9-11] as seen in other TRIMEB complexes. Average bond lengths and angles for the host are within the standard deviation of those reported for other TRIMEB complexes, except in the case of some of the disordered atoms, as already mentioned. The values calculated for the parameters in Tables 6.26 and 6.27 are comparable with those of the TRIMEB-*p*-iodophenol complex,[6] as this TRIMEB molecule was used as the isomorphous replacement structure.

Guest geometry and interactions for the BPTMB structure

The conformation of the butyl paraben guest may be defined by five torsion angles. The torsion angles listed below will be used to describe the rotation around each of the corresponding bonds [Figure 6.34]. This conformation is favoured as it reduces the width of the paraben molecule.

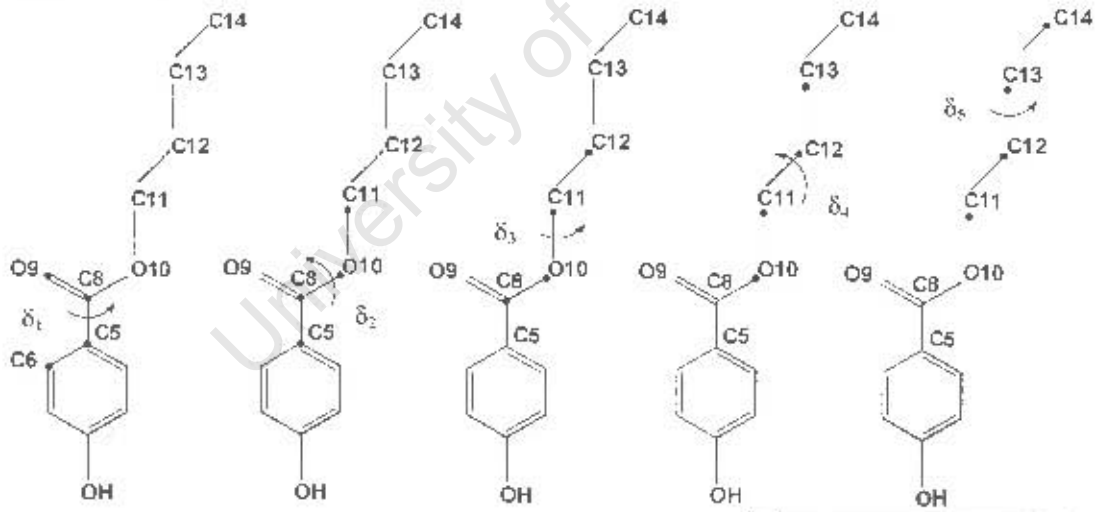

δ_1 C(6)–C(5)–C(8)–O(9)	➡	C(5)–C(8)
δ_2 C(5)–C(8)–O(10)–C(11)	➡	C(8)–O(10)
δ_3 C(8)–O(10)–C(11)–C(12)	➡	O(10)–C(11)
δ_4 O(10)–C(11)–C(12)–C(13)	➡	C(11)–C(12)
δ_5 C(11)–C(12)–C(13))–C(14)	➡	C(12)–C(13)

BP in complex:

δ_1 = +20 (2)

δ_2 = +157 (1)

δ_3 = +105 (2)

δ_4 = -136 (2)

δ_5 = -125 (2)

Figure 6.34 Torsion angles δ_1, δ_2, δ_3, δ_4 and δ_5 of the butyl paraben

The close contact distances for the relevant interactions between the host and guest molecule are listed in Table 6.28. As can be seen from this table there are many close contacts with the hydrogen atoms on C(14), however this was the best position located for this atom in WebLab Viewer.[17]

Table 6.28 Close contact distances for the BPTMB structure

Interaction	Distance (Å)
H(4) ··· H(521)	2.24
C(6) ··· H(641)	2.89 (2)
C(6) ··· C(6G7)	3.36 (2)
C(6) ··· H(672)	2.81 (2)
H(6) ··· O(65A)	2.44 (2)
C(7) ··· H(551)	2.79 (2)
H(7) ··· H(551)	2.03
O(1) ··· H(13B)^{i}	2.49 (3)
O(1) ··· C(14)^{i}	3.03 (3)
O(1) ··· H(14C)^{i}	2.30 (3)
C(2) ··· C(14)^{i}	3.35 (2)
C(2) ··· H(14C)^{i}	2.57 (2)
C(7) ··· H(14C)^{i}	2.62 (2)
H(7) ··· H(14C)^{i}	2.31
H(11B) ··· C(8G6)^{i}	2.48 (2)
H(11B) ··· H(862)^{i}	2.20 (1)
H(11B) ··· H(863)^{i}	2.19
C(13) ··· O(2G3)^{i}	2.98 (4)
H(13A) ··· C(73A)^{i}	2.59 (2)
H(13A) ··· H(732)^{i}	2.33
H(13A) ··· O(2G3)^{i}	2.04 (1)
C(14) ··· C(3G4)^{i}	3.07 (1)
C(14) ··· H(341)^{i}	2.17 (1)
C(14) ··· O(4G4)^{i}	2.98 (1)
C(14) ··· O(4G4)^{i}	3.37 (1)
H(14A) ··· C(3G4)^{i}	2.72 (1)
H(14A) ··· H(341)^{i}	1.74
H(14B) ··· C(3G4)^{i}	2.54 (1)
H(14B) ··· H(341)^{i}	1.86
H(14B) ··· O(4G4)^{i}	2.00 (1)
H(14B) ··· C(4G4)^{i}	2.53 (1)
H(14B) ··· H(541)^{i}	2.38

^{i}Related by symmetry operation: 2-x, $^{1}/_{2}$+y, $^{1}/_{2}$-z

The ester moiety of the guest molecule protrudes from the primary rim of the host while the phenolic hydroxyl group is situated at the secondary face of the host. The phenyl ring of the guest forms an angle of 89.6 (4)° with the mean O(4) plane. The tilting permits the guest to occupy most of the available space in the cavity. Figures 6.35 and 6.36 show CPK diagrams of the BPTMB structure, and include the O(4W) and O(5W) water oxygen atoms [which are light blue in colour].

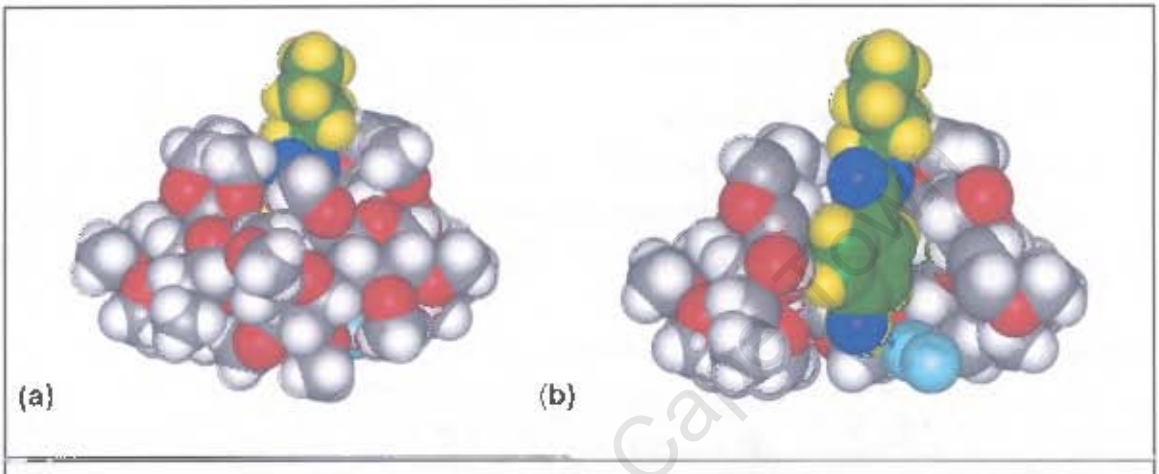

Figure 6.35 Space-filling diagram of the BPTMB structure (a) side view (b) sectioned view of the same orientation

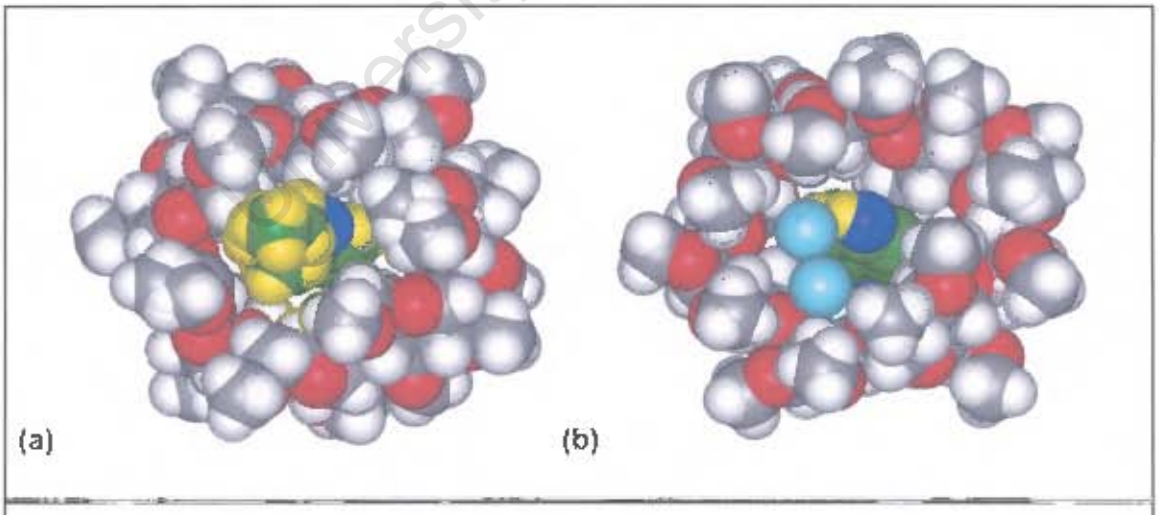

Figure 6.36 Space-filling diagram of the BPTMB structure (a) viewed from the primary rim (b) viewed from the secondary rim

Hydrogen bonding interactions of the BPTMB structure

Host interactions

The conformation of the TRIMEB molecule is stabilised by sixteen intramolecular C–H•••O hydrogen bonds [Table 6.29], three of which are of the type C(6)–H•••O(5'). In addition, there are two C(1)–H•••O(3') hydrogen bonds, a C(1)–H•••O(6') hydrogen bond, three C(8)–H•••O(2') hydrogen bonds, a C(7)–H•••O(3') hydrogen bond and a C(9)–H•••O(5') hydrogen bond linking adjacent glucose residues in the TRIMEB molecule. Furthermore there are stabilising intramolecular hydrogen bonds within some of the glucose units, namely two C(7)–H•••O(3) hydrogen bonds, two C(8)–H•••O(2) hydrogen bonds and a C(9)–H•••O(5) hydrogen bond. Additionally there is one intermolecular C(7)–H•••O(6') hydrogen bond that adds stability to the crystal structure. All the C•••O distances are in the range 3.0-3.4 Å.

Table 6.29 Intramolecular C–H•••O hydrogen bonds in the BPTMB structure*

			Distance (Å)			Angle (°)
C	H	O	C–H	H•••O	C•••O	C–H•••O
C(1G3)	H(131)	O(3G4)	1.00	2.54	3.14 (1)	118.2 (5)
C(1G5)	H(151)	O(6G6)	1.00	2.42	3.16 (1)	130.7 (5)
C(1G6)	H(161)	O(3G7)	1.00	2.41	3.11 (1)	126.5 (5)
C(6G1)	H(612)	O(5G7)	0.99	2.51	3.13 (1)	120.7 (6)
C(6G3)	H(632)	O(5G2)	0.99	2.55	3.30 (1)	132.1 (5)
C(6G6)	H(662)	O(5G5)	0.99	2.33	3.10 (1)	134.3 (5)
C(73A)	H(733)	O(3G3)	0.98	2.44	3.08 (2)	122 (1)
C(7G4)	H(741)	O(3G5)	0.98	2.74	3.37 (1)	122.0 (6)
C(7G6)	H(763)	O(3G6)	0.98	2.48	3.12 (2)	122.3 (8)
C(8G1)	H(812)	O(2G7)	0.98	2.56	3.28 (2)	129.0 (9)
C(8G2)	H(821)	O(2G1)	0.98	2.50	3.19 (1)	127.4 (6)
C(8G3)	H(832)	O(2G2)	0.98	2.44	3.07 (2)	121.5 (9)
C(85A)	H(853)	O(2G5)	0.98	2.54	3.14 (2)	120 (1)
C(8G7)	H(873)	O(2G7)	0.98	2.60	3.16 (1)	116.7 (5)
C(9G1)	H(913)	O(5G7)	0.98	2.77	3.40 (1)	122.9 (7)
C(9G6)	H(961)	O(5G6)	0.98	2.41	3.03 (1)	121.0 (8)
C(7G7)	H(771)	O(65B)'	0.98	2.53	3.17 (2)	122.6 (7)

' Related by symmetry operation: $1^1/_2 - x$, $1 - y$, $^1/_2 + z$

* Hydrogen bonding parameters based on idealised hydrogen atom positions.

Guest interactions

The hydroxyl oxygen atom is in hydrogen bonding contact with one water O(4W) oxygen atom. This water molecule is also involved in hydrogen bonding to one of the aromatic carbons. C(13) and C(14) are hydrogen bonded to the guest hydroxyl oxygen atom by the symmetry operation 2 - x, $^1/_2$ + y, $^1/_2$ - z. The guest is furthermore stabilised by a hydrogen bond with the host, of the type C(14)–H•••O(4). These interactions are listed in Table 6.30.

Table 6.30 Hydrogen bonding distances and C–H•••O hydrogen bonds involving the guest*

			Distance (Å)			Angle (°)
Donor (D)	H	Acceptor (A)	D–H	H•••A	D•••A	D–H•••A
O(1)	H(1)	O(4W)	0.84	2.05	2.74 (4)	140 (2)
C(3)	H(3)	O(4W)	0.95	2.84	3.45 (3)	122.9 (7)
C(13)	H(13B)	O(1)^i	0.99	2.49	3.18 (4)	126 (1)
C(14)	H(14A)	O(4G5)^i	0.98	2.73	3.356 (5)	122.2 (1)
C(14)	H(14B)	O(1)^i	0.98	2.31	3.03 (3)	129.8 (8)

^{i} Related by symmetry operation: 2 - x, $^1/_2$ + y, $^1/_2$ - z

* Hydrogen bonding parameters based on idealised hydrogen atom positions.

Water interactions

Four of the water molecules [O(1W), O(2W), O(3W) and O(6W)] are situated at the periphery of the cyclodextrin molecule, filling a small intermolecular space between complex units. The other two water molecules [O(4W) and O(5W)] are located within the TRIMEB cavity, near the secondary rim. The O(4W), O(5W) and O(6W) water molecules do not bond to the host, but are within hydrogen bonding distances to other water molecules. Furthermore the O(4W) water molecule is involved in hydrogen bonding to the guest molecule. The hydrogen bonding distances between the host and these water molecules are listed in Table 6.31 and are illustrated in Figure 6.37.

Table 6.31 Hydrogen bonding distances involving the water molecules

Interaction	Distance (A)	Symmetry operator for the second oxygen atom listed
O(1W) ••• O(5G3)	2.84 (1)	-1+x, y, z
O(1W) ••• O(6G7)	2.76 (1)	x, y, z
O(2W) ••• O(3G2)	2.82 (1)	x, y, z
O(3W) ••• O(6G4)	2.78 (1)	x, y, z
O(6W) ••• O(5G4)	3.00 (2)	$2^1/_2$-x, 1-y, $^1/_2$+z
O(1W) ••• O(3W)	2.68 (1)	-1+x, y, z
O(2W) ••• O(3W)	2.77 (1)	$2^1/_2$-x, 1-y, $^1/_2$+z
O(2W) ••• O(5W)	2.81 (2)	$^1/_2$+x, $^1/_2$-y, 1-z
O(2W) ••• O(6W)	2.89 (2)	x, y, z
O(4W) ••• O(5W)	2.62 (3)	x, y, z

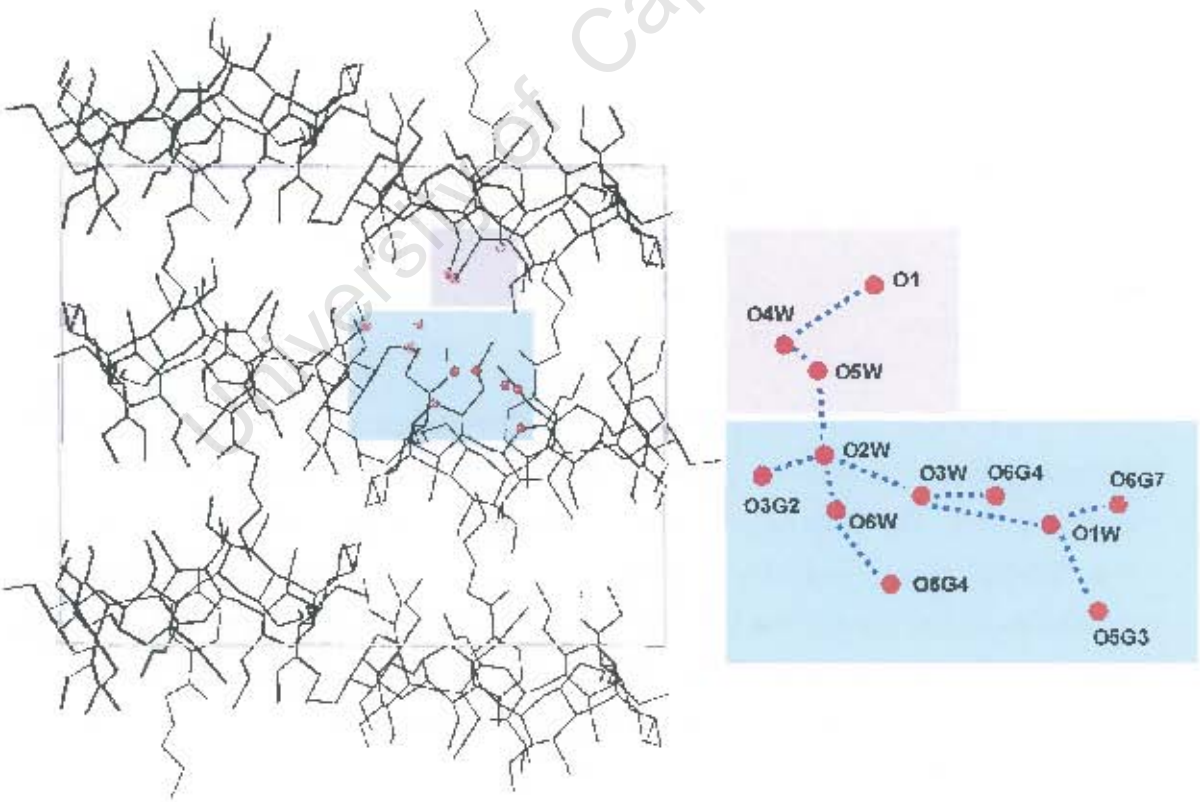

Figure 6.37 A schematic representation of guest and water interactions that connect adjacent host units

Crystal packing of the BPTMB structure

Figures 6.38 and 6.39 are extended stereo packing diagrams of the BPTMB structure showing projections as viewed down the *a*- and *b*-axes. Complex units pack in a screw-channel mode in a head-to-tail fashion with their axes almost parallel to the *b*-axis and the complex units arranged parallel to the *ac*-plane. Since the centre of the molecule is laterally shifted from the two-fold screw axis, the cavity does not form a continuous channel. Figure 6.38 illustrates how the alkyl chain of the butyl paraben molecule penetrates into the secondary side of the neighbouring host molecule.

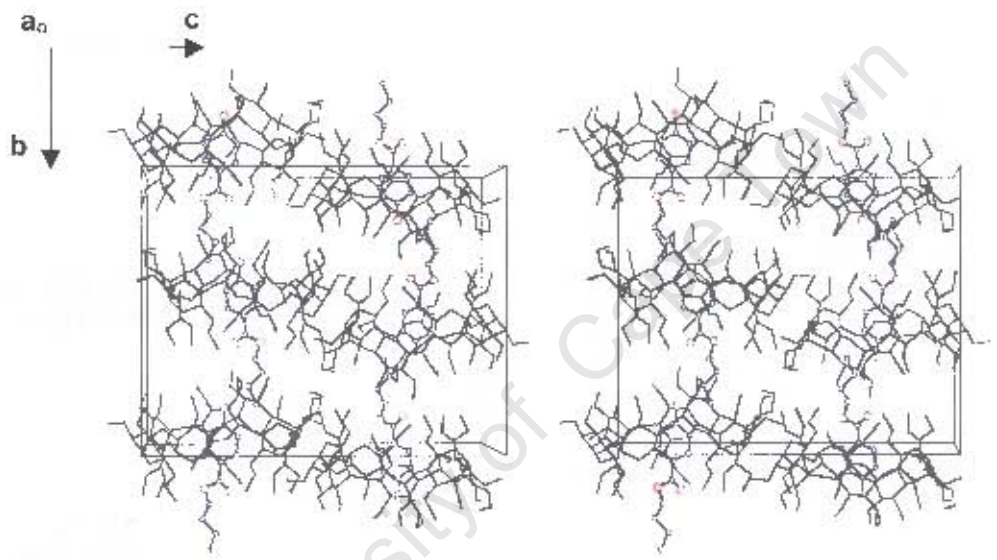

Figure 6.38 Stereo packing diagram of the BPTMB structure [*a*-axis projection]

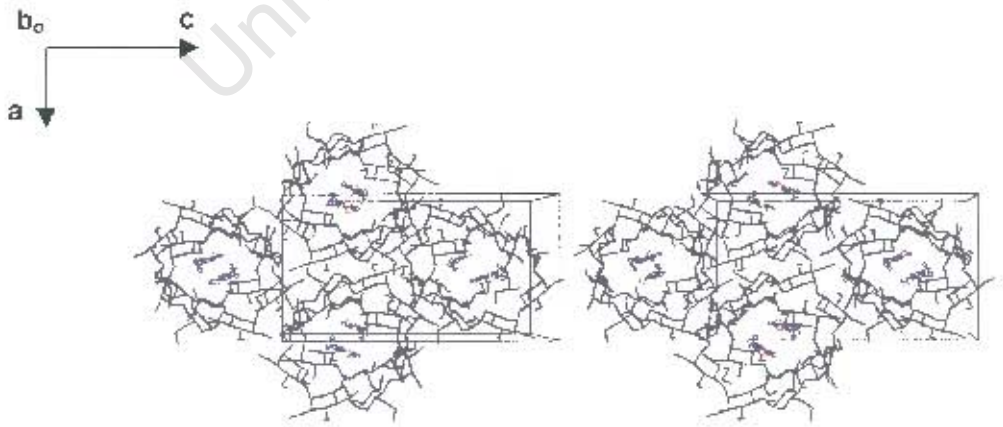

Figure 6.39 Stereo packing diagram of the BPTMB structure [*b*-axis projection]

Comparative XRD

The calculated and experimental XRD patterns for the BPTMB complex were successfully matched and are shown in Figure 6.40. The very close match in peak positions (2θ) shows that the experimental pattern represents a homogeneous preparation of the BPTMB. The differences in relative intensities between the two patterns are due to preferred orientation of the crystallites.

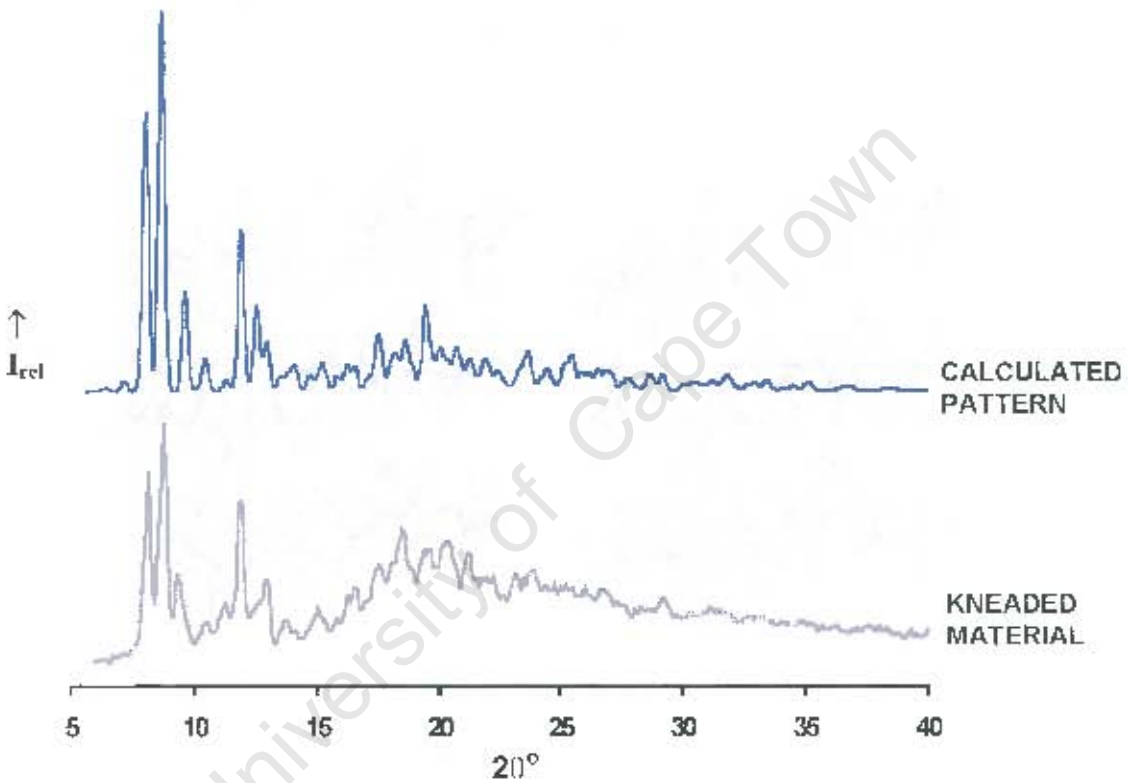

Figure 6.40 Experimental and calculated patterns for the BPTMB structure

DISCUSSION

Permethylation of β-CD renders it many times more soluble than β-CD and, as such, potentially more useful in the pharmaceutical industry.[18] Hence complexes with heptakis(2,3,6-tri-O-methyl)-β-cyclodextrin and the paraben preservatives were investigated in this study. To date the CSD[3] houses twelve TRIMEB structures, of which one is the hydrated form. TRIMEB and its complexes crystallise in the orthorhombic space $P2_12_12_1$ in four different packing modes, of which the screw-channel type packing mode along the *b*-axis is predominant [Table 6.32].

In most of these complexes the TRIMEB molecule takes on a similar conformation despite a range of guests and different packing arrangements. In these structures the CD molecule is cup shaped and five of the glucose residues have a positive tilt angle, while the other two have a negative tilt angle. Exceptions are observed in the ethyl laurate, methylcyclohexane and *S*-(1,7)dioxaspiro(5,5)undecane complexes where all the glucose units adopt a positive tilt angle. A marked difference in the conformations of one of the pyranose rings is observed in two instances, namely the monohydrate and the *m*-iodophenol structures. In both these structures one of the glucopyranose residues adopts an alternative conformation to the "normal" $^4C_1$ chair conformation. In the monohydrate structure the $^1C_4$ inverted chair conformation is observed, while in the *m*-iodophenol-TRIMEB complex a $^0S_2$ twist conformation is found.

All the structures reported to date have larger tilt angles than those observed in complexes of native β-CD and this can be attributed to two factors, namely steric hindrance involving the methyl groups attached to O(3) which are directed towards the cavity, and the host's inability to form O(2)•••O(3') intramolecular hydrogen bonds.[9] The absence of these hydrogen bonds allows the TRIMEB macrocycle to be more flexible and therefore the insertion of a guest molecule into the cavity will alter the conformation of the ring to accommodate the guest, i.e. an induced fit is achieved.[19] The conformation of TRIMEB is however stabilised by several C(6)–H•••O(5') intramolecular hydrogen bonds and these are said to account for the similarities found among TRIMEB structures.[20]

Table 6.32 TRIMEB structures from the CSD

Guest	H : G : W	a (Å)	b (Å)	c (Å)	α (°)	β (°)	γ (°)	Refcode	Ref.
Space group – $P2_12_12_1$									
Herringbone type									
Hydrate	1 : 0 : 1	14.818	19.362	26.510	90	90	90	HEZWAK	19, 14
m-iodophenol	1 : 1 : 0	15.669	20.798	25.486	90	90	90	GELKEN	11, 21
Cage type									
L-menthol	1 : 1 : 2	11.060	26.138	29.669	90	90	90	NIZHAF	22
methylcyclohexane	1 : 1 : 0	11.149	25.664	29.427	90	90	90	XAQJII	23
Screw-channel type									
p-iodophenol	1 : 1 : 4	14.997	21.368	28.205	90	90	90	CAMPIP	6, 9
R-flurbiprofen	1 : 1 : 1	15.092	21.714	28.269	90	90	90	COYXAP	10, 24
S-flurbiprofen	1 : 1 : 0	15.271	21.451	27.895	90	90	90	COYXET	9-10
4-biphenylacetic acid	1 : 1 : 1	14.890	21.407	28.540	90	90	90	PAFSOE	11
ethyl laurate	1 : 1 : 0.92	14.796	22.444	27.720	90	90	90	PINMAA	12
S-ibuprofen	1 : 1 : 0	15.232	21.327	27.597	90	90	90	RONWOG	25
S-naproxen	1 : 1 : 0	15.179	21.407	27.670	90	90	90	ZIFQOU	26
Channel type									
S-(1,7)dioxaspiro(5,5) undecane	1 : 1 : 0.57	10.936	25.530	29.640	90	90	90	QOYLIZ	27

In this study, complexes of TRIMEB with each paraben have been crystallised and the crystal structures have been elucidated. A comparison of the four crystal structures and the interaction between the cyclodextrin, water molecules and the guest compounds are discussed in this section. Physicochemical methods of analysis showed that the parabens form well defined inclusion complexes with TRIMEB by kneading. This was determined by comparison of the measured X-ray powder diffraction pattern of the ground product with the calculated pattern obtained from the single crystal structure. Each complex crystallised in the space group $P2_12_12_1$ with Z = 4 and a host to guest ratio of 1:1. Comparison of the cell dimensions and XRD traces of the four structures indicated that the EPTMB, PPTMB and BPTMB complexes were isostructural, while the MPTMB structure stood apart, as shown in Table 6.33.

Table 6.33 The unit cell parameters of the TRIMEB-paraben inclusion complexes

Guest	H : G : W	a (Å)	b (Å)	c (Å)	α (°)	β (°)	γ (°)
MPTMB	1 : 1 : 2.6	10.718	26.353	30.018	90	90	90
EPTMB	1 : 1 : 5.0	14.886	22.024	27.602	90	90	90
PPTMB	1 : 1 : 5.2	14.863	21.862	27.627	90	90	90
BPTMB	1 : 1 : 5.6	14.866	21.967	27.635	90	90	90

Conformation of the TRIMEB host molecule

Comparison of the paraben complexes indicates that the geometries of the TRIMEB molecule in the EPTMB, PPTMB and BPTMB complexes are all closely related to each other, while the geometry of the TRIMEB molecule of the MPTMB complex differs more significantly from the other three complexes. This point is more clearly illustrated in Figure 6.41(b), which shows how the macrocycle of the MPTMB complex differs in the relative orientations of the glucose residues from that of the EPTMB complex and is therefore not superimposable with the latter.

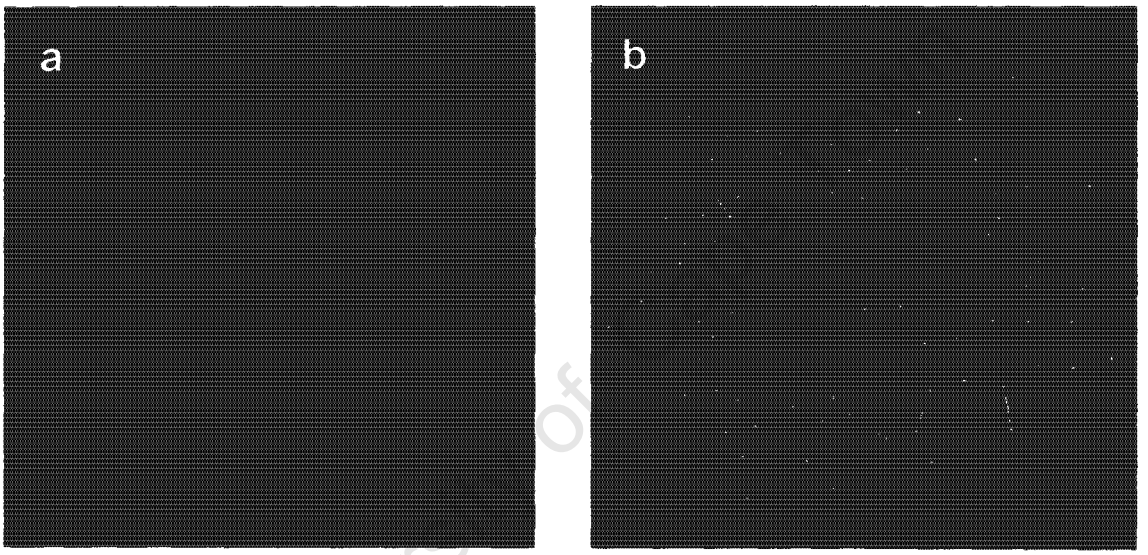

Figure 6.41 Conformation of the TRIMEB macrocycle **(a)** EPTMB [red], PPTMB [blue] and BPTMB [yellow]; **(b)** MPTMB [purple] and EPTMB [red]

In all four complexes the extensive distortion of the macrocycle from the symmetrical shape of the parent β-CD is reflected in the geometrical parameters of the O(4) heptagonal rings [Tables 6.5, 6.12, 6.19 and 6.26]. This is manifested in the deviation of the O(4) atoms from their mean plane, which range from 0.01 to 0.67 Å in the TRIMEB structures, while the corresponding deviation in the β-CD dimeric structures is less than 0.02 Å.[28]

Another remarkable difference is found in the tilt angles of the TRIMEB residues. The tilt angles are in the range -8.1 to 33.2° (τ_1) and -6.6 to 47.4° (τ_2). Five residues incline with their O(6) side towards the inside of the macrocycle, while the other two are rotated in the opposite direction. Steric reasons seem to induce the negative tilting of the two glycosidic residues. Hence the O(6) rim is narrowed and the molecule assumes a cup shaped appearance. In the MPTMB complex, the residues G1, G3, G4, G5 and G7 incline with their O(6) side nearer to the molecular axis of TRIMEB, while the G2 and G6 residues incline so that their O(2) and O(3) sides are nearer to each other. For the other three complexes the G1, G2, G4, G5 and G7 residues are tilted inwards and the G3 and G6 residues are tilted outwards. It should be noted that the numbering scheme "Gn" used for the MPTMB differs from that used for the EPTMB, PPTMB and BPTMB complexes, since MPTMB is not isostructural with the latter three complexes. Thus residues G2 and G6 in MPTMB physically correspond with residues G3 and G6 respectively in the EPTMB, PPTMB and BPTMB complexes. Since the G6 and G7 residues are oppositely rotated to each other with respect to the O(4) plane, a large tilt angle of 47.3°, 46.1° and 46.3° in the EPTMB, PPTMB and BPTMB complexes respectively, is observed between the planes through O(4'), C(1), C(4) and O(4) of these residues. A similar twisted conformation is observed between the G3 and G4 residues. In the MPTMB complex this twisted conformation is observed between the G1 and G2 residues and the G5 and G6 residues. The tilt angles can therefore be described as a measure of the macrocyclic shape.

The distortion of the macrocycle is due to the methylation at the O(3) position, since DIMEB, in which all O(2) and O(6) hydroxyl groups are methylated, still maintains the round structure.[29-30] The methylation of the O(3) hydroxyl groups, firstly, breaks the intramolecular O(2)•••O(3') hydrogen bonds and makes the macrocyclic conformation less symmetrical. Secondly, it causes steric hindrance which can only be relieved by increasing the O(2), O(3) distance, which requires a larger inclination of each residue.[6] The O(2)•••O(3') distances between the adjacent TRIMEB residues are in the range 3.14-3.82 Å, with an average value of 3.44 Å. These differences in the O(2)•••O(3') distances, deviations of the O(4) atoms from their mean plane and the tilt angle suggest that the 2,3,6-tri-O-methylglucose residue has more flexibility around the glycosidic linkage. The structure is, however, stabilised by numerous C(6)–H•••O(5') intramolecular hydrogen bonds. The EPTMB, PPTMB and BPTMB structures have three analogous C(6)–H•••O(5') hydrogen bonds. The MPTMB structure has an additional C(6)–H•••O(5') hydrogen bond, which has the effect of narrowing the O(6) rim and producing a more cup shaped and "sealed" macrocyclic conformation. Numerous other C–H•••O hydrogen bonds involving O(2), O(3) and O(6) add to the conformational stability of the macrocycle, the BPTMB complexes having significantly more of these types of interactions.

Paraben guest molecules

In the TRIMEB-paraben complexes each of the paraben guests is inserted into the TRIMEB cavity. The protrusions of the four guests can be seen in the CPK diagrams, illustrated in Figure 6.42. A schematic representation of the inclusion features of all the CD complexes is shown in Figure 6.43. Noticeable differences are observed in the position and orientation of the guest molecules within the CD cavity.

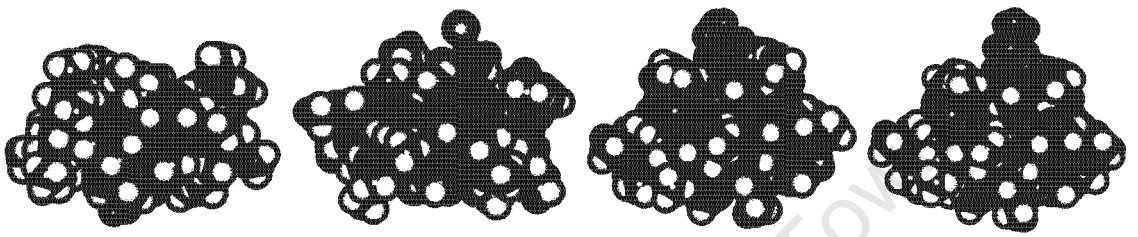

(a) (b) (c) (d)

Figure 6.42 Space-filling diagram of the (a) MPTMB, (b) EPTMB, (c) PPTMB, (d) BPTMB structures

In the MPTMB complex the phenolic hydroxyl group protrudes from the O(2), O(3) face of the host, while the ester moiety of the guest molecule occupies the centre of the host cavity. The molecule is included not parallel to the molecular axis of TRIMEB, but tilted, with the benzene plane making an angle of 50.4 (2)° with the mean O(4) plane. The large tilt of the glucose residues and the extra C(6)–H•••O(5') hydrogen bond make the primary side very narrow and almost sealed over the guest. As a result the benzene ring is more suitably accommodated to the wider O(2), O(3) side of the cavity.

The guest of the EPTMB complex is flipped with respect to the guest in the other three complexes, in that the phenolic hydroxyl group protrudes from the primary rim of the host enabling it to be in a polar environment. The ester moiety of the guest molecule is situated at the secondary rim. The phenyl ring of the guest forms an angle of 87.8 (3)° with the mean O(4) plane. This orientation corresponds to the Lichtenthaler *et al* [31-32] theory in which it is suggested that the primary rim of the TRIMEB molecule is relatively hydrophilic and so the hydrophilic portion of the guest will be located there.

In the PPTMB and BPTMB complexes, the guest has the same orientation and is included almost parallel to the molecular axis of TRIMEB with the aromatic ring located near the centroid of the cyclodextrin. Since the depth of the TRIMEB molecule [~9.8 Å] is not enough to cover the entire length of the propyl- and butyl paraben guests [being approximately 10.5 Å and 11.8 Å in length respectively] the alkyl chain protrudes through the narrow opening of the primary rim. These hydrophobic ends "protect" themselves by entering the secondary side of the adjacent host molecule, forming a channel with the original and related by the two-fold screw axis parallel to the *b*-axis. Since the butyl paraben alkyl chain protrudes into the host "above" it the C(14) atom is within hydrogen bonding distance to the guest hydroxyl oxygen atom found in this CD.

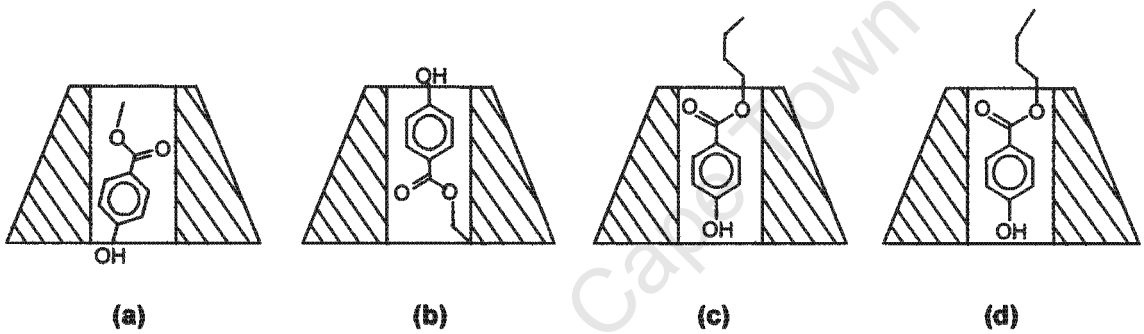

Figure 6.43 Orientation of the guest in the TRIMEB cavity (a) MPTMB, (b) EPTMB, (c) PPTMB, (d) BPTMB

Water molecules

TRIMEB complexes contain few or no water molecules and this is presumably because of their decreased hydrogen bonding capability and the presence of methyl groups which have a greater degree of rotational freedom and so help to maximise the efficiency of crystal packing. However, with the paraben complexes the water molecules are vital in maintaining the crystal structure and the crystallinity is reduced upon their removal.

One common feature in the four complexes is that the hydroxyl oxygen atom is in hydrogen bonding contact distance to one water oxygen atom. This interaction adds stability to the crystal structure. Another similarity is that in each complex at least one water atom is found within the cavity and has a site-occupancy factor of less than one. The remaining waters fill the intermolecular spaces between complex units and are linked together by O(W)•••O(W) type hydrogen bonds and interact with the host, to stabilise the crystal structure.

The MPTMB complex has fewer water molecules per asymmetric unit than the other three complexes and this can be ascribed to the fact that the MPTMB complex has a more efficient packing arrangement. In the MPTMB structure the cavity water molecule is in hydrogen bonding contact distance to the O(9) atom of the guest, and appears to act as a "filler" of the space that is created by i) the small guest size and ii) the inclination of 50.4° that the benzene plane makes with the mean O(4) plane. The guest is indirectly connected to the host by this water molecule as the latter acts as a bridging atom and therefore holds the guest in place relative to the host.

In the EPTMB complex the hydroxyl oxygen atom of the guest is in hydrogen bonding contact distance to a water molecule, which acts as a bridging atom to the TRIMEB host molecule. In the PPTMB and BPTMB structures the cavity water molecule is in hydrogen bonding contact distance to the hydroxyl oxygen atom of the guest and is linked to another water molecule, found inside the cavity with a s.o.f. of less than one.

Crystal packing

In the EPTMB, PPTMB and BPTMB structures, the TRIMEB molecules are linked by the two-fold screw axis parallel to the *b*-axis and are nearly parallel to the *ac*-plane. These structures have been characterised as a screw-channel type packing mode and pack in a head-to-tail fashion that is observed in the dimeric β-CD structures [space group $P2_1$]. Two adjacent TRIMEB molecules, which are related by the two-fold screw axis parallel to the *b*-axis, are laterally shifted with respect to each other. As a result the channel runs in a zigzag. The zigzag packing enables the guest molecules to have contact with the water molecules, which are located outside the TRIMEB rim.

In the MPTMB structure, complex units stack in columns in a head-to-tail mode, forming what appear to be continuous channels along the *a*-axis in a modified herringbone type packing mode. However the O(6)-C(9) methoxy groups almost completely block off the O(6) side of the molecule and therefore the packing is more accurately described as a cage type packing. The cell volume of the MPTMB complex is approximately 6% less than the mean of the cell volumes of the three isostructural complexes. This suggests that the MPTMB complex has a closer packing arrangement.

REFERENCES

1) F. Giordano, R. Bettini, C. Donini, A. Gazzaniga, M. R. Caira, G. G. Z. Zhang, D. J. W. Grant, *J. Pharm. Sci.*, **1999**, 88, 11, 1210.
2) Paratone N oil (Exxon Chemical Co., TX, USA).
3) *Cambridge Structural Database and Cambridge Structural Database System,* Version 5.23, April **2002**, Cambridge Crystallographic Data Centre, University Chemical Laboratory, Cambridge, England.
4) E. Egert, *Acta Crystallogr.*, **1983**, A39, 936.
5) E. Egert, G. M. Sheldrick, *Acta Crystallogr.*, **1985**, A41, 262.
6) K. Harata, K. Uekama, M. Otagiri, F. Hirayama, *Bull. Chem. Soc. Jpn.*, **1983**, 56, 1732.
7) G. M. Sheldrick, *SHELXL-97, Program for the Refinement of Crystal Structures*, University of Göttingen, Germany, **1997**.
8) X. Lin, *J. Struct. Chem.*, **1983**, 2, 213.
9) K. Harata, K. Uekama, M. Otagiri, F. Hirayama, *J. Incl. Phenom.*, **1984**, 1, 279.
10) K. Harata, K. Uekama, T. Imai, F. Hirayama, *J. Incl. Phenom.*, **1988**, 6, 443.
11) K. Harata, F. Hirayama, H. Arima, K. Uekama, T. Miyaji, *J. Chem. Soc., Perkin Trans. 2,* **1992**, 1159.
12) D. Mentzafos, I. M. Mavridis, H. Schenk, *Carbohydr. Res.*, **1994**, 253, 39.
13) T. Steiner, W. Saenger, *J. Am. Chem. Soc.*, **1992**, 114, 10146.
14) M. R. Caira, V. J. Griffith, L. R. Nassimbeni, B. van Oudtshoorn, *J. Chem. Soc., Perkin Trans. 2,* **1994**, 2071.
15) X. Lin, *J. Struct. Chem.*, **1986**, 5, 281.
16) G. A. Jeffery, *An Introduction to Hydrogen Bonding,* Oxford University Press, Oxford, **1997**, p.50.
17) *WebLab ViewerPro Version 3.5* (Copyright **1999** by Molecular Simulations Inc., San Diego, CA).
18) J. Szejtli, *J. Incl. Phenom.*, **1992**, 14, 25.
19) T. Steiner, W. Saenger, *Angew. Chem., Int. Ed. Engl.*, **1998**, 37, 3404.
20) V. J. Griffith, *PhD Thesis, Physiochemical Characterisation of Cyclodextrin - Drug Complexes,* University of Cape Town, South Africa, **1996**.
21) K. Harata, *J. Chem. Soc., Chem. Commun.*, **1988**, 928.

22) M. R. Caira, V. J. Griffith, L. R. Nassimbeni, B. van Oudtshoorn, *Supramol. Chem.*, **1996**, 7, 119.

23) A. Rontoyianni, I. M. Mavridis, R. Israel, G. Beurskens, *J. Incl. Phenom.*, **1998**, 32, 415.

24) K. Harata, F. Hirayama, T. Imai, K. Uekama, M. Otagiri, *Chem. Lett.*, **1984**, 1549.

25) G. R. Brown, M. R. Caira, L. R. Nassimbeni, B. van Oudtshoorn, *J. Incl. Phenom.*, **1996**, 26, 281.

26) M. R. Caira, V. J. Griffith, L. R. Nassimbeni, B. van Oudtshoorn, *J. Incl. Phenom.*, **1995**, 20, 277.

27) S. Makedonopoulou, K. Yannakopoulou, D. Mentzafos, V. Lamzin, A. Popov, I. M. Mavridis, *Acta Crystallogr.*, **2001**, B57, 399.

28) D. Mentzafos, I. M. Mavridis, G. le Bas, G. Tsoucaris, *Acta Crystallogr.*, **1992**, B47, 746.

29) M. Czugler, E. Eckle, J. J. Stezowski, *J. Chem. Soc., Chem. Commun.*, **1981**, 1291.

30) K. Harata, *Chem. Lett.*, **1984**, 1641.

31) F. W. Lichtenthaler, S. Immel, *Starch*, **1996**, 48, 4, 145.

32) F. W. Lichtenthaler, S. Immel, *Starch*, **1996**, 48, 6, 225.

Chapter 7

CONCLUSION

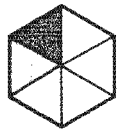
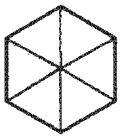
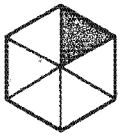
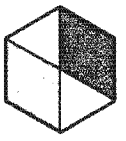
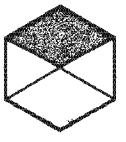
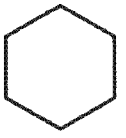
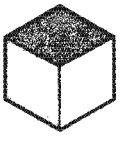

CONCLUSION

In this study a number of solid state complexes have been prepared and properties such as H:G:W stoichiometry, thermal behaviour and X-ray diffraction characteristics have been recorded. Where crystals of suitable size have been grown, single crystal X-ray photography and X-ray intensity data-collections were performed. In addition ^{1}H NMR solution studies were performed on the β-CD series.

Complex preparation, identification and determination of the stoichiometry

Inclusion complexes of alkylparabens with γ-CD, β-CD, DIMEB and TRIMEB were prepared and have been characterised by physicochemical methods. Indications of complex formation were based on the assumption that the included guest would no longer exhibit its bulk crystalline properties when it was interspersed in the CD crystalline framework.

Formation of a CD complex was characterised by the disappearance of the fusion event of the guest in the DSC trace, as well as by a change in the profile of the XRD trace. Shifts in prominent IR bands of a guest also indicated that certain interactions of the guest had changed in the presence of a CD. These trends were all observed for the interaction of each paraben with each of the host CDs and so it was evident that sixteen different CD-guest inclusion complexes had been prepared.

A combination of UV spectrophotometric analysis, thermogravimetric analysis and microanalysis were the principal means of determining the stoichiometry of the inclusion complexes. In most cases, the stoichiometry was calculated from microanalysis results using the percentage of water in the sample and values for the content of carbon and hydrogen. The number of water molecules of crystallisation was based on the mass loss determined by TGA. The results obtained from microanalysis were supported by UV spectrophotometric analysis. The stoichiometries of all the complexes were 1:1, except in the γ-CD complexes where a 1:2 host-to-guest ratio was observed. Solution state NMR studies also indicated 1:1 β-CD to paraben stoichiometries, although it has been noted that the stoichiometry in solution and in the solid state do not always coincide.[1-6]

Thermal analysis of the CD complexes

Thermal analysis is commonly used as a routine method for a rapid preliminary qualitative investigation. As already mentioned, it is one of the principal techniques used to establish if complexation has occurred. In this regard the approach was almost always the same: comparison of the thermal behaviour of single components, their physical mixtures and the inclusion compound candidate prepared by kneading or co-precipitation. Evidence for the formation of an inclusion complex was provided when differences between the physical mixtures and the putative inclusion complex existed, as observed by the disappearance of the fusion endotherm of the guest in the DSC trace.

Thermal analysis also provided information on the physical characteristics of the inclusion complexes and proved to be the most useful technique in determining the presence of two different forms of the β-CD-methyl paraben inclusion complex.

DSC indicated that water losses from complexes of native CDs and DIMEB were multi-step processes, pointing to different populations of water molecules in the inclusion complexes. Weight loss and endotherms associated with the loss of water could be seen in the TGA and DSC traces, respectively. Weight losses obtained for dehydration were generally very reproducible, emphasising the reliability of thermogravimetric analysis in estimating the water content of CD complexes as opposed to crystal structure solution, where high thermal motion and disorder often caused uncertainty in the placement of water molecules.

In the DSC traces, endotherms related to decomposition could also be identified. The γ-CD inclusion complexes revealed a correlation between the onset of decomposition of the inclusion complex and the onset of decomposition of the appropriate uncomplexed guest. A similar trend was observed with the β-CD complexes. This observation suggests that the inclusion of the guest by the CD does confer additional stability to that particular guest but that the thermal stability of the uncomplexed guest is still an important overall determinant.

The decomposition of the complexes began at a lower temperature than the decomposition of the pure host. This decrease in thermal stability of the inclusion complexes was associated with the thermal stability of the guests they include. In contrast, the lower melting points of the TRIMEB complexes, compared to those of native cyclodextrins, were indicative of the weaker intermolecular interactions.

XRD analysis of the CD complexes

In much the same way that thermal analysis can be used to determine if an inclusion complex has formed, so can XRD, as inclusion complexes showed characteristic XRD powder patterns, which are distinguished from those of the uncomplexed guest, pure host or physical mixtures of the two compounds. In addition XRD traces are useful as predictive indicators of structural characteristics of CD complexes and in this regard are effective in detecting polymorphs.

The essential structural characteristics of the γ-CD inclusion complexes could be determined from their XRD traces, a great benefit, as single crystals could not be obtained for these complexes. The XRD patterns of the γ-CD complexes were all closely matching implying an analogous packing arrangement for the host structures of these complexes. Comparison of these patterns with the reference patterns indicated that these γ-CD complexes belong to an isostructural series crystallising in the space group $P42_12$.[7] Based on the consideration of their space group and H:G stoichiometries the structures of these complexes would exhibit disorder of the guest molecule.

A similar trend was observed for the β-CD complexes in that the XRD traces resemble one another closely and these complexes could therefore be considered as isostructural. Comparison of these patterns with the reference patterns indicated that these β-CD complexes crystallise in the space group C2 or P1, both with channel type packing.[7] X-ray photographic analysis was used to determine the space group unequivocally and indicated that the complexes crystallise in the monoclinic space group C2.

Although it was not possible to collect X-ray intensity data for the EPBCD and BPBCD complexes, it was expected from the XRD results that the crystal structures would be similar to those of MPBCD and PPBCD complexes whose crystal structures were successfully elucidated.

Both the DIMEB and TRIMEB complexes crystallised in the most commonly observed space group for these host inclusion complexes, namely $P2_12_12_1$. However, compared to the γ- and β-CD complexes, where only a single isostructural series was observed in each case, single crystal XRD of the DIMEB complexes indicated two different isostructural packing arrangements, namely MPDMB and EPDMB as one isostructural pair and PPDMB and BPDMB as the other. Similarly, two different packing arrangements were observed for the TRIMEB complexes. The XRD traces of the EPTMB, PPTMB and BPTMB complexes were closely matched and these species could therefore be considered to be isostructural with each other,[7] while the MPTMB complex formed an inclusion complex that crystallised with a different packing arrangement. These XRD results indicate that the elongation of the alkyl chain directly affects the packing arrangements of the complexes. No differences in the packing arrangements of the β-CD complexes were observed as the C2 complexes crystallise as a dimer, thus allowing the parabens with the longer alkyl chain to be included within the CD cavity.

X-ray structure solution of the CD complexes

Patterson search and isomorphous replacement techniques proved to be useful for the structure solution of the CD complexes, accounting for the solution of ten of the sixteen crystal structures investigated in this study. In addition one other crystal structure was solved as the complex between β-CD and methyl paraben exhibited pseudo-polymorphism. It was not possible to collect X-ray intensity data for the γ-CD complexes and two of the β-CD complexes due to inferior crystal quality, despite repeated efforts to grow better crystals. In all other cases, crystal structure solution of CD-drug complexes has provided unambiguous confirmation of complex formation and detailed information regarding the stoichiometry, mode of inclusion and host-guest interactions.

Structural characteristics of CD geometry

The geometrical parameters that define the conformation of the macrocycle show that the ring of β-CD adopts a more rigid relative positioning of the glucose residues than DIMEB or TRIMEB, as illustrated by the radius of the heptagon, deviation of the O(4) atoms from the mean O(4) plane of the macrocycle and glycosidic oxygen angles. In the β-CD complexes an intrinsic network of intramolecular and intermolecular hydrogen bonds maintain these geometric parameters.

Methylation of the hydroxyl groups enlarges the whole cavity of the host molecules and gives rise to a narrower primary rim than that of native CDs and this steric effect is important in guest orientation. Additionally it adds length to the CD leading to a deeper cavity. Besides these differences the conformation of DIMEB was found to be similar to that of β-CD, and this can be ascribed to the formation of a network of intramolecular O(2)•••O(3') hydrogen bonds found in both structures. Permethylation in contrast makes the formation of such hydrogen bonds impossible and hence the macrocyclic conformation is more flexible than β-CD or DIMEB.

The crystal structures of the TRIMEB complexes reveal a rather distorted conformation of this host in comparison with β-CD. The cavity is no longer open but closed by "inwards" rotation of the O(6)-CH_3 groups so that the host is cup shaped. The permethylation markedly affects the planarity of the O(4) heptagon of the macrocycle and increases the deviations of the O(4) atoms from the mean O(4) plane. The effect of permethylation appears more clearly in the change of the O(2)•••O(3') distances and tilt angles. The average O(2)•••O(3') distances are enlarged to avoid steric hindrance and are about 0.6 Å larger than those in β-CD. Steric hindrance also results in larger tilt angles of the glucose residues, which are about three times those in the native CD. Such a macrocyclic conformation produces a cavity with a shape and size different from that of the parent CD.

It was noted that the TRIMEB molecule in this study adopts a similar conformation to that observed in all of its complexes reported to date. This is attributed to a series of C(6)–H•••O(5') intramolecular hydrogen bonds which maintain and stabilise the conformation of the macrocycle in the solid state in much the same way as the O(2)•••O(3') hydrogen bonds do in β-CD and DIMEB.

Mode of guest inclusion and orientation

The orientation of the guest molecule within the CD cavity is dependent on a number of factors. These include geometric compatibility, hydrophobicity and polarity. In general the included molecules are normally orientated in the host in such a way as to achieve the maximum contact between the hydrophobic part of the guest and the apolar cavity of the cyclodextrin. The hydrophilic part will remain as far as possible at the outer face of the cyclodextrin cavity to maximise contacts with the solvent and/or hydroxyl groups of the host.

The guests of the pseudo-polymorphic β-CD-methyl paraben structures show very similar modes of inclusion. In both cases, two disordered guest molecules were included in the β-CD dimeric unit. The ester moieties of the guest molecules were centralised in the cavities of the β-CD molecules and the guest hydroxyl groups were located at the primary rims. The position of the guest -OH group at the rims of the CD allows for hydrogen bonding with water molecules and CD-hydroxyl groups in the P1 and C2 complexes respectively.

A parallel study of the inclusion of the paraben drugs in β-CD in solution was performed. Additional arrangements of the β-CD complex are possible in solution, as the secondary hydroxyl end is open, allowing for solvation of the hydroxylic group at either end of the CD cavity.[8] NOE experiments indicated that the orientation of the methyl paraben guest was indeed inverted, as the guest –OH group was now found to be located at the wider secondary rim.

Similarly, in the DIMEB complexes, where both ends of the cavity are exposed to water, the guest hydroxyl group of the MPDMB and EPDMB structures were found at the secondary rim. However, the orientation of the guests in the PPDMB and BPDMB structures differed in that the guest aromatic ring extends well beyond the primary rim of the host and the alkyl chain is embedded in the cavity. The guest orientation of the latter two compounds corresponds to Lichtenthaler's [9-10] study in that the hydrophilic and hydrophobic portions of the guest aligns with the hydrophilic and hydrophobic portions of the host respectively. These results clearly show how the elongation of the alkyl chain affects the mode of inclusion of the guest, as both propyl- and butyl paraben are too long to be fully included within the DIMEB cavity.

In all of the TRIMEB complexes, except EPTMB, the guest orientation corresponds with that found in the DIMEB structures MPDMB and EPDMB. The hydroxyl group of the guest is located at the secondary rim and the alkyl chain is located at the primary rim. The orientation of the EPTMB guest corresponds to the Lichtenthaler *et al* [9-10] model in which it is suggested that the primary rim of the TRIMEB molecule is relatively hydrophilic and so the hydrophilic portion of the guest will be located there. Here again the propyl- and butyl paraben guests are too long to be fully included within the TRIMEB cavity and thus the alkyl chain protrudes into the neighbouring CD.

From this analysis it can be seen that the size of the guest is an important factor in complex formation and differences in the inclusion geometry can be ascribed to changes in the shape and size of the host cavities.

Host-guest interactions and hydrogen bonding

Hydrogen bonding remains the most important intermolecular interaction in complexes of the type examined in this study. It is these intermolecular forces which make a significant contribution to the structure and thermal stability of the inclusion compound.

It is well known that the β-CD host has a strong tendency to form head-to-head dimeric units held together by multiple O-H•••O hydrogen bonds across the secondary rims[11] and these hydrogen bonds show a remarkable consistency in the constitution of their network. Strong hydrogen bonds form between the O(2) and O(3) hydroxyl groups of adjacent glucose units in the same molecule, giving rise to an intramolecular ring of hydrogen bonds. The hydrogen bonds are of the flip-flop type and so contribute to the stability of the individual CDs. In addition to these intramolecular hydrogen bonds, intermolecular O(3)•••O(3) hydrogen bonding was observed in these dimeric β-CD structures.

The DIMEB and TRIMEB studies illustrate the predominant role of the intermolecular C-H•••O interactions involving the methoxyl groups when methylation of the O(6), O(2) and/or O(3) hydroxyl groups negates the formation of O-H•••O hydrogen bonds. Although C-H groups form much weaker hydrogen bonds [*ca* 2-8 kJ mol^{-1}] than O-H groups, their donor potentials should not be neglected as C-H•••O hydrogen bonds have been shown to occur frequently and play crucial roles in many organic and biological structures.[12-13]

In most of the DIMEB and TRIMEB structures there are also C-H•••O interactions between the host cavity walls and guest molecules. This has been observed before when polar guest molecules, which are included in the relatively hydrophobic cavity, cannot satisfy their acceptor potential with conventional partners and therefore resort to weaker C-H•••O hydrogen bonds involving the cavity wall.[14-16] From quantum chemical calculations, the energies of these interactions are estimated to be slightly more then 4 kJ mol^{-1}, i.e. about a quarter to a third of those of conventional hydrogen bonds.[17]

Structural role of water

The water molecules in CD complexes can act as "space-fillers", maintaining the crystal structure through a network of hydrogen bonds, and/or as a participant in the inclusion mode.[18] The water structure in these complexes plays an important role in determining the equilibrium, complex stability, and consequently the effect of the cyclodextrin on the guest. DSC results indicated that water losses from complexes of native CDs and DIMEB are multi-step processes, pointing to different populations of water molecules. This can be rationalised with the respective crystal structures, where some water molecules are involved in a complex network of hydrogen bonds.

All the complexes contain water molecules in the interstices between the cyclodextrins in the crystal structure. These water molecules interact through hydrogen bonding with the -OH groups on the primary and secondary rims of the CD molecules in the case of DIMEB and β-CD.

The relatively hydrophobic environment of the methylated CD crystal structure generally excludes water molecules. However, in this study the TRIMEB host molecules included water molecules and these play an important part in the overall stabilisation of the complex, as the water molecules are in hydrogen bonding contact of the guest molecule which, are in turn in contact with the host molecule.

Crystal packing of the CD complexes

The structure analyses indicate that the packing arrangements of the complexes are directly affected by i) the temperature of crystallisation and ii) the elongation of the alkyl chain. A variation in crystallisation temperature resulted in the β-CD-methyl paraben inclusion complex crystallising in both the space groups P1 and C2 with IM and CH type packing modes respectively.

A possible explanation for this pseudo-polymorphic occurrence is that when the crystals are grown at low temperature the degree of motion of the guest is reduced and the hydration shell is more ordered, thereby favouring the IM packing mode. When the crystals are grown at a higher temperature, the guest has a greater degree of motion and therefore the interactions with the water molecules are destabilised, allowing for the CH type packing mode to form.

The previous XRD results indicated that elongation of the alkyl chain leads to two different packing arrangements of the DIMEB and TRIMEB complexes, and these differences were confirmed by the crystal structure analyses. The crystal packing of complexes of the methylated CDs indicated that the smaller paraben guests, which can be fully included within the cavity, allow for a close packed arrangement of the molecules. This is evident in the MPDMB and EPDMB complexes, where the complex units stack in infinite channels in a modified herringbone scheme, and a similar packing arrangement is seen in the MPTMB complex. In contrast, parabens with a longer alkyl chain yielded CD complex structures characterised by a more zigzag type packing than those already discussed.

Final remarks

Parabens have a long history of use in drug products and were first employed as preservatives in pharmaceutical products in the mid-1920s.[19] The antimicrobial activity of alkylparabens increases as the chain length of the ester group increases, but the solubility decreases with increasing chain length. This study has shown that alkylparabens are favourable candidates for inclusion by CDs, thereby improving their aqueous solubility. Physicochemical characterisations of the solid state complexes provided indisputable evidence for complex formation. XRD was one of the techniques used in this regard and it additionally enabled the prediction of the packing arrangements of the complexes. Physicochemical characterisation therefore accomplished a comprehensive understanding of the solid state properties of these complexes by relating molecular scale properties and bulk properties. The NMR spectroscopy study provided additional information on the relative stability, stoichiometry and geometry of the inclusion compounds in solution. This study, based on the continuous variation method, represents a significant advance on that reported by Chan *et al*[20] whose NMR measurements were performed at only a single concentration of each paraben.

The results of the X-ray analyses for a number of complexes, and the unique unit cell data obtained, indicate that the mode of inclusion and properties of the complexes in the solid state are more varied than have been reported to date. The methyl- and ethyl parabens allow for a close, channel type packing complex to form, that until now was not as prevalent among DIMEB and TRIMEB inclusion complexes. Differences in the temperature of crystallisation also yielded some unique findings. In conclusion, the application of X-ray diffraction methods, thermal analysis, and in some cases solution NMR spectroscopy, has therefore enhanced the understanding of the inclusion capabilities of these compounds.

REFERENCES

1) K. Harata, *Bull. Chem. Soc. Jpn.*, **1976**, 49, 1493.
2) Y. Yamamoto, M. Onda, M. Kitagawa, Y. Inoue, R. Chujo, *Carbohyr. Res.*, **1987**, 167, C11.
3) R. L. Gelb, L. M. Schwartz, B. Cardelino, H. S. Fuhrman, R. F. Johnson, D. A. Laufer, *J. Am. Chem. Soc.*, **1981**, 103, 1750.
4) M. Sakurai, M. Kitagawa, H. Hoshi, Y. Inoue, R. Chujo, *Bull. Chem. Soc. Jpn.*, **1989**, 62, 2067.
5) K. Harata, H. Uedaira, J. Tanaka, *Bull. Chem. Soc. Jpn.*, **1978**, 51, 1627.
6) Y. Inoue, T. Okuda, R. Chujo, *Carbohyr. Res.*, **1985**, 141, 179.
7) M. R. Caira, *Roum. Chim. Rev.*, **2001**, 46, 4, 371.
8) J. A. Hamilton, M. N. Sabesan, *Acta Crystallogr.*, **1982**, B38, 3063.
9) F. W. Lichtenthaler, S. Immel, *Starch*, **1996**, 48, 4, 145.
10) F. W. Lichtenthaler, S. Immel, *Starch*, **1996**, 48, 6, 225.
11) W. Saenger, *J. Incl. Phenom,* **1984**, 2, 445.
12) G. T. Desiraju, *Acc. Chem. Res.*, **1996**, 29, 441.
13) T. Steiner, *J. Chem. Soc., Chem. Commun.*, **1997**, 727.
14) T. Steiner, W. Saenger, *J. Am. Chem. Soc.*, **1993**, 115, 4540.
15) T. Steiner, W. Saenger, *J. Chem. Soc., Chem. Commun.*, **1995**, 2087.
16) T. Steiner, A. M. Moreira da Silva, J. J. C. Teixeira-Dias, J. Müller, W. Saenger, *Angew. Chem., Int. Ed. Engl.*, **1995**, 34, 1452.
17) E. B. Starikov, W. Saenger, T. Steiner, *Carbohydr. Res.*, **1998**, 307, 343.
18) D. Giron, *Thermochim. Acta,* **1965**, 248, 1.
19) T. Sabalitschka, *Archives of Pharmacology,* **1930**, 268, 653.
20) L. W. Chan, T. R. R. Kurup, A. Muthaiah, J. C. Thenmozhiyal, *Int. J. Pharm.*, **2000**, 195, 71.

Appendices

APPENDIX A

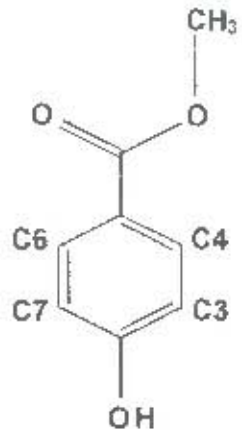

r = [BCD] / [BCD] [G] or
r = [G] / [BCD] [G]

Table 1 BCD protons of the MPBCD complex in D_2O at 298K

r	[BCD]	H1	H2	H3	H4	H5	H6
1	10	5.1143	3.6927	4.0099	3.6273	3.8936	3.9240
0.9	9	5.1062	3.6851	3.9895	3.6200	3.8672	3.9093
0.8	8	5.0953	3.6755	3.9718	3.6137	3.8311	3.9039
0.7	7	5.0897	3.6675	3.9505	3.6134	3.7940	3.8982
0.6	6	5.0909	3.6762	3.9325	3.6138	3.7645	3.8971
0.5	5	5.0831	3.6598	3.9086	3.6104	3.7261	3.8857
0.4	4	5.0779	3.6609	3.8991	3.6101	3.7036	3.8836
0.3	3	5.0917	3.6708	3.8973	3.6151	3.6909	3.8828
0.2	2	5.0873	3.6541	3.8899	3.6109	3.6801	3.8816
0.1	1	5.0871	3.6530	3.8839	3.6113	3.6704	3.8789

Table 2 Methyl paraben protons of the MPBCD complex in D_2O at 298K

r	[M]	H3, H7	H4, H6	CH_3
1	10	7.9863	6.9987	3.9337
0.9	9	7.9875	6.9968	3.9331
0.8	8	7.9884	6.9935	3.9378
0.7	7	7.9897	6.9910	3.9455
0.6	6	7.9872	6.9848	3.9485
0.5	5	7.9833	6.9779	3.9517
0.4	4	7.9855	6.9790	3.9511
0.3	3	7.9817	6.9741	-
0.2	2	7.9745	6.9690	-
0.1	1	7.9787	6.9716	-

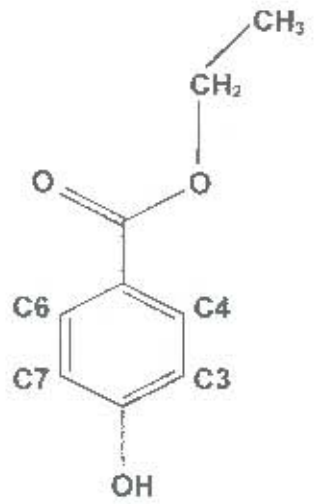

r = [BCD] / [BCD] [G] or
r = [G] / [BCD] [G]

Table 3 BCD protons of the EPBCD complex in D_2O at 298K

r	[BCD]	H1	H2	H3	H4	H5	H6
1	5.0	5.1160	3.6953	4.0115	3.6292	3.8952	3.9258
0.9	4.5	5.1138	3.6936	3.9920	3.6289	3.8741	3.920
0.8	4.0	5.1112	3.6913	3.9847	3.6289	3.8436	3.9111
0.7	3.5	5.1060	3.6862	3.9679	3.6272	3.8118	3.9077
0.6	3.0	5.1058	3.6869	3.9550	3.6273	3.7820	3.9006
0.5	2.5	5.0968	3.6788	3.9338	3.6228	3.7478	3.8936
0.4	2.0	5.0968	3.6849	3.9230	3.6228	3.7215	3.8882
0.3	1.5	5.0966	3.6798	3.9149	3.6234	3.7036	3.8840
0.2	1.0	5.0936	3.6890	3.9049	3.6208	-	3.8775
0.1	0.5	5.0904	3.6908	3.8982	3.6205	-	3.8731

Table 4 Ethyl paraben protons of the EPBCD complex in D_2O at 298K

r	[E]	H3, H7	H4, H6	CH_2	CH_3
1	5.0	8.0029	7.0039	4.4004	1.4116
0.9	4.5	7.9983	6.9978	4.4040	1.4173
0.8	4.0	7.9963	6.9961	4.4070	1.4193
0.7	3.5	7.9948	6.9934	4.4144	1.4233
0.6	3.0	7.9880	6.9863	4.4176	1.4248
0.5	2.5	7.9848	6.9821	4.4220	1.4282
0.4	2.0	7.9831	6.9788	4.4261	1.4319
0.3	1.5	7.9792	6.9734	4.4277	1.4339
0.2	1.0	7.9735	6.9654	4.4288	1.4344
0.1	0.5	7.9718	6.9706	4.4303	1.4353

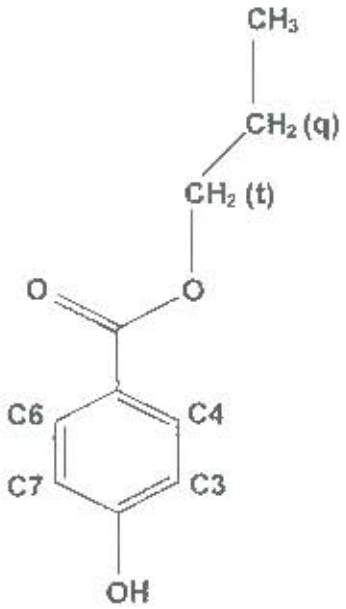

r = [BCD] / [BCD] [G] or
r = [G] / [BCD] [G]

Table 5 BCD protons of the PPBCD complex in D_2O at 298K

r	[BCD]	H1	H2	H3	H4	H5	H6
1	1.50	5.1095	3.6884	4.0048	3.6239	3.8872	3.9191
0.9	1.35	5.1100	3.6853	3.9947	3.6230	3.8711	3.9118
0.8	1.20	5.1094	3.6814	3.9828	3.6214	3.8526	3.9073
0.7	1.05	5.1017	3.6803	3.9714	3.6213	3.8313	3.9035
0.6	0.90	5.1073	3.6782	3.9609	3.6205	3.8086	3.8975
0.5	0.75	5.0973	3.6769	3.9510	3.6252	3.7841	3.8903
0.4	0.60	5.0989	3.6768	3.9405	3.6238	3.7614	3.8841
0.3	0.45	5.0946	3.6733	3.9300	3.6220	3.7420	3.8756
0.2	0.30	5.0937	3.6684	3.9172	3.6166	3.7249	3.8722
0.1	0.15	5.0930	3.6748	3.9101	3.6144	3.7057	3.8710

Table 6 Propyl paraben protons of the PPBCD complex in D_2O at 298K

r	[P]	H3, H7	H4, H6	CH_2 (t)	CH_2 (q)	CH_3
1	1.50	8.0037	6.9800	4.3120	1.8181	1.0272
0.9	1.35	7.9927	6.9770	4.3135	1.8208	1.0259
0.8	1.20	7.9859	6.9738	4.3194	1.8231	1.0279
0.7	1.05	7.9805	6.9715	4.3310	1.8206	1.0343
0.6	0.90	7.9750	6.9699	4.3371	1.8266	1.0368
0.5	0.75	7.9696	6.9670	4.3399	1.8273	1.0365
0.4	0.60	7.9626	6.9642	4.3427	1.8255	1.0362
0.3	0.45	7.9578	6.9611	4.3470	1.8265	1.0377
0.2	0.30	7.9540	6.9580	4.3483	1.8264	1.0385
0.1	0.15	7.9526	6.9530	4.3550	1.8309	1.0415

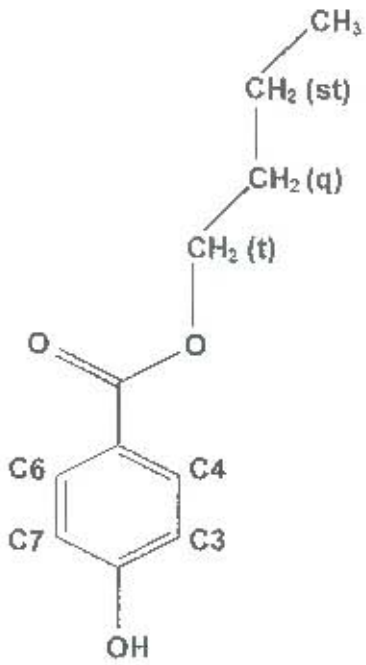

r = [BCD] / [BCD] [G] or
r = [G] / [BCD] [G]

Table 7 BCD protons of the BPBCD complex in D_2O at 298K

r	[BCD]	H1	H2	H3	H4	H5	H6
1	0.7	5.1116	3.6892	4.0061	3.6254	3.8877	3.9205
0.9	0.63	5.1106	3.6885	3.9991	3.6267	3.8746	3.9121
0.8	0.56	5.1100	3.6884	3.9920	3.6280	3.8620	3.9063
0.7	0.49	5.1080	3.6864	3.9824	3.6282	3.8420	3.9027
0.6	0.42	5.1068	3.6855	3.9737	3.6295	3.8200	3.8960
0.5	0.35	5.1051	3.6856	3.9629	3.6287	3.8013	3.8901
0.4	0.28	5.1022	3.6852	3.9552	3.6294	3.7826	3.8831
0.3	0.21	5.1009	3.6793	3.9482	3.6289	3.7663	3.8767
0.2	0.14	5.0988	3.6820	3.9407	3.6294	3.7514	3.8727
0.1	0.07	5.0989	3.6824	3.9360	3.6310	3.7411	3.8681

Table 8 Butyl paraben protons of the BPBCD complex in D_2O at 298K

r	[B]	H3, H7	H4, H6	CH_2 (t)	CH_2 (q)	CH_2 (st)	CH_3
0.9	0.63	7.9944	6.9895	4.3764	1.7963	1.4982	0.9894
0.8	0.56	7.9855	6.9853	4.3806	1.7992	1.4985	0.9965
0.7	0.49	7.9745	6.9791	4.3837	1.8005	1.4987	0.9995
0.6	0.42	7.9675	6.9789	4.3903	1.8037	1.5005	1.0031
0.5	0.35	7.9577	6.9751	4.3919	1.8045	1.5009	1.0051
0.4	0.28	7.9518	6.9744	4.3996	1.8051	1.5013	1.0080
0.3	0.21	7.9456	6.9741	4.4033	1.8091	1.5021	1.0116
0.2	0.14	7.9376	6.9682	4.4079	1.8110	1.5027	1.0136
0.1	0.07	7.9338	6.9663	4.4080	1.8145	1.5032	1.0109

APPENDIX B

The NMR traces of the free and complexed states of the β-CD solution state complexes can be found on the CD-ROM attached. There are eleven NMR traces for each β-CD complex and these are grouped under a filename bearing the same name as that of the complex. Each trace is labelled according to the β-CD concentration of that sample.

APPENDIX C

Supplementary material can be found on the CD-ROM attached. Seven files are included for each of the structures elucidated in this thesis, namely:

EXTENSION	CONTENTS
Filename.HKL	Reflection data
Filename.RES Filename.CIF	SHELX type co-ordinate file SHELX type co-ordinate file
Filename.SFT Filename.FCF	Structure factor tables
Filename.TEX	atomic co-ordinates bond lengths bond angles torsion angles displacement parameters
Filename.LST	atomic co-ordinates bond lengths bond angles torsion angles displacement parameters geometry between non-bonded atoms intermolecular and inter-atomic contacts

For each structure these seven files are grouped into a subdirectory bearing the same name as the filename. The files have been saved as text files and can be opened in a text editor such as WORDPAD in Windows95 and Windows98.